Ines Aline Aschenbrenner, MSc

Stability and change in the lichen microbiome

DOCTORAL THESIS

to achieve the university degree of

Doktorin der Naturwissenschaften

submitted to

Graz University of Technology

Supervisor

Univ.-Prof. Dipl.-Biol. Dr.rer.nat. Gabriele Berg

Institute of Environmental Biotechnology - Graz University of Technology
and

Ao.Univ.-Prof. Mag. Dr.rer.nat. Martin Grube
Institute of Plant Sciences - University of Graz

Graz, September 2015

AFFIDAVIT

I declare that I have authored this thesis independently, that I have not used other than the declared sources/resources, and that I have explicitly indicated all material which has been quoted either literally or by content from the sources used. The text document uploaded to TUGRAZonline is identical to the present doctoral thesis.

16. 09. 2015
Date

Aschenbrenner Ines
Signature

TABLE OF CONTENTS

ABSTRACT

Traditionally, lichens are regarded as symbiotic association of a mycobiont (fungus) and a photobiont (green alga and/or cyanobacterium). To maintain this kind of lifestyle each partner within symbiosis succeeds at certain tasks. While the fungus provides a suitable habitat for the photobiont, the photosynthetic partner produces energy for the whole system in form of fixed carbon. In the last years this classical point of view was challenged by advanced microbiome research accompanied with new technologies. Similar to a wide range of other organisms, the positive effect of a microbiome on its host might also contribute to the wellbeing of lichens. If and which role these bacteria play for the lichen symbiosis and which taxa are in particular involved, was mostly unknown. The aim of this study was to characterize the structure and diversity of the lichen-associated microbiome by sequencing and microscopy, and to shed light on its potential contribution to the symbiosis on different molecular levels (metagenome, transcriptome, proteome).

Focusing on the lichen *Lobaria pulmonaria* as model system, we could show that *Alphaproteobacteria,* and *Rhizobiales* in particular, was the dominant group within the bacterial community. The microbiome, which was high in alpha diversity, indicated variations in community composition across large scale geography. Nevertheless, a core microbiome shared by distant *Lobaria* populations could be identified, indicating a correlation between specific bacterial taxa and the lichen species itself. Vertical transmission of a bacterial delegation with the lichen vegetative propagules over short distances might to some extent shape and explain the microbiome composition within a region, but this fails for large-scale geography. However, inter-microbiome transfer of bacteria among naturally co-occurring, but not related host-organisms, such as moss or tree bark, is another factor in shaping the bacterial community in lichens. These adjoining hosts are each associated with a specific microbiome, nonetheless bacterial generalists, which might have a beneficial effect on the host and therefore might be shared among them, were also identified. Potential functions attributed to representatives of a generalist or specialist emphasized the general occurrence or the specific adaption to the host, respectively. In detail, it could be shown that the symbiotic lifestyle is supported and supplemented by various potential functions. These include the syntheses and provision of nutrients, vitamins and hormones as well as chemical defense mechanisms against various stress factors. The latter one comprises protection against reactive oxygen species and detoxification of toxic inorganic compounds such as arsenic. Several of these

encoded functions were also found in a metatranscriptomic approach reflecting the metabolically active bacterial fraction of the microbiome supporting the metagenomic findings. Additionally, lichens were identified as potential bio-resources for bacteria with antagonistic activities against pathogenic bacteria and fungi.

Results obtained in this study on functions, dispersal, habitat-specificity and inter-microbiome relations were discussed based on recent literature and concluded in a holistic view on lichen-bacteria interactions.

KURZFASSUNG

Traditionell werden Flechten als symbiotische Verbindung zwischen einem Mycobionten (Pilz) und einem Photobionten (Grünalgen- und /oder Cyanobakterien) gesehen. Um diesen Lebensstil aufrecht zu erhalten, übernimmt jeder dieser Partner innerhalb dieser Symbiose eine bestimmte Aufgabe. Während der Pilz einen geeigneten Lebensraum für den Photobionten bereitstellt, produziert dieser Energie in Form von fixiertem Kohlenstoff für das gesamte symbiotische System. Diese klassische Sichtweise wurde in den letzten Jahren durch fortschreitende Mikrobiom-Forschung und den damit einhergegangenen neuen Technologien in Frage gestellt. Ähnlich wie bei anderen Organismen, könnte das Mikrobiom einen positiven Effekt auf seinen Wirt haben und damit zum Wohlergehen der Flechte beitragen. Ob und welche Rolle diese Bakterien für die Flechten Symbiose jedoch wirklich spielen und welche Taxa darin beteiligt sind, war noch weitestgehend unbekannt. Das Ziel dieser Studie war es, das Flechten-assoziierte Mikrobiom in Hinblick auf seine Struktur und Diversität durch Sequenzierung und Mikroskopie zu charakterisieren, sowie dessen potentiellen Beitrag zur Symbiose auf verschiedenen molekularen Ebenen (Metagenom, Transkriptom und Proteom) zu beleuchten.

Mit Fokus auf das Model System *Lobaria pulmonaria* konnte gezeigt werden, dass *Alphaproteobakterien* und *Rhizobiales* im speziellen die dominante Gruppe innerhalb der bakteriellen Gemeinschaft darstellen. Das Mikrobiom zeigte neben einer hohen Alpha-Diversität auch Abweichungen in den *Lobaria*-assoziierten bakteriellen Gemeinschaften über große räumliche Entfernungen. Dennoch konnte auch ein Core-Mikrobiom identifiziert werden, das entfernt liegende *Lobaria* Populationen gemeinsam hatten und damit auf eine Verbindung zwischen speziellen Bakterien Arten und der Flechtenart selbst hindeutet. Eine vertikale Übertragung einer Bakterien Delegation mit den vegetativen Ausbreitungseinheiten der Flechte über kurze Distanzen dürfte das Flechten-assoziierte Mikrobiom innerhalb einer Region teilweise formen und auch die Zusammensetzung erklären. Dies trifft jedoch nicht auf größere Distanzen zu. Der Inter-Mikrobiom-Transfer von Bakterien zwischen natürlich vorkommenden, aber nicht miteinander verwandten Wirtsorganismen, wie das Moos oder die Baumrinde, ist ein weiterer Faktor der die Zusammensetzung der bakteriellen Gemeinschaft wahrscheinlich beeinflusst. Obwohl jeder dieser benachbarten Wirte mit einem spezifischen Mikrobiom assoziiert ist, konnten auch Generalisten identifiziert werden, die womöglich einen positiven Effekt auf den Wirt haben könnten und deshalb auch zwischen ihnen geteilt

werden. Vertretern eines Generalisten sowie Spezialisten konnten potentielle Funktionen zugewiesen werden und damit das allgemeine Vorkommen bzw. spezifische Adaptierung an den Wirt unterstreichen. Im Detail konnte gezeigt werden, dass das Flechten-assoziierte Mikrobiom den symbiotischen Lebensstil durch verschiedene Funktionen potentiell unterstützen bzw. ergänzen kann. Dazu gehören die Bereitstellung von verschiedenen Nährstoffen, Vitaminen und Hormonen, aber auch chemische Abwehrmechanismen gegen verschiedene Stress Faktoren. Letzteres inkludiert den Schutz vor reaktiven Sauerstoffspezies oder die Detoxifizierung von schädlichen anorganischen Verbindungen wie Arsen. Mehrere dieser kodierten Funktionen konnten auch in einem Metatranskriptom Ansatz, das die metabolisch aktiven Bakterien innerhalb des Mikrobioms wiederspiegelt, gefunden und damit die Ergebnisse aus dem Metagenom bekräftigt werden. Zusätzlich wurden Flechten als potentielle Bioressource für Bakterien mit antagonistischen Aktivitäten gegen pathogene Bakterien und Pilze entdeckt.

Die erhaltenen Erkenntnisse über die Funktionen, Ausbreitung, Habitat-Spezifität und Inter-Mikrobiom Relationen wurden anhand aktueller Literatur diskutiert und in einem holistischen Betrachtungsschema der Flechten-Mikrobiom-Interaktionen resümiert.

Review Article in preparation*

Lichens: obligate symbioses and their indispensable microbiome

Ines Aline Aschenbrenner,[1,2] Tomislav Cernava,[1] Gabriele Berg,[1] Martin Grube[2]

[1]Institute of Environmental Biotechnology
Graz University of Technology, Austria

[2]Institute of Plant Sciences
University of Graz, Austria

*Passages in this review article indicated with square brackets were adapted from the doctoral thesis "*Exploring the substantial contributions and the global interactions of the microbiome in an ancient symbiosis*" (Cernava Tomislav, Graz University of Technology, 2015)

Lichens: obligate symbioses and their indispensable microbiome

Ines Aline Aschenbrenner,[1,2] Tomislav Cernava,[1] Gabriele Berg,[1] Martin Grube[2]

[1]Institute of Environmental Biotechnology, Graz University of Technology, Petersgasse 12, 8010 Graz, Austria

[2]Institute of Plant Sciences, University of Graz, Holteigasse 6, 8010 Graz, Austria

Corresponding Author

Martin Grube
University of Graz
Institute of Plant Sciences
Holteigasse 6, A-8010 Graz
email: martin.grube@uni-graz.at
telephone: +43 316 380 5655

Introduction

More than 130 years ago the mycologist de Bary coined the term "symbiosis" referring to it as "the living together of unequal organism" (de Bary, 1879). Now, a wide variety of symbiotic lifestyles was demonstrated comprising mutualistic, commensalistic or parasitic interactions (e.g., fungi: Frey-Klett et al., 2011; animals: McFall-Ngai et al., 2013; humans: Eloe-Fadrosh & Rasko, 2013; plants: Berg et al., 2014). A detailed account on the historic development of the term and concept of symbiosis is provided by Sapp (2010).

[In the context of symbioses, bacterial-fungal interactions were more recently identified as key elements in many natural environments (Frey-Klett *et al.*, 2011). One of the most prominent bacterial-fungal interactions is represented by the lichen symbiosis.] Lichens are an obligate association between a fungal (mycobiont) and a photosynthetic partner (photobiont), which can be either cyanobacteria and/or green algae (Nash, 2008). Thereby, the photobionts supply nutrients by carbon dioxide fixation and the mycobiont provides the habitat with the formation of a vegetative body. [The first ancestors of lichens can be tracked back to the Devonian 400 million years ago (Remy *et al.*, 1994; Honegger *et al.*, 2013) – a first fossil glance of a symbiosis, which diversified to more than 18,000 known lichen species until now.] The successful symbiosis is characterized by its poikilohydric lifestyle and enables lichens to colonize almost all terrestrial environments from tropic to polar climatic zones. Moreover, they can grow on almost every kind of substrate including bare soils, rocks and plants, but they can be also found in freshwater streams and in marine intertidal zones (Nash, 2008). The vegetative bodies vary in color, size (a few millimeters to meters) and growth forms, and some few can persist for several thousands of years (Denton and Karlén, 1973). The wide variety of lichen thallus structures, which are primarily determined by the fungal partner, can be roughly divided into three main morphological types, namely the crustose, foliose and fruticose growth forms. The vegetative body can be either homoiomerous, where the mycobiont and photobiont are evenly distributed in the lichen thallus, or heteromerous with a stratified thallus subdivided into upper and lower cortex with a photobiont layer and a medulla in-between. Crustose lichens are characterized by the attachment of the entire lower surface to the substrate, whereas foliose and fruticose lichens are only partially attached (Büdel & Scheidegger, 2008). Sexual reproduction of the fungal partner obligatory requires the association with appropriate algae, since sexual structures of lichenized fungi are only produced on a properly developed lichen thallus. For rapid asexual reproduction of the

symbiosis, numerous lichens also evolved vegetative reproduction to disperse both symbiotic partners together in joint propagules (Büdel & Scheidegger, 2008).

Even though lichens produce a wide variety of secondary metabolites, some of which are known for antifungal or antibacterial activities, their long-lived thalli provide various distinct microhabitats for other eukaryotic and prokaryotic (both bacteria and archaea) microorganisms (Lawrey & Diederich, 2003; Grube & Berg, 2009a; Bjelland et al., 2010; Bates et al., 2012). [In previous years attention was increasingly drawn to lichen-associated bacteria that were not recognized as being an integral part of the symbiosis. Biofilm-like communities that mainly consist of *Alphaproteobacteria* were detected on the surface of various lichen species (Cardinale *et al.*, 2008, 2012a, b). Furthermore, it was shown that such communities display a certain degree of host specificity when different species were compared (Grube *et al.*, 2009b; Hodkinson *et al.*, 2012; Bates *et al.*, 2011). Related to these findings, experiments based on cultivable bacteria from lichens have provided additional evidence for their beneficial contributions to the overall symbiosis (Liba *et al.*, 2006; Grube *et al.*, 2009b). However, the detailed roles of these bacteria were previously unknown and therefore required further exploration to facilitate a more holistic lichen model.]

[For this reason, the lung lichen *Lobaria pulmonaria* (L.) Hoffm. was extensively used as model system due to its relatively fast growth and other facilitative characteristics, *e.g.* epiphytic growth on tree bark and a low number of secondary metabolites, which could interfere with the conducted analyses. *L. pulmonaria* is characterized by a leaf-like structure (foliose lichen) and mainly found in old-growth forests with unpolluted air. Its sensitivity to air pollution can be employed for indirect evaluations of air quality and ecosystem integrity (Scheidegger and Werth, 2009). It harbors two photosynthetic partners, a phenomenon observed for approximately 4% of all described lichens (Honegger, 1991). However, only the green alga *Dictyochloropsis reticulata* forms a continuous layer, whereas cyanobacterial *Nostoc* strains are maintained in spaced, nodule-like internal compartments (cephalodia).]

In this review we discuss recent literature on lichen-associated microbiota with focus on diversity, functions, dispersal, habitat specificity and inter-microbiome relations of the *L. pulmonaria*-associated bacterial community and conclude with an outline to promote a holistic view on lichen-bacteria interactions.

Unraveling the lichen-associated microbiome – a brief review on applied methods: now and then

Bacteria in context with lichens were initially mentioned in the first half of the 20th century (Uphof, 1925; Henkel & Yuzhakova, 1936; Iskina, 1938). During these early studies various bacterial genera were reported to be associated with lichens such as *Azotobacter, Pseudomonas* (*Gammaproteobacteria*), *Beijerinckia* (*Alphaproteobacteria*), and the *Firmicutes* genera *Bacillus* and *Clostridium* (Iskina, 1938; Panosyan & Nikogosyan, 1966; Henkel & Plotnikova, 1973). At that time descriptions of bacteria underlay solely phenotypical and physiological characterizations indicating a possible role in nitrogen fixation for some of these bacteria. Nevertheless, Lenova & Blum (1983) already estimated that millions of bacterial cells per gram could colonize a lichen thallus. Several decades passed before the first molecular analyses started using bacterial isolates, e.g. Gonzalez et al. 2005, Cardinale et al. 2006, Liba et al. 2006, or Selbmann et al., 2009. While Gonzalez et al. (2005) only focused on culturable *Actinomycetes* (with *Micromonospora* and *Streptomyces* as predominant genera) of various lichen species from tropical and cold areas, Cardinale et al. (2006) attempted to describe the overall bacterial community composition associated with seven different lichen species from temperate habitats. The latter enabled the identification of several genera affiliated to *Firmicutes, Actinobacteria* and *Proteobacteria*, highlighting *Paenibacillus* and *Burkholderia* to be ubiquitous genera in lichens. However, culture-dependent methods capture only 0.001-15% of the bacterial diversity in environmental samples (Amann et al., 1995), whereas the majority remains unobserved (Rappe et al., 2003). To overcome the limitations of selective bacterial isolation from environmental samples and to obtain a more unbiased and less restricted view on the microbial communities, new techniques were employed to complement the traditional methods.

First culture-independent investigations on lichen-associated microbiota were assessed with different fingerprinting methods (Cardinale et al., 2006; Grube et al., 2009b; Bjelland et al., 2010; Mushegian et al., 2011, Cardinale et al., 2012a) and molecular cloning approaches (Hodkinson & Lutzoni, 2009). Such techniques (e.g., DGGE: Muyzer & Smalla, 1998; T-RFLP: Liu et al., 1997; SSCP: Schwieger & Tebbe, 1998) were used to generate microbial community profiles by amplifying genetic markers (e.g., 16S ribosomal DNA) with universal primers. Based on sequence or length polymorphisms PCR products are separated and the degree of sample similarity according to the specific band patterns can be characterized (Smalla et al., 2007). Although many samples can be analyzed in parallel and their profiles

can be compared with each other easily, the identification of the bacterial community members in detail is tedious and limited. In 2005, Margulies and colleagues introduced a new time reduced and cost efficient technology to study community compositions and diversity of environmental samples in depth by large-scale high throughput sequencing. Bates and colleagues (2011) described lichen-associated bacteria for the first time based on this next generation pyrosequencing technology, followed by Hodkinson et al. (2012), Grube et al. (2012), and Aschenbrenner et al. (2014). Besides various advantages coming along with these PCR-based techniques, there are also various disadvantages (addressed in e.g., Marzorati et al. 2008; Gonzalez et al. 2012; Pinto & Raskin, 2012; Klindworth et al. 2013). Species abundances of amplicon-based pyrosequencing, in particular, can only roughly be estimated (Davenport & Tümmler, 2013), since multiple rRNA gene copies (up to 15) can be present per bacterial genome (Klappenbach et al., 2000). Although there were method-based limitations, the understanding of community composition and diversity, however, expanded tremendously and it was shown to be higher than previously expected. Genera, previously considered to be ubiquitous in lichens based on culture-dependent methods of earlier studies, were found to represent only a small proportion, if at all, of the entire bacterial community detected with high-throughput sequencing techniques (Grube et al., 2009b; Hodkinson et al., 2012).

With the improvement of sequencing technologies and bioinformatics tools the focus in microbial ecology research shifted from the basic taxonomical descriptions to a more detailed and holistic view on microbial communities. Metagenomic, transcriptomic and proteomic analyses can now shed light on the questions “Who is there?”, “What are they capable of?” and “Who is actively doing what?” (Schneider et al., 2011; Grube et al., 2015; Aschenbrenner et al., 2015b). However, the lack of standard guidelines in sample preparation as well as bioinformatics analyses leads to variations in the final results and makes comparisons of different studies difficult or even impossible.

Composition and diversity of the lichen-associated microbiome driven by various abiotic and biotic factors

It is estimated that about 10^{30} microbial cells can be found on Earth (Turnbaugh and Gordon, 2008) currently comprising about 9300 microbial species (Saleem, 2015). Soils are one of the most diverse habitats with about 10^{10} cells/cm^3. Contrarily, a leaf surface comprises

only 10^5 cells/cm^2 and one so far analyzed lichen species, e.g. *Cladonia* sp., is colonized by approximately 10^7-10^8 bacteria per gram of lichen thallus (Cardinale et al., 2008, Grube et al., 2009, Saleem, 2015). Alpha diversity indices (Shannon index) of bacterial communities were shown to vary between different lichens, e.g., from in average 4.5 (*Solorina crocea*) to 7.0 (*L. pulmonaria*) at a genetic distance of 3% (Grube et al., 2012, Aschenbrenner et al., 2014) indicating differences in lichens as suitable microhabitats.

L. pulmonaria is mainly colonized by *Alphaproteobacteria* with *Sphingomonadales* as predominant order, followed by *Sphingobacteria*, *Actinobacteria* and *Spartobacteria* (Aschenbrenner et al., 2014). Contrarily, shotgun sequencing-based studies suggested *Rhizobiales* as the main order within *Alphaproteobacteria* (Grube et al., 2015; Erlacher et al., 2015). These results were additionally confirmed with adapted visualizing techniques. Thereby, the predominance of *Alphaproteobacteria* and *Rhizobiales* on lichen surfaces were shown with a combined approach of fluorescence in situ hybridization (FISH) and confocal laser scanning microscopy (CLSM). Related to these findings, the lichen-associated *Rhizobiales* group (LAR1) was reported to be a lichen-specific lineage of *Alphaproteobacteria*, which can be found among many examined species (Hodkinson & Lutzoni, 2009; Bates et al., 2011; Hodkinson et al., 2012). However, this lineage could not be detected in other species such as *L. pulmonaria* (Aschenbrenner et al., 2014). The observed compositional differences within the same lichen species can be attributed to various reasons such as sequencing platforms (amplicon vs. shotgun sequencing), utilized databases, or activity of the bacteria in case of metatranscriptomic analysis (Aschenbrenner et al., 2015b) since less than 10% of a microbial community is metabolically active at one time (Locey, 2010).

While the predominance of *Alphaproteobacteria* was also reported in other studies (Bates et al., 2011; Hodkinson et al., 2012), bacterial community composition in general differed among distinct lichens. These variations are supposed to be driven by various biotic and abiotic factors. Hodkinson et al. (2012) who thoroughly studied the bacterial communities associated with various lichen species comprising 24 mycobiont types with all photobiont combinations of different sampling locations (tropical and arctic regions) highlighted the photobiont type (chlorolichens vs. cyanolichens) and large-scale geography as the main driving forces.

Photobiont and mycobiont type. Hodkinson et al. (2012) argued that the differences in community composition could be ascribed to both the availability of fixed nitrogen and the

type of fixed carbon. Regarding to the first one bacteria associated with cyanolichens have access to fixed atmospheric nitrogen due to the cyanobacterial photobiont, whereas those of chlorolichens lack this benefit in nitrogen-restricted environments. According to that chlorolichens would preferably enrich species capable of nitrogen fixation rather than cyanolichens. Another suggestion was that green algae release different types of fixed carbon (sugar alcohols: ribitol, erythritol, or sorbitol) than cyanobacteria (glucose; Elix & Stocker-Wörgötter, 2008), thereby shaping the bacterial community with respect to carbon utilization. Both explanations can only partly declare community differences based on taxonomical descriptions as bacteria can exchange and share genes encoding for certain functions via horizontal gene transfer. This agrees with Burke et al. (2011) who argued that ecological niches are colonized randomly by bacteria equipped with suitable functions rather than following bacterial taxonomy. The attempt to explanations gets more complicated with regard to tripartite lichens as they carry both types of photobionts as it is the case in *L. pulmonaria*.

Species-specificity for bacterial communities associated with chlorolichens was already indicated in previous studies (Grube et al., 2009b; Bates et al., 2011). Lichenized fungi are able to produce secondary metabolites, which are unique to lichens and comprise several hundred compounds which can be deposited on the extracellular surface of the fungal hyphae (Elix & Stocker-Wörgötter, 2008). As already suggested by Hodkinson et al. (2012) these secondary metabolites with many of them having antimicrobial activities (Kosanic & Rankovic, 2015) might cause a selective pressure on lichen colonizing bacteria as well. However, as *L. pulmonaria* contains only low concentrations of lichen-specific substances like many other lichens of the suborder *Peltigerineae* (Beckett et al., 2003), secondary metabolites might play only a minor role in shaping the community structure of *Lobaria*-associated bacteria.

Growth type. Differences in bacterial community composition might be also due to the lichen growth type as for instance previous studies reported that the bacterial community compositions of crustose lichens differed from those of foliose or fruticose lichens (Grube et al., 2009b; Hodkinson et al., 2012). While the foliose lichens were mainly colonized by *Alphaproteobacteria*, the crustose lichen *Ophioparma* sp. was predominated by *Acidobacteria* (Hodkinson et al., 2012). Another rock inhabiting crustose lichen *Hydropunctaria* sp. was mainly colonized by *Cyanobacteria*, *Actinobacteria* and *Deinococcus* (Bjelland et al., 2011). But growth type on its own does not explain the predominance of certain taxa since the foliose lichen *Solorina* sp. was also predominated by *Acidobacteria* (Grube et al., 2012). This

agrees with previous results of Cardinale et al. (2012b) who showed that growth types do not affect the main bacterial community structure.

Bacteria are spatially distributed on lichen surfaces

Thallus sub-compartments of varying age as well as external and internal surfaces offer chemically and physiologically distinct micro-niches and facilitate the formation of various distinct bacterial communities.

Ectobiont vs. endobiont. Based on FISH-CLSM the lichen-associated eubacteria as well as specific bacterial taxa therein were demonstrated to colonize distinct lichen thallus parts in different abundances and patterns (Cardinale et al., 2008). Confocal laser scanning microscopy of the *L. pulmonaria* surfaces showed that both the upper and the lower cortexes were densely colonized by *Alphaproteobacteria* among other eubacteria (Cardinale et al., 2012a; Grube et al., 2015). This was also demonstrated for other dorsiventral organized lichen thalli such as *Umbilicaria* sp. (Grube et al., 2009b). In the case of the fruticose species *Cladonia* the outer cortex of the radial organized hollow thallus (podetium) was merely colonized by single cell colonies and smaller colony clusters, while the highest bacterial density examined on this lichen was found on the internal layer of the podetia forming a biofilm-like coat (Cardinale et al., 2008, 2012b). Contrarily, bacterial colonization on crustose lichens such as *Lecanora* sp. was only shown for the lateral parts of adjacent thalli (Grube et al., 2009b). There were also indications for endobiotic bacteria within the cell walls of fungal hyphae (Cardinale et al., 2008). Erlacher et al. (2015) previously reported in *L. pulmonaria* endosymbiotic *Rhizobiales*, localized in varying depths of the interhyphal gelatinous matrix of the upper cortex and seldom in the interior of fungal hyphae. So far, there is no documentation of bacterial growth in other compartments of *L. pulmonaria* such as the internal thalline tissue (medulla) or the photobiont layer.

Old vs. young thallus parts. The establishment and aging of a lichen thallus starting with symbiotic propagules to mature thallus structures might influence and shape bacterial community structure following similar adaptions to the community succession in the apple flower microbiome (Shade et al., 2013). A recent study has shown that the vegetative propagules of *L. pulmonaria* were colonized by a more distinct bacterial community than the mature lichen thallus (Aschenbrenner et al., 2014) indicating that the community structure

might change over time. In detail, only 37% of thallus-associated bacterial OTUs were shared with the vegetative propagules, conversely, shared OTUs associated with the propagules comprised 55%. While both lichen parts were mainly colonized by *Alphaproteobacteria*, the lichen thallus was additionally predominated by *Deltaproteobacteria*, whereas the vegetative propagules were also colonized in higher abundances by *Spartobacteria* and *Sphingobacteria*.

Cardinale et al. (2012b) already reported that older thallus parts hosted significantly higher amounts of bacteria than the younger thallus structures including a change of the predominant *Alphaproteobacteria* to other taxa such as *Actinobacteria*, *Gamma-*, and *Betaproteobacteria*. Also Mushegian et al. (2011) observed a spatial diversification of the bacterial compositions between the more diverse and consistent thallus centers (older parts) and those of the more variable and species poor edges (younger parts). Cardinale et al. (2012b) referred to this bacterial distribution patterns as anabolic centers in the growing and catabolic sinks in the senescing parts of the lichen thallus, respectively. The hypothesis of recycling nutrients in the decaying lichen parts by bacteria can be also underpinned by the presence of specific taxa known for their degradation potential. *Sphingomonas* spp., which are known to degrade organic matter and xenobiotic substances, were previously isolated from lichens sampled in Arctic and Antarctic regions (Lee et al., 2014), but also reported in other studies (Grube et al., 2009; Hodkinson et al., 2012; Grube et al, 2012; Aschenbrenner et al., 2015a). However, also other genera such as *Paenibacillus* and *Streptomyces* were mentioned for their functions (e.g. chitinolytic activity) in the degradation of lichen tissues (Cardinale et al., 2006).

Inter-microbiome transfer of host-associated bacteria

Vertical transmission. Analyses of lichen-associated bacteria revealed differences in community composition and diversity among geographically distant habitats (Printzen et al., 2012; Aschenbrenner et al., 2014). Hodkinson et al. (2012) explained these large-scale geographical effects by the dispersal efficiency of the lichen hosts. Thereby, dispersal happens on small spatial scales rather than on large-scale distances resulting in a geographical differentiation of the community composition. Printzen et al. (2012) analyzed the geographic structure of lichen-associated *Alphaproteobacteria* in Antarctic regions indicating that this group is affected by environmental parameters as they are more similar within these regions than to those of extrapolar regions. Moreover, it was suggested that the highly abundant

Alphaproteobacteria might be crucial for the establishment of the dispersed young lichen structures in the new environment (Cardinale et al., 2012a), whereas less abundant species and therefore less important for the lichen wellbeing are replaced by locally more adapted species, related to the vertical transmission of primary symbionts and the horizontal transfer of facultative symbionts. This was underpinned by the presented results indicating a geographical influence on the diversity of *Alphaproteobacteria*, whereas other groups such as *Burkholderia* were not affected.

Aschenbrenner et al. (2014) visualized and described the bacterial colonization of such lichen propagules demonstrating that at least a certain proportion of the lichen microbiome is transferred vertically via these symbiotic structures. These bacterial communities were predominated by *Alphaproteobacteria*, as already supposed by Cardinale et al. (2012a). Interestingly, the bacterial consortia of the lichen propagules were more than only a delegation of the thallus microbiome as they also comprised unique species, which were not shared with the maternal thallus at all. Thus, Aschenbrenner et al. (2014) put forward the hypothesis that the vegetative propagules are equipped with a bacterial starter community rather than a *de novo* recruitment of the entire lichen microbiome. Moreover, these early colonizing bacteria might influence the subsequent recruitment of new bacteria either positively (promoting effect) or negatively (inhibitory effect; Fukami, 2010), thereby shaping the community composition. The importance of the lichen-associated bacteria during the establishment of the lichen symbiosis was already suggested by Hodkinson & Lutzoni (2009) as the growth of stratified lichen thalli was only successful in cultures based on lichen fragments, which established in nature, but failed under axenic conditions. Although vertical transmission of lichen-associated bacteria was only shown in a single lichen species, it is very likely that this strategy of microbiome transfer is also common in other species utilizing vegetative diaspores for reproduction.

Vertical transfer of valuable host-associated bacteria is not restricted to the lichen symbioses, but a more universal phenomenon observed in many plants and animals. There are various examples reporting on a transmission of host-associated bacteria (Bright & Bulgheresi, 2010), e.g. invertebrates such as marine sponges (Wilkinson, 1984; Li et al., 1998). Bacteria associated with terrestrial invertebrates such as insects are known to assist in nutrient uptake and provision of essential amino acids and vitamins (Douglas, 1998; Feldhaar & Gross, 2009), but their vertical transmission strategy varies among distinct insects (Sacchi et al., 1988; Attardo et al., 2008; Prado & Zucchi, 2012). In vertebrates including human

beings the transfer of maternal microbes to the child through natural birth and breast feeding as first inoculum was reported to be important for the baby's health, in particular by shaping the microbiome structure with beneficial microbes (Funkhouser & Bordenstein, 2013). But also in the plant kingdom transfer of plant-associated bacteria, in particular of seeds, from the mother plant was reported (van Overbeek et al., 2011), although it is more common in higher plants (rhizosphere) to recruit their microorganisms from the surrounding soil (Berg & Smalla, 2009). Vertical transmission was previously shown for the oldest group of land plants. In mosses, which belong together with lichens to the group of poikilohydric cryptogams, associated bacteria, especially specific *Burkholderia* strains, are transferred from the sporophyte to the gametophyte via spores (Bragina et al., 2012, 2013).

Lichens as bacterial hubs. Lichens are pioneers in the colonization of ecologically forbidding environments with extreme temperatures, desiccation and high salinity, but they may also become very old either as individuals (some reach several thousands of years, Denton and Karlén, 1973), or as associations (it is assumed that some non-glaciated sites were colonized by lichens since the tertiary). Colonized habitats include arid and semi-arid regions where bare soil can be colonized by e.g. cryptogamic soil crusts (an association between soil particles, lichens, cyanobacteria, algae, fungi and bryophytes; Beckett et al., 2008), but also more extreme regions such as deserts, where lichens are one of the few successful colonizers. In particular, their capability to become hydrated without contact to liquid water (Printzen et al., 2012) only by fog, dew or high air humidity (Beckett et al., 2008) ensures survival in these dry areas. This suggests that lichens as slow-growing and long-living host organisms might serve as bacterial hubs in these environments facilitating their survival by nutrient and water supply, offering a habitat with various micro-niches and ensuring their distribution over short distances by the dispersal strategies of the lichen host. Thereby the lichens could be important sources/reservoirs of beneficial bacterial strains for other habitats in an environment as well.

Habitat specificity. So far most of the host-associated bacterial communities were described without any correlation to adjacent habitats and their inter-microbiome relationships. A recent study focused on this topic unraveling the specificity of the lichen-associated microbiome compared to the naturally adjoining habitats – moss and bark – and highlighted potential habitat specialists and generalists (Aschenbrenner et al., 2015a). Host specificity for both cryptogams (lichen and moss) was already reported in previous independent studies (Grube et al., 2009b; Bragina et al., 2012). In this survey, members of the

genus *Sphingomonas* were identified as ubiquitous in the three habitats, whereas members of *Mucilaginibacter* were described as potential specialists of lichens. While functions of the generalist indicated a more universal role in the symbioses comprising hormone production, phosphate solubilization and ammonia assimilation, the functions of the specialist indicated a more adapted lifestyle such as defense strategies against oxidative stress caused by the lichen. Specialists or primary symbionts often have reduced genomes with retained gene sets specifically adapted to their hosts. These specialists can be shared with other individuals of the same host species whereas generalists can be shared among distinct hosts under similar environmental conditions. In particular, beneficial strains facilitating the survival and the overall fitness of the host under certain abiotic stresses (reactive oxygen species, periodic desiccation) might be shared. In the study of lichen/moss inter-microbiome relationships this was shown for certain *Nostoc* strains which were shared between both cryptogams indicating their need for fixed nitrogen (Aschenbrenner et al., 2015a).

Host specificity in the context of lichens was already reported in previous studies where the lichen-associated communities were distinct from those of the surrounding substrate (soil or rock) and of other lichen species (Bjelland et al., 2010; Bates et al., 2011; Lee et al., 2014). Bates et al. (2011) also showed that various bacterial species can be found in distinct lichen species, even across large distances indicating bacterial generalists. Furthermore, Hodkinson et al. (2009) suggested that these ubiquitous lichen-associated bacteria might encode some of the known "symbiosis genes" such as *nod*, *nif*/*fix* and *exo*.

[The lichen-associated microbiome plays a central functional role in the lichen holobiont]

[Although the biofilm-like colonization of various lichen species by highly diversified bacterial populations has been described in previous studies, their functions remained largely unknown. Meta-omic techniques were identified as suitable tools to globally identify potentially beneficial contributions of the bacterial population. Recently, the *L. pulmonaria* associated microbiome was investigated with an integrated metagenomics and metaproteomics approach to screen for present genetic information and to verify the expression at the protein level (Grube et al., 2015).] A pioneering metaproteomics-based study conducted by Schneider et al. (2011) provided the first evidence for a complex and widespread involvement of bacterial functions in the lichen symbiosis. [The results of Grube

et al. (2015) provided strong evidence that the bacterial microbiome is involved in nutrient provision and degradation of older lichen thallus parts, biosynthesis of vitamins and hormones, detoxification processes, and the protection against biotic as well as abiotic stress. Additionally, the high prevalence of bacterial nitrogen fixation was confirmed with –omic data and quantitative RT-PCR. Moreover, a comparison of the whole *Lobaria*-associated metagenome with a representative set of publicly available metagenomes highlighted its uniqueness. The closest related metagenomes were found to be those obtained from plant-associated habitats.]

In particular, [*Rhizobiales* (*Alphaproteobacteria*) were previously shown to be remarkably abundant in the *L. pulmonaria* microbiome mainly represented by the families: *Methylobacteriaceae*, *Bradyrhizobiaceae*, and *Rhizobiaceae*. Although they are well known for their beneficial interactions with many higher plants, less is known about their specific roles in terms of the lichens. According to Erlacher et al. (2015) functional assignments based on hierarchical SEED classification indicated an involvement of *Rhizobiales* in various beneficial functions (*e.g.* auxin, folate, and vitamin B_{12} biosynthesis). A further breakdown demonstrated that the predominant *Methylobacteriaceae* were also the most potent producers of the examined metabolites. These findings suggest the potential for various biotechnological applications of this group.]

[The pathogen defense is supported by antagonistic members of the microbiome.] Recently, it was shown that the *L. pulmonaria* associated microbiome include also various bacteria with antagonistic potential (Cernava et al., 2015a). [The most abundant antagonists were assigned to *Stenotrophomonas*, *Pseudomonas*, *Micorcoccus* and *Burkholderia*. These genera accounted for 67% of all identified antagonistic bacteria. Metagenomic screening revealed the presence of genes involved in the biosynthesis of stress-reducing metabolites. Complementary HPLC-MS analyses enabled the detection of *Stenotrophomonas*-produced spermidine which is known to reduce desiccation- and high salinity-induced stress in plants. It was also tested if these protective effects can be transferred to non-lichen hosts such as primed tomato (*Solanum lycopersicum*) strains. Results indicated a significant increase in the root and stem lengths under water-limited conditions. The application of lichen-associated bacteria in plant protection and growth promotion may prove to be a useful alternative to conventional approaches. However, further studies are required to evaluate the host range and to elucidate the overall applicability (Cernava et al., 2015a).]

[Furthermore, VOCs (volatile organic compounds) profiles from bacterial isolates showed that lichen-associated bacteria are emitting a broad range of volatile substances. These molecules are most likely involved in various interactions (*e.g*. communication between microorganisms and the host) and might also increase the overall resistance against various pathogens (Cernava et al., 2015b).]

[**The microbiome provides complementary detoxification mechanisms.**] As already mentioned, lichen-associated bacteria encode [for a variety of defense mechanisms conferring enhanced resistance against biotic as well as abiotic stress. While global studies of the microbiome provided a first evidence for the involvement in the detoxification of inorganic substances (*e.g*. As, Cu, Zn), the detailed mechanisms remained unknown. In order to obtain a deeper insight into these beneficial contributions, the effects of elevated arsenic concentration on the microbiome were analyzed (Cernava et al., 2015c). Metagenomic analyses have revealed that the global microbial community structures from different lichens were similar irrespective of the arsenic concentrations at the sampling locations, while the spectrum of arsenic related functions was extended. These functions include bioconversion mechanisms that are involved in the methylation of inorganic arsenic and consequently generate less toxic substances. Furthermore, the abundance of numerous detoxification related genes was enhanced in arsenic-polluted samples. Supplementary qPCR approaches have shown that the arsM gene copy number is not strictly related to the determined arsenic concentrations. Additionally, a culture collection of bacterial isolates obtained from three lichen species was screened for the arsM gene. Detected carriers of arsM were later identified as members of the genera *Leifsonia, Micrococcus, Pedobacter, Staphylococcus*, and *Streptomycetes*. The overall results reinforced the important role of the microbiome in host protection and provided detailed insights into the taxonomic structure of involved microorganisms.]

Holistic view on lichen-bacteria interactions

The obligate lichen symbiosis with its various physical and chemical distinct micro-niches represents a miniature ecosystem for microorganisms. While lichen-associated bacteria were previously seen as negligible occurrence upon lichen thalli, recent research considers them with increasing evidence as important and crucial component of the lichen holobiont (Fig.1). These bacterial communities are species specific and their composition and diversity

are shaped by various abiotic (e.g., large-scale geography) and biotic (e.g., photobiont and mycobiont type) factors. Colonization patterns vary within lichen thalli from single cell colonies to biofilm like structures as well as in abundance, diversity and spatial distribution. Vegetative propagules are equipped with a core fraction of this lichen microbiome and transmitted vertically with the symbiotic structures during dispersal events. Lichen thallus development in the new habitat is likely accompanied with the recruitment of locally adapted facultative bacterial symbionts. Ancillary inter-microbiome relations between the lichen and adjacent habitats such as bark or moss enables the interexchange and transfer of beneficial bacteria. The overall bacterial community supports the lichen symbiosis with various functional contributions including nutrient supply and provision of vitamins and hormones. Additionally, specific community members provide protection against biotic and abiotic stresses by detoxifying inorganic substances such as Arsenic or pathogen defense.

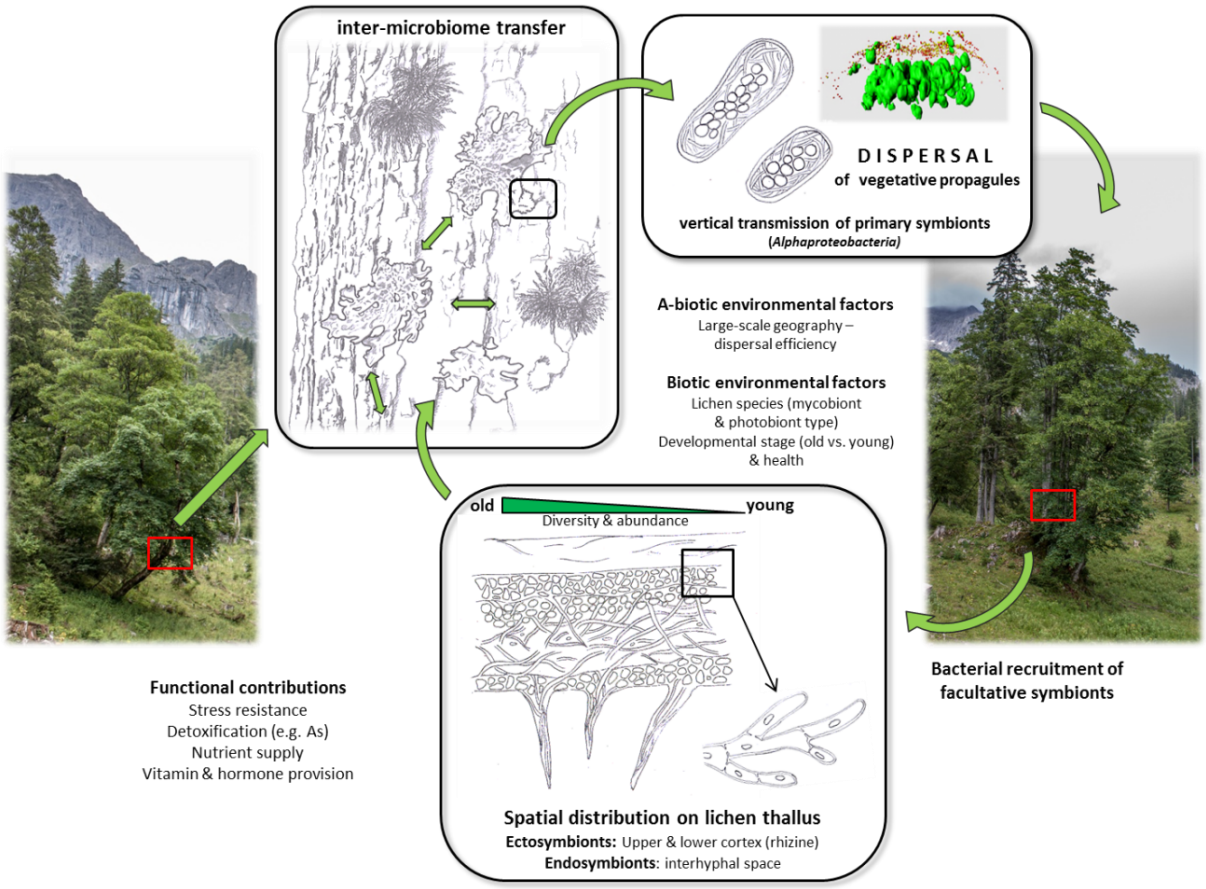

Figure 1: Holistic view on lichen-bacteria interactions including functional contributions, intermicrobiome transfer of beneficial members and vertical transmission via vegetative propagules.

References

Amann, R. I., Ludwig, W., and Schleifer, K. H. (1995). Phylogenetic identification and in situ detection of individual microbial cells without cultivation. *Microbiol. Rev.* 59, 143–169.

Aschenbrenner, I. A., Cardinale, M., Berg, G., and Grube, M. (2014). Microbial cargo: do bacteria on symbiotic propagules reinforce the microbiome of lichens? *Environ. Microbiol*. 16, 3743–3752.

Aschenbrenner, I. A., Cernava, T., Erlacher, A., Berg G., and Grube, M. (2015b). An integrative omics approach identifies bacterial key players in a complex microenvironment. Manuscript in preparation.

Aschenbrenner, I. A., Cernava, T., Erlacher, A., Berg, G., and Grube, M. (2015a). Inter-microbiome relations: spatially close hosts show a common network with specific components. Submitted.

Attardo, G. M., Lohs, C., Heddi, A., Alam, U. H., Yildirim, S., and Aksoy, S. (2008). Analysis of milk gland structure and function in Glossina morsitans: milk protein production, symbiont populations and fecundity. *J. Insect. Physiol.* 54, 1236–1242.

Bates, S. T., Berg-Lyons, D., Lauber, C. L., Walters, W. a., Knight, R., and Fierer, N. (2012). A preliminary survey of lichen associated eukaryotes using pyrosequencing. *Lichenologist* 44, 137–146.

Bates, S. T., Cropsey, G. W. G., Caporaso, J. G., Knight, R., and Fierer, N. (2011). Bacterial communities associated with the lichen symbiosis. *App. Environ. Microb.* 77, 1309–14.

Beckett, R. P., Kranner, I., and Minibayeva, F. V. (2008). "Physiological ecology of carbon dioxide exchange", in *Lichen Biology*, ed. T. H. Nash (Cambridge, UK: Cambridge University Press), 152–181.

Beckett, R. P., Minibayeva, F. V., Vylegzhanina, N. N., and Tolpysheva, T. (2003). High rates of extracellular superoxide production by lichens in the suborder *Peltigerineae* correlate with indices of high. *Plant Cell Environ.* 26, 1827–1837.

Berg, G., and Smalla, K. (2009). Plant species and soil type cooperatively shape the structure and function of microbial communities in the rhizosphere. *FEMS Microbiol. Ecol*. 68, 1–13.

Berg, G., Grube, M., Schloter, M., and Smalla, K. (2014). Unraveling the plant microbiome: looking back and future perspectives. *Front. Microbiol.* 5:148. doi: 10.3389/fmicb.2014.00148

Bjelland, T., Grube, M., Hoem, S., Jorgensen, S. L., Daae, F. L., Thorseth, I. H., et al. (2010). Microbial metacommunities in the lichen-rock habitat. *Environ. Microbiol. Rep.* 3, 434–442.

Bragina, A., Berg, C., Cardinale, M., Shcherbakov, A., Chebotar, V., and Berg, G. (2012). Sphagnum mosses harbour highly specific bacterial diversity during their whole lifecycle. *ISME J. 6*, 802–13.

Bragina, A., Cardinale, M., Berg, C., & Berg, G. (2013). Vertical transmission explains the specific Burkholderia pattern in Sphagnum mosses at multi-geographic scale. *Front. Microbiol*. 4:394. doi: 10.3389/fmicb.2013.00394

Bright, M., and Bulgheresi, S. (2010). A complex journey: transmission of microbial symbionts. *Nat. Rev. Microbiol.* 8, 218–230.

Büdel, B., and Scheidegger, C. (2008). "Thallus morphology and anatomy", in *Lichen Biology*, ed. T. H. Nash (Cambridge, UK: Cambridge University Press), 40–68.

Burke, C., Steinberg, P., Rusch, D., Kjelleberg, S., and Thomas, T. (2011). Bacterial community assembly based on functional genes rather than species. *PNAS*. 108, 14288–14293

Cardinale, M., Grube, M., Castro, J. V., Müller, H., and Berg, G. (2012a). Bacterial taxa associated with the lung lichen *Lobaria pulmonaria* are differentially shaped by geography and habitat. *FEMS Microbiol. Lett.* 329, 111–115.

Cardinale, M., Puglia, A. M., and Grube, M. (2006). Molecular analysis of lichen-associated bacterial communities. *FEMS Microbiol. Ecol.* 57, 484–495.

Cardinale, M., Steinová, J., Rabensteiner, J., Berg, G., and Grube, M. (2012b). Age, sun and substrate: triggers of bacterial communities in lichens. *Environ. Microbiol. Rep.* 4, 23–28.

Cardinale, M., Vieira de Castro, J., Müller, H., Berg, G., and Grube, M. (2008). *In situ* analysis of the bacterial community associated with the reindeer lichen *Cladonia arbuscula* reveals predominance of Alphaproteobacteria. *FEMS Microbiol. Ecol.* 66, 63–71.

Cernava, T. (2015c). *Exploring the substantial contributions and the global interactions of the microbiome in an ancient symbiosis* (Doctoral thesis). Graz University of Technology. p. 15-16.

Cernava, T., Aschenbrenner, I. A., Grube, M., Liebminger, S., and Berg, G. (2015b). A novel assay for the detection of bioactive volatiles evaluated by screening of lichen-associated bacteria. *Front. Microbiol.* 6:398. doi: 10.3389/fmicb.2015.00398

Cernava, T., Müller, H., Aschenbrenner, I. A., Grube, M., and Berg, G. (2015a). Analyzing the antagonistic potential of the lichen microbiome against pathogens by bridging metagenomic with culture studies. *Front. Microbiol.* 6:620. doi: 10.3389/fmicb.2015.00620

Davenport, C. F., and Tümmler, B. (2013). Advances in computational analysis of metagenome sequences. *Environ. Microbiol.* 15, 1–5.

De Bary, A. (1879). *Die Erscheinung der Symbiose*. Strasburg.

Denton, G. H., and Karlén, W. (1973). Lichenometry: its application to Holocene moraine studies in southern Alaska and Swedish Lapland. *Arctic Alpine Res.* 347–372.

Douglas, A. E. (1998). Nutritional interactions in insect-microbial symbioses: aphids and their symbiotic bacteria *Buchnera*. *Annu. Rev. Entomol.* 43, 17–37.

Elix, J. A. and Stocker-Wörgötter, E. (2008). "Biochemistry and secondary metabolites", in *Lichen Biology*, ed. T. H. Nash (Cambridge, UK: Cambridge University Press), 104–133.

Eloe-Fadrosh, E. A., and Rasko, D. A. (2013). The human microbiome: from symbiosis to pathogenesis. *Annu. Rev. Med.* 64, 145.

Erlacher, A., Cernava, T., Cardinale, M., Soh, J., Sensen, C. W., Grube, M., et al. (2015). *Rhizobiales* as functional and endosymbiontic members in the lichen symbiosis of *Lobaria pulmonaria* L. *Front. Microbiol.* 6:53. doi: 10.3389/fmicb.2015.00053.

Feldhaar, H., and Gross, R. (2009). Insects as hosts for mutualistic bacteria. *Int. J. Med. Microbiol.* 299, 1–8.

Frey-Klett, P., Burlinson, P., Deveau, A., Barret, M., Tarkka, M., and Sarniguet, A. (2011). Bacterial-fungal interactions: hyphens between agricultural, clinical, environmental, and food microbiologists. *Microbiol. Mol. Biol. Rev.* 75, 583–609.

Fukami, T. (2010). "Community assembly dynamics in space", in *Community ecology: processes, models and applications*, ed. H. A. Verhoef, P. J. Morin (Oxford, United Kingdom, Oxford University Press), 45–53.

Funkhouser, L. J., and Bordenstein, S. R. (2013). Mom Knows Best: The Universality of Maternal Microbial Transmission. *PLoS Biol.* 11, doi: 10.1371/journal.pbio.1001631

González, I., Ayuso-Sacido, A., Anderson, A., and Genilloud, O. (2005). *Actinomycetes* isolated from lichens: evaluation of their diversity and detection of biosynthetic gene sequences. *FEMS Microbiol. Ecol.* 54, 401–415.

Gonzalez, J. M., Portillo, M. C., Belda-Ferre, P., and Mira, A. (2012). Amplification by PCR artificially reduces the proportion of the rare biosphere in microbial communities. *PLoS One* 7, doi: 10.1371/journal.pone.0029973.

Grube, M., and Berg, G. (2009a). Microbial consortia of bacteria and fungi with focus on the lichen symbiosis. *Fungal Biol.Rev.* 23, 72–85.

Grube, M., Cardinale, M., de Castro, J. V., Müller, H., and Berg, G. (2009b). Species-specific structural and functional diversity of bacterial communities in lichen symbioses. *ISME J.* 3, 1105–1115.

Grube, M., Cernava, T., Soh, J., Fuchs, S., Aschenbrenner, I., Lassek, C., et al. (2015). Exploring functional contexts of symbiotic sustain within lichen-associated bacteria by comparative omics. *ISME J.* 9, 412–424.

Grube, M., Köberl, M., Lackner, S., Berg, C., and Berg, G. (2012). Host-parasite interaction and microbiome response: Effects of fungal infections on the bacterial community of the Alpine lichen *Solorina crocea*. *FEMS Microbiol. Ecol.* 82, 472–481.

Henkel, P. A, Yuzhakova, L. A. (1936). Nitrogen-fixing bacteria in lichens. *Izv Biol Inst Permsk Gos Univ* 10*:* 9–10.

Henkel, P. A., and Plotnikova, T. T. (1973). Nitrogen-fixing bacteria in lichens. *Izv Akad Nauk SSR Ser Biol* 807–813

Hodkinson, B. P., and Lutzoni, F. (2009). A microbiotic survey of lichen-associated bacteria reveals a new lineage from the *Rhizobiales*. *Symbiosis* 49, 163–180.

Hodkinson, B. P., Gottel, N. R., Schadt, C. W., and Lutzoni, F. (2012). Photoautotrophic symbiont and geography are major factors affecting highly structured and diverse bacterial communities in the lichen microbiome. *Environ. Microbiol.* 4, 147–61.

Honegger, R. (1991). Functional aspects of the lichen symbiosis. *Annu. Rev. Plant Biol.* 42, 553–578.

Honegger, R., Edwards, D., and Axe, L. (2013). The earliest records of internally stratified cyanobacterial and algal lichens from the Lower Devonian of the Welsh Borderland. *New Phytol.* 197, 264–275.

Iskina, R.Y. (1938). On nitrogen fixing bacteria in lichens. *Bulletin of the Perm (Molotov) Biological Research Institute* 11, 113–139.

Klappenbach, J. A., Dunbar, J. M., & Schmidt, T. M. (2000). rRNA operon copy number reflects ecological strategies of bacteria. *Appl. Environ. Microbiol.* 66, 1328–1333.

Klindworth, A., Pruesse, E., Schweer, T., Peplies, J., Quast, C., Horn, M., et al. (2013). Evaluation of general 16S ribosomal RNA gene PCR primers for classical and next-generation sequencing-based diversity studies. *Nucleic Acids Res.* 41, doi: 10.1093/nar/gks808

Kosanić M., and Ranković B. (2015). "Lichen secondary metabolites as potential antibiotic agents", in *Lichen secondary metabolites,* ed. B. Ranković (Springer, Berlin), 81–104.

Lawrey, J. D., and Diederich, P. (2003). Lichenicolous Fungi : Interactions , Evolution , and Biodiversity. *Bryologist* 106, 80–120.

Lee, Y. M., Kim, E. H., Lee, H. K., and Hong, S. G. (2014). Biodiversity and physiological characteristics of Antarctic and Arctic lichens-associated bacteria. *World J. Microbiol. Biotechnol.* 30, 2711–2721.

Lenova, L. I., and Blum, O. (1983). To the question on the third component of lichens. *Bot J*, 68, 21–28.

Li, C. W., Chen, J. Y., and Hua, T. E. (1998). Precambrian sponges with cellular structures. *Science* 279, 879–882.

Liba, C. M., Ferrara, F. I. S., Manfio, G. P., Fantinatti-Garboggini, F., Albuquerque, R. C., Pavan, C., et al. (2006). Nitrogen-fixing chemo-organotrophic bacteria isolated from cyanobacteria-deprived lichens and their ability to solubilize phosphate and to release amino acids and phytohormones. *J. Appl. Microbiol.* 101, 1076–1086.

Liu, W. T., Marsh, T. L., Cheng, H., and Forney, L. J. (1997). Characterization of microbial diversity by determining terminal restriction fragment length polymorphisms of genes encoding 16S rRNA. *Appl. Environ. Microbiol.* 63, 4516–4522.

Locey, K. J. (2010). Synthesizing traditional biogeography with microbial ecology: the importance of dormancy. *J. Biogeogr*. 37, 1835–1841.

Margulies, M., Egholm, M., Altman, W. E., Attiya, S., Bader, J. S., Bemben, L. A., et al. (2005). Genome sequencing in microfabricated high-density picolitre reactors. *Nature* 437, 376–380.

Marzorati, M., Wittebolle, L., Boon, N., Daffonchio, D., and Verstraete, W. (2008). How to get more out of molecular fingerprints: practical tools for microbial ecology. *Environ. Microbiol.* 10, 1571–1581.

McFall-Ngai, M., Hadfield, M. G., Bosch, T. C., Carey, H. V., Domazet-Lošo, T., Douglas, A. E., et al. (2013). Animals in a bacterial world, a new imperative for the life sciences. *PNAS.* 110, 3229–3236.

Mushegian, A. A, Peterson, C. N., Baker, C. C. M., & Pringle, A. (2011). Bacterial diversity across individual lichens. *Appl. Environ. Microbiol.* 77, 4249–52.

Muyzer, G., and Smalla, K. (1998). Application of denaturing gradient gel electrophoresis (DGGE) and temperature gradient gel electrophoresis (TGGE) in microbial ecology. A*ntonie van Leeuwenhoek*, 73, 127–141.

Nash, T.H. III. (2008, ed.). *Lichen Biology*. Cambridge, UK: Cambridge University Press, pp 1–8.

Panosyan, A. K., and Nikogosyan, V. G. (1966). The presence of *Azotobacter* in lichens. *Akad Nauk Armian SSR, Biol Zhurn Armen*, 19, 3–11.

Pinto, A. J., and Raskin, L. (2012). PCR biases distort bacterial and archaeal community structure in pyrosequencing datasets. *PloS one* 7, doi: 10.1371/journal.pone.0043093

Prado, S. S., Zucchi, T. D. (2012). Host-symbiont interactions for potentially managing heteropteran pests. *Psyche*

Printzen, C., Fernández-Mendoza, F., Muggia, L., Berg, G., and Grube, M. (2012). Alphaproteobacterial communities in geographically distant populations of the lichen *Cetraria aculeata*. *FEMS Microbiol. Ecol.* 82, 316–25.

Rappé, M. S., and Giovannoni, S. J. (2003). The uncultured microbial majority. *Annu. Rev. Microbiol.* 57, 369–394.

Remy, W., Taylor, T. N., Hass H., and Kerp, H. (1994). Four hundred-million-year-oldvesicular arbuscular mycorrhizae. *PNAS* 91, 11841–11843.

Sacchi, L., Grigolo, A., Mazzini, M., Bigliardi, E., Baccetti, B., and Laudani, U. (1988). Symbionts in the oocytes of *Blattella germanica* (L.)(Dictyoptera: Blattellidae): their mode of transmission. *Int. J. Insect Morphol.* 7, 437–446.

Saleem, M. (2015). "Microbiome Ecosystem Ecology: Unseen Majority in an Anthropogenic Ecosystem", in *Microbiome Community Ecology*, ed. M. Saleem (Springer International Publishing), 1-11.

Sapp J 2010. On the Origin of Symbiosis. In Seckbach J & Grube M (eds) Symbioses and Stress. Springer, Dordrecht. pp. 5-18.

Scheidegger, C., and Werth, S. (2009). Conservation strategies for lichens: insights from population biology. *Fungal Biol. Rev.* 23, 55–66.

Schneider, T., Schmid, E., de Castro, J. V, Cardinale, M., Eberl, L., Grube, M., et al. (2011). Structure and function of the symbiosis partners of the lung lichen (*Lobaria pulmonaria* L. Hoffm.) analyzed by metaproteomics. *Proteomics* 11, 2752–2756.

Schwieger, F., and Tebbe, C. C. (1998). A new approach to utilize PCR–single-strand-conformation polymorphism for 16S rRNA gene-based microbial community analysis. *Appl. Environ. Microbiol.* 64, 4870–4876.

Selbmann, L., Zucconi, L., Ruisi, S., Grube, M., Cardinale, M., and Onofri, S. (2009). Culturable bacteria associated with Antarctic lichens: affiliation and psychrotolerance. *Polar Biol.* 33, 71–83.

Shade, A., Mcmanus, P. S., and Handelsman, J. (2013). Unexpected Diversity during Community Succession in the Apple. *mBio* 4, doi: 10.1128/mBio.00602-12

Smalla, K., Oros-Sichler, M., Milling, A., Heuer, H., Baumgarte, S., Becker, R., et al. (2007). Bacterial diversity of soils assessed by DGGE, T-RFLP and SSCP fingerprints of PCR-amplified 16S rRNA gene fragments: do the different methods provide similar results? *J Microbiol. Meth.* 69, 470–479.

Turnbaugh, P. J., and Gordon, J. I. (2008). An invitation to the marriage of metagenomics and metabolomics. *Cell* 134, 708–13.

Uphof**,** J. C. 1925. Purple bacteria as symbionts of a lichen. Science 61**:**67.

van Overbeek, L. S., Franke, A. C., Nijhuis, E. H., Groeneveld, R. M., da Rocha, U. N., and Lotz, L. A. (2011). Bacterial communities associated with Chenopodium album and Stellaria media seeds from arable soils. *Microb. Ecol.* 62, 257–264.

Wilkinson, C. R. (1984). Immunological evidence for the Precambrian origin of bacterial symbioses in marine sponges. *Proc. R. Soc. Lond. [Biol]*. 220, 509–518.

PUBLICATION I

Environmental Microbiology (2014) **16**, 3743–3752

Microbial cargo: Do bacteria on symbiotic propagules reinforce the microbiome of lichens?

Ines Aline Aschenbrenner,[1,2] Massimiliano Cardinale,[1,2] Gabriele Berg,[1] and Martin Grube[2]

[1]Institute of Environmental Biotechnology
Graz University of Technology, Austria

[2]Institute of Plant Sciences
University of Graz, Austria

environmental microbiology

Environmental Microbiology (2014) **16**(12), 3743–3752 doi:10.1111/1462-2920.12658

Microbial cargo: do bacteria on symbiotic propagules reinforce the microbiome of lichens?

Ines Aline Aschenbrenner,[1,2] Massimiliano Cardinale,[1,2] Gabriele Berg[1] and Martin Grube[2]*

[1] *Institute of Environmental Biotechnology, Graz University of Technology, Petersgasse 12, 8010 Graz, Austria.*

[2] *Institute of Plant Sciences, University of Graz, Holteigasse 6, 8010 Graz, Austria.*

Summary

According to recent research, bacteria contribute as recurrent associates to the lichen symbiosis. Yet, the variation of the microbiomes within species and across geographically separated populations remained largely elusive. As a quite common dispersal mode, lichens evolved vertical transmission of both fungal and algal partners in specifically designed mitotic propagules. Bacteria, if co-transmitted with these symbiotic propagules, could contribute to a geographical structure of lichen-associated microbiomes.

The lung lichen was sampled from three localities in eastern Austria to analyse their associated bacterial communities by bar-coded pyrosequencing, network analysis and fluorescence in situ hybridization. For the first time, bacteria were documented to colonize symbiotic propagules of lichens developed for short-distance transmission of the symbionts. The propagules share the overall bacterial community structure with the thalli at class level, except for filamentous *Cyanobacteria* (*Nostocophycideae*), and with *Alphaproteobacteria* as predominant group. All three sampling sites share a core fraction of the microbiome. Bacterial communities of lichen thalli from the same sampling site showed higher similarity than those of distant populations. This variation and the potential co-dispersal of a microbiome fraction with structures of the host organism contribute new aspects to the 'everything is everywhere' hypothesis.

Received 14 April, 2014; revised 30 September, 2014; accepted 1 October, 2014. *For correspondence. E-mail martin.grube @uni-graz.at; Tel. (+43) 316 380 5655; Fax (+43) 316 380 9880.

Introduction

Lichens are known as ecologically diversified symbioses that colonize almost all climate zones and occur on a wide range of substrates (Nash, 2008). In the symbiotic stage, the microscopic fungi (mycobionts) produce macroscopic thalli of characteristic appearance. They provide a long-living habitat for the photoautotrophic partners (alga and/or cyanobacterium), which are sheltered between peripheral fungal layers (Honegger, 2012). Despite a general ubiquity of lichens, individual species of lichen-forming fungi may be highly specialized for their ecological niches. One prominent example for ecological specialization is the lung lichen, a conspicuous foliose species adapted to old-growth forests and highly sensitive to air pollution (Scheidegger, 1995; Scheidegger and Werth, 2009). This species is among the most intensely studied lichens because of its importance as indicator species (Rose, 1992). Detailed studies have assessed chemical, ecological and ecophysiological aspects in lung lichens (e.g. McEvoy *et al*., 2007; Bidussi *et al*., 2013), as well as in population genetics, phylogeography and reproductive biology (e.g., Jüriado *et al*., 2011; Widmer *et al*., 2012). The lung lichen represents a tripartite lichen as it hosts additionally to the mycobiont (*Lobaria pulmonaria*) two distinct photobionts internally. The green-algae *Dictyochloropsis reticulata* is found beneath more than 90% of the lichen surface and strains of cyanobacterium *Nostoc* are locally restricted to gall-like colonies, in so-called internal cephalodia (Myllys *et al*., 2007). These *Nostoc* strains are generally captured from the surface to become gradually integrated into the lichen thallus, where they primarily contribute to the symbiotic system by nitrogen fixation (Jordan, 1970; Cornejo and Scheidegger, 2013).

Although the lung lichen is among the fastest growing lichens, it is only fertile under rare optimal habitat conditions. Apothecia are usually only found on older and sometimes even senescing thallus lobes. On the other hand, mitotic propagules for simultaneous dispersal of both symbionts (fungus and alga), a common propagation strategy of many lichens, are almost generally present in this species. Their function as dispersal units has also been shown experimentally (Scheidegger, 1995), and a recent microsatellite analysis revealed co-dispersal of

both symbionts as one of the key factors shaping the genetic structure of this species (Werth and Scheidegger, 2012). The symbiotic propagules of the lung lichen can be called isidioid soredia, which are developed at margins and ridges of the upper thallus surfaces as dust-like particles comprising a few algal and fungal cells, as typical for soredia structures. Before the propagules detach, they normally develop a peripheral cortex to resemble isidia (stratified propagules). These symbiotic propagules of the lung lichen are much larger and heavier than the sexual fungal spores of this species. Therefore, the propagules appear to be less suitable for long-distance dispersal, compared with the much smaller meiotically produced fungal ascospores. Previous work underlined that symbiotic dispersal with isidioid soredia is rather local in this species (Walser, 2004). More recently, Dal Grande and colleagues (2012) provided a quantitative assessment of both propagation strategies and showed that vertical transmission decreases significantly within short distance (approximately cut in half over distances of 10 m).

Long-living lichen thalli provide various niches for associated microorganisms, of which colonizing fungi have been well studied (Lawrey and Diederich, 2003; Werth *et al*., 2013). Even though earlier culture-dependent search for microorganisms revealed the presence of lichen-associated bacteria (Grube and Berg, 2009), the molecular characterization has only just started in the last few years. According to fluorescence in situ hybridization and confocal laser scanning microscopy (FISH-CLSM), bacteria colonize lichens in a biofilm-like manner (Cardinale *et al*., 2008). The composition of these communities is host specific (Grube *et al*., 2009; Bates *et al*., 2011), with *Alphaproteobacteria* as the prominent bacterial class on many lichens (e.g. Grube *et al*., 2009; Schneider *et al*., 2011). Other lineages may also be detected at considerable relative abundances, including *Acidobacteria*, *Actinobacteria*, *Betaproteobacteria*, *Spartobacteria* and *Sphingobacteria*, among others (Bjelland *et al*., 2010; Mushegian *et al*., 2011; Grube *et al*., 2012; Hodkinson *et al*., 2012). These surface-colonizing bacteria of lichens are supposed to play a beneficial role for lichens by contributing to the lichen metabolism with release of nitrogen compounds like amino acids, vitamins and phytohormones, or by solubilization of phosphate (Liba *et al*., 2006; Grube *et al*., 2009; 2014; Schneider *et al*., 2011).

Despite new insights into the structure and function of lichen-associated bacteria, little is known so far about the intraspecific variation of microbiome composition, and also, how lichens acquire their specific bacterial communities. In the present study, we set out to study whether symbiotic propagules of lichens could contribute to a co-dispersal of lichen-associated bacteria. Multiple symbiont dispersal has not been addressed before. We assume that this process could reinforce the composition of the lichen-associated microbiome and contribute to its geographical structure. We studied this possibility by microcopy to assess bacterial colonization on the propagules and by analyses of pyrosequencing data and community fingerprinting patterns.

Results

First insights into the bacterial communities on the lichen thalli and symbiotic propagules

Single strand conformation analysis (SSCP) of 16S rRNA gene fragments obtained from three sampling sites (Tamischbachgraben, St. Oswald/Eibiswald, Johnsbach in Styria, Austria) revealed generally high numbers of bands (> 20) in samples of both thalli and vegetative propagules (isidioid soredia). The entire thalli were characterized by several additional strong bands, which were not present in the samples of the symbiotic propagules (Fig. S2).

Microbial community composition of lichen thalli and symbiotic propagules

A comparison of the lichen-associated bacterial community compositions on both thallus and isidioid soredia by amplicon sequencing showed that the lichen propagules shared most of the dominant taxa (at class level) with entire thalli except for the filamentous *Nostocophycideae* (*Cyanobacteria*), which were only present on thalli (Fig. 1A). *Alphaproteobacteria* were the predominant taxon on both lichen parts [on average: soredia 33%, standard deviation (SD) 6.7%; thalli 26%, SD 4.7%] followed by *Sphingobacteria* (on average: soredia 23%, SD 8.9%; thalli 14%, SD 2.8%). The relative abundance of *Betaproteobacteria*, *Gammaproteobacteria* and *Deltaproteobacteria* as well as *Actinobacteria* on thalli was at least twofold higher compared with that on the propagules, and in contrast, the relative abundance of *Spartobacteria* was twofold higher on the propagules than on thalli (Fig. 1A). The lichen-associated communities on thalli and symbiotic propagules were high in alpha diversity and richness indices (Table S1).

More than 89% of all sequences were shared by both thalli and propagules and represented 28% of all observed operational taxonomic units (OTUs) within this data set (Fig. S3A). Only 9% of the sequences were unique for the thalli and 2% for the propagules. The majority of the OTUs (49%) occurred exclusively on lichen thalli; about 23% were unique on propagules. The distribution of the OTUs between isidioid soredia and thalli was visualized in a Venn diagram (Fig. S3B).

The predominant class within this shared microbiome was *Deltaproteobacteria* (17%; Fig. S4). The most abun-

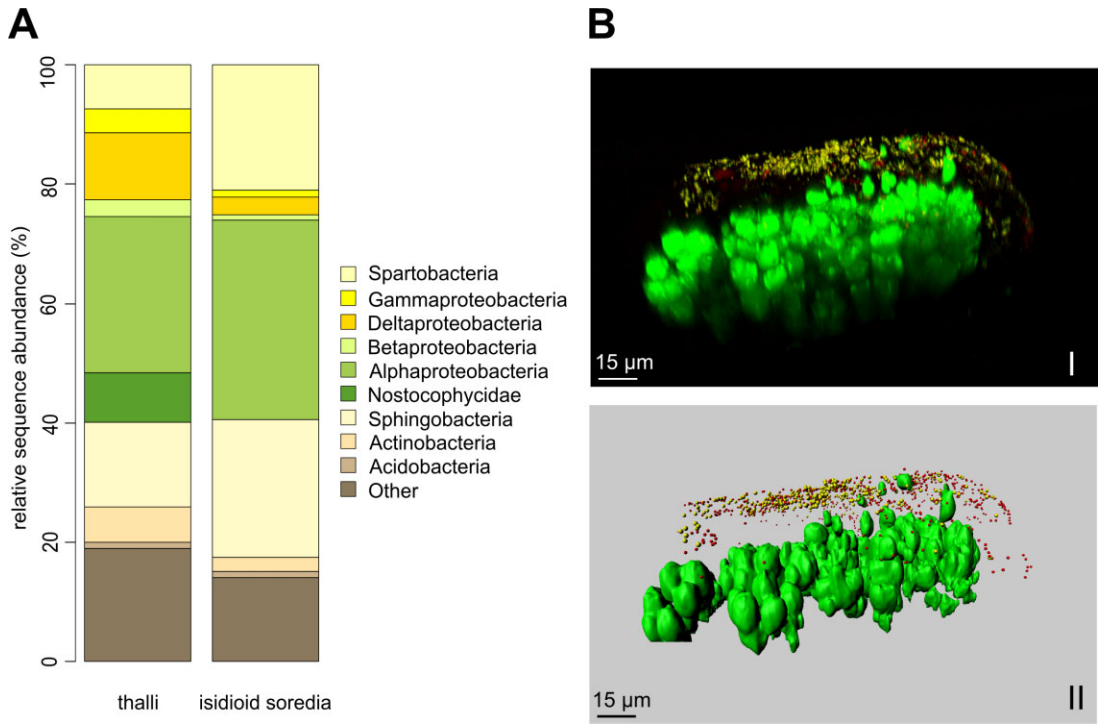

Fig. 1. A. Comparison of microbial community composition of lichen thalli and isidioid soredia at class level sampled in Johnsbach. Besides *Alphaproteobacteria*, thalli were mainly colonized by *Sphingoproteobacteria* and *Deltaproteobacteria* and soredia by *Sphingobacteria* and *Spartobacteria*. *Nostocophycideae* were only present on thalli, but missing on lichen propagules. Taxa representing less than 1% of relative abundance were summarized in the category 'Other'. B. Bacterial colonization on isidioid soredia of *Lobaria pulmonaria* with *Alphaproteobacteria* as dominant group. Volume rendering (I) and 3D reconstruction (II) of confocal stacks were created with IMARIS 7.0; green, algae; yellow, *Alphaproteobacteria*; red, other *Eubacteria* (*Tamischbachgraben*).

dant family within *Deltaproteobacteria* was *Cystobacterineae* (42%), which belongs to the order *Myxococcales*. *Alphaproteobacteria* were only reaching 11%. Other dominant classes were *Sphingobacteria* (14%), *Actinobacteria* (14%), *Phycisphaerae* (9%), *Spartobacteria* (4%) and *Acidobacteria* (2%). The beta diversity of the microbial communities of lichen thalli and propagules showed also a difference between those lichen parts (Anosim; $P < 0.022$; Fig. S5A), and one of the propagule samples was clearly separated from the others of that kind but had closer similarity with the thallus samples.

Colonization patterns of bacterial communities on propagules

The predominance of *Alphaproteobacteria* on lichen propagules was confirmed by FISH-CLSM experiments (Fig. 1B). By using taxon-specific probes for *Alphaproteobacteria* in combination with universal probes for eubacteria, we could show that bacteria form a cover of evenly distributed *Alphaproteobacteria*, intermingled by other eubacteria. The three-dimensional (3D) reconstruction (Fig. 1B-II) of the volume rendered confocal stack (Fig. 1B-I) showed that bacteria colonize the surfaces of the propagules, whereas no bacterial signals were detected in the internal parts of the isidioid soredia.

Sphingomonadaceae was the most dominant family of *Alphaproteobacteria* on symbiotic propagules, comprising more than 65% of alphaproteobacterial reads (Fig. S6). Besides alphaproteobacterial sequences, which could not be assigned to a family (denoted as 'other'), the remaining 8% of the sequences represented diverse families, including *Acetobacteraceae*, *Caulobacteraceae*, *Methylobacteriaceae*, *Bradyrhizobiaceae*, *Rhizobiaceae*, *Rickettsiaceae*, *Hyphomicrobiaceae*, *Hyphomonadaceae*, *Rhodospirillaceae* and *Aurantimonadaceae*.

Composition and diversity of microbial communities within sampling sites

At phylum level, the only difference in composition and relative abundance within all three sampling sites was found for *Actinobacteria* and *Deltaproteobacteria*. *Actinobacteria* showed a threefold higher relative abundance at one site (St. Oswald/Eibiswald), whereas *Deltaproteobacteria* was two times more abundant at another site (Johnsbach; Fig. 2A). The microbial

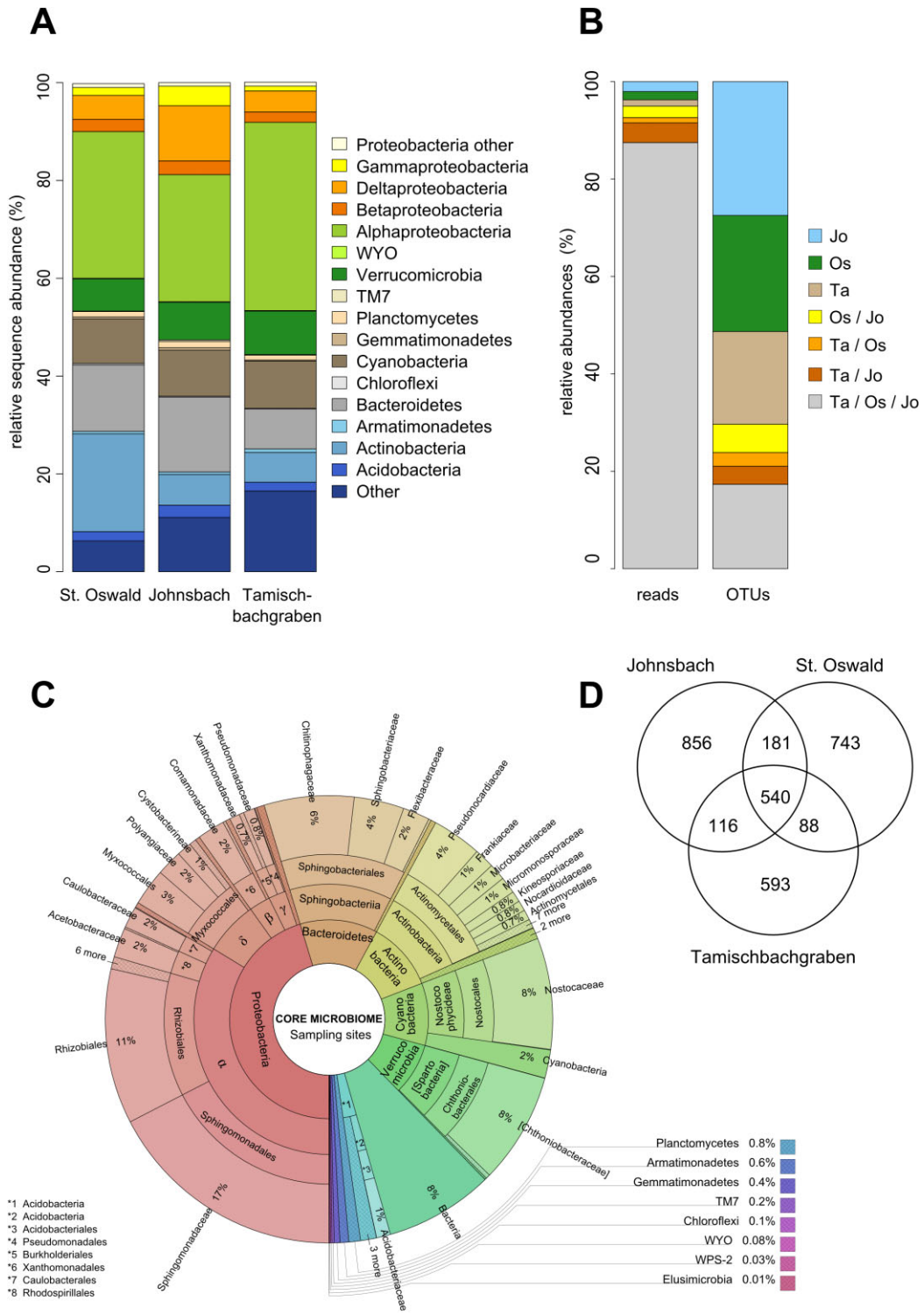

Fig. 2. A. Composition of bacterial communities among the three sampling sites at phylum level. *Proteobacteria* were subdivided to class level in *Alphaproteobacteria*, *Betaproteobacteria*, *Gammaproteobacteria* and *Deltaproteobacteria*. *Alphaproteobacteria* was the predominant group followed by *Sphingobacteria* (*Bacteroidetes*) and *Actinobacteria* (*Actinobacteria*). B. Distribution of the relative abundances of either sequence reads or OTUs across sampling sites. Jo, Johnsbach; Os, St. Oswald/Eibiswald; Ta, Tamischbachgraben. C. Composition of the core microbial community among the three sampling sites at phylum, class, order and family level (starting at the inner circle). *Alphaproteobacteria* (34%) was the predominant class followed by *Sphingobacteria* (12%) and *Actinobacteria* (10%). D. Distribution of the microbial communities (3117 observed OTUs) of the lichen thalli within the three locations. Samples of each location were pooled. All locations shared a core microbiome, which represented about 87% of all sequences, but only 16% of all observed OTUs.

community composition of all 15 thallus samples included seven dominant phyla (Fig. 2A shows the taxa summaries for each location; the following data are given as minimum and maximum sequence abundances across the locations): *Proteobacteria* (39.8–44.9%), *Bacteroidetes* (8.2–15.3%), *Actinobacteria* (6.1–20.0%), *Cyanobacteria* (9.1–9.7%), *Verrucomicrobia* (6.6–8.9%), *Acidobacteria* (1.8–2.5%) and *Planctomycetes* (1.0–1.3%), whereas the remaining 6.3–16.5% of the reads could not be assigned to any bacterial phylum (denoted as 'other'). Within the predominant phylum *Proteobacteria*, 58–83% of the sequences were assigned to *Alphaproteobacteria*, followed by *Deltaproteobacteria*, *Betaproteobacteria* and *Gammaproteobacteria*. A comparison of microbial community composition on lichen thalli shown by principal coordinate analysis (PCoA) revealed clear differences among the three sampling sites (Anosim; $P < 0.001$; Fig. S5B).

Alphaproteobacterial families, which were found at all localities, are *Caulobacteraceae*, *Aurantimonadaceae*, *Rhizobiaceae*, *Acetobacteraceae*, *Rhodospirillaceae*, *Bradyrhizobiaceae*, *Hyphomicrobiaceae*, *Methylobacteriaceae*, *Methylocystaceae* and *Sphingomonadaceae*. The latter family represented the most dominant group, reaching up to 43–57% of all *Alphaproteobacteria*. Families only occurring on thalli from St. Oswald/Eibiswald and Tamischbachgraben are *Beijerinckiaceae*, *Phyllobacteriaceae* and *Xanthobacteraceae*, whereas *Rickettsiaceae* was only found in the two northern sampling sites (Johnsbach and Tamischbachgraben; Table S2).

Core microbiome across lung lichen populations

Network analysis of the microbial communities among the three localities revealed that 87% of all sequence reads are shared across sites (Fig. 2B). However, these represent only 16% of the total 3117 observed OTUs. Each sampling site also has unique OTUs as well as OTUs shared only among two sampling sites (see Fig. 2D; samples for each location were pooled). The dominant classes within this core microbiome were *Alphaproteobacteria* (34%), *Sphingobacteria* (12%), *Actinobacteria* (10%), *Nostocophycideae* (8%), *Spartobacteria* (8%) and *Deltaproteobacteria* (6%; Fig. 2C). On the other hand, less abundant phyla like *Chlorobia*, *Deinococcales*, *Firmicutes* and *Chlamydiales* were not present in the shared microbiome.

Discussion

Here, we present first indication that local dispersal via symbiotic propagules also includes a part of the bacterial communities associated with the lung lichen. Rather than depending on a de novo recruitment of bacteria on the developing lichen structure, a 'starter' community is packaged with the vegetative propagules of this lichen. It is likely that such mode of microbiome transfer is not exclusive in this lichen, but rather, a widespread phenomenon associated with vegetative dispersal. This example for community dispersal also raises interesting new questions about the dispersal of bacteria and microbial biogeography, e.g. to what extent do propagated communities generally influence the subsequent recruitment and succession in bacterial communities?

Symbiotic propagules

Using the lung lichen, we demonstrated – for the first time – the bacterial colonization on symbiotic propagules. An initial overview of bacterial diversity using microbial fingerprints already indicated a high number of bacterial strains associated with the lung lichen, and variation among the samples. While FISH-CLS found bacterial colonization to be localized on the surface, insight in the taxonomic composition of this bacterial niche was then achieved by amplicon library sequencing. Symbiotic propagules largely shared the general taxonomic composition of the microbiome with the lichen thalli at class level. However, the PCoA plot of thalli and symbiotic propagules suggested a shift in the community composition mostly at the species level of bacteria. The difference may result from the morphological and positional constraints of the symbiotic propagules. While the total thallus with its age structure and its upper and lower surface (i.e. fungal formed cortex) enables the formation of specific bacterial communities, symbiotic propagules are young and comprise only an upper cortex at maturity. The upper surface of the thalli could preferentially enrich desiccation-tolerant bacterial taxa originating from the rain, wind or small animals (e.g. insects, snails); the shaded lower surface offers different ecological conditions for enrichment. The symbiotic propagules are produced on the upper surface of the lichen thalli and might therefore lack bacterial taxa that might be more common on the lower surface of the thalli.

Distant lung lichen populations share a core microbiome

The overall compositional pattern of bacterial phyla across the locations in our study was fairly similar and reflected an overall ecological resemblance of the lichen habitats. A limited number of highly abundant bacterial OTUs were shared by all sampling sites (16% of all OTUs, ~ 87% of all sequences). The geographical range of the sampling sites represents a small fraction of the global lung lichen distribution. We therefore consider it as a regional core microbiome. The majority of the bacterial

OTUs (70% of all observed OTUs), however, only referred to 5% of all sequences and was specific for each sampling site. It remains unresolved (also because of the unfeasibility to evenly cover all microniches in forests) whether these unique species are adaptations to the specific environmental conditions at each sampling site or if they might be more common in these forest sites.

These results also address the recurrent question about the presence of 'core' microbiomes in host-associated bacterial communities (Shade and Handelsman, 2012). Assessing the 'global' core microbiome of lichens would require a thorough sampling across the entire geographic range. This was beyond the scope of this study and will remain challenging because of the remoteness of appropriate sites colonized by the worldwide-distributed lung lichen. However, our results suggest a differentiation of the lichen thallus microbiomes by distance. A first hint of geographic pattern in lichen-associated *Alphaproteobacteria* was indicated already in Cardinale and colleagues (2012). The only other analysis of geographic structure in a different lichen species, *Cetraria aculeata*, was presented by Printzen and colleagues (2012), which propagates asexually by fragments of the thalli (while sexual fruiting bodies are rare). In this species, alphaproteobacterial communities of high latitudes are depauperate and more closely related to each other than to those of extrapolar habitats. This pattern also agreed with findings for their fungal and algal symbionts (Fernández Mendoza *et al*., 2011).

Lichen-associated microbiomes in comparison

The predominance of *Alphaproteobacteria* agrees well not only with the results obtained from other foliose lichens with a green photobiont (e.g., *Parmelia sulcata, Rhizoplaca chrysoleuca*, *Umbilicaria* sp. and *Flavocetraria*), but also in lichens with cyanobacterial photobionts (e.g., *Leptogium*, *Peltigera* and *Sticta*), as well as lichens with other growth forms beyond foliose lichens (Cardinale *et al*., 2008; Grube *et al*., 2009; Bates *et al*., 2011; Hodkinson *et al*., 2012). However, some lichens displayed altered patterns, e.g. the intertidal *Hydropunctaria maura* was dominated by *Actinobacteria* (Bjelland *et al*., 2010), whereas the acid-rock inhabitant *Ophioparma ventosum* was dominated by *Acidobacteria* (Hodkinson *et al*., 2012). *Rhizobiales* is usually the most abundant order of *Alphaproteobacteria*, followed by *Sphingomonadales* and *Rhodospirillales* (Bates *et al*., 2011; Hodkinson *et al*., 2012). However, in the case of the lung lichen, *Sphingomonadales* appeared to be the prominent order. Within alphaproteobacterial families, *Acetobacteraceae* (*Rhodospirillales*) appeared to be fairly dominant in lichens from acid rock and soil habitats (Cardinale *et al*., 2008; Bates *et al*., 2011), whereas *Sphingomonadaceae* were found to be more prominent in lichens with cyanobacterial photobionts (Hodkinson *et al*., 2012). However, this observation is not well supported by our present findings of high amounts of *Sphingomonadaceae* on the symbiotic propagules, which are generally devoid of the cyanobacterial photobiont. Based on our current sampling, we did not detect LAR1 (order *Rhizobiales*), which was characterized as a lichen-specific lineage of *Alphaproteobacteria* in other studies (Hodkinson and Lutzoni, 2009; Bates *et al*., 2011; Hodkinson *et al*., 2012). LAR1, which has not been taxonomically described up to now, seems to occur on several phylogenetically unrelated species of lichenized fungi. LAR1 was so far detected in lichens from North America and in a sequence library derived from Antarctic lichens (de la Torre *et al*., 2003), but not in our data set. Bacterial communities of the lung lichen differ among geographically distant sites, which leads to an interesting aspect in relation to the Baas-Becking hypothesis ('everything is everywhere, but the environment selects'). The biogeography of host-associated bacteria could at least partly be structured by the dispersal-capacities and -modes of the host organisms and may contribute to a phenomenon of microbiome 'dissimilarity by distance', which may also be found in other plant-alike systems hosting microbial communities.

A more detailed statistical analysis was used to survey to which extent the differences in community composition can be explained – by geographic factors and by the tissue origin (non-parametric analysis of variance and a redundancy analysis (RDA)-based variation partitioning; see Supporting information). Both pyrosequencing-based OTUs and community fingerprinting patterns suggested that approximately 60–70 % of variation is still unexplained by statistical analyses. This high number prevents a conclusive answer to the question whether the microbiome structure is reinforced exclusively by vertical transmission. Nonetheless, microscopic evidence clearly supports that a bacterial fraction is vertically inherited by lichen vegetative propagules. It might also be possible that bacterial communities undergo successional change by the development of thalli starting from germinating propagules (similar to Shade *et al*., 2013). Even the comparison of mature thalli did not reveal a strict dominance of particular bacterial species. Burke and colleagues (2011) argue that the colonization of ecological niches is based on a random selection of species with similar functions suitable for certain habitats and not following bacterial taxonomy. It will be a further informative step to analyse the correlation between the lichen host and its microbiome by large-scale metagenomic and metatranscriptomic approaches in the future.

Vertical transmission in other systems

Increasing evidence suggests a universal role of vertical transmission for structural stability of host-associated microbiomes. Vertical transmission is common in animals, ranging from invertebrates to humans (Funkhouser and Bordenstein, 2013), as well as in plants. A microbiome core fraction is transmitted from a moss sporophyte to the gametophyte (Bragina *et al*., 2013), an invasive plant shares endobacteria in grass rhizomes across generations (Rout *et al*., 2013) and the transmission of endophytic bacteria via seeds seems to be widespread (e.g. Ferreira *et al*., 2008, López-López *et al*., 2010). Comparing bacterial communities, vertical transmission was suggested also in invasive macroalgae (Aires *et al*., 2013). In fungi, vertical transmission of symbiotic bacteria has so far been found in mycorrhizal fungi (Bianciotto *et al*., 2004; Sharma *et al*., 2008), as well as in plant pathogens (Lackner *et al*., 2009). In the fungal kingdom, however, vertical transmission of entire communities is so far unique, because it requires particular morphological structures of propagules, here resulting from pre-established symbiotic interactions, to create the habitat for its own bacterial cargo.

Experimental procedures

Sampling strategy

Lichen thalli were collected at three sampling sites in Austria: Tamischbachgraben (Styria, N 47°38′22″ E 14°41′45″; 8 June 2012), Johnsbach (Styria, N 47°32′35″, E 14°37′38″; 5 October 2012) and St. Oswald/Eibiswald (Styria, N 46°44′50″, E 15°04′26″; 9 July 2012). The sampling sites in upper Styria (Johnsbach, Tamischbachgraben) have a linear distance of about 15 km (separated by a mountain range up to 2500 m of altitude), and both of them are in about 100 km of linear distance from St. Oswald/Eibiswald. The sites differed in bedrock type – siliceous at St. Oswald and calcareous at Tamischbachgraben and Johnsbach. The substrate was uniformly bark of maple trees (*Acer pseudoplatanus*), where the lichen thalli develop either on or adjacent to pleurocarpous mosses at heights of 1–2 m above the ground. At each sampling site, five lichen samples were collected from different *Acer pseudoplatanus* trees by using sterile tweezers. Each sample consisted of about five thallus replicates with symbiotic propagules (Fig. S1). Samples were stored separately in sterile polyethylene bags and cooled on dry ice until further processing, within 4 h after sampling.

Sample preparation and DNA extraction

Prior to DNA extraction, isidioid soredia were separated from lichen thalli under a binocular microscope by using a sterile razor blade and stored separately at −20°C until processing. About 1.5 g of thalli of each sample was homogenized with sterile pestle and mortar, resuspended in 0.85% NaCl-peptone solution and centrifuged in 2 ml of fractions at 13 000 r.p.m. for 20 min at 4°C. The pellets were stored at −20°C until processing. DNA of thalli and vegetative propagules was isolated with PowerSoil® DNA Isolation Kit (MoBio, Germany) and DNeasy Plant Mini Kit (Qiagen, Austria). DNA was purified using E.Z.N.A.® Cycle-Pure Kits, Omega Bio-tek (VWR). Extraction and purification was done according to the manufacturer's protocol.

Community fingerprinting using SSCP of 16S rRNA genes

SSCP of the lichen-associated microbiome was carried out as described by Schwieger and Tebbe (1998). For bacterial 16S rRNA amplification universal bacterial primers Com1/Com2^{P} (Schwieger and Tebbe, 1998) were used. Thermocycling was conducted in a G-STORM™ GS482 instrument (AlphaMetrix Biotech), starting with an initial denaturation for 3 min at 95°C. Each of the 35 cycles included 45 s at 95°C, 45 s at 55°C and 60 s at 72°C. The final extension step was done for 4 min at 72°C. The amplicons were separated using TGGE Maxi System (Biometra). Electrophoresis was carried out in an 8% Polyacrylamide gel at 26°C and 400 V. Silver-staining visualized band patterns.

FISH-CLSM

Symbiotic propagules (also called isidioid soredia) were fixed with 4% paraformaldehyde/phosphate-buffered saline (PBS) (v/v, 3:1) at 4°C for at least 4 h, followed by three washing steps with ice-cold 1x PBS. The samples were stored at −20°C in ethanol absolute/PBS (v/v, 1:1). The isidioid soredia were used for hybridization without cryosectioning in 1.5 ml tubes (following Cardinale *et al*., 2008). For detection of *Alphaproteobacteria*, the Cy5-labelled probe ALF968 (46°C, 45% formamide) and for eubacteria an equimolar mixture of the Cy3-labelled probes EUB338, EUB338II, EUB338III (46°C, 10% formamide) were used (Amann *et al*., 1990; Neef, 1997; Daims *et al*., 1999). Details on oligonucleotide probes are available at probeBase (Loy *et al*., 2007). Confocal laser scanning microscopy was carried out with a Leica TCS (Leica Microsystems). IMARIS 7.0 (Bitplane) was used for volume rendering and 3D reconstructions of the confocal stacks.

454-Pyrosequencing of 16S rRNA genes

The microbiome of *L. pulmonaria* was studied using a 454-pyrosequencing approach. From each sample (15 thallus and 5 isidiod soredia samples) 50 ng of bacterial template DNA was amplified with a universal bacterial primer set, 515F/806R (Caporaso *et al*., 2011), and the Taq&Go Ready-to-use PCR Mix (MP Biomedicals). From each template, a triplet of PCR amplicons was pooled and purified with E.Z.N.A.® Cycle-Pure Kits (Omega Bio-tek, VWR). High-throughput DNA sequencing was carried out by Macrogen Korea using 454 GS FLX Titanium platform. 16S rRNA gene sequences from the lichen microbiome were analysed using the open-source software package QIIME 1.6.0 (Quantitative Insights Into Microbial Ecology; Caporaso *et al*., 2010a,b). Raw 16S rRNA 454 reads were filtered by quality (minimal quality

score: 25) and length (≥ 250 nt; ≤ 550 nt), followed by a denoising step (denoise wrapper and denoiser script; Reeder and Knight, 2010) and trimming of the reverse primer. OTUs were clustered with UCLUST (Edgar, 2010) at a similarity of 97%, 95% and 90%, which correlates with the taxonomic levels of species, genus and family. Sequence alignment was done with PYNAST using the Greengenes core set as template sequences (DeSantis *et al*., 2006; Caporaso *et al*., 2010a,b). For chimera identification the method Chimera Slayer was used, and taxonomy was assigned with the Ribosomal Database Project (RDP) classifier (Wang *et al*., 2007; Haas *et al*., 2011). Mitochondrial and Chloroplast sequences were excluded as well as sequences assigned to the genus *Nostoc*, because it represents the second photobiont of the lung lichen, and therefore, these sequences were not evaluated as part of the microbiome. Singletons were not removed. Alpha rarefaction was analysed at 97%, 95% and 90% sequence similarity. Normalization of the data set to the same sequence count per sample was carried out before calculation of diversity indices and richness estimation. Based on jackknifed, unweighted UNIFRAC distance matrix the beta diversity was calculated and shown as PCoA plots created with QIIME (Lozupone and Knight, 2005). Determination of richness was done at family level (genetic distance: 10%). Alpha diversity was resolved using Shannon diversity index and Simpson diversity calculated at 3% genetic distance. Network analysis was performed with QIIME and visualized as Venn diagrams. Therefore, the five thallus/propagules samples of each sampling location were pooled. Pie charts were created with KRONA (Ondov *et al*., 2011). Statistical analysis was performed with the R packages VEGAN and APE (http://www.r-project.org/; see also Supporting information).

Acknowledgements

We are grateful to Tomislav Cernava (TU Graz) and Christian Westendorf (KFU Graz) for critical remarks on the manuscript, to Stefanie Maier (KFU Graz) for the valuable discussions about bioinformatic analyses and to Fernando Fernandez Mendoza (KFU Graz) for the statistical analysis. The authors declare that they have no conflict of interest. This research was supported by a grant of FWF to GB and MG (FWF-DACH I882).

References

Aires, T., Serrão, E.A., Kendrick, G., Duarte, C.M., and Arnaud-Haond, S. (2013) Invasion is a community affair: clandestine followers in the bacterial community associated to green algae, *Caulerpa racemosa*, track the invasion source. *PLoS ONE* **8:** e68429.

Amann, R.I., Binder, B.J., Olson, R.J., Chisholm, S.W., Devereux, R., and Stahl, D.A. (1990) Combination of 16S rRNA-targeted oligonucleotide probes with flow cytometry for analyzing mixed microbial populations. *Appl Environ Microbiol* **56:** 1919–1925.

Bates, S.T., Cropsey, G.W., Caporaso, J.G., Knight, R., and Fierer, N. (2011) Bacterial communities associated with the lichen symbiosis. *Appl Environ Microbiol* **77:** 1309–1314.

Bianciotto, V., Genre, A., Jargeat, P., Lumini, E., Bécard, G., and Bonfante, P. (2004) Vertical transmission of endobacteria in the arbuscular mycorrhizal fungus *Gigaspora margarita* through generation of vegetative spores. *Appl Environ Microbiol* **70:** 3600–3608.

Bidussi, M., Gauslaa, Y., and Solhaug, K.A. (2013) Prolonging the hydration and active metabolism from light periods into nights substantially enhances lichen growth. *Planta* **237:** 1359–1366.

Bjelland, T., Grube, M., Hoem, S., Jorgensen, S.L., Daae, F.L., Thorseth, I.H., and Øvreas, L. (2010) Microbial metacommunities in the lichen–rock habitat. *Environ Microbiol Rep* **3:** 434–443.

Bragina, A., Cardinale, M., Berg, C., and Berg, G. (2013) Vertical transmission explains the specific *Burkholderia* pattern in *Sphagnum* mosses at multi-geographic scale. *Front Microbiol* **4:** 394.

Burke, C., Steinberg, P., Rusch, D., Kjelleberg, S., and Thomas, T. (2011) Bacterial community assembly based on functional genes rather than species. *Proc Natl Acad Sci* **108:** 14288–14293.

Caporaso, J.G., Bittinger, K., Bushman, F.D., DeSantis, T.Z., Andersen, G.L., and Knight, R. (2010a) PyNAST: a flexible tool for aligning sequences to a template alignment. *Bioinformatics* **26:** 266–267.

Caporaso, J.G., Kuczynski, J., Stombaugh, J., Bittinger, K., Bushman, F.D., Costello, E.K., *et al*. (2010b) QIIME allows analysis of high-throughput community sequencing data. *Nat Methods* **7:** 335–336.

Caporaso, J.G., Lauber, C.L., Walters, W.A., Berg-Lyons, D., Lozupone, C.A., Turnbaugh, P.J., *et al*. (2011) Global patterns of 16S rRNA diversity at a depth of millions of sequences per sample. *Proc Natl Acad Sci* **108:** 4516–4522.

Cardinale, M., De Castro, J.V., Müller, H., Berg, G., and Grube, M. (2008) In situ analysis of the bacterial community associated with the reindeer lichen *Cladonia arbuscula* reveals predominance of *Alphaproteobacteria*. *FEMS Microbiol Ecol* **66:** 63–71.

Cardinale, M., Grube, M., de Castro, J.V., Jr, Müller, H., and Berg, G. (2012) Bacterial taxa associated with the lung lichen *Lobaria pulmonaria* are differentially shaped by geography and habitat. *FEMS Microbiol Lett* **329:** 111–115.

Cornejo, C., and Scheidegger, C. (2013) New morphological aspects of cephalodium formation in the lichen *Lobaria pulmonaria* (Lecanorales, Ascomycota). *The Lichenologist* **45:** 77–78.

Daims, H., Brühl, A., Amann, R., Schleifer, K.H., and Wagner, M. (1999) The domain-specific probe EUB338 is insufficient fort the detection of all Bacteria: development and evaluation of a more comprehensive probe set. *Syst Appl Microbiol* **22:** 434–444.

Dal Grande, F., Widmer, I., Wagner, H., and Scheidegger, C. (2012) Vertical and horizontal photobiont transmission within populations of a lichen symbiosis. *Mol Ecol* **21:** 3159–3172.

DeSantis, T.Z., Hugenholtz, P., Larsen, N., Rojas, M., Brodie, E.L., Keller, K., *et al*. (2006) Greengenes, a chimera-checked 16S rRNA gene database and workbench compatible with ARB. *Appl Environ Microbiol* **72:** 5069–5072.

Edgar, R.C. (2010) Search and clustering orders of magnitude faster than BLAST. *Bioinformatics* **26:** 2460–2461.

Fernández Mendoza, F., Domaschke, S., García, M.A., Jordan, P., Martín, M.P., and Printzen, C. (2011) Population structure of mycobionts and photobionts of the widespread lichen *Cetraria aculeata*. *Mol Ecol* **20:** 1208–1232.

Ferreira, A., Quecine, M.C., Lacava, P.T., Oda, S., Azevedo, J.L., and Araújo, W.L. (2008) Diversity of endophytic bacteria from *Eucalyptus* species seeds and colonization of seedlings by *Pantoea agglomerans*. *FEMS Microbiol Lett* **287:** 8–14.

Funkhouser, L.J., and Bordenstein, S.R. (2013) Mom knows best: the universality of maternal microbial transmission. *PLoS Biol* **11:** e1001631.

Grube, M., and Berg, G. (2009) Microbial consortia of bacteria and fungi with focus on the lichen symbiosis. *Fung Biol Rev* **23:** 72–85.

Grube, M., Cardinale, M., Vieira de Castro, J., Müller, H., and Berg, G. (2009) Species-specific structural and functional diversity of bacterial communities in lichen symbiosis. *ISME J* **3:** 1105–1115.

Grube, M., Köberl, M., Lackner, S., Berg, C., and Berg, G. (2012) Host-parasite interaction and microbiome response: effects of fungal infections on the bacterial community of the Alpine lichen *Solorina crocea*. *FEMS Microbiol Ecol* **82:** 472–481.

Grube, M., Cernava, T., Soh, J., Fuchs, S., Aschenbrenner, I., Lassek, C., *et al*. (2014) Exploring functional contexts of symbiotic sustain within lichen-associated bacteria by comparative omics. *ISME J* doi:10.1038/ismej.2014.138.

Haas, B.J., Gevers, D., Earl, A.M., Feldgarden, M., Ward, D.V., Giannoukos, G., *et al*. (2011) Chimeric 16S rRNA sequence formation and detection in Sanger and 454-pyrosequenced PCR amplicons. *Genome Res* **21:** 494–504.

Hodkinson, B., and Lutzoni, F. (2009) A microbiotic survey of lichen-associated bacteria reveals a new lineage from the Rhizobiales. *Symbiosis* **49:** 163–180.

Hodkinson, B.P., Gottel, N.R., Schadt, C.W., and Lutzoni, F. (2012) Photoautotrophic symbiont and geography are major factors affecting highly structured and diverse bacterial communities in the lichen microbiome. *Environ Microbiol* **14:** 147–161.

Honegger, R. (2012) The symbiotic phenotype of lichen-forming ascomycetes and their endo- and epibionts. In *Fungal Associations (The Mycota)*. Hock, B. (ed.). Berlin, Germany: Springer, pp. 287–339.

Jordan, W. (1970) The internal cephalodia of the genus *Lobaria*. *Bryologist* **73:** 669–681.

Jüriado, I., Liira, J., Csencsics, D., Widmer, I., Adolf, C., Kohv, K., and Scheidegger, C. (2011) Dispersal ecology of the endangered woodland lichen Lobaria pulmonaria in managed hemiboreal forest landscape. *Biodivers Conserv* **20:** 1803–1819.

Lackner, G., Möbius, N., Scherlach, K., Partida-Martinez, L.P., Winkler, R., Schmitt, I., and Hertweck, C. (2009) Global distribution and evolution of a toxigenic *Burkholderia-Rhizopus* symbiosis. *Appl Environ Microbiol* **75:** 2982–2986.

Lawrey, J.D., and Diederich, P. (2003) Lichenicolous fungi: interactions, evolution, and biodiversity. *Bryologist* **106:** 81–120.

Liba, C.M., Ferrara, F.I.S., Mangio, G.P., Fantinatti-Garboggini, F., Albuquerque, R.C., Pavan, C., *et al*. (2006) Nitrogen-fixing chemo-organotrophic bacteria isolated from cyanobacteria-deprived lichens and their ability to solubilize phosphate and to release amino acids and phytohormones. *J Appl Microbiol* **101:** 1076–1086.

López-López, A., Rogel, M.A., Ormeno-Orillo, E., Martínez-Romero, J., and Martínez-Romero, E. (2010) *Phaseolus vulgaris* seed-borne endophytic community with novel bacterial species such as *Rhizobium endophyticum* sp. nov. *Syst Appl Microbiol* **33:** 322–327.

Loy, A., Maixner, F., Wagner, M., and Horn, M. (2007) probeBase – an online resource for rRNA-targeted oligonucleotide probes: new features 2007. *Nucleic Acids Res* **35:** D800–D804.

Lozupone, C., and Knight, R. (2005) UniFrac: a new phylogenetic method for comparing microbial communities. *Appl Environ Microbiol* **71:** 8228–8235.

McEvoy, M., Gauslaa, Y., and Solhaug, K.A. (2007) Changes in pools of depsidones and melanins, and their function, during growth and acclimation under contrasting natural light in the lichen *Lobaria pulmonaria*. *New Phytol* **175:** 271–282.

Mushegian, A.A., Peterson, C.N., Baker, C.C.M., and Pringle, A. (2011) Bacterial diversity across individual lichens. *Appl Environ Microbiol* **77:** 4249–4252.

Myllys, L., Stenroos, S., Thell, A., and Kuusinen, M. (2007) High cyanobiont selectivity of epiphytic lichens in old growth boreal forest of Finland. *New Phytol* **173:** 621–629.

Nash, T.H.I.I.I. (2008) Introduction. In *Lichen Biology*. Nash, T.H. (ed.). Cambridge, UK: Cambridge University Press, pp. 1–8.

Neef, A. (1997) Anwendung der in situ Einzelzell-Identifizierung von Bakterien zur Populationsanalyse in komplexen mikrobiellen Biozönosen. PhD Thesis. Munich, Germany: Munich Technological University.

Ondov, B.D., Bergman, N.H., and Phillippy, A.M. (2011) Interactive metagenomic visualization in a Web browser. *BMC Bioinformatics* **12:** 385.

Printzen, C., Fernández-Mendoza, F., Muggia, L., Berg, G., and Grube, M. (2012) Alphaproteobacterial communities in geographically distant populations of the lichen *Cetraria aculeata*. *FEMS Microbiol Ecol* **82:** 316–325.

Reeder, J., and Knight, R. (2010) Rapidly denoising pyrosequencing amplicon reads by exploiting rank-abundance distributions. *Nat Methods* **7:** 668–669.

Rose, F. (1992) Temperate forest management: its effect on bryophyte and lichen floras and habitats. In *Bryophytes and Lichens in a Changing Environment*. Bates, J.W., and Farmer, A.M. (eds). Oxford, UK: Oxford University Press, pp. 211–233.

Rout, M.E., Chrzanowski, T.H., Westlie, T.K., DeLuca, T.H., Callaway, R.M., and Holben, W.E. (2013) Bacterial endophytes enhance competition by invasive plants. *Am J Bot* **100:** 1726–1737.

Scheidegger, C. (1995) Early development of transplanted isidioid soredia of *Lobaria pulmonaria* in an endangered population. *Lichenologist* **27:** 361–374.

Scheidegger, C., and Werth, S. (2009) Conservation strategies for lichens: insights from population biology. *Fung Biol Rev* **23:** 55–66.

Schneider, T., Schmid, E., Vieria de Castro, J., Jr, Cardinale, M., Eberl, L., Grube, M., *et al*. (2011) Structure and function of the symbiosis partners of the lung lichen (*Lobaria pulmonaria* L. Hoffm.) analyzed by metaproteomics. *Proteomics* **11:** 2752–2756.

Schwieger, F., and Tebbe, C.C. (1998) A new approach to utilize PCR-single-strand-conformation polymorphism for 16S rRNA gene-based microbial community analysis. *Appl Environ Microbiol* **64:** 4870–4876.

Shade, A., and Handelsman, J. (2012) Beyond the Venn diagram: the hunt for a core microbiome. *Environ Microbiol* **14:** 4–12.

Shade, A., McManus, P.S., and Handelsman, J. (2013) Unexpected diversity during community succession in the apple flower microbiome. *mBio* **4:** e602–e612. doi:10.1128/mBio.00602-12.

Sharma, M., Schmid, M., Rothballer, M., Hause, G., Zuccaro, A., Imani, J., *et al*. (2008) Detection and identification of bacteria intimately associated with fungi of the order Sebacinales. *Cell Microbiol* **10:** 2235–2246.

de la Torre, J.R., Goebel, B.M., Friedmann, E.I., and Pace, N.R. (2003) Microbial diversity of cryptoendolithic communities from the McMurdo Dry Valleys, Antarctica. *Appl Environ Microbiol* **69:** 3858–3867.

Walser, J.C. (2004) Molecular evidence for limited dispersal of vegetative propagules in the epiphytic lichen *Lobaria pulmonaria*. *Am J Bot* **91:** 1273–1276.

Wang, Q., Garrity, G.M., Tiedje, J.M., and Cole, J.R. (2007) Naive Bayesian classifier for rapid assignment of rRNA sequences into the new bacterial taxonomy. *Appl Environ Microbiol* **73:** 5261–5267.

Werth, S., and Scheidegger, C. (2012) Congruent genetic structure in the lichen-forming fungus *Lobaria pulmonaria* and its green-algal photobiont. *Mol Plant Microbe Interact* **25:** 220–230.

Werth, S., Millanes, A.M., Wedin, M., and Scheidegger, C. (2013) Lichenicolous fungi show population subdivision by host species but do not share population history with their hosts. *Fung Biol* **117:** 71–84.

Widmer, I., Dal Grande, F., Excoffier, L., Holderegger, R., Keller, C., Mikryukov, V.S., and Scheidegger, C. (2012) European phylogeography of the epiphytic lichen fungus *Lobaria pulmonaria* and its green algal symbiont. *Mol Ecol* **21:** 5827–5844.

Supporting information

Additional Supporting Information may be found in the online version of this article at the publisher's web-site:

Fig. S1. Microscopic pictures of the vegetative propagules of lung lichen. A. young stage of propagules (soredia) made up of algal cell clusters wrapped by fungal hyphae (wet state). B. late developmental stage of propagules as cylindrical outgrowths stratified with fungal cortex (isidioid soredia; dry state).

Fig. S2. Single strand conformation polymorphism analysis of the lung lichen thalli and vegetative propagules of the three sampling sites (Tamischbachgraben, St. Oswald/Eibiswald, Johnsbach, white bars). M: marker; red bar: vegetative propagules; blue bar: thalli.

Fig. S3. A. Distribution of the relative abundances of either sequences or OTUs across lichen parts. B. Venn diagram of OTUs from lichen thalli and propagules (sampled at Johnsbach). Thalli and propagules shared 689 OTUs, but had also unique OTUs for each lichen part.

Fig. S4. Composition of the core microbial community of the two lichen parts at phylum, class, order and family level (starting from the inner circle). Within the *Proteobacteria*, *Deltaproteobacteria* was the predominant group (52%).

Fig. S5. Principal coordinate analysis (PCoA) of bacterial communities based on unweighted, jackknifed unifrac distance matrix. A. Beta diversity of the bacterial communities of lichen thalli and propagules sampled at Johnsbach (Data set I; 5 thallus and 5 propagule samples). Samples were represented by: blue rectangles – lichen thalli, red points – isidioid soredia; $P < 0.022$ (Anosim) B. Beta diversity of the bacterial communities of the three different sampling sites (Data set II; 5 thallus samples at each site); $P < 0.001$ (Anosim). Samples were represented by: green rectangles – St. Oswald/Eibiswald, blue points – Johnsbach and brown triangles – Tamischbachgraben.

Fig. S6. Alphaproteobacterial families on isidiod soredia. The most dominant one was *Sphingomonadaceae* comprising more than 60%. Alphaproteobacterial sequences, which could not be assigned to a certain family taxon are summarized in the category 'Other'. All further families found comprised only 8%.

Table S1. Alpha diversity* and richness indices of lichen thalli and vegetative propagules.

Table S2. Distribution of alphaproteobacterial families across all three sampling sites.

Table S3. Multivariate analysis. Statistical significance was tested with Adonis and ANOVA on the testable RDA fractions. Support values are indicated by an asterisk (*) when $P < 0.05$ and by two asterisks (**) when $P < 0.01$.

Publication I – Supplementary data

Supplementary materials and methods

Pyrosequencing: Barcoded 454-pyrosequencing followed by quality filtering yielded in an average sequence length of about 300 nt. After exclusion of reads assigned to chloroplasts, mitochondria and the cyanobacterial genus *Nostoc*, which is harbored in internal cephalodia of the thalli, two pyrosequencing data sets at a genetic distance of 3% were generated. The first one was used for the comparison of the lichen thalli with its propagules and was made up of 10 samples (5 thallus- and 5 propagule-samples) collected in Johnsbach. It comprised 74,180 sequences (min: 4,891 seq., max: 10,512 seq.) representing 3,273 operational taxonomic units (OTUs). The second one was used for comparison of lichen thalli within sampling sites and was made up of 15 thallus samples (5 samples for each sampling site). It comprised 83,080 sequences (min: 3,635 seq.; max: 8,021 seq.) representing 3,972 OTUs. Due to the difference in sequence counts among the samples both datasets were normalized to the minimal sequence count in each dataset resulting in 41,890 sequences representing 2,439 OTUs for dataset 1 and a total number of 3,117 OTUs with 54,525 sequences for data set 2. None of the rarefaction curves were saturated, resulting in a coverage of ~51-53%.

Statistics: A non-parametric analysis of variance and a RDA based variation partitioning were used to survey the extent to which the differences in community composition can be explained - by geographic factors and by the tissue origin. Both analyses were carried out in R (http://www.R-project.org) using adonis and varpart as implemented in package vegan (http://vegan.r-forge.r-project.org).

Both analyses are similar, despite of their conceptual differences. Adonis uses the localities as categorical variables, while for variation partitioning a geographic distance matrix was used to capture geographic relatedness. Both analyses were run twice using different response matrices: a) the OTU community matrix obtained in QIIME, standardized using “total” method in vegan function *decostand* and a pairwise dissimilarity matrix obtained by analyzing the SSCP band pattern with GelCompare II 6.5 created by Applied Maths NV (http://www.applied-maths.com/).

The results of all four analyses are highly coherent and are summarized in table S3. Only a small fraction of the variability in the datasets is explained by the analyzed factors,

ranging between 30% and 41% in all analyses. This apparent lack of explanative power is coherent with the methodological constraints in amplicon studies like having identified thousands of OTUs in a small number of samples resulting in a high variability between samples. Across all analyses, most of the explained variation in community composition was due to the tissue of origin (e.g. 24-25% in adonis).

However, when the co-structuring between tissue of origin and distance was partialled out using variation partitioning in the Qiime dataset, this percentage dropped to ca. 14%. Also, an additional 5% to 9% of the variability in the studied datasets was explained by the differences between localities or by geographic distance across all analyses. However, the strong co-structuring between tissue of origin and locality found in the QIIME dataset might reflect the lack of complete nestedness of this dataset. Meanwhile, when using the fully nested SSCP band dataset, geographic distances became more explanative than the tissue of origin, explaining up to 24% of the variability.

Supplementary Figures

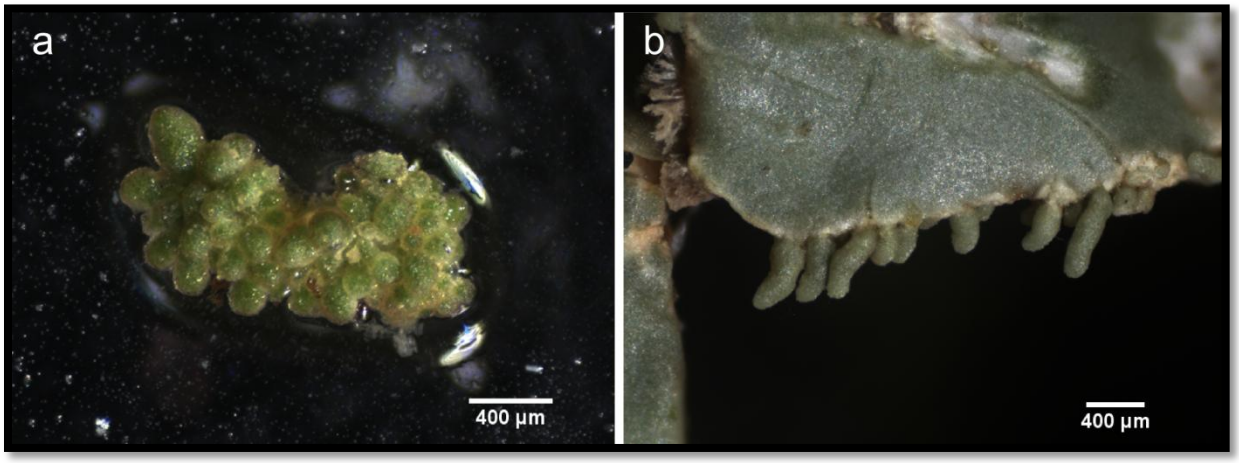

Figure S1: Microscopic pictures of the vegetative propagules of lung lichen. a) young stage of propagules (soredia) made up of algal cell clusters wrapped by fungal hyphae (wet state). b) late developmental stage of propagules as cylindrical outgrowths stratified with fungal cortex (isidioid soredia; dry state).

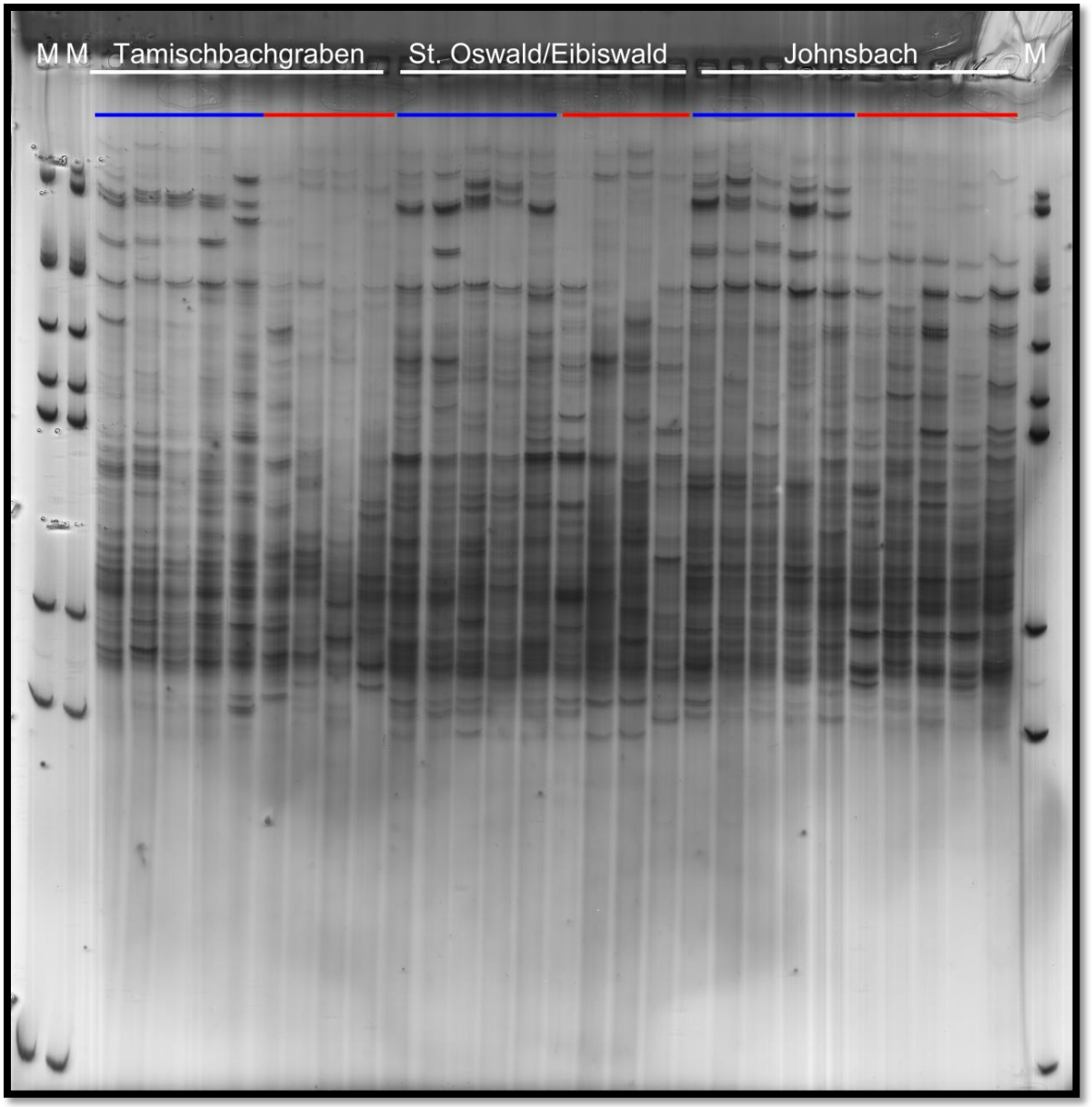

Figure S2: Single strand conformation polymorphism analysis of the lung lichen thalli and vegetative propagules of the three sampling sites (Tamischbachgraben, St. Oswald/Eibiswald, Johnsbach, white bars). M: marker; red bar: vegetative propagules; blue bar: thalli

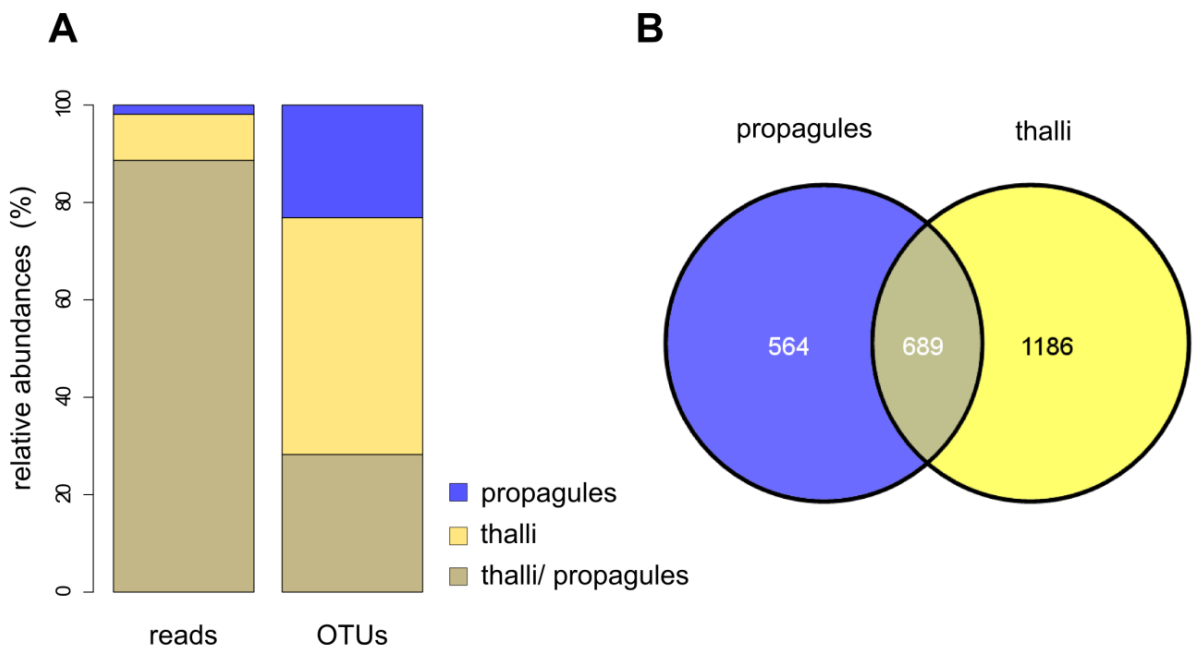

Figure S3: A) Distribution of the relative abundances of either sequences or OTUs across lichen parts. B) Venn diagram of OTUs from lichen thalli and propagules (sampled at Johnsbach). Thalli and propagules shared 689 OTUs, but had also unique OTUs for each lichen part.

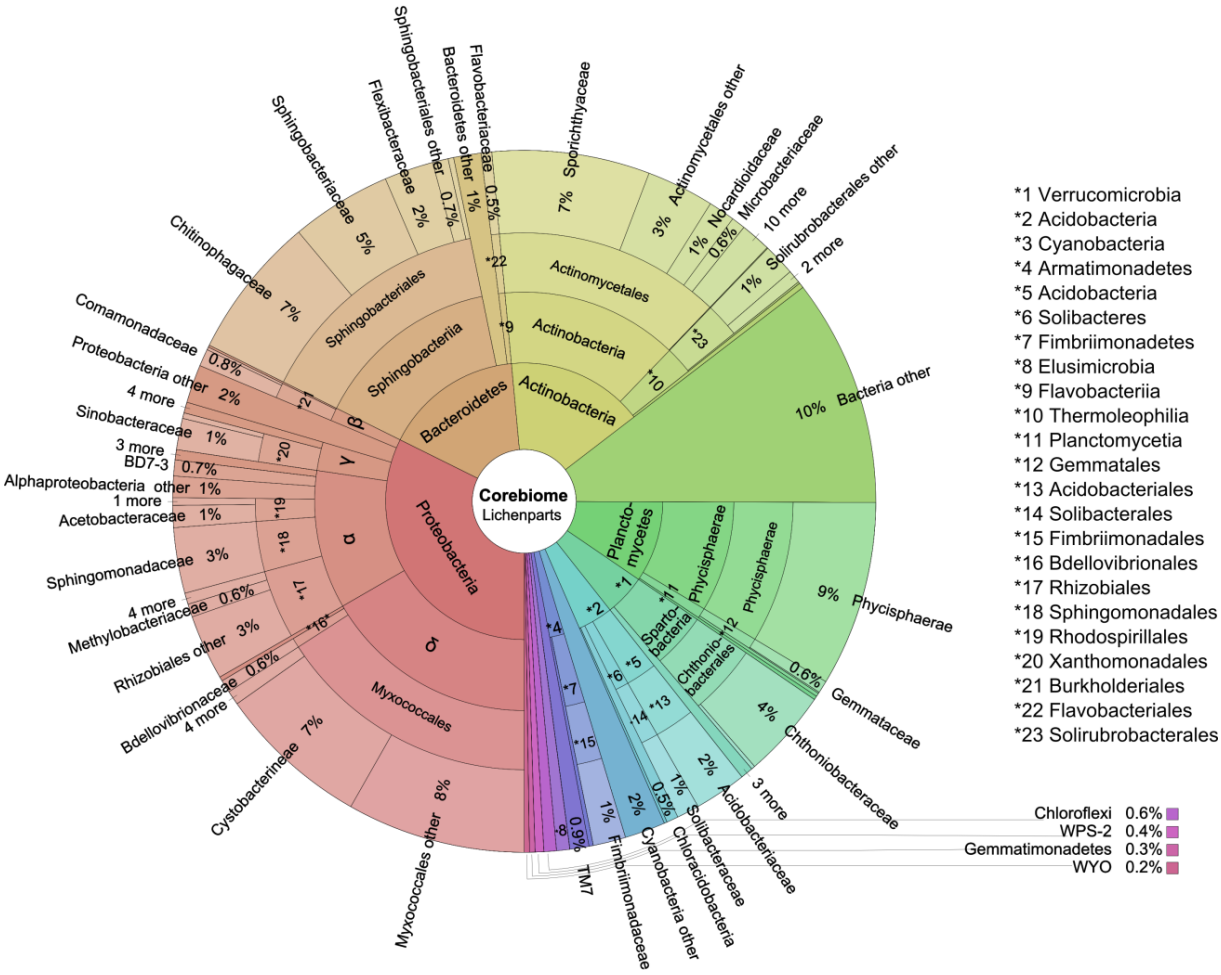

Figure S4: Composition of the core microbial community of the two lichen parts at phylum, class, order and family level (starting from the inner circle). Within the *Proteobacteria*, *Deltaproteobacteria* was the predominant group (52%).

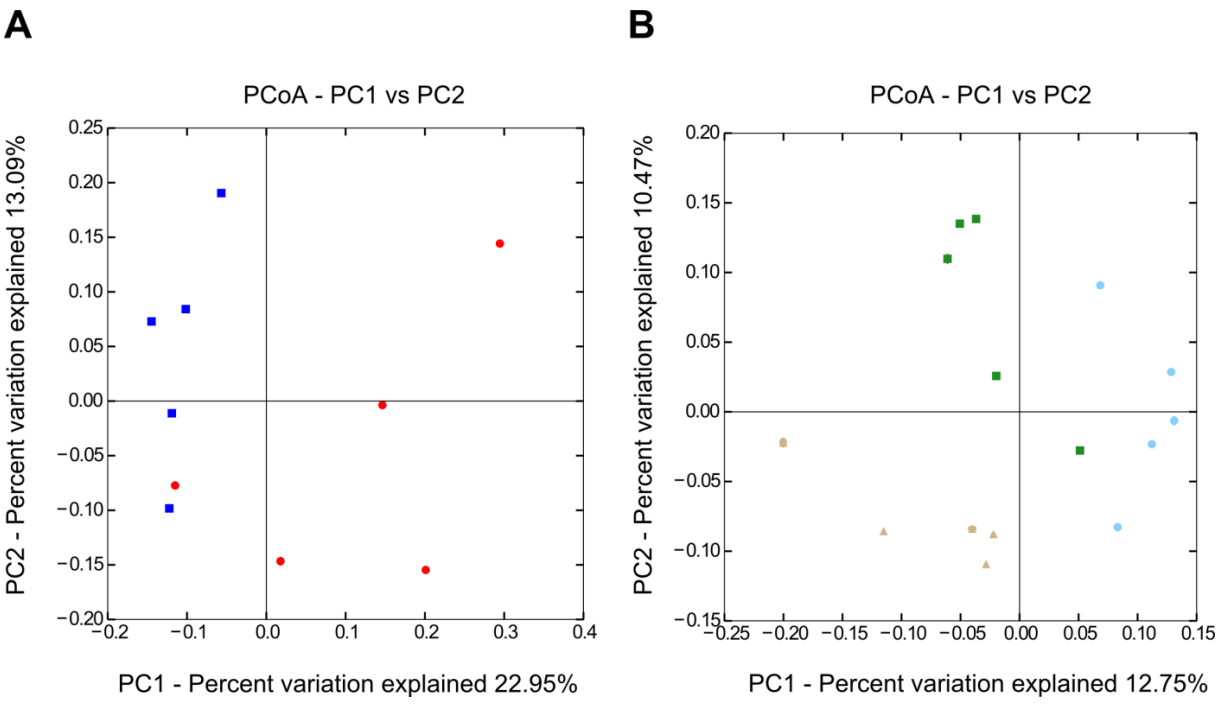

Figure S5: Principal coordinate analysis (PCoA) of bacterial communities based on unweighted, jackknifed unifrac distance matrix. A) Beta diversity of the bacterial communities of lichen thalli and propagules sampled at Johnsbach (Dataset I; 5 thallus and 5 propagule samples). Samples were represented by: blue rectangles – lichen thalli, red points – isidioid soredia; $p < 0.022$ (Anosim) B) Beta diversity of the bacterial communities of the three different sampling sites (Dataset II; 5 thallus samples at each site); $p < 0.001$ (Anosim). Samples were represented by: green rectangles - St. Oswald/Eibiswald, blue points - Johnsbach and brown triangles - Tamischbachgraben.

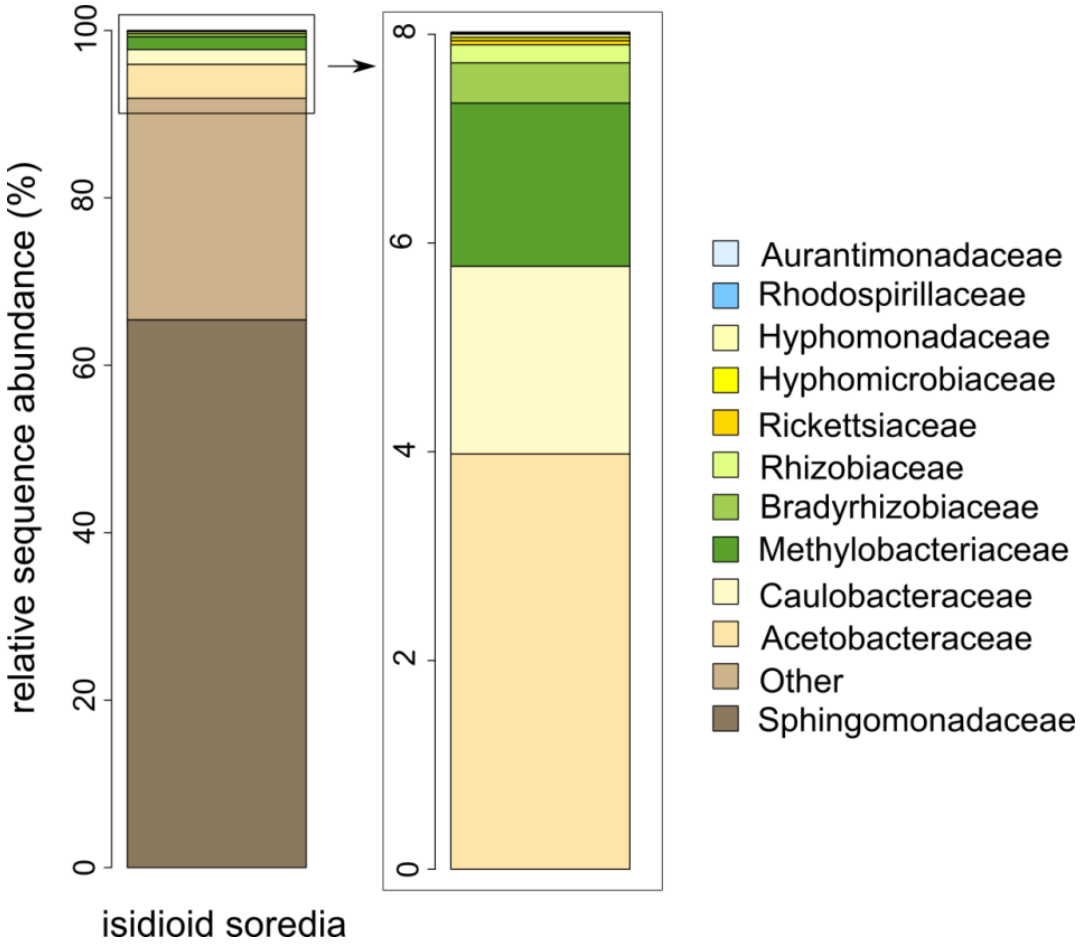

Figure S6: Alphaproteobacterial families on isidioid soredia. The most dominant one was *Sphingomonadaceae* comprising more than 60%. Alphaproteobacterial sequences, which could not be assigned to a certain family taxon are summarized in the category "Other". All further families found comprised only 8%.

Supplementary Tables

Table S1: Alpha diversity* and richness indices of lichen thalli and vegetative propagules.

		Shannon	Simpson	observed species	chao1
Tamischbach-graben thalli	MID1	7.1	0.97	595	1173
	MID2	6.17	0.93	484	951
	MID3	6.71	0.96	570	1131
	MID4	6.83	0.97	563	1122
	MID5	5	0.87	369	722
St. Oswald/ Eibiswald Thalli	MID6	7.08	0.97	570	1118
	MID7	6.76	0.97	531	1065
	MID8	6.98	0.97	580	1194
	MID10	7.6	0.99	672	1444
	MID11	7.21	0.98	567	1188
Johnsbach Thalli	MID13	7.28	0.98	634	1268
	MID14	7.65	0.99	702	1490
	MID15	7.54	0.98	658	1367
	MID16	7.1	0.97	647	1229
	MID17	7.33	0.98	606	1249
Johnsbach propagules	MID18	5.98	0.95	472	975
	MID19	7.07	0.97	616	1207
	MID40	6.05	0.96	419	799
	MID21	5.59	0.94	327	672
	MID22	4.97	0.92	275	594

*normalized to 3635 sequences/sample; 3% genetic distance.

Table S2: Distribution of alphaproteobacterial families across all three sampling sites

order	family	St. Oswald	Johnsbach	Tamischbachgraben
***Alphaproteobacteria* other**	other	1.65	2.58	0.93
BD7-3	other	0.18	0.85	0.17
Caulobacterales	other	0.26	0.21	0.23
	Caulobacteraceae	5.04	3.61	4.39
Ellin329	other	0.07	0.49	0.10
Rhizobiales	other	39.47	34.71	27.57
	Aurantimonadaceae	0.02	0.02	0.07
	Beijerinckiaceae	0.02	0	0.03
	Bradyrhizobiaceae	0.62	1.04	0.53
	Hyphomicrobiaceae	0.06	0.08	0.10
	Methylobacteriaceae	0.84	1.16	2.51
	Methylocystaceae	0.17	0.06	0.07
	Phyllobacteriaceae	0.09	0	0.01
	Rhizobiaceae	0.28	0.38	0.21
	Xanthobacteraceae	0.02	0	0.01
Rhodospirillales	other	0.66	0.30	0.77
	Acetobacteraceae	7.21	8.41	4.96
	Rhodospirillaceae	0.17	0.15	0.04
Rickettsiales	other	0.07	0.36	0.03
	Rickettsiaceae	0	0.08	0.04
Sphingomonadales	other	0.11	0	0.14
	Sphingomonadaceae	42.99	45.51	57.07
		100.00%	100.00%	100.00%

Table S3: Multivariate analysis. Statistical significance was tested with Adonis and ANOVA on the testable RDA fractions. Support values are indicated by an asterisk (*) when $p<0.05$ and by two (**) when $p<0.01$

	SSCP band patterns		**Qiime data (OTUs)**	
	Adonis [R2]	Variation partitioning [Adjusted R2]	Adonis [R2]	Variation partitioning [Adjusted R2]
lichen parts	0.24761 **	0.17163 **	0.24142 **	0.13545 **
locality/ geographic distance	0.04580	0.23556 **	0.08653 *	0.09173 *
combination of both	0.07204 *	-0.00098	0	0.07405
unexplained variation	0.63455	0.59379	0.67205	0.69877

MANUSCRIPT I

Submitted as Journal Article

Inter-microbiome relations: spatially close hosts show a common network with specific components

Ines Aline Aschenbrenner,[1,2] Tomislav Cernava,[1] Armin Erlacher,[1] Gabriele Berg,[1] Martin Grube[2]

[1]Institute of Environmental Biotechnology
Graz University of Technology, Austria

[2]Institute of Plant Sciences
University of Graz, Austria

Inter-microbiome relations: spatially close hosts show a common network with specific components

Ines Aline Aschenbrenner,[1,2] Tomislav Cernava,[1] Armin Erlacher,[1] Gabriele Berg,[1] Martin Grube[2]

[1]Institute of Environmental Biotechnology, Graz University of Technology, Petersgasse 12, 8010 Graz, Austria

[2]Institute of Plant Sciences, University of Graz, Holteigasse 6, 8010 Graz, Austria

Correspondence:

Martin Grube
University of Graz
Institute of Plant Sciences
Holteigasse 6, A-8010 Graz
email: martin.grube@uni-graz.at
telephone: +43 316 380 5655

Submitted to: The ISME Journal

Subject Category: Microbial population and community ecology

Running title: inter-microbiome relations

Abstract

A wealth of information exists about specificity and diversity of host-associated bacterial communities, but the inter-microbiome relationships of unrelated but naturally co-occurring host organisms are surprisingly little understood. We provide a first insight into three typical habitats of tree trunks, comprising lichens, mosses and the bare bark. Overall, an exceptionally high number of more than 33,000 OTUs was found for the interrelated biosphere. The microbiomes were significantly different to each other, particularly at lower taxonomic ranks. A limited number of highly abundant OTUs were identified as generalists, mainly affiliated to *Proteobacteria* (*Alpha-* and *Betaproteobacteria*) and with *Sphingomonas* as most abundant genus. The taxonomic spectrum of specialists differed for each habitat and moss-associated specialists were highly diverse. The analyses of inter-microbiome relationships improve understanding of the supra-organismal structure of microbiomes in their environmental contexts and reveal the effect of close spatial proximity of distinct hosts by their bacterial communities. Moreover, the metagenomic analysis of a generalist and a specialist revealed functional segregation and a broader scope of functions in the generalist. We suggest that a narrow spatial mosaic of hosts maintains an optimal network of associated generalist and specialist bacteria which contribute to the sustainability of a healthy host community.

Keywords: *Lobaria pulmonaria*, *Pterigynandrum filiforme*, *Acer pseudoplatanus*, 16S rRNA amplicon, metagenome, co-occurrences

Introduction

The understanding of symbiosis has significantly progressed since it was originally characterized as the "living-together of unequal organisms" (de Bary, 1879). Formerly seen as a curiosity of biology, symbioses are now confirmed as a fundamental biological principle, especially since bacteria were shown to associate with all macroscopic organisms, including humans or plants (Blaser et al., 2013; Berg et al., 2014). Bacteria are also known for their supportive functions in ecologically important fungal symbioses, such as in below-ground mycorrhiza (Frey-Klett et al., 2007), or more recently, also in lichens above the ground (Grube et al., 2009; 2015; Erlacher et al. 2015). Owing to their potential as microbial underpinning of ecosystems, it is important to understand how host-associated bacterial communities are correlated in their wider context of habitats (Berg, 2015). Bacterial communities at plant roots, including the mycorrhiza, are primarily recruited from the microbiota of the surrounding soil (Berg and Smalla; 2009), whereas the origin of above-ground, atmosphere-exposed communities is less clear (e.g. the phyllosphere; Vorholt, 2012).

Trees represent complex habitats, which, despite their significance, have so far hardly been studied using contemporary culture-independent approaches. Recently, Leff et al. (2014) focused on bark and leaf samples of the Ginkgo tree, but trees, in their native environment, usually host also unrelated epiphytic organisms, which colonize the bark surface in mosaic-like patterns. The most frequent epiphytes in forests of temperate latitudes are mosses and lichens. They therefore represent ideal and distinct objects for a comparative analysis of adjoining microbial habitats.

Lichens produce macroscopic thalli, as fungal-dominated morphs to shelter internalized photosynthetic partners. This joint morphology also creates unique habitats. Culture-independent approaches revealed the diversity of lichen-associated bacteria (Cardinale et al., 2006; Bjelland et al. 2010; Mushegian et al., 2011; Hodkinson et al., 2012). The dominant bacterial group in most lichens is *Alphaproteobacteria*, along with other lineages present in lower abundances (Cardinale et al., 2008; Bates et al., 2011; Aschenbrenner et al., 2014). Bacterial communities are specific for their host lichens (Grube et al., 2009), and bacteria primarily colonize surfaces of lichens, but eventually intrude more deeply into their hosts (Cardinale et al., 2008; Erlacher et al. 2015). Potential metabolic contributions by bacteria to the lichen holobiont were recently summarized by metagenomics and metaproteomics (Grube et al., 2015). These functions include phosphate solubilization, nitrogen fixation and release

of amino acids (Grube et al., 2009; Sigurbjörnsdóttir et al., 2015), besides provision of vitamins, detoxification and stress resistance mechanisms (Grube et al., 2015). Similar to lichens, mosses also host complex bacterial communities (e.g., Opelt et al., 2004; Bragina et al., 2012, 2014). The moss microbiome is supposed to have an impact on the entire forest ecosystem by nitrogen-fixation – primarily by associated *cyanobacteria* (Lindo et al., 2011), whereas some of the culturable strains were also shown to have host growth promoting effects (Tani et al., 2011). With the discovery of specific bacterial communities in lichens and mosses, a gap of knowledge arises about their inter-microbiome relationships in their natural habitats, e.g. on tree trunks. A comparison of adjacent moss and lichen microbiomes might nevertheless be informative, as both hosts – commonly also known as "cryptogams" – are poikilohydric organisms which endure periodic desiccation and thus both might share, similar and possibly ecologically robust bacteria.

The aim of this study was to explore the specificity of the lichen-associated microbiome (*Lobaria pulmonaria* (L.) Hoffm.) in comparison to the bacterial communities of the surrounding hosts, i.e. tree bark (*Acer pseudoplatanus* (L.)) and a predominant moss (*Pterigynandrum filiforme* (Hedw.)), using a high-throughput sequencing approach. *L. pulmonaria*, which is adapted to old-growth forests devoid of any air pollutants, harbors the photosynthetic partner *Dictyochloropsis reticulata* (Tschermak-Woess, 1995), and in addition also internal *Nostoc* (*Cyanobacteria*) clusters for nitrogen fixation (Millbank & Kershaw, 1970). The prevailing moss of the study site, *P. filiforme*, is quite common in cool montane environments of circumboreal latitudes. We hypothesized that the specific conditions provided by the hosts differed among the three (micro-)habitats, and that this is reflected by clearly different bacterial communities. Moreover, we supposed that the vital mosses and lichens would have more similar communities than the suberin-rich bark, which should also be reflected by potentially specialized bacteria in each of these ecological niches. We were also interested in a comparison of the co-occurrence patterns of the distinct habitats to assess potential differences of bacterial correlations. Finally, metagenomic analysis was used to reveal potential functional characteristics of a generalist and a lichen specialist.

Materials and Methods

Sampling procedure, DNA extraction and sequencing

To explore bacterial community composition and diversity in adjacent habitats (moss: *Pterigynandrum filiforme* (Hedw.); lichen: *Lobaria pulmonaria* (L.) Hoffm.; bark: from *Acer pseudoplatanus* (L.)) in Johnsbach (Styria, Austria, N 47°32‘35‘‘, E 14°37‘38‘‘, 1175 m above sea level; October/2014) 24 moss, lichen, and bark samples (in total 72) from 6 trees (*Acer pseudoplatanus*) were collected in an open patch of a montane forest dominated by maple. Samples were collected from the tree trunk below the primary branching in a height between 1-2 meters above ground. Moss and lichen samples were ground with mortar and pestle, while bark samples were ground with a hand mill. DNA was extracted using the MoBio Power Soil DNA isolation kit according to manufacturer's protocol. Each DNA extract was supplemented with peptide nucleic acid PCR clamps (0.75 µM of each PNA in the final reaction in a ratio pPNA:mPNA 1:1) as described by Lundberg et al. (2013) and then used as template for PCR amplifications (triplicates with subsequent pooling) with a universal bacterial primer set 515f/806r (Caporaso et al., 2011). Barcoded samples were pooled equimolar and sent for paired end Illumina MiSeq sequencing (MWG Eurofins, Germany).

Initial data analysis

Data analysis was performed using the Qiime 1.9.0 pipeline (Caporaso et al., 2010). Raw Illumina MiSeq forward and reverse reads for each of the 72 samples were initially joined and demultiplexed with a minimal phred quality threshold of Q=20. Additionally, the obtained sequences were quality-checked for chimeric sequences (usearch61; Edgar, 2010). Subsequently, the OTU table was generated with the script "pick_open_reference_otus.py" using default settings except for the reference database. The SILVA database (release 119) was employed for reference sequences and for taxonomy assignment (Pruesse et al., 2007). OTU clustering was done with a sequence similarity threshold of 94% and 97% representing theoretical taxonomic units at genus and species level, respectively. Chloroplast, mitochondrial and other non-bacterial sequences were excluded from the dataset.

General diversity and structure of bacterial communities across the habitats

For a general description of the bacterial community structure and alpha-diversity the initial OTU tables (94% and 97% similarity) were rarefied. All beta-diversity indices as well as statistical analysis were calculated with the 97% similarity OTU table. Significance between sample groupings (grouped per habitat type) was calculated with Adonis based on weighted and unweighted UniFrac distance metrices (Lozupone & Knight, 2005).

Bacterial generalists and specialists across the habitats

In order to determine generalists and specialists (OTUs) across the habitats the initial OTU table (97% similarity) was reduced to OTUs, which were present in at least 3 out of 4 replicates per habitat per tree prior to sequence rarefaction. To identify generalists, OTUs, which occurred in more than 90% of all samples, were taken into consideration. OTUs occurring uniquely on a specific habitat and detected in at least one third of these samples (with a minimal count of 20 sequences) were categorized as specialists. For further descriptions these OTUs were taxonomically summarized at genus level. For the identification of the lichen specific strain "Lichen-associated-*Rhizobiales* 1" (LAR1) in our data set we used 19 LAR1 sequences from GenBank (accession numbers: GU191849.1, GU191851.1-GU191857.1, GU191859.1, GU191860.1, GU191864.1-GU191872.1). The representative sequences of all OTUs assigned to the order *Rhizobiales* (despite the habitat affiliation) and LAR1 sequences were aligned with ClustalX2 (Larkin et al., 2007) and the alignment was used to create a bootstrapped neighbor-joining tree. *Cyanobacteria* were extracted and filtered for OTUs with at least 20 sequences and which occurred in at least 8 samples. Additional BLASTn searches were performed with the representative sequences of the observed OTUs (Zhang et al., 2000).

Co-occurrence patterns of Alphaproteobacteria for each habitat

Co-occurrence patterns of alphaproteobacterial families were determined for each habitat separately. Therefore, the data set (at 97% similarity) for each habitat was rarefied and then summarized at species level. Spearman's correlation and corresponding significance was calculated in R version 3.2.0 (Hmisc package; http://www.r-project.org/; R core team, 2013). Spearman's correlations ($\rho \geq 0.7$ and $\rho \leq -0.7$), which were statistically significant (p-value < 0.001) were considered as positive or negative correlation with focus on *Alphaproteobacteria*.

Co-occurrence patterns were visualized as networks using Cytoscape version 3.2.1 (Shannon et al., 2003).

FISH/CLSM

Fluorescence in situ hybridization (FISH) was performed to visualize the colonization pattern of *Alphaproteobacteria* among other eubacteria on the lichen thallus. For this purpose, thalli were fixed with 4% paraformaldehyde/phosphate-buffered saline (PBS) with a ratio of 3:1 at 4°C for at least 4 h. Prior to FISH application (according to Cardinale et al., 2008), cross-sections of the thalli were prepared. For the detection of *Alphaproteobacteria* the Cy5-labled probe ALF968 (42°C, 35% formamide; Neef, 1997) and an equimolar mixture of the Cy3-labled probes EUB338, EUB338II, EUB338III (42°C, 15% formamide) for eubacteria were used (Amann et al., 1990; Daims et al., 1999). Additionally, NONEUB probes (Wallner et al., 1993) labeled with the respective fluorochromes were used as negative controls. Details on oligonucleotide probes are available on probeBase (Loy et al., 2007). SlowFade Gold antifade reagent (Molecular Probes, Eugene, USA) was used to suppress photobleaching of the fluorescently labeled probes. Visualization was performed with a Leica TCS SPE confocal laser-scanning microscope (Leica Microsystems, Mannheim, Germany). Confocal stacks were processed with Imaris 7.3 (Bitplane, Zurich, Switzerland). Overlapping micrographs were processed with Microsoft Image Composite Editor to create stitched panorama images.

Functional analysis of a generalist and a specialist

The potential functional contributions of a generalist and a lichen-associated specialist were examined based on the *Lobaria* metagenome (ID 4530091.3) deposited on the metagenomics analysis server MG-RAST (Meyer et al., 2008). Meta-genomic sequences were compared to GenBank using a maximum e-value of 1e-5 and a minimum identity cutoff of 70%. All reads assigned to the genera *Sphingomonas* (*Proteobacteria) and Mucilaginibacter* (*Bacteroidetes*) were aligned to the protein reference database NCBI-NR using DIAMOND (version 0.7.9; Buchfink et al., 2014). Functional assignments were performed with MEGAN5 (version 5.10.5; Huson et al., 2011) based on SEED classification (Overbeek et al., 2005). The abundances of function-assigned sequences were subsampled for comparison.

Results

Bacterial community composition and diversity across habitats

The bacterial community composition and diversity of the adjoining microhabitats (Fig. 1) *L. pulmonaria* (lichen), *P. filiforme* (moss) and *A. pseudoplatanus* (maple, bark of the trunk) were assessed using Illumina-based high throughput sequencing of 16S ribosomal RNA gene amplicons. After quality filtering and removal of chloroplast, mitochondrial and other nonbacterial sequences 33,817 operational taxonomic units (OTUs) were identified at species level (97% sequence identity) with a total read count of 1,121,997 sequences (min: 2,455; max: 45,032) representing 24 bark, moss and lichen specimens, respectively.

All analyzed habitats were high in alpha diversity as shown by Shannon diversity (bark: 7.4, moss: 8.10, lichen: 7.54) and Simpson diversity indices (bark: 0.98, moss: 0.98, lichen: 0.97; Table S1; Fig. S1). Overall, moss specimens showed the highest alpha diversity, which was also reflected by the number of observed OTUs (bark: 5,246, moss: 6,918, lichen 6,069 OTUs after normalization). The phylogenetic beta-diversity of the bacterial communities across the three habitats was significantly different, both quantitatively and qualitatively (weighted and unweighted UniFrac distance matrices, respectively), according to nonparametric Adonis ($p \leq 0.001$; Fig. 2). The samples covered between 50-65%, 51-60%, and 42-56% of the estimated OTUs (chao1) at genus level for bark, moss and lichen samples, respectively.

Although the most abundant phyla (more than 2% relative sequence abundance within each habitat) were shared by all three habitats, differences in the community composition in terms of the relative taxon abundances of each phylum were noticeable (Fig. 3). Taxonomic assignments revealed that the majority of the reads, independent from the sequence origin, was assigned to the phylum *Proteobacteria* (bark: 54.7%, moss: 37.0%, lichen: 42.6%,), with *Alphaproteobacteria* as the predominant class. Additionally, *Cyanobacteria* and *Bacteroidetes* were overrepresented in at least one of the habitats by accounting about 20% of all sequences (*Cyanobacteria*: 1.0%, 13.0%, 20.2%; *Bacteroidetes*: 11.0%, 21.3%, 10.6% on bark, moss and lichen, respectively). Other highly abundant phyla, in particular on bark, were *Actinobacteria* (12.6%, 3.5%, 5.6%) and *Acidobacteria* (10.7%, 7.1%, 3.9%), whereas both cryptogams showed higher relative abundances of *Verrucomicrobia* (4.0%, 8.4%, 9.6%) and *Planctomycetes* (2.7%, 5.6%, 5.1%).

Similar to the phylum level, also deeper analysis at family level revealed habitat preferences for certain taxa (Fig. 4). Bacterial families within *Proteobacteria* such as *Sphingomonadaceae, Acetobacteraceae* and *Enterobacteriaceae* predominated on bark relative to the two other habitats, but also *Acidobacteriaceae* (*Acidobacteria*) and *Microbacteriaceae* (*Actinobacteria*) were more frequent. In contrast, the lichens were dominated by informal cyanobacterial "Family I", which mainly comprises the genus *Nostoc,* as well as *Rhizobiales* group 1174-901-12 (*Proteobacteria*) and a family within the order *Chthoniobacterales* (*Verrucomicrobia*). Moreover, the mosses contained higher proportions of the *Bacteroidetes* families *Chitinophagaceae* and *Cytophagaceae* and the proteobacterial family *Comamonadaceae*, among others.

Unraveling the host-associated microbiomes revealed bacterial generalists across all and specialists for each habitat

In order to identify habitat related generalists and specialists at OTU level (97% similarity) the data set was reduced to OTUs, which were present in at least three out of four replicates per habitat per tree. OTUs occurring in more than 90% of all samples were here termed generalists. Conversely, OTUs detected uniquely in one habitat (in at least one third of the samples) were termed as specialists. Applying these criteria, about 1.2% of these OTUs (52 OTUs; 19.9% of the sequences) were identified as generalists, while 2.5% (109 OTUs; 2.7% of all sequences) were categorized as specialists (Fig. 5).

About 50% of the generalists (27 out of 52 OTUs) belonged to *Alphaproteobacteria* and were represented by four taxonomical orders. The most abundant genus was *Sphingomonas* (*Sphingomonadales*) followed by bacteria affiliated to various other lineages, such as *Bradyrhizobium, Methylobacterium* (*Rhizobiales*), *Acidiphilium* (*Rhodospirillales*) and *Sandarakinorhabdus* (*Sphingomonadales*). Other proteobacterial genera among the generalists were *Limnobacter, Aquincola*, *Piscinibacter, Massilia* and *Rhizobacter* (*Betaproteobacteria*). Generalists assigned to other phyla were, e.g. *Chthoniobacter* (*Verrucomicrobia*), *Ferruginibacter, Pedobacter* and *Mucilaginibacter* (*Bacteroidetes*) and *Jatrophihabitans* and *Marmoricola* (*Actinobacteria*), among others.

Bark, moss and lichen specimens revealed 49, 31 and 29 OTUs, respectively, as putative specialists. Yet, moss specialists were taxonomically more diverse than the other two

habitats. Specialists on bark were mainly assigned to the phyla *Proteobacteria* (mainly *Alphaproteobacteria)*, *Actinobacteria* and *Acidobacteria* with high abundant genera such as *Asticcacaulis, Sphingomonas* and *Rhodovastum* (*Alphaproteobacteria*), *Burkholderia* and *Achromobacter* (*Betaproteobacteria*), *Pseudomonas* (*Gammaproteobacteria*), *Bryocella* (*Acidobacteria*), *Jatrophihabitans and Actinomycetospora* (*Actinobacteria*). Contrary, moss-specific OTUs were mainly assigned to *Bacteroidetes* such as *Spirosoma, Ferruginibacter,* and *Mucilaginibacter*, followed by *Proteobacteria* (mainly *Beta-*, and *Deltaproteobacteria*) like *Sorangium* and *Haliangium* and genera within *Planctomycetes*. *Lobaria* specialists belonged mainly to *Proteobacteria*, especially *Alphaproteobacteria*, represented by genera such as *Sphingomonas* and *Acidiphilium.* Notably, sequences of the lichen specific strain LAR1 (Lichen-associated-*Rhizobiales* 1) did not cluster with the representative sequences of the lichen specific *Rhizobiales* OTUs. In contrast, *Chthoniobacterales* (*Verrucomicrobia)* was highly abundant among the lichen specialists. The most abundant specialist of lichens, however, was *Mucilaginibacter* (*Bacteroidetes*). While two rare abundant OTUs assigned to the genus *Nostoc* (*Cyanobacteria*) were identified as putative lichen specialists, there was a common share of abundant cyanobacterial OTUs among mosses and lichens.

About 68% of the cyanobacterial OTUs were assigned to the genus *Nostoc* and 30% of them were exclusively shared between mosses and lichens, but generally *Nostoc* were proportionally more abundant on lichen species. Although *Leptolyngbya* sp. and *Gloeotrichia* sp. were also shared by mosses and lichens, both of these genera appeared to be more abundant on mosses. Representative sequences of cyanobacterial OTUs were additionally analyzed with BLASTn (NCBI nt database) for a more detailed characterization. According to these analyses, most of the sequences showed a high similarity (95-99%) to *Nostoc punctiforme* strain PCC73102. Of the low abundance cyanobacteria, an uncultured bacterium (according to SILVA database release 119) had high similarity (98%) to the species *Oscillatoria nigro-viridis* (*Oscillatoriales*) and another one to *Calochaete cimrmanii* (*Nostocales*). Moreover, the representative sequence of *Leptolyngbya* sp. (SILVA database, release 119) was assigned to *Spirulina* (*Oscillatoriales*, 89% similarity) based on the BLASTn search.

Co-occurrence patterns of *Alphaproteobacteria* differ for each habitat

Co-occurrence patterns for each habitat were determined based on Spearman's correlations between bacterial taxa at species level. Robust and statistically significant correlations ($\rho \pm 0.7$; p-value < 0.001) were visualized in co-occurrence networks (Fig. 6). Overall, the networks consisted of 387, 478 and 314 nodes (bacterial species) and 1236, 1491 and 343 edges (node connections) for bark, moss and lichen co-occurrence patterns, respectively. Particularly, 24.2% (bark), 25.5% (moss) and 21.9% (lichen) of the nodes of each network belonged to *Alphaproteobacteria,* which was mainly represented by the orders *Rhizobiales, Rhodospirillales, Caulobacterales* and *Sphingomonadales.* Figure 6 shows that the bacteria co-occurrence networks differ to a great extent between the habitats. However, most co-occurrences (bark: 93%, moss: 75% and lichen: 80%) were positively correlated. Specifically, *Alphaproteobacteria* revealed 494, 517 and 101 positive correlations to other nodes on bark, moss and lichen, respectively, but comparatively few negative correlations (36, 169, 25).

Positive correlations between *Alphaproteobacteria* and other taxa in all three habitats were mainly associated to *Rhizobiales* (bark: 50%, moss: 51% and lichen: 56%). Across all habitats *Rhizobiales* was identified to positively co-occur with members assigned to seven other phyla, namely: *Acidobacteria*, *Actinobacteria*, *Proteobacteria* (*Alpha-*, *Beta-*, *Gamma-* and *Deltaproteobacteria*), *Bacteroidetes*, *Chloroflexi*, *Cyanobacteria* and *Verrucomicrobia*. *Rhodospirillales* also showed positive correlations to various phyla, whereas co-occurrences of *Sphingomonadales*, *Caulobacterales* and *Rhodobacterales* were restricted to two or three, with *Bacteroidetes* as common phylum among them. *Rickettsiales* co-occurred on both cryptogams with *Actinobacteria*, *Verrucomicrobia* and *Alphaproteobacteria*.

Negative correlations found in the moss- and lichen-associated bacterial communities were also mainly associated with the order *Rhizobiales* (moss: 62%, lichen: 56%). In contrast, most negative correlations on bark were assigned to *Rhodospirillales* (47%). Across all three habitats *Rhizobiales* correlated negatively with members assigned to *Acidobacteria, Actinobacteria, Chloroflexi* and *Alphaproteobacteria*, but also *Rhodospirillales* and *Caulobacterales* recurrently showed negative correlations with *Planctomycetes* or *Betaproteobacteria* over all habitats. While there were no clear patterns of co-occurrences between *Rhizobiales* and interacting nodes at deeper taxonomic level, *Rhodospirillales* and *Caulobacterales* also showed consistent negative associations at family level. Specifically,

Acetobacteraceae correlated negatively with members of *Planctomycetaceae*, and *Caulobacteraceae* with members of *Comamonadaceae* and *Burkholderiaceae*. *Rhodospirillales* and *Rhizobiales* members of the two cryptogams showed various negative correlations to members assigned to *Bacteroidetes* and *Verrucomicrobia*, especially *Cytophagales* and *Chthoniobacterales*. Finally, in case of the moss and lichen there were also negative correlations with the cyanobacterial genus *Nostoc* with *Bradyrhizobium* (*Rhizobiales*) and *Sphingobium* (*Sphingomonadales*).

Functional analysis of a generalist and a lichen specialist

To characterize the potential functional contributions of the generalist *Sphingomonas* and the lichen-associated specialist *Mucilaginibacter* to the lichen symbiosis we utilized the metagenome of *L. pulmonaria*. For a functional comparison between the two genera of interest, the reads were subsampled and visualized schematically in Figure 7. Hits assigned to functions within the primary metabolic pathways such as DNA, RNA or protein metabolism among others were indicated in grey and not examined in more detail. On the other hand, functional categories of potential interest were visualized as pie charts reflecting the relative contributions of each genus.

Genes attributed to both nitrogen (ammonia assimilation) and phosphate metabolisms were exclusively found for the generalist. In contrast, sulfur and iron metabolism was predominantly found for the specialist. In particular, a TonB-dependent receptor for iron acquisition was detected. Contrary to the specialist, *Sphingomonas* was involved in various pathways of aromatic compound metabolisms, such as transport and degradation of benzoate, catabolism of salicylate and gentisate or the degradation of phenylpropanoid compounds. However, *Mucilaginibacter* was only found to contribute to the degradation of n-phenylalkanoic acid. Both genera also differ in the detected secondary metabolites. While the generalist was exclusively found to produce the plant hormone auxin, the specialist was found to synthesize quinolinic acids and its derivates as biologically active compounds in metazoan cell defense and differentiation. Both genera were able to produce the vitamin biotin, whereas genes attributed to the synthesis of pyridoxine (vitamin B6) were only found for the generalist.

For the functional category virulence, disease and defense two main resistance mechanisms to antibiotics and toxic compounds were detected. The specialist exclusively encoded for beta-lactamases, whereas the generalist additionally had multidrug resistance efflux pumps and MLST. Additionally, integrated gene transfer elements (Bacteroides conjugative transposons) were detected for *Mucilaginibacter*. Genes attributed to oxidative stress response, such as catalases, glutathiones, or transcriptional regulators, were only found for the generalist.

Discussion

In the present study we have compared three adjoining microhabitats on tree trunks: lichen, moss and the bare bark. Previous works already demonstrated specificity of separated lichen- and moss-associated bacterial communities (Grube et al., 2009; Bragina et al., 2012). Here we have expanded these findings and integrated them to analyze inter-microbiome relationships among the two co-occurring representatives of phototrophic cryptogams and the tree bark. Our results clearly revealed overlaps in the community structures at all taxonomic ranks, with more complex patterns at deeper taxonomic resolution, which revealed OTUs shared among the habitats and those specific for each of the habitats.

Several potential generalists and specialists were identified for the selected environmental niches. The majority of the bacterial generalists belonged to *Alpha-* and *Betaproteobacteria*, mainly represented by the orders *Rhizobiales, Sphingomonadales and Burkholderiales*. *Sphingomonas* is a ubiquitously occurring and facultatively photosynthetic genus, which was recently also isolated from the endosphere of the maple species *Acer negundo* (Shen and Fulthorpe, 2015). While the quantitative distribution of the generalists was relatively uniform in all habitats, the potential specialists differed in both their taxonomic affiliation and relative abundances for each habitat. Specialists for bark and lichen specimens belonged mainly to *Proteobacteria* (especially *Alphaproteobacteria*). Members of *Rhizobiales* were shown to be particularly abundant in lichens. Previously, this order was linked to potential symbiotic functions, including provision of specific secondary metabolites and nutrient cycling in lichens (Erlacher et al., 2015; Grube et al., 2015). They are also well known for their nitrogen fixing symbiosis with plants (Long, 1989). *Burkholderia* and *Pseudomonas* (*Beta-* and *Gammaproteobacteria,* respectively*)* were generally detected in each habitat, but as specialist OTUs they were only identified on bark. *Burkholderia* species

are beneficial for plants by nitrogen fixation or aromatic compound degradation (Suárez-Moreno et al., 2012), and more recently, *Burkholderia* was also identified as member of the moss core microbiome with beneficial, but also potentially pathogenic features (Bragina et al., 2013). Moreover, *Burkholderia* and *Pseudomonas* isolated from lichens were also found to represent highly effective antagonists of certain bacterial and fungal pathogens (Cernava et al., 2015 a,b). Thus, an essential role of this bacterial fraction in pathogen defense and microbial community stabilization is very likely. On moss, specialists affiliated to *Proteobacteria* (*Deltaproteobacteria*) were less abundant than *Bacteroidetes*. While moss-associated *Bacteroidetes* specialists were highly diverse, lichen-associated specialists affiliated to this phylum were represented only by the genus *Mucilaginibacter,* which was also the most abundant specialist on lichens. However, members of *Mucilaginibacter* could serve as nutrient suppliers for other members within the microbial community or the host species itself as they are able to produce and release extracellular polysaccharides (Urai et al., 2008). Additionally, *Mucilaginibacter* is a potential contributor to the nutrient (re-)cycling because it can degrade various polysaccharides like pectin and hemicellulose (Pankratov et al., 2007). Specialists assigned to *Actinobacteria* were primarily found on bark, whereas only the genus *Pseudonocardia* was identified to occur specifically on moss. Members in this genus effectively produce antibiotics, and some strains are also known to provide important symbiotic functions: leaf-cutter ants carry them to ward off fungal pathogens in their nests (Zhang et al., 2007). While other studies already demonstrated the antagonistic potential of various moss-associated bacteria (Opelt et al., 2007), the specific roles of *Pseudonocardia* in this particular context remains to be elucidated.

Nostoc clusters were commonly shared between both cryptogams, but occurred in higher abundances on lichens. *Nostoc* is of particular importance for the lung lichen, as this genus is utilized as secondary photobiont for nitrogen fixation. The cyanobacterial colonies are recruited from external sources, primarily via uptake from the surface of the growing thallus to become finally integrated as internalized cephalodia, i.e. clustered *Cyanobacteria* in a fungal cover (Cornejo & Scheidegger 2013). Our results indicate that mosses may serve as rich reservoir of compatible *Nostoc* strains. This fits well with the common field observation that *Lobaria* develops readily on mosses over barks (unpublished observations). Since also other bacterial groups were shared by *L. pulmonaria* and *P. filiforme*, e.g. photosynthetically active *Sphingomonas,* we hypothesize that there might be a broader beneficial effect on the lichen establishment on mosses by additional associated bacteria. As both, lichens and mosses, are organisms that are well adapted to poikilohydric conditions, they might also share

further bacteria that tolerate periodic desiccation and production of reactive oxygen species (Beckett et al., 2003).

Comparison of the bacterial co-occurrence networks – for the first time connecting different neighboring habitats – revealed similarities as well as striking differences among them. Interestingly, more than 75% of all correlations were positive, suggesting fairly stable situations. In contrast to the primarily large concentrated clusters of bark- and moss-associated communities, the network structure for lichen-associated *Alphaproteobacteria* was relatively loose with several small networks comprising few nodes. The reasons for these differences can be diverse and require further research, including complementary microscopic studies. According to our FISH-CLSM analyses of the lung lichen thalli (Grube et al., 2015; Erlacher et al., 2015), we can confirm that *Alphaproteobacteria* are forming larger colonies on the lichen surface, whereas other eubacteria are usually present in much smaller clusters (see also Fig. 1 B). We argue that this pattern could explain the observed loose network, that could result from a strict control of bacterial colonization on the lichen.

The generalist functions include metabolism of primary goods shared in microbial symbioses. Production of hormones such as auxin is useful in broad spectrum of symbioses with photosynthetic eukaryotes such as plants, mosses and likely algae. The same holds true for phosphate solubilization and ammonia assimilation. The generalist also has a greater range of aromatic compound metabolism, which agrees with a wide range of such compounds in mosses, lichens, and tree bark. The specialist has a more restricted capacity in this respect, and revealed more specific defense functions than found in the generalist. The latter also shows general signatures of responses to oxidative stress, which is of prevalent periodicity in the entire habitat. The segregation of potentially beneficially functions between generalist and specialist bacterial associates is of particular interest for ecology in a wider sense. Specialists rely only their genuine host as natural reservoir, thus the nearby conspecifics of the same host may share beneficial strains to contribute to ecological continuity. Generalists, on the other hand, can be shared among very different hosts, and might have a higher functional redundancy, to facilitate the maintenance of a convivial host community. A narrow spatial pattern of diverse hosts thus is optimal to keep a valuable mix of generalist and specialist bacterial fractions for sustaining a healthy community of hosts.

By now, only a few studies dealt with inter-microbiome relationships of different environmental habitats. While host-associated bacterial microbiomes are well known for different plant species and are shown to be clearly different from surrounding soil

communities (e.g., Knief et al., 2012; Vorholt, 2012; Bragina et al., 2014, Berg et al., 2014), more recently, also fluctuations and shifts in the community structures were detected among neighboring plants (Schlatter et al. 2015). Warmink and colleagues (2009) showed that there are also species-specific bacteria associated with the mycospheres of different basidiomycetous fungi compared to the corresponding bulk soils, which might be due to their capability to utilize specific fungal compounds. Bjelland et al. (2010) compared lichen-associated bacteria with those of the subtending rock substrate using clone library sequencing. Their study showed a higher diversity of bacteria in the rocks than in the lichen thalli, whereas the abundance of certain bacteria is significantly increased in lichens. However, this study cannot be compared directly with our present work. The slow growing rock-inhabiting crust-forming lichens analyzed by Bjelland et al. are tightly attached to the rock surface with the entire thallus, which influenced the sampled substrate beneath.

In the present study, *Lobaria pulmonaria* was sampled from separate, yet more or less neighboring locations on the bark (the mosses were not influenced by any products from the lichen). As the lung lichen is very frequently found to grow over mosses, we recognize facilitative effects, as suggested for soil lichens (Colesie et al. 2012), where physiological or microclimatic benefits result in facilitation of lichens. We think that this concept could be extended to include the host-associated microbiomes, as lichens may apparently recruit cyanobacteria (and likely other bacteria) from mosses for facilitated establishment. Hence, we argue that a specific share of bacteria associated with different hosts (even representing different kingdoms) could have positive effects on the overall fitness of the hosts in their common environment. The study of inter-microbiome relationships may therefore also provide valuable information on the stability of co-occurring host communities. Up to the present date there are only a few examples of synergisms among microbiomes, which have shown that there are important relationships between adjoining microbiomes (e.g. the root-soil connection, or food-human gut connection; Berg et al., 2014; David et al., 2014). With our contribution, we hope to raise interest in studying inter-microbiome relationships in a wider context as these may have a broad ecological significance in nature.

Acknowledgments

This work was supported by a grant of the Austrian and German Science Foundation to GB and MG (FWF-DACH Project I882).

Conflict of Interest

The authors of this paper declare no conflict of interest.

References

Amann RI, Binder BJ, Olson RJ, Chisholm SW, Devereux R, Stahl DA. (1990). Combination of 16S rRNA-targeted oligonucleotide probes with flow cytometry for analyzing mixed microbial populations. *Appl Environ Microbiol* **56**: 1919–1925.

Aschenbrenner IA, Cardinale M, Berg G, Grube M. (2014). Microbial cargo: do bacteria on symbiotic propagules reinforce the microbiome of lichens? *Environ Microbiol* **16**: 3743–52.

Bates ST, Cropsey GW, Caporaso JG, Knight R, Fierer N. (2011). Bacterial communities associated with the lichen symbiosis. *Appl Environ Microbiol* **77**: 1309–1314.

Beckett RP, Minibayeva FV, Vylegzhanina NN, Tolpysheva T. (2003). High rates of extracellular superoxide production by lichens in the suborder *Peltigerineae* correlate with indices of high metabolic activity. *Plant Cell Environ* **26**: 1827–1837.

Berg G, Grube M, Schloter M, Smalla K. (2014). Unraveling the plant microbiome: looking back and future perspectives. *Front Microbiol* **5**: 148.

Berg G, Smalla K. (2009). Plant species and soil type cooperatively shape the structure and function of microbial communities in the rhizosphere. *FEMS Microbiol Ecol* **68**: 1–13.

Berg G. (2015). Beyond borders: investigating microbiome interactivity and diversity for advanced biocontrol technologies. *Microb Biotechnol* **8**: 5–7.

Bjelland T, Grube M, Hoem S, Jorgensen SL, Daae FL, Thorseth IH, *et al.* (2010). Microbial metacommunities in the lichen-rock habitat. *Environ Microbiol* **3**: 434–442.

Blaser M, Bork P, Fraser C, Knight R, Wang J. (2013). The microbiome explored: recent insights and future challenges. *Nat Rev Microbiol* **11**: 213–7.

Bragina A, Berg C, Cardinale M. Shcherbakov A, Chebotar V, Berg G. (2012). *Sphagnum* mosses harbour highly specific bacterial diversity during their whole lifecycle. *ISME J* **6**: 802–813.

Bragina A, Cardinale M, Berg C, Berg G. (2013). Vertical transmission explains the specific *Burkholderia* pattern in *Sphagnum* mosses at multi-geographic scale. *Front Microbiol* **4**: 394.

Bragina A, Oberauner-Wappis L, Zachow C, Halwachs B, Thallinger GG, Müller H, *et al.* (2014). The *Sphagnum* microbiome supports bog ecosystem functioning under extreme conditions. *Mol Ecol* **23**: 4498–4510.

Buchfink B, Xie C, & Huson DH. (2014). Fast and sensitive protein alignment using DIAMOND. *Nat methods* **12**: 59-60

Caporaso JG, Kuczynski J, Stombaugh J, Bittinger K, Bushman FD, Costello EK, *et al.* (2010). QIIME allows analysis of high-throughput community sequencing data. *Nat Methods* **7**: 335–336.

Caporaso JG, Lauber CL, Walter WA, Berg-Lyons D, Lozupone CA, Turnbaugh PJ, *et al.* (2011). Global patterns of 16S rRNA diversity at a depth of millions of sequences per sample. *Proc Natl Acad Sci USA* **108**: 4516–4522.

Cardinale M, De Castro JV, Müller H, Berg G, Grube M. (2008). *In situ* analysis of the bacterial community associated with the reindeer lichen *Cladonia arbuscula* reveals predominance of *Alphaproteobacteria*. *FEMS Microbiol Ecol* **66**: 63–71.

Cardinale M, Puglia AM, Grube M. (2006). Molecular analysis of lichen-associated bacterial communities. *FEMS Microbiol Ecol* **57**: 484–95.

Cernava T, Aschenbrenner IA, Grube M, Liebminger S, Berg G. (2015 a). A novel assay for the detection of bioactive volatiles evaluated by screening of lichen-associated bacteria. *Front Microbiol* **6**: 398.

Cernava T, Mueller H, Aschenbrenner IA, Grube M, Berg G. (2015 b). Analyzing the antagonistic potential of the lichen microbiome against pathogens by bridging metagenomic with culture studies. *Front Microbiol* **6**: 620.

Colesie C, Scheu S, Green TG, Weber B, Wirth R, Büdel B. (2012). The advantage of growing on moss: facilitative effects on photosynthetic performance and growth in the cyanobacterial lichen *Peltigera rufescens*. *Oecol* **169**: 599–607.

Cornejo C, Scheidegger C. (2013). New morphological aspects of cephalodium formation in the lichen *Lobaria pulmonaria* (*Lecanorales, Ascomycota*). *Lichenologist* **45**: 77–87.

Daims H, Brühl A, Amann R, Schleifer KH, Wagner M. (1999). The domain-specific probe EUB338 is insufficient for the detection of all Bacteria: Development and evaluation of a more comprehensive probe set. *Syst and Appl Microbiol* **22**: 434–444.

David LA, Maurice CF, Carmody RN, Gootenberg DB, Button JE, Wolfe BE, *et al*. (2014). Diet rapidly and reproducibly alters the human gut microbiome. *Nature* **505**: 559–563.

De Bary A. (1879). Die Erscheinung der Symbiose. Strasbourg.

Edgar RC. (2010). Search and clustering orders of magnitude faster than BLAST. *Bioinformatics* **26**: 2460–2461.

Erlacher A, Cernava T, Cardinale M, Soh J, Sensen CW, Grube M, *et al.* (2015). *Rhizobiales* as functional and endosymbiontic members in the lichen symbiosis of *Lobaria pulmonaria* L. *Front Microbiol* **6**: 53.

Frey-Klett P, Garbaye J, Tarkka M. (2007). The mycorrhiza helper bacteria revisited. *New Phytol* **176**: 22–36.

Grube M, Cardinale M, Vieira de Castro J, Müller H, and Berg G. (2009). Species-specific structural and functional diversity of bacterial communities in lichen symbiosis. *ISME J* **3**: 1105–1115.

Grube M, Cernava T, Soh J, Fuchs S, Aschenbrenner I, Lassek C, *et al.* (2015). Exploring functional contexts of symbiotic sustain within lichen-associated bacteria by comparative omics. *ISME J* **9**: 412–424.

Hodkinson BP, Gottel NR, Schadt CW, Lutzoni F. (2012). Photoautotrophic symbiont and geography are major factors affecting highly structured and diverse bacterial communities in the lichen microbiome. *Environ Microbiol* **14**: 147–61.

Huson DH, Mitra S, Weber N, Ruscheweyh H, Schuster SC. (2011). Integrative analysis of environmental sequences using MEGAN4. *Genome Res* **21**: 1552–1560.

Knief C, Delmotte N, Chaffron S, Stark M, Innerebner G, Wassmann R, *et al.* (2012). Metaproteogenomic analysis of microbial communities in the phyllosphere and rhizosphere of rice. *ISME J* **6**: 1378–1390.

Larkin MA, Blackshields G, Brown NP, Chenna R, McGettigan PA, McWilliam H, *et al.* (2007). Clustal W and Clustal X version 2.0. *Bioinformatics* **23**: 2947–2948.

Leff JW, Del Tredici P, Friedman WE, Fierer N. Spatial structuring of bacterial communities within individual *Ginkgo biloba* trees. *Environ Microbiol* 2014; e-pub ahead of print 3 Nov 2014, doi: 10.1111/1462-2920.12695.

Lindo Z, Whiteley JA. (2011). Old trees contribute bio-available nitrogen through canopy bryophytes. *Plant and Soil* **342**: 141–148.

Long SR. (1989). *Rhizobium*-legume nodulation: Life together in the underground. *Cell* **56**: 203–214.

Loy A, Maixner F, Wagner M, Horn M. (2007). probeBase - an online resource for rRNA-targeted oligonucleotide probes: new features 2007. *Nucleic Acids Res* **35**: 800–804.

Lozupone C, Knight R. (2005). UniFrac: a new phylogenetic method for comparing microbial communities. *Appl Environ Microbiol* **71**: 8228–8235.

Lundberg DS, Yourstone S, Mieczkowski P, Jones CD, Dangl JL. (2013). Practical innovations for high-throughput amplicon sequencing. *Nat Methods* **10**: 999–1002.

Millbank JW, Kershaw KA. (1970). Nitrogen metabolism in lichens III. Nitrogen fixation by internal cephalodia in *Lobaria pulmonaria*. *New Phytol* **69**: 595–597.

Mushegian AA, Peterson CN, Baker CC, Pringle A. (2011). Bacterial diversity across individual lichens. *Appl Environ Microbiol* ***77***: 4249–4252.

Neef A. (1997). Anwendung der in situ Einzelzell-Identifizierung von Bakterien zur Populationsanalyse in komplexen mikrobiellen Biozönosen. Doctoral thesis (Technische Universität München).

Opelt K, Berg C, Schönmann S, Eberl L, Berg G. (2007). High specificity but contrasting biodiversity of *Sphagnum*-associated bacterial and plant communities in bog ecosystems independent of the geographical region. *ISME J* **1**: 502–16.

Opelt K, Berg G. (2004). Diversity and antagonistic potential of bacterial associated with bryophytes from nutrient-poor habitats of the Baltic Sea coast. *Appl Environ Microbiol* **70**: 6569–6579.

Overbeek R, Begley T, Butler RM, Choudhuri JV, Chuang HY, Cohoon M, *et al*. (2005). The subsystems approach to genome annotation and its use in the project to annotate 1000 genomes. *Nucleic Acids Res* **33**: 5691–702.

Pankratov TA, Tindall BJ, Liesack W, Dedysh SN. (2007). *Mucilaginibacter paludis* gen. nov., sp. nov. and *Mucilaginibacter gracilis* sp. nov., pectin-, xylan-and laminarin-degrading members of the family *Sphingobacteriaceae* from acidic *Sphagnum* peat bog. *Int J Syst Evol Microbiol* **57**: 2349–2354.

Pruesse E, Quast C, Knittel K, Fuchs BM, Ludwig WG, Peplies J, *et al.* (2007). SILVA: a comprehensive online resource for quality checked and aligned ribosomal RNA sequence data compatible with ARB. *Nucleic Acids Res* **35**: 7188–7196.

R Core Team. (2013). R: A language and environment for statistical computing. R Foundation for Statistical Computing, Vienna, Austria.

Schlatter DC, Bakker MG, Bradeen JM, Kinkel LL. (2015). Plant community richness and microbial interactions structure bacterial communities in soil. *Ecology* **96**: 134–142.

Shannon P, Markiel A, Ozier O, Baliga NS, Wang JT, Ramage D, *et al.* (2003). Cytoscape: a software environment for integrated models of biomolecular interaction networks. *Genome Res* **13**: 2498–2504.

Shen SY, Fulthorpe R. (2015). Seasonal variation of bacterial endophytes in urban trees. *Front Microbiol* **6**: 427

Sigurbjörnsdóttir MA, Andrésson ÓS, Vilhelmsson O. (2015). Analysis of the *Peltigera membranacea* metagenome indicates that lichen-associated bacteria are involved in phosphate solubilization. *Microbiology* **161**: 989–96.

Suárez-Moreno ZR, Caballero-Mellado J, Coutinho BG, Mendonça-Previato L, James EK, Venturi V. (2012). Common features of environmental and potentially beneficial plant-associated *Burkholderia*. *Microb Ecol* **63**: 249–266.

Tani A, Akita M, Murase H, Kimbara K. (2011). Culturable bacteria in hydroponic cultures of moss *Racomitrium japonicum* and their potential as biofertilizers for moss production. *J Biosci Bioeng* **112**: 32–39.

Tschermak-Woess E. (1995). *Dictyochloropsis splendida* (*Chlorophyta*), the correct phycobiont of *Phlyctis argena* and the high degree of selectivity or specificity involved. *Lichenologist* **27**: 169–187.

Urai M, Aizawa T, Nakagawa Y, Nakajima M, Sunairi M. (2008). *Mucilaginibacter kameinonensis* sp., nov., isolated from garden soil. *Int J Syst Evol Microbiol* **58**: 2046–2050.

Vorholt JA. (2012). Microbial life in the phyllosphere. *Nat Rev Microbiol* **10**: 828–840.

Wallner G, Amann R, Beisker W. (1993). Optimizing fluorescent in situ hybridization with rRNA-targeted oligonucleotide probes for flow cytometric identification of microorganisms. *Cytometry* **14**: 136–143.

Warmink JA, Nazir R, van Elsas JD. (2009). Universal and species-specific bacterial 'fungiphiles' in the mycospheres of different basidiomycetous fungi. *Environ Microbiol* **11**: 300–312

Zhang MM, Poulsen M, Currie CR. (2007). Symbiont recognition of mutualistic bacteria by Acromyrmex leaf-cutting ants. *ISME J* **1**: 313–320.

Zhang Z, Schwartz S, Wagner L, Miller W. (2000). A greedy algorithm for aligning DNA sequences. *J Comput Biol* **7**: 203–214.

Data Accessibility

All data represented in this study have been deposited in the NCBI Sequence Read Archive and are accessible through the Accession number PRJNA290145.

Figure legends

Figure 1: A) Macroscopic picture of a maple tree indicating the adjacent (micro-)habitats: *L. pulmonaria* (L.) Hoffm., *P. filiforme (*Hedw.) and tree bark of *Acer pseudoplatanus* (L.); B) Confocal laser scanning microscopy of a *L. pulmonaria* cross-section. *Alphaproteobacteria* (yellow) and other eubacteria (red) colonize the upper and lower cortex of the lichen thallus. C) Stitched panorama micrograph showing in situ growth and interaction of moss and lichen.

Figure 2: Two dimensional PCoA plots of the three habitats based on weighted Unifrac distance matrix. Red: bark samples; orange: moss samples and blue: lichen samples; significance of sample groupings (bark, moss and lichen) based on Adonis $p \leq 0{,}001$.

Figure 3: iTOL tree of the eight most abundant bacterial phyla across the habitats. Bootstrapped neighbor-joining tree based on clustalX alignment. An additional heatmap represents the sequence abundances of each taxon and habitat.

Figure 4: Heatmap of the most abundant families across all three habitats. Relative abundances of each family were visualized in a heatmap.

Figure 5: Specialists and generalists on bark, lichen and moss summarized at family level.

Figure 6: Co-occurrence network of *Alphaproteobacteria* for each habitat. A: co-occurrence on bark, B: on moss and C: on lichen. Nodes represent taxa on species level (colors: species assigned to *Alphaproteobacteria* blue; other species grey; size: reflects degree of connections between nodes). Edges represent the positive or negative connections (green and red, respectively) based on Spearman's correlation (±0.7; $p \leq 0.001$).

Figure 7: Scheme of the functional assignments based on SEED-classification to a generalist *Mucilaginibacter* (*Bacteroidetes*) and a lichen specialist *Sphingomonas* (*Proteobacteria*). Functional categories of interest were visualized as pie charts representing the relative contributions of two genera to each category. Functions associated with the primary metabolism and other categories are indicated in grey.

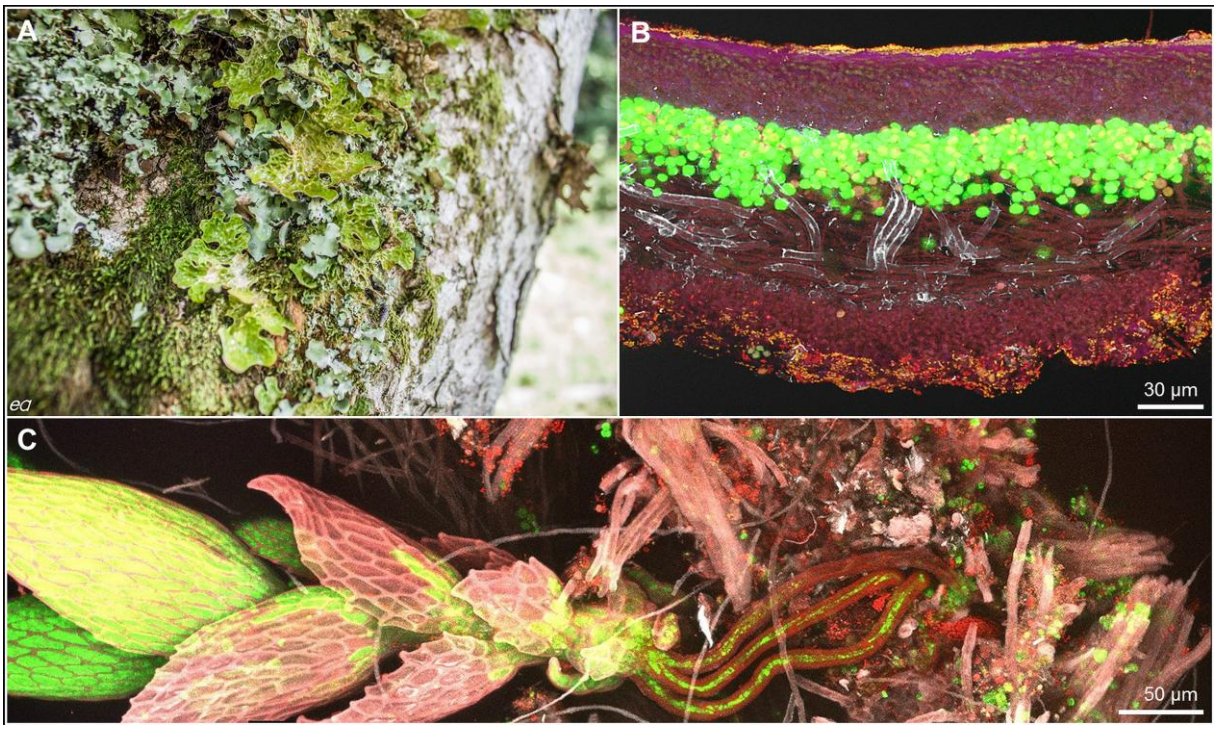

Figure 1

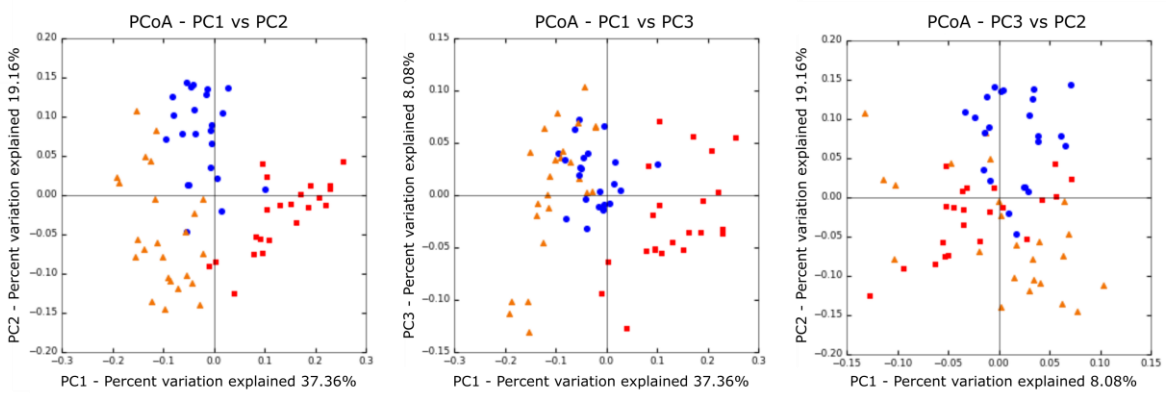
PCoA - PC1 vs PC2
PC2 - Percent variation explained 19.16%
PC1 - Percent variation explained 37.36%
PCoA - PC1 vs PC3
PC3 - Percent variation explained 8.08%
PC1 - Percent variation explained 37.36%
PCoA - PC3 vs PC2
PC2 - Percent variation explained 19.16%
PC1 - Percent variation explained 8.08%

Figure 2

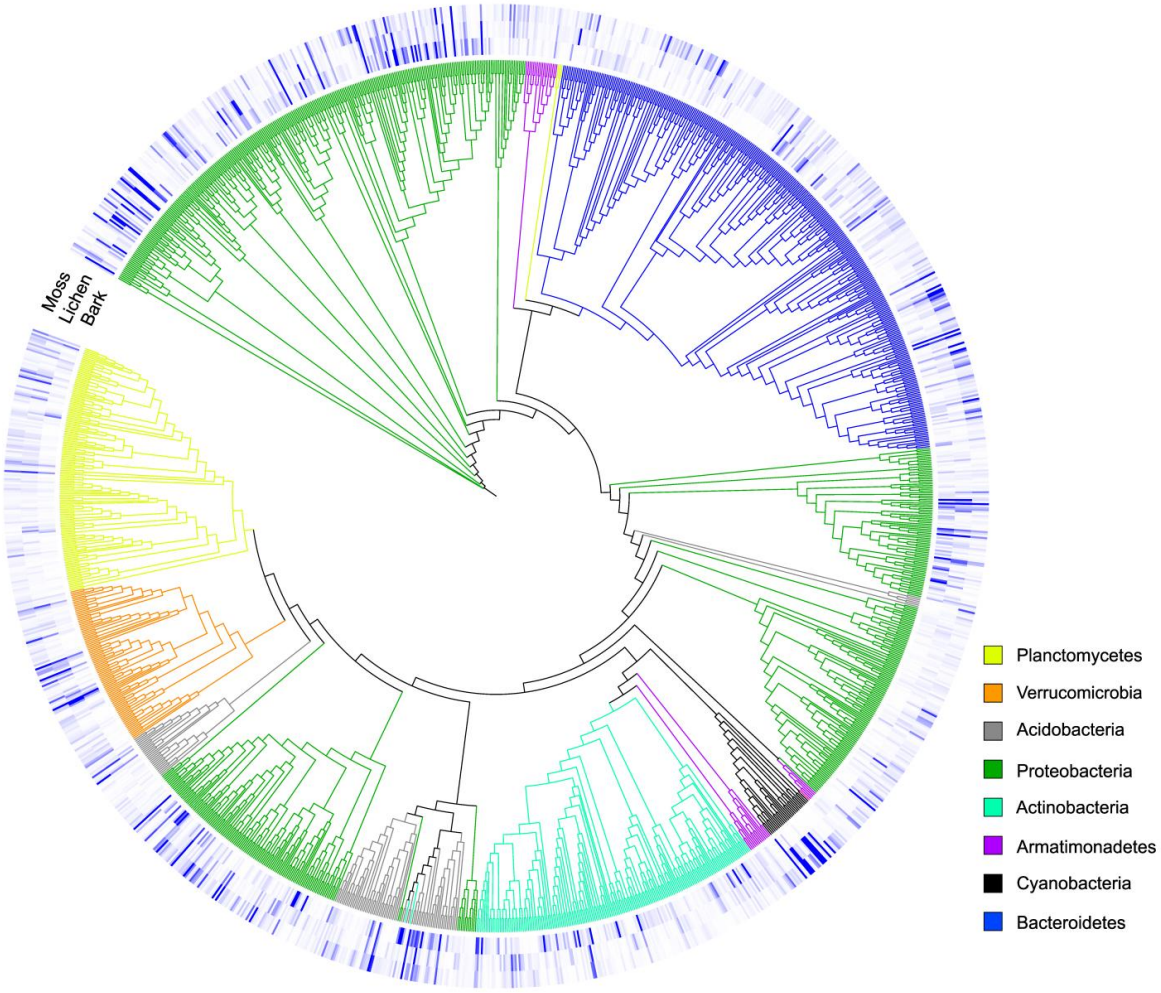
Moss
Lichen
Bark
Planctomycetes
Verrucomicrobia
Acidobacteria
Proteobacteria
Actinobacteria
Armatimonadetes
Cyanobacteria
Bacteroidetes

Figure 3

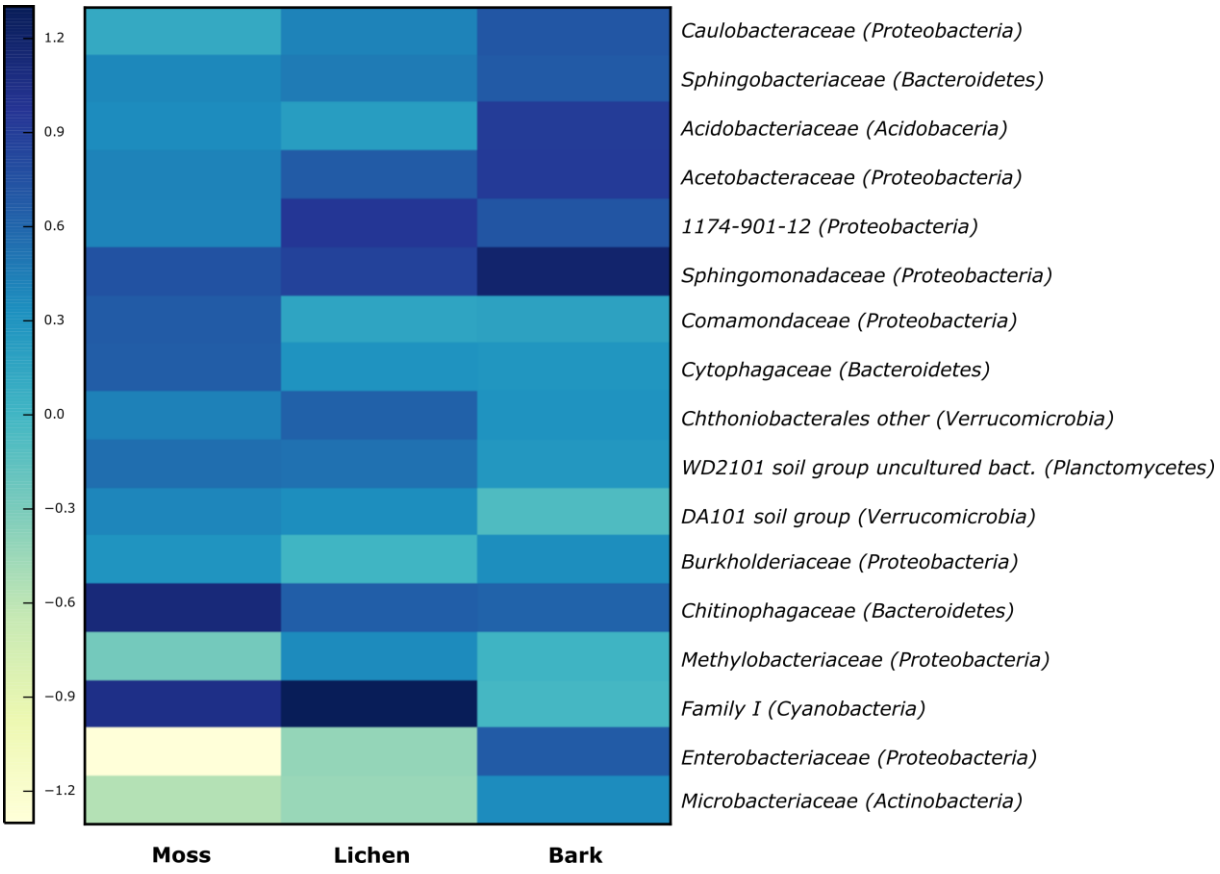
1.2
0.9
0.6
0.3
0.0
−0.3
−0.6
−0.9
−1.2
Caulobacteraceae (Proteobacteria)
Sphingobacteriaceae (Bacteroidetes)
Acidobacteriaceae (Acidobaceria)
Acetobacteraceae (Proteobacteria)
1174-901-12 (Proteobacteria)
Sphingomonadaceae (Proteobacteria)
Comamondaceae (Proteobacteria)
Cytophagaceae (Bacteroidetes)
Chthoniobacterales other (Verrucomicrobia)
WD2101 soil group uncultured bact. (Planctomycetes)
DA101 soil group (Verrucomicrobia)
Burkholderiaceae (Proteobacteria)
Chitinophagaceae (Bacteroidetes)
Methylobacteriaceae (Proteobacteria)
Family I (Cyanobacteria)
Enterobacteriaceae (Proteobacteria)
Microbacteriaceae (Actinobacteria)
Moss
Lichen
Bark

Figure 4

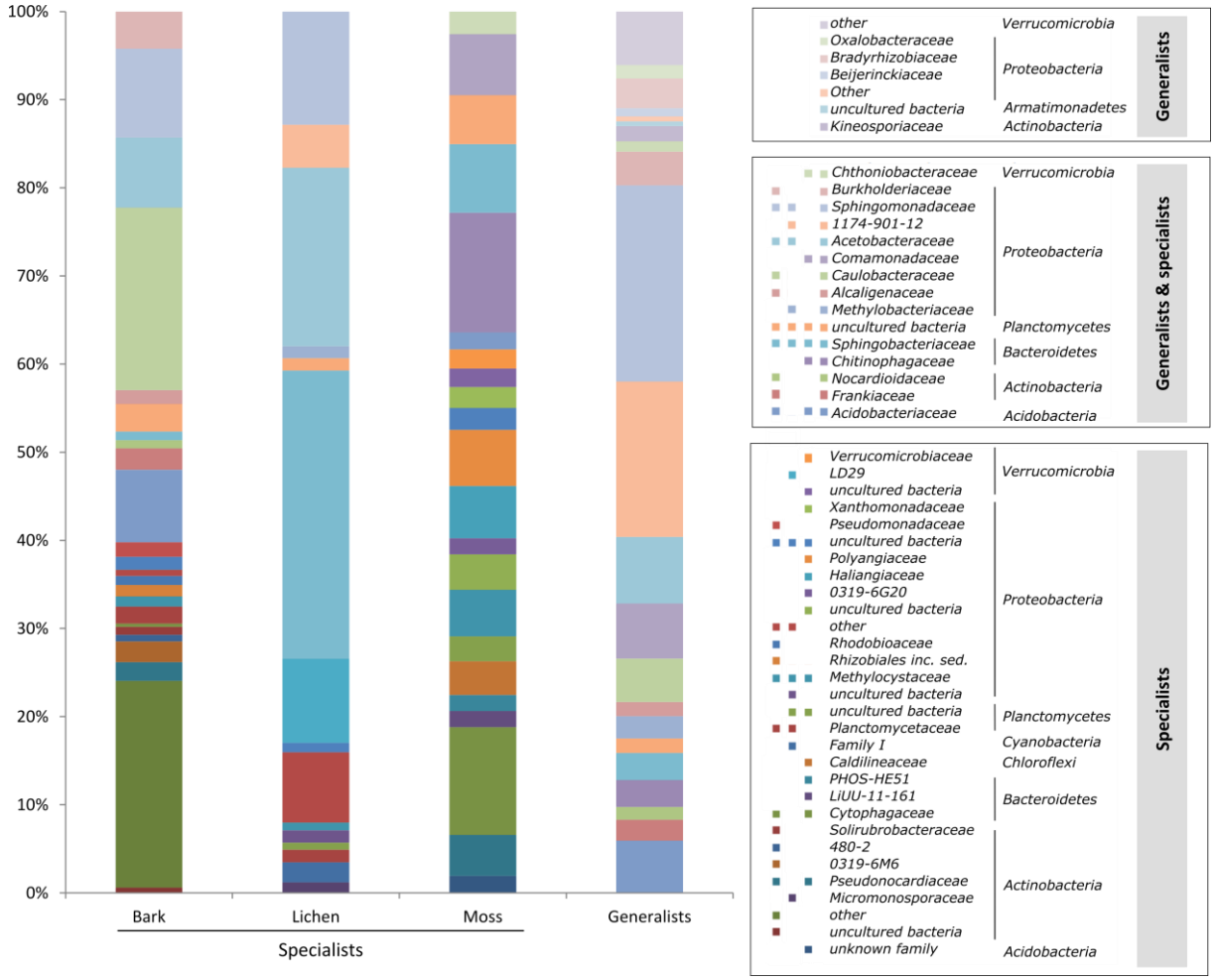
100%
90%
80%
70%
60%
50%
40%
30%
20%
10%
0%
Bark
Lichen
Moss
Generalists
Specialists
other
Oxalobacteraceae
Bradyrhizobiaceae
Beijerinckiaceae
Other
uncultured bacteria
Kineosporiaceae
Verrucomicrobia
Proteobacteria
Armatimonadetes
Actinobacteria
Generalists
Chthoniobacteraceae
Burkholderiaceae
Sphingomonadaceae
1174-901-12
Acetobacteraceae
Comamonadaceae
Caulobacteraceae
Alcaligenaceae
Methylobacteriaceae
uncultured bacteria
Sphingobacteriaceae
Chitinophagaceae
Nocardioidaceae
Frankiaceae
Acidobacteriaceae
Verrucomicrobia
Proteobacteria
Planctomycetes
Bacteroidetes
Actinobacteria
Acidobacteria
Generalists & specialists
Verrucomicrobiaceae
LD29
uncultured bacteria
Xanthomonadaceae
Pseudomonadaceae
uncultured bacteria
Polyangiaceae
Haliangiaceae
0319-6G20
uncultured bacteria
other
Rhodobioaceae
Rhizobiales inc. sed.
Methylocystaceae
uncultured bacteria
uncultured bacteria
Planctomycetaceae
Family I
Caldilineaceae
PHOS-HE51
LiUU-11-161
Cytophagaceae
Solirubrobacteraceae
480-2
0319-6M6
Pseudonocardiaceae
Micromonosporaceae
other
uncultured bacteria
unknown family
Verrucomicrobia
Proteobacteria
Planctomycetes
Cyanobacteria
Chloroflexi
Bacteroidetes
Actinobacteria
Acidobacteria
Specialists

Figure 5

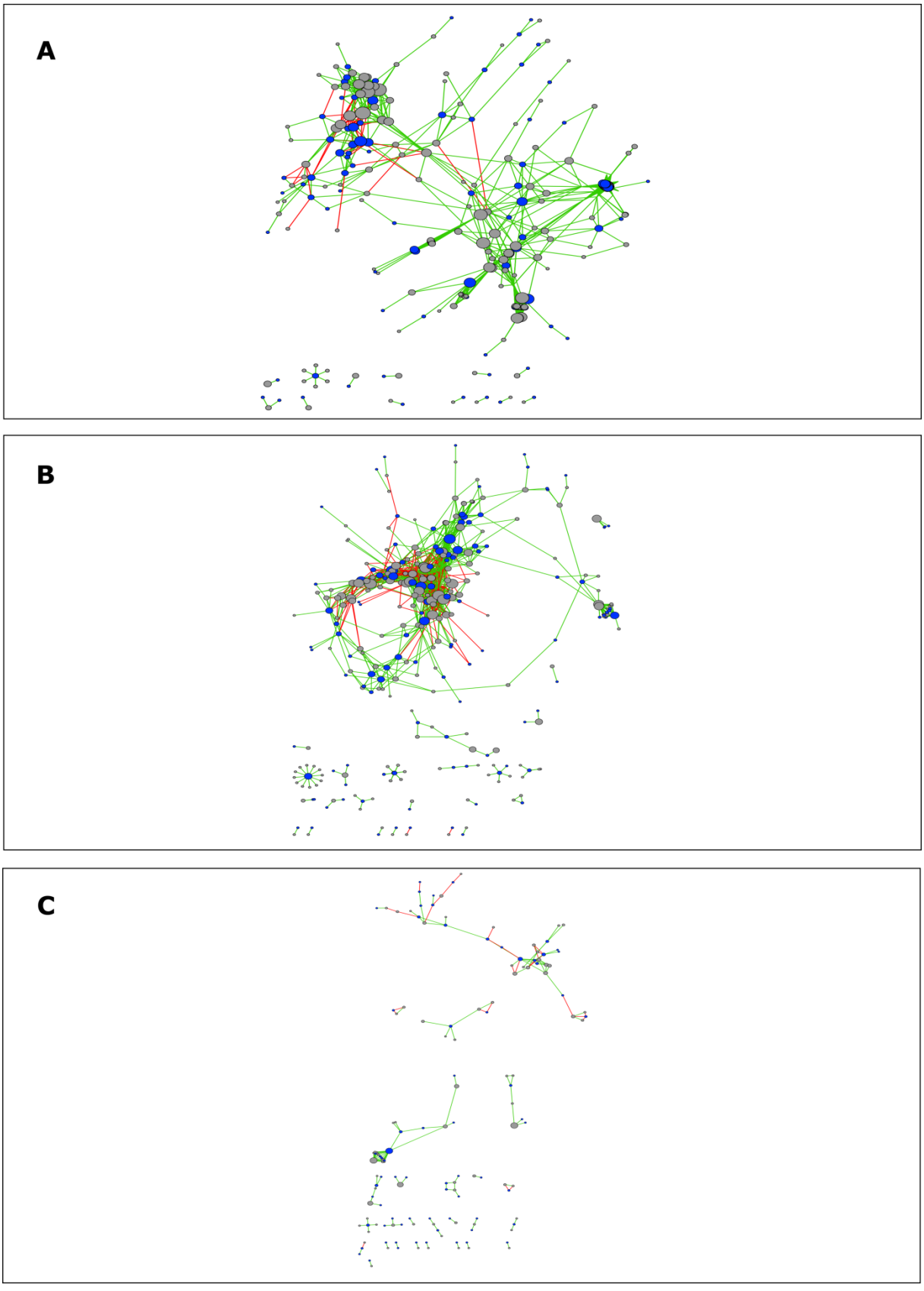

Figure 6

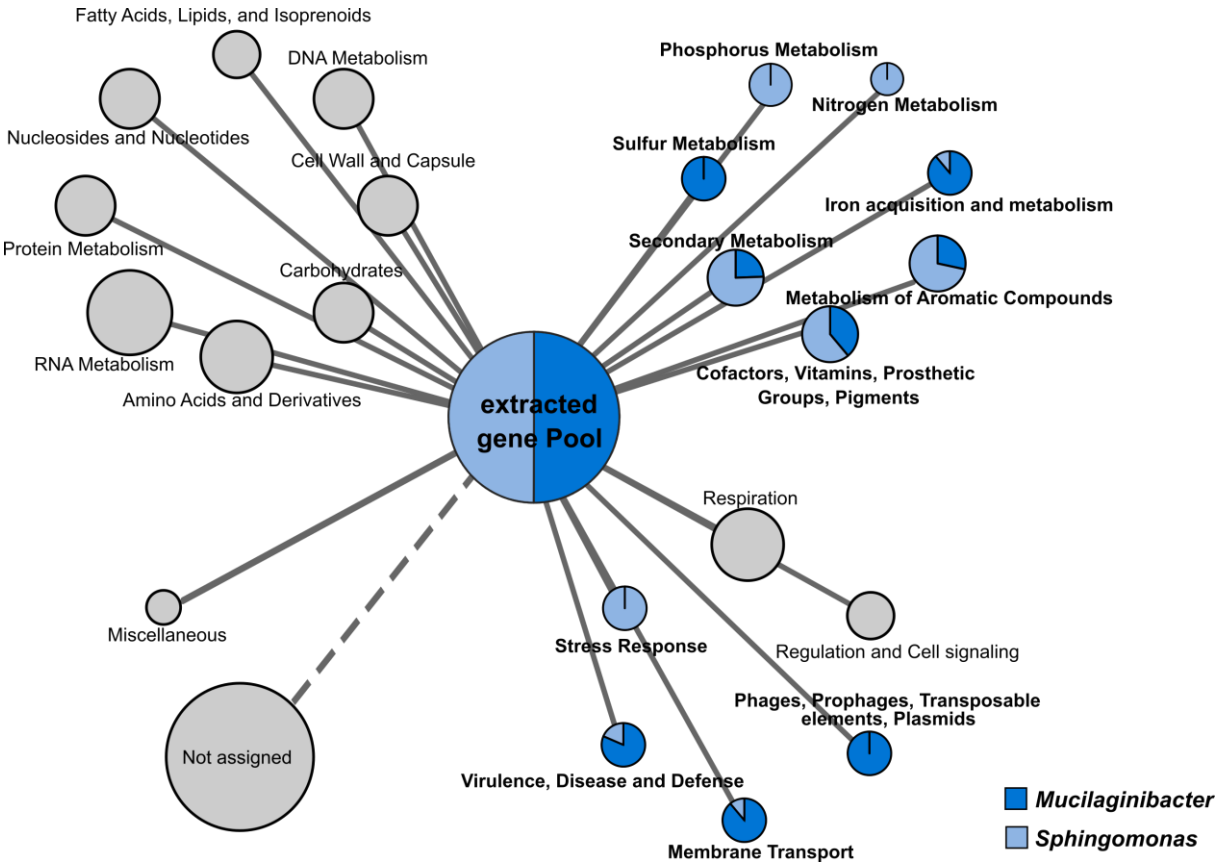
Fatty Acids, Lipids, and Isoprenoids
DNA Metabolism
Nucleosides and Nucleotides
Cell Wall and Capsule
Protein Metabolism
Carbohydrates
RNA Metabolism
Amino Acids and Derivatives
extracted gene Pool
Phosphorus Metabolism
Nitrogen Metabolism
Sulfur Metabolism
Iron acquisition and metabolism
Secondary Metabolism
Metabolism of Aromatic Compounds
Cofactors, Vitamins, Prosthetic Groups, Pigments
Respiration
Miscellaneous
Stress Response
Regulation and Cell signaling
Phages, Prophages, Transposable elements, Plasmids
Not assigned
Virulence, Disease and Defense
Membrane Transport
Mucilaginibacter
Sphingomonas

Figure 7

Manuscript I – Supplementary Data

Supplementary Figure

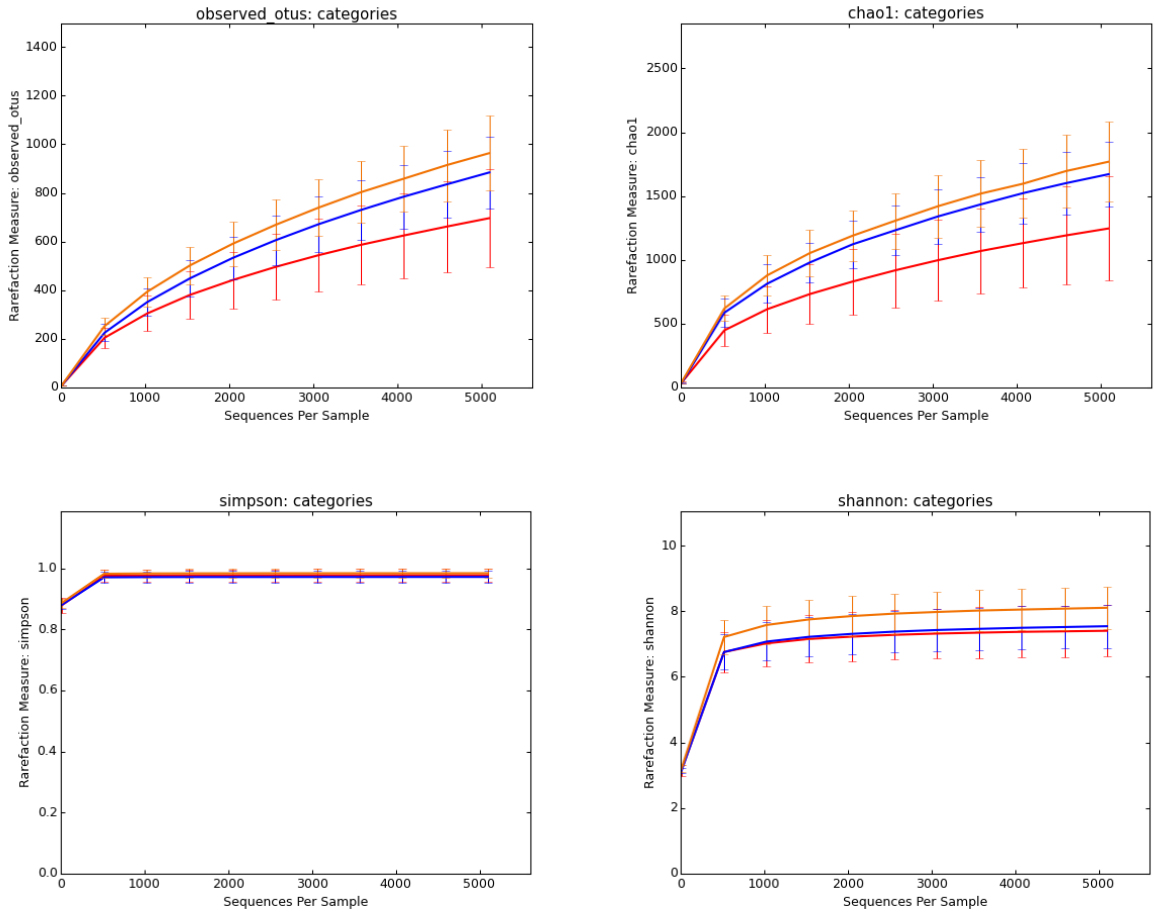

Figure S1: Alpha diversity indices of the pooled bark, moss and lichen samples. Bark: red, Moss: orange, Lichen: blue

Supplementary Table

Table S1: Alpha diversity indices at 94% sequence identity

Sample ID	observed OTUs	chao1	coverage	Simpson	Shannon
Moss					
BC49	1204.7	2299.0	52.4	0.996	9.0
BC50	1161.1	2122.3	54.7	0.996	9.0
BC51	1118.6	1878.1	59.6	0.993	8.7
BC52	904.4	1579.3	57.3	0.992	8.3
BC61	820.2	1557.9	52.6	0.989	7.8
BC62	956.6	1711.5	55.9	0.991	8.3
BC63	813.7	1407.5	57.8	0.987	7.9
BC64	752.9	1321.4	57.0	0.988	7.8
BC73	1155.8	2254.6	51.3	0.995	8.8
BC74	1064.8	1937.6	55.0	0.995	8.7
BC75	1127.1	1982.7	56.8	0.995	8.8
BC76	1108.3	2128.4	52.1	0.995	8.7
BC85	913.1	1679.2	54.4	0.967	7.4
BC86	758.4	1402.0	54.1	0.937	6.7
BC87	1259.0	2437.5	51.7	0.990	8.8
BC88	1003.7	1873.2	53.6	0.973	7.8
BC97	816.5	1506.3	54.2	0.983	7.8
BC98	790.5	1468.0	53.8	0.971	7.3
Lichen					
BC53	1108.7	2060.3	53.8	0.993	8.6
BC54	836.6	1502.5	55.7	0.985	7.8
BC55	839.1	1617.7	51.9	0.965	7.4
BC56	942.0	1741.2	54.1	0.974	7.6
BC65	773.4	1498.6	51.6	0.972	7.1
BC66	1005.4	1879.1	53.5	0.981	7.9
BC67	1054.9	1874.5	56.3	0.988	8.2
BC68	898.2	1606.8	55.9	0.982	7.8
BC77	930.7	1690.0	55.1	0.989	8.1
BC78	759.7	1572.1	48.3	0.956	6.8
BC79	835.8	1645.4	50.8	0.965	7.1
BC80	774.1	1376.6	56.2	0.989	7.7
BC89	899.6	1807.7	49.8	0.976	7.5
BC90	1177.7	2339.7	50.3	0.989	8.4
BC91	698.9	1349.2	51.8	0.908	6.4
BC92	1046.7	1926.3	54.3	0.991	8.4
BC101	1058.5	1895.6	55.8	0.991	8.6
BC102	788.6	1525.1	51.7	0.940	6.9

Bark					
BC57	517.5	916.3	56.5	0.914	6.1
BC58	946.8	1733.9	54.6	0.967	7.7
BC59	694.5	1246.0	55.7	0.990	7.8
BC60	969.7	1946.5	49.8	0.991	8.2
BC69	806.6	1488.9	54.2	0.986	7.7
BC70	756.6	1274.4	59.4	0.988	7.7
BC71	892.5	1639.9	54.4	0.991	8.1
BC72	1174.0	2167.6	54.2	0.995	8.9
BC81	834.8	1430.0	58.4	0.991	8.0
BC82	660.8	1172.1	56.4	0.973	7.3
BC83	601.5	1127.2	53.4	0.979	7.1
BC84	635.9	1055.6	60.2	0.988	7.5
BC93	602.6	1096.0	55.0	0.975	7.2
BC94	577.3	1067.4	54.1	0.982	7.1
BC95	325.8	563.6	57.8	0.937	5.5
BC96	518.8	996.5	52.1	0.939	5.9
BC105	412.6	638.7	64.6	0.976	6.7
BC107	533.0	854.1	62.4	0.985	7.3

MANUSCRIPT II

Journal Article in preparation

An integrative omics approach identifies bacterial key players in a complex microenvironment

Ines Aline Aschenbrenner,[1,2] Tomislav Cernava,[1] Armin Erlacher,[1] Gabriele Berg,[1] Martin Grube[2]

[1]Institute of Environmental Biotechnology
Graz University of Technology, Austria

[2]Institute of Plant Sciences
University of Graz, Austria

An integrative omics approach identifies bacterial key players in a complex microenvironment

Ines Aline Aschenbrenner,[1,2] Tomislav Cernava,[1] Armin Erlacher,[1] Gabriele Berg,[1] Martin Grube[2]

[1]Institute of Environmental Biotechnology, Graz University of Technology, Petersgasse 12, 8010 Graz, Austria

[2]Institute of Plant Sciences, University of Graz, Holteigasse 6, 8010 Graz, Austria

Correspondence:

Martin Grube
University of Graz
Institute of Plant Sciences
Holteigasse 6, A-8010 Graz
email: martin.grube@uni-graz.at
telephone: +43 316 380 5655

Abstract

Lichen symbioses develop long-persisting structures that are readily colonized by bacterial communities. The high diversity and host specificity of bacterial communities is now better understood, but their functional roles require a more targeted study by an integrative omics-approach. Metagenome, metatranscriptome, 16S amplicon sequencing data are here used to obtain more detailed insight into (a) the taxonomy of five highly abundant bacterial groups and (b) their functional contributions to the symbiotic system. Analyses indicate specific functions for each group of the bacterial fraction, reaching from general features such as nutrient supply and vitamin syntheses to more specific roles. These include various defense strategies against oxidative bursts, associated with the poikilohydric life-style of lichens, and antimicrobial lichen substances such as phenolic compounds. In particular, the under-recognized group *Chthoniobacterales* (*Verrucomicrobia*) was involved in defense mechanisms. Based on FISH-CLSM we were also able to selectively visualize this group in lichens for the first time. Our data suggest that the lichen-associated microbiome seems to be adapted to the fluctuating microclimatic conditions suggesting their involvement in coordinated response to periodic desiccation.

Introduction

The lichen symbiotic lifestyle of fungi with phototrophic organisms arose with the evolution of terrestrial life in the Devonian more than 400 million years ago (Remy et al., 1994; Honegger et al., 2013). This self-sustaining lifestyle enables the lichenized fungus and the photobiont to colonize substrates almost all over the world (Nash, 2008). Even in environments at the edge of life lichens can form long-lasting and landscape-dominating communities. With their persisting structures, lichens provide a microhabitat for various eukaryotic microorganisms, such as fungi or other eukaryotic life forms (Lawrey & Diederich, 2003; Bates et al., 2012), but in particular also a high number of prokaryotes. It was shown that lichen-associated bacteria are highly diverse and form host-specific communities (Grube et al., 2009; Bates et al.; 2011). The community structure is shaped not only by the lichen-forming fungal species, but to some extent also by the photobiont and geographic parameters, as shown by Hodkinson and colleagues (2012). Microscopic studies revealed colonization by bacteria, usually in a biofilm-like manner predominantly of lichen surfaces (Cardinale et al., 2008).

Grube et al. (2015) analyzed the potential metabolic contributions of the associated microbiome to the lichen symbiosis by metagenomic and metaproteomic tools. Besides the solubilization of phosphate and the release of phytohormones and amino acids (Liba et al., 2006; Grube et al., 2009; Schneider et al., 2011), the bacteria potentially provide vitamin B12, detoxify metabolites and promote resistance against biotic and abiotic stress factors. *Alphaproteobacteria* are the dominant bacterial group on many studied lichen species (Cardinale et al., 2008; Grube et al., 2009; Schneider et al., 2011; Bates et al., 2011). This applies also to the lung lichen *Lobaria pulmonaria* (L.) Hoffm. (Aschenbrenner et al., 2014), which has been the focus of our recent studies. This foliose lichen is adapted to old-growth forests with high ecological continuity (Rose, 1992; Gauslaa, 1994; Scheidegger, 1995) and belongs to the approximately 4% of lichens, which harbor two photosynthetic partners, a green algal species (*Dictyochoropsis reticulata*, representing 90% of the photobiont community) and cyanobacteria (*Nostoc* sp., representing 10%).

A detailed study by Erlacher et al. (2015) of the highly abundant alphaproteobacterial order *Rhizobiales*, also known as beneficial associates of plants, highlighted potential functions for nitrogen fixation, phytohormone and vitamin syntheses as functional contributions to the lichen symbiosis. This was the first study unraveling the potential

functional roles of a specific taxonomic group within the lichen associated bacterial community. Besides *Rhizobiales*, *Sphingomonadales* was also reported to be high abundant within the *Lobaria*-associated microbiome (Aschenbrenner et al., 2014), whereas less attention so far was paid to other lineages present, such as *Spartobacteria* (*Verrucomicrobia*). This poorly investigated group was found to be highly abundant in soil and aquatic environments (Zwart et al., 1998; Janssen et al., 2011, Bergman et al., 2011), but also on lichen thalli and their vegetative propagules as previously reported by Aschenbrenner et al. (2014). More recently, members of *Chthoniobacterales* (*Spartobacteria),* and other lineages such as *Sphingobacteriales* (*Bacteroidetes*) were shown to specifically colonize *L. pulmonaria* (Aschenbrenner et al., 2015).

In this study we combined three different omic-approaches (meta-genome, meta-transcriptome and 16S rRNA amplicon sequencing) to assess the taxonomical composition of five highly abundant bacterial groups associated with *L. pulmonaria* and to get a more detailed insight into their specific functional contributions to the symbiosis.

Materials and Methods

Sampling

Lichen thalli of *Lobaria pulmonaria* were sampled in the Austrian Alps (Johnsbach, N 47°32’35’’, E 14°37’38’’; 1175 m above sea level) from a rich population on a mountain maple bark (*Acer pseudoplatanus*) on 05/October/2012 (meta-genome), on 28/June/2014 (meta-transcriptome) and on 17/October/2014 (16S rRNA amplicon analysis). Sampling was conducted in the late morning hours, when thalli were humidified and flexible (rather than dry and brittle). The samples were collected with sterile tweezers and cleaned from contaminations (*e.g*. moss, bark, and insects). Lichen specimens for meta-genome and amplicon studies were stored separately in sterile polyethylene bags and cooled on dry ice. For the meta-transcriptome analysis lichen thalli were immediately transferred in RNAlater®Stabilization solution (Ambion; Life Technologies Germany) and stored at -20°C until further processing.

Sample preparation and sequencing

L. pulmonaria specimens were processed as described in Aschenbrenner et al. (2015). Briefly, lichen thalli were ground in liquid nitrogen with sterile pestle and mortar. The lichen powder was resuspended in 0.85% NaCl solution and centrifuged prior to DNA extraction (PowerSoil® DNA Isolation Kit, MoBio, Germany). Each DNA extract was supplemented with peptide nucleic acid PCR clamps as described in Lundberg et al. (2013) and then used as a template for PCR amplifications with universal bacterial primer 515f/806r (Caporaso et al., 2011), which enclose the variable region 4 in the 16S rRNA gene (which is also studied for the Earth Microbiome project; http://www.earthmicrobiome.org/; Gilbert et al. 2014). Barcoded samples were pooled in equimolar amounts and submitted to paired-end Illumina MiSeq sequencing (MWG Eurofins, Germany).

For metagenomic analysis (Grube et al. 2015), thalli were similarly homogenized in liquid nitrogen, but enriched for bacteria by sieving the suspension (in 0.85% NaCl) and additional centrifugation steps afterwards. The pellet was used for DNA isolation (MoBio PowerSoil® DNA Isolation Kit; Carlsbad, USA). Total metagenomic DNA was sequenced by paired-end Illumina HiSeq 2000 (GATC Biotech; Konstanz, Germany).

TRIZOL plus RNA purification kit was used to isolate total RNA according to manufacturer's protocol. The lichen tissue was homogenized with a FastPrep®-24 Instrument and FastPrep™ Lysing Matrix E (MP Biomedicals, Germany) for 3 x 30'' at 6.0 m/s with 1 min cooling on ice in-between. Total RNA was purified with RNeasy mini kit (Qiagen, Germany) and RNA integrity was measured with Agilent 2100 Bioanalyzer (Agilent Technologies). To enrich the messenger RNA for functional analyses, eukaryotic and prokaryotic ribosomal RNA was depleted (Stewart et al., 2010; Kukutla et al.; 2013). For this purpose rRNA probes specific for the eukaryotic and prokaryotic SSU and LSU rRNA regions were designed based on corresponding metagenomic DNA sequences. Briefly, small and large subunits of the rRNA gene fragments were amplified with specific primer sets (see Table S1). Purified PCR products (Wizard ® SV Gel and PCR Clean-Up System, Promega, Germany) were used as DNA templates for the production of biotinylated anti-sense rRNA probes via *in vitro* transcription according to manufacturer's protocol (MEGAscript T7 kit, Ambion, Life Technologies, Germany). Finally, rRNA was subtracted from total RNA with streptavidin-coated magnetic beads after hybridization with the biotinylated anti-sense rRNA probes. Quality-checked RNA of three separately processed lichen thalli was pooled

equimolar. Strand-specific cDNA library preparation of total and depleted RNA, and Illumina HiSeq 2500 paired-end sequencing was performed by GATC Biotech AG (Konstanz, Germany).

Taxonomic analysis

Downstream sequence analysis for taxonomical assignments was done with QIIME 1.9.0 (Quantitative Insights Into Microbial Ecology, Caporaso et al., 2010). Therefore the 16S rRNA gene sequences of the meta-genome (MG-RAST ID 4530091.3) and meta-transcriptome datasets were filtered with SortMeRNA (Kopylova et al., 2012) based on the integrated bacterial 16S rRNA database (SILVA SSU Ref NR v.119). Sequences were clustered at 97% similarity based on the "pick_closed_reference_OTUs.py" script. The SILVA database (release 119; Quast et al., 2013) was used as reference sequence set and for taxonomical assignment (Pruesse et al., 2007). Additionally, mitochondrial and chloroplast sequences were removed from datasets. Taxonomic composition for each omic-approach was visualized in Krona-charts (Ondov et al., 2011).

Functional analysis

The functional analysis is based on a meta-genomic (MG-RAST ID 4530091.3) and metatranscriptomic dataset deposited on the metagenomics analysis server MG-RAST (Meyer et al., 2008). Meta-genomic and transcriptomic sequences were compared to GenBank using a maximum e-value of 1e-5 and a minimum identity cutoff of 70%. All reads assigned to the orders *Sphingobacteriales* (*Bacteroidetes*), *Chthoniobacterales* (*Verrucomicrobia*), *Myxococcales*, *Sphingomonadales* and *Rhodospirillales* (*Proteobacteria*) were exported for further analysis. The short DNA/cDNA reads were aligned to the protein reference database NCBI-NR (version May 2015) using DIAMOND (version 0.7.9; Buchfink et al., 2015). Functional assignment was performed with MEGAN5 (Huson et al., 2011) based on SEED classification (Overbeek et al., 2005). The abundances of function-assigned sequences of the specified taxonomic orders were subsampled (1000 times randomly subsampled; default settings in MEGAN5) for comparison.

FISH/CLSM

Fluorescence *in situ* hybridization (FISH) was performed to specifically visualize the colonization pattern of *Chthoniobacterales* (class: *Spartobacteria*, phylum: *Verrucomicrobia*)

among other eubacteria. *L. pulmonaria* thalli were fixed with 4% paraformaldehyde/phosphate-buffered saline (PBS) with a ratio of 3:1 at 4°C for at least 4 h. Prior to *in situ* hybridization according to Cardinale et al. (2008), thallus cross-sections were prepared. For the detection of *Spartobacteria* as well as *Verrucomicrobia* the Cy5-labled probes SPA714 (42°C, 35% formamide; Arnds et al., 2010) and EUB338III (42°C, 15% formamide) were used. Other eubacteria were detected with an equimolar mixture of the Cy3-labled probes EUB338, EUB338II, EUB338III (42°C, 15% formamide; Amann et al., 1990; Daims et al., 1999). Additionally, NONEUB probes (Wallner et al., 1993) labeled with the respective fluorochromes were used as negative controls. Details on oligonucleotide probes are available on probeBase (Loy et al., 2007). To suppress photobleaching of the fluorescently labeled probes SlowFade Diamond antifade reagent (Molecular Probes, Eugene, USA) was used. Targeted *Chthoniobacterales* and all other eubacteria were visualized with a Leica TCS SPE confocal laser-scanning microscope (Leica Microsystems, Mannheim, Germany). Confocal stacks were processed with Imaris 7.3 (Bitplane, Zurich, Switzerland).

Results

Taxonomical analysis of *Lobaria*-associated bacteria

To assess the taxonomical composition of the *Lobaria*-associated microbiome the 16S ribosomal RNA gene sequences of a meta-genomic and a meta-transcriptomic data set was compared together with 16S rRNA gene amplicon sequences. Each omics dataset derived from independent studies, two of them (metagenomic and 16S rRNA gene amplicon data sets) were already published in Grube et al. (2015) and Aschenbrenner et al. (2015). The new meta-transcriptome dataset was deposited on MG-RAST. The total sequence counts and mean sequence length within these datasets varied (with sequencing platform) between around 400 thousand and more than 67 million reads with respective lengths between 105 bp and 290 bp (Table S2).

As already shown in previous studies, *Proteobacteria* and more specifically *Rhizobiales* among *Alphaproteobacteria* was the predominant group in the bacterial community of *L. pulmonaria* (Erlacher et al.; 2015). The general taxonomic composition at phylum and class level was largely similar in all three omic-approaches, but varied in the relative abundances at deeper taxonomic levels such as family and genus affiliations. A

detailed visualization of the taxonomic compositions for each omic-approach up to family level is shown in Krona-charts (Fig. 1). In particular, *Cyanobacteria* showed remarkably high differences among the datasets. Within the amplicon dataset *Cyanobacteria* comprised almost 30%, in contrast to the metagenome, where they accounted for less than 1% of the total reads. According to the metatranscriptomic analysis the apparently small fraction of them, however, comprised 8% of the metabolically active community.

Besides *Rhizobiales* and *Cyanobacteria*, the predominant orders within the lichen-associated microbiome across all three omics approaches were 10.2% (mean) *Sphingomonadales*, 5.8% *Rhodospirillales*, 4.7% *Myxococcales* (*Proteobacteria*), 4.3% *Chthoniobacterales* (*Verrucomicrobia*) and 5.8% *Sphingobacteriales* (*Bacteroidetes*). With focus on these taxa their composition and relative abundances at family level were visualized in more detail in Figure 2, whereas unassigned or unclassified families were grouped into "others". Within the order *Sphingobacteriales* two main families were identified: *Sphingobacteriaceae* and *Chitinophagaceae*. The *Chitinophagaceae* were overrepresented in the amplicon dataset when compared with the metagenome, whereas *Sphingobacteriaceae* were underrepresented in the former dataset. *Chthoniobacterales* was represented by the families *Chthoniobacteraceae* and *Xiphinematobacteraceae*. Also groups within *Chthoniobacteraceae* seemed to be underrepresented within the amplicon dataset, but they appear metabolically active according to the metatranscriptome. Highly abundant families identified within the alphaproteobacterial orders *Sphingomonadales* were represented by *Sphingomonadaceae* and *Erythrobacteraceae*, as well as *Acetobacteraceae* and *Rhodospirillaceae* in *Rhodospirillales*. Both *Sphingomonadaceae* and *Acetobacteraceae* were not fully recovered within the amplicon analysis and they also seemed not to be as metabolically active as other families compared to the respective metagenome data. The order *Myxococcales* was represented by various distinct families, whereas *Polyangiaceae*, *Phaselicystidaceae* and *Cystobacteraceae* had a higher relative abundance within the metatranscriptome than in the other two -omic approaches. Other detected families within this order were *Haliangiaceae* and *Sandaracinaceae*.

Functional analysis of *Lobaria*-associated bacteria

Metagenomic and metatranscriptomic data were utilized to unravel the genetic potential and actually expressed functions of the five highly abundant bacterial orders

Sphingomonadales, *Rhodospirillales*, *Myxococcales*, *Chthoniobacterales* and *Sphingobacteriales* within the *L. pulmonaria*-associated microbiome.

Functional assignments for each bacterial group based on SEED classification are visualized schematically in Figure 3. Hits assigned to functions within the primary metabolic pathways such as DNA, RNA or protein metabolism among others are indicated in grey and not examined in more detail. Functional categories of interest are visualized in pie charts reflecting the relative contributions of each bacterial order.

Metabolic pathways. Based on the metagenome, genes attributed to potassium and nitrogen metabolism were both predominantly (96%) assigned to the alphaproteobacterial order *Rhodospirillales* and to a minor extent to *Sphingobacteriales* (potassium metabolism) and *Sphingomonadales* (nitrogen metabolism). *Rhodospirillales* contributed to 94% and 96% of the hits for the assimilation of ammonia and potassium uptake and transport, respectively. There were also functional assignments to nitrate and nitrite ammonification and the production of nitric oxides. Sulfur and iron metabolism was predominately represented by *Sphingobacteriales*. With respect to iron metabolism all *Sphingobacteriales*-specific reads contributed to the TonB-dependent receptor of Gram-negative bacteria, but also all three proteobacterial taxa were involved in this iron acquisition strategy. Other identified iron transport mechanisms were systems based on siderophores or hemin. Functional genes within the phosphate metabolism were mainly assigned to *Proteobacteria*, especially *Myxococcales*. Contrarily, in the metatranscriptome dataset nitrogen metabolism (ammonia assimilation) was mainly detected for *Chthoniobacterales* and only to a minor extent for *Rhodospirillales*. Also in context of the sulfur metabolism the metagenome results could not be confirmed by transcriptomic data, instead *Rhodospirillales* was the main contributor in the latter. Iron acquisition and metabolism was only detected for *Sphingobacteriales* and *Sphingomonadales* in the transcriptome, including hemin transport system and TonB-dependent receptor.

Involvement in the metabolism of aromatic compounds was found for all examined taxa according to the analyzed metagenome. The majority of these functions was assigned to various degradation mechanisms. *Chthoniobacterales* was the primary contributor to the degradation of n-phenylalkanoic acid. *Alphaproteobacteria* were involved in the degradation of phenylpropanoid, xylenols and cresols (mainly by *Rhodospirillales*) and chloroaromatic compounds (by *Myxococcales*). Especially *Proteobacteria* were identified to potentially synthesize the plant hormone auxin. *Rhodospirillales* was also found to be involved in biosynthesis of phenazine. Based on the metatranscriptome, the phenazine and auxin

production could not be confirmed. Instead, degradation and transport mechanisms of various compounds were found, such as biphenyl, carbazol, benzoate (*Sphingomonadales*) as well as gentisate and salicylate (*Rhodospirillales, Myxococcales*).

Potential synthesis of cofactors, vitamins, prosthetic groups and pigments was generally found among all observed taxa based on the metagenome. Particularly, *Chthoniobacterales* was found to contribute mainly to the synthesis of the vitamins riboflavin and biotin, whereas, genes for the syntheses of the vitamins thiamin, pyridoxine and folate were predominantly assigned to *Proteobacteria*. Cofactors like coenzyme A and B or NAD and NADP were mainly assigned to *Alphaproteobacteria*. Contrary to the metagenome data, in the metatranscriptome *Chthoniobacterales* synthesized biotin and folate. Vitamins such as riboflavin, pyridoxine and thiamin, were mainly produced by *Rhodospirillales*,. Interestingly, *Sphingomonadales* expressed the cobalamin-adenosyltransferase PduO (EC 2.5.1.17), which is involved in the biosynthesis of vitamin B12. Quinone cofactors were found to be synthesized by *Sphingobacteriales* (menaquinone) and *Myxococcales*, whereas the latter one expressed 4-hydroxyphenylpyruvate dioxygenase (EC 1.13.11.27) which is involved in the biosynthesis of plastoquinone and tocopherol.

Stress response. Functional genes within the category stress response focused on oxidative stress and heat shock. The latter one was mainly represented by the chaperones DnaK and GroEL within the metagenome, where sequences of both of them were predominantly assigned to *Myxococcales* and *Sphingobacteriales*. DnaK was also found to be expressed by *Myxococcales* according to the metatranscriptome data. Additionally hits for transcribed RpoH and the Hfl operon were found for *Rhodospirillales*. Notably, all of the observed taxa encoded to a certain extent defense mechanisms against oxidative stress. In particular, *Chthoniobacterales* encoded for a redox-sensitive transcriptional regulator and *Rhodospirillales* for rubrerythrin, which facilitates oxidative stress tolerance. All *Proteobacteria* encoded for the same catalase (EC 1.11.1.6), but also for glutathione-dependent protection against oxidative damage by ROS (reactive oxygen species). Contrarily, the metatranscriptome analysis revealed defense mechanisms against oxidative stress only for *Chthoniobacterales, Myxococcales* and *Rhodospirillales*. According to that all of them expressed glutaredoxin-related proteins. Additionally, *Chthoniobacterales* expressed glutaredoxin, whereas *Rhodospirillales* was also found to synthesize rubrerythrin and glutathione for non-redox reactions. The catalase EC 1.11.1.6 was only found to be expressed

by *Myxococcales*. Resistance mechanisms against acid stress were only encoded by *Myxococcales* by a biosynthetic arginine decarboxylase (EC 4.1.1.19).

Virulence, disease and defense. *Chthoniobacterales* and *Myxococcales* were mainly involved in resistance to antibiotics and toxic compounds. *Myxococcales* encoded for resistances against the metals arsenic and zinc. In addition to zinc resistance, *Sphingomonadales* and *Sphingobacteriales* showed also cobalt and cadmium resistance. In contrast, the metatranscriptome data revealed that only *Myxococcales* was found to express a response regulator of zinc sigma-54-dependent two-component system.

Regarding antibiotic resistance all taxa encoded functions for resistance against fluoroquinolones according to the metagenome, with *Chthoniobacterales* as the predominant contributor. Especially, hits for beta-lactamases were detected for *Alphaproteobacteria* and *Sphingobacteriales*. Multidrug resistance *e.g*. via efflux pumps were found for all taxa, except for *Myxococcales*. According to the metatranscriptome *Sphingobacteriales*, *Myxococcales* and *Chthoniobacterales* were found to be involved in fluoroquinolone resistance and the latter one also against acriflavin.

Membrane transport. Various kinds of transport systems were present in the metagenome dataset, such as protein secretion systems type II, III and IV. Secretion systems type IV was found in *Alphaproteobacteria*, especially *Sphingomonadales,* and *Sphingobacteriales* but not for *Chthoniobacterales*. Additionally, *Rhodospirillales* encoded exclusively for the sec-independent twin-arginine translocation pathway to transport folded proteins as well as manganese, zinc, nickel and cobalt. Functional assignments for Ton- and Tol-dependent transport systems were found for all observed taxa. Metatranscriptome data displayed the expression of Ton and Tol transport systems for *Sphingomonadales* and *Sphingobacteriales*, as well as hits for parts of the type IV secretion system in *Rhodospirillales*.

Motility and chemotaxis. *Proteobacteria* were the main contributors to this category, particularly *Myxococcales* was involved in chemotaxis encoding the proteins methyltransferase CheR (EC 2.1.1.80) and the response regulator protein-glutamate methylesterase CheB (EC 3.1.1.61). According to the metatranscriptome only the signal transduction histidine kinase CheA was detected for *Myxococcales*. *Rhodospirillales* predominantly encoded for flagellar motility. Contrarily, in the metatranscriptome the main

contributor to flagellar motility was *Sphingobacteriales*, followed by *Chthoniobacterales* and *Myxococcales*.

Phages, Prophages, Transposable elements, Plasmids. Functional assignments within this category were only found for *Sphingomonadales* and *Sphingobacteriales*, including transposable elements like Tn552 encoding for a beta-lactamase or the staphylococcal phi-Mu50B-like prophages. In the metatranscriptome analysis transcripts for the staphylococcal pathogenicity island SaPI were found for *Sphingobacteriales* and *Myxococcales*.

Regulation and cell signaling. Orphan regulatory proteins were particularly found for *Myxococcales*, both in the metagenome and transcriptome data. Furthermore, numerous hits were found for the two-component regulatory system as well as cAMP signaling in bacteria according to the metagenome and additionally quorum sensing involved proteins in the metatranscriptome.

Visualization of *Lobaria*-associated *Chthoniobacterales*

According to probeBase no specific probes for the order *Chthoniobacterales* are available. However, within our datasets all sequences of the verrucomicrobial class *Spartobacteria* were assigned to *Chthoniobacterales*. Thus, we used the probe SPA714 to detect specifically bacteria within this class. However, this probe only targets about 66% (2553/3874 hits) of all *Chthoniobacterales* sequences according to RDP probe-match. Fluorescence *in situ* hybridization of *Spartobacteria* revealed consistent colonization of both the upper and the lower cortex of *L. pulmonaria* (Fig. 4 A,B). Volume rendering of the confocal stacks clearly visualized a general tendency of *Spartobacteria* to form single colonies between biofilm-like structures of other unspecifically labeled eubacteria. Although there were also small areas with higher cell-densities (Fig.4 B), no larger colonies of *Spartobacteria* were detected.

Additionally, we evaluated the FISH probe EUB338III, which should specifically target the order *Verrucomicrobiales* (class *Verrucomicrobiae*) besides the non-target taxon *Chloroflexi* besides others. Sequence alignments to the Probematch database (Cole et al., 2005) revealed that this probe does not only match to *Verrucomicrobiae* (6930/7266), but also covers the verrucomicrobial classes Subdivision 3 (3064/3647), *Opitutae* (4223/4460) and

Spartobacteria (4441/4734). According to our data about 89% (mean) of the verrucomicrobial sequences were assigned to the class *Spartobacteria*, followed by *Opitutae* (7%). Hence, this FISH probe is also suitable to detect *Chthoniobacterales* on *L. pulmonaria*. A three-dimensional reconstruction visualizes the EUB338III labeled bacteria on the upper cortex of the lichen thallus among other eubacteria (Fig. 4 C).

Discussion

By application of multiple omics approaches (metagenome, metatranscriptome and 16S rRNA amplicon sequencing) the taxonomic composition of the lichen-associated microbiome was assessed on different molecular levels (DNA and RNA). So far several studies have described the *L. pulmonaria*-associated bacterial community structure and diversity based on simple fingerprinting methods, 16S rRNA sequencing (Cardinale et al., 2012; Aschenbrenner et al., 2014) or by metagenome (Grube et al., 2015). Based on these DNA-dependent methods all bacteria regardless of whether they are active, dormant or dead were detected. In the current study we present for the first time insights into the composition of the metabolically active bacterial community of a lichen-associated microbiome based on a metatranscriptomic approach.

The taxonomical compositions of all data sets were very similar at higher taxonomic levels (*e.g*. *Alphaproteobacteria* as predominant class) but differed especially towards family and genus level. We do not have indications that variations are due to different sampling dates, as the main composition of the microbiomes seem fairly stable on the lichen structures (Grube et al. 2009), but several other causes may explain these differences. Slight biases may occur by differences associated with sample preparation (Stach et al., 2001), or with gene-specific amplification (Gonzalez et al. 2012; Pinto & Raskin, 2012), where selection of the primers may also play a role (Klindworth et al. 2013, Rajendhran & Gunasekaran, 2011). The most likely cause of variation, however, might be due to copy number variation in the rRNA operons (Klappenbach et al., 2000; Rajendhran & Gunasekaran, 2011). The presence of multiple copies in *Nostoc* genomes (usually four copies; Schirrmeister et al. 2012) could account for the differences in abundances in either amplicon or metagenomic data sets. Especially for the metatranscriptomic data, the metabolic activity at the sampling time might explain some variations in the bacterial community. Therefore we sampled at the same time of

the day, when thalli were humid and in a state when the lichen partners are known to be metabolically active.

Focusing on five highly abundant bacterial orders, namely *Sphingomonadales*, *Rhodospirillales*, *Myxococcales* (all *Proteobacteria*), *Chthoniobacterales* (*Verrucomicrobia*) and *Sphingobacteriales* (*Bacteroidetes*), specific functional contributions to the overall symbiosis were explored. Metagenomic and metatranscriptomic analyses revealed various defense strategies of the associated bacteria against stressful environmental conditions in the lichen microhabitat.

Lichens are known to produce extracellular reactive oxygen species (ROS) including *e.g*. superoxide, hydroxyl radicals, and hydrogen peroxide (Beckett et al, 2005). Particularly, members of the suborder *Peltigerineae* (including *L. pulmonaria*) are supposed to produce high rates of extracellular superoxide after desiccation-rehydration events. According to Beckett et al. (2003) extracellular ROS production helps defending against bacterial and fungal pathogens, especially in this lineage of lichenized fungi, which lack crystallized secondary metabolites with potential antimicrobial properties in the upper surface layers. Indeed bacterial pathogens are not known in lichens in general, and by far, many of the colonizing bacteria seem to represent stress-tolerant commensals or even beneficials, which potentially contribute various functions to the lichen meta-organism (Grube et al., 2015; Erlacher et al., 2015). These bacteria must be adapted to periodic desiccation and rehydration with associated oxidative bursts. According to our metagenomic data all bacteria encoded corresponding protection mechanisms against oxidative stress, such as catalase and low-molecular-weight antioxidants (e.g., glutathione), which were also found in the metatranscriptome.

Oxidative stress conditions also induce the expression of various heat shock proteins (Susin et al., 2006). In particular, the chaperones GroEL and DnaK, which were highly abundant in our data, can be induced by various oxygen species such as superoxide or hydrogen peroxide, respectively (Farr and Kogoma, 1991). These chaperones can also be induced by the presence of toxic compounds like antibiotics, heavy metals and aromatic compounds (Susin et al., 2006). Indeed, several functions, which protect against such toxic compounds, were also reflected in our data, e.g. those contributing to resistance to the toxic metals arsenic and cadmium, cobalt or zinc. In addition resistance mechanisms for antibiotics, such as fluoroquinolones, were also found, like beta-lactamases and efflux pumps for multidrug resistances. As secondary metabolites (including depsides, depsidones and

dibenzofurans) produced by the lichenized fungus have anti-microbial activities to defend the host against fungal and bacterial pathogens (Kosanic and Rankovic, 2015). Lichen- as well as plant-associated bacteria developed different defense mechanisms against these specific aromatic compounds. Our data confirmed the presence of potential functions to degrade these metabolites such as phenylpropanoid, which is the carbon skeleton of a wide range of polyphenols. In contrast, there were also hints for the production of phenolic compounds by bacteria itself. Especially, *Rhodospirillales* was found to be involved in the production of phenazines, which are known to inhibit the bacterial and fungal growth (Mavrodi et al., 2009) thereby increasing its own competitiveness and ecological fitness (Pierson and Pierson, 2010). This could have also a positive effect for the lichen itself as these broad-specificity antibiotics might also control bacterial and fungal pathogens.

Besides more general transport machineries such as Ton- and Tol- dependent transport systems, also different secretion systems were detected. Especially, the type four secretion system (T4SS), which is not only involved in the DNA uptake/release to the environment or in the conjugal DNA transfer to other bacteria, but also in the translocation of effector molecules to eukaryotic target cells (Ding et al., 2003). These trans-kingdom transfers include fungi, plants and mammalian cells (Bundock et al., 1995, Waters, 2001, Cascales and Christie, 2003). The phytopathogen *Rhizobium radiobacter* (Syn. *Agrobacterium tumefaciens*) is one of the most prominent examples for such effects of T4SS. However, the transferred macromolecules can not only suppress host-defense mechanisms and cause infectious diseases, but also stimulate the host to synthesize specific nutrients beneficial for bacterial colonization (Cascales & Christie, 2003). In the case of the Rhizobia-legumes symbiosis, *Mesorhizobium loti* (*Alphaproteobacteria*) uses the T4SS to transfer proteins, which then affect the host nodulation and control plant defense responses e.g. via Nod factors (Soto et al., 2006, Gourion et al., 2014). Related to these findings, the T4SS might be also used for inter-kingdom "cross-talking" between the lichen and the associated microbiome. However, their precise functions in lichens still need to be elucidated.

While lichen-associated *Alphaproteobacteria* have been illustrated on lichen surfaces several times in the last few years, *Chthoniobacterales (Spartobacteria)*, despite their abundance, have not selectively visualized so far in lichens. After the first representative of this class, *Chthoniobacter flavus,* was isolated from soil (Sangwan et al., 2004), only few studies focused on this particular class (Sangwan et al, 2005; Kant et al., 2011), but our study shows the significance in lichens for the first time. Metagenomic analysis of an aquatic

Spartobacteria-representative revealed potential functions in the degradation of various complex carbohydrates, such as cellulose, assuming it has an important role in the carbon cycle (Herlemann et al., 2013). However, in our study *Chthoniobacterales* was mainly involved in the metabolism of aromatic compounds (degradation of phenolic substances), production of vitamins and defense against antibiotics (fluoroquinolone) and oxidative stress.

In this study we revealed the potential functions of predominant bacterial groups in a complex microenvironment with an integrative omics approach. Metagenomic and metatranscriptomic analyses indicated specific functional roles for each group in the bacterial community reaching from nutrient and vitamin supply to different defense strategies against harsh conditions, which might be evolved over a long time of co-existence. We nevertheless observed some obvious differences between the signals in the metatranscriptome versus the metagenome. This is not surprising since the metagenomes encodes the potential functionality of the bacterial microbiome, whereas the metatranscriptome represents a snapshot of active functions in the lichen at a particular metabolic state. We hypothesize that the metatranscriptome is particularly responsive to the hydration conditions of the lichen, which varies between a completely water saturated state, e.g. during rainfall or complete hydration by dew (e.g. in cool morning hours), and dry states. Our sampling at late morning hours represents a moderately water saturated stage following a rainy period of more than one week (but the lichen was not directly exposed to rain). While water supra-saturation impedes lichen activity of the eukaryotic partners, both in nature and laboratory experiments (Lange et al. 2001), the bacteria could be fully active in this stage and contribute hydration stage-specific functions to the lichen symbiosis, which is characteristically exposed to periodic drought. The wealth of functions found in the metagenome will point future investigations in this direction. Pending further studies, we suppose that the pattern of metatranscriptomic gene expressions will vary specifically with depletion of hydration towards more pronounced desiccation stages of the lichens. The next step of investigations thus needs to study the interplay with eukaryotic partners at a transcriptomic level at different hydration stages. Indicators for gene expression related to stress tolerance were meanwhile also found in a transcriptomic study of eukaryotic partners in the lichen *Cladonia rangiferina* in the course of desiccation (Juntilla et al., 2013). We think that the reaction to desiccation by eukaryotic partners could be sequentially coordinated by bacterial stress responses. Such future integrated approaches could test whether bacteria could trigger the process of stress response in the lichen symbiosis as an early alert system.

References

Amann RI, Binder BJ, Olson RJ, Chisholm SW, Devereux R, Stahl DA. Combination of 16S rRNA-targeted oligonucleotide probes with flow cytometry for analyzing mixed microbial populations. *Appl Environ Microbiol* 1990;**56**:1919–1925

Arnds J, Knittel K, Buck U, Winkel M, Amann R. Development of a 16S rRNA-targeted probe set for Verrucomicrobia and its application for fluorescence in situ hybridization in a humic lake. Syst *Appl Microbiol* 2010;**33**:139–48.

Aschenbrenner IA, Cardinale M, Berg G, Grube M. Microbial cargo: do bacteria on symbiotic propagules reinforce the microbiome of lichens? *Environ Microbiol* 2014;**16**:3743–3752.

Aschenbrenner IA, Cernava T, Erlacher A, Berg G, Grube M. Inter-microbiome relations: spatially close hosts show a common network with specific components. 2015; Submitted.

Bates ST, Berg-Lyons D, Lauber CL, Walters W, Knight R, Fierer N. A preliminary survey of lichen associated eukaryotes using pyrosequencing. *Lichenologist* 2012;***44*:**137–146.

Bates ST, Cropsey GW, Caporaso JG, Knight R, Fierer N. Bacterial communities associated with the lichen symbiosis. *Appl Environ Microbiol* 2011;**77**:1309–1314.

Beckett RP, Minibayeva FV, Laufer Z. Extracellular reactive oxygen species production by lichens. *Lichenologist* 2005;**37**:397.

Beckett RP, Minibayeva FV, Vylegzhanina NN, Tolpysheva T. High rates of extracellular superoxide production by lichens in the suborder Peltigerineae correlate with indices of high. *Plant Cell Environ* 2003;**26**:1827–1837.

Bergmann GT, Bates ST, Eilers KG, Lauber CL, Caporaso JG, Walters WA, et al. The under-recognized dominance of Verrucomicrobia in soil bacterial communities. *Soil Biol Bioch* 2011;***43***:1450–1455.

Buchfink B, Xie C, Huson DH. Fast and sensitive protein alignment using DIAMOND. *Nature Methods*. 2015;12:59–60

Bundock P, den Dulk Ras A, Beijersbergen A, Hooykaas PJ. Trans-kingdom T-DNA transfer from *Agrobacterium tumefaciens* to *Saccharomyces cerevisiae*. *EMBO J* 1995;**14**:3206–3214.

Caporaso JG, Kuczynski J, Stombaugh J, Bittinger K, Bushman FD, Costello EK, Fierer N, Gonzalez Pena A, Goodrich JK, Gordon JI, Huttley GA, Kelley ST, Knights D, Koenig JE, Ley RE, Lozupone CA, McDonald D, Muegge BD, Pirrung M, Reeder J, Sevinsky JR, Turnbaugh PJ, Walters WA, Widmann J, Yatsunenko T, Zaneveld J, Knight R. QIIME allows analysis of high-throughput community sequencing data. *Nat Meth* 2010;**7**:335-336.

Caporaso JG, Lauber CL, Walter WA, Berg-Lyons D, Lozupone CA, Turnbaugh PJ, Fierer N, Knight R. Global patterns of 16S rRNA diversity at a depth of millions of sequences per sample. *Proc Natl Acad Sci* USA 2011;**108**:4516–4522.

Cardinale M, De Castro JV, Müller H, Berg G, Grube M. *In situ* analysis of the bacterial community associated with the reindeer lichen *Cladonia arbuscula* reveals predominance of *Alphaproteobacteria*. *FEMS Microbiol Ecol* 2008;**66**:63–71.

Cardinale M, Grube M, Castro Jr JV, Müller H, Berg G. Bacterial taxa associated with the lung lichen *Lobaria pulmonaria* are differentially shaped by geography and habitat. *FEMS Microbiol Lett* 2012;***329***:111–115.

Cascales E, Christie PJ. The versatile bacterial type IV secretion systems. *Nat Rev Microbiol* 2003;**1**:137–149.

Cole JR, Chai B, Farris RJ, Wang Q, Kulam SA, McGarrell DM, et al. The Ribosomal Database Project (RDP-II): sequences and tools for high-throughput rRNA analysis. *Nucleic Acids Res*. 2005;33:294–296.

Daims H, Brühl A, Amann R, Schleifer KH, Wagner M. The domain-specific probe EUB338 is insufficient for the detection of all Bacteria: Development and evaluation of a more comprehensive probe set. *Syst Appl Microbiol* 1999;**22**:434–444.

Ding Z, Atmakuri K, Christie PJ. The outs and ins of bacterial type IV secretion substrates. *Trends Microbiol* 2003;**11**:527–535.

Erlacher A, Cernava T, Cardinale M, Soh J, Sensen CW, Grube M, Berg G. Rhizobiales as functional and endosymbiontic members in the lichen symbiosis of *Lobaria pulmonaria* L. *Front Microbiol* 2015;***6***.

Farr SB, Kogoma T. Oxidative stress responses in *Escherichia coli* and *Salmonella typhimurium*. *Microbiol Rev* 1991;**55:**561–585.

Gauslaa Y. *Lobaria pulmonaria*, an indicator of species-rich forests of long ecological continuity. *Blyttia* 1994;**52**:119–128.

Gilbert JA, Jansson JK, Knight R. The Earth Microbiome project: successes and aspirations. *BMC Biol* 2014;**12**:69.

Gonzalez JM, Portillo MC, Belda-Ferre P, Mira, A. Amplification by PCR artificially reduces the proportion of the rare biosphere in microbial communities. *PloS One* 2012;**7**:e29973.

Gourion B, Berrabah F, Ratet P, and Stacey G. Rhizobium–legume symbioses: the crucial role of plant immunity. *Trends Plant Sci* 2015;**20**:186–194.

Grube M, Cardinale M, Vieira de Castro J, Müller H, and Berg G. Species-specific structural and functional diversity of bacterial communities in lichen symbiosis. *ISME J* 2009;**3**:1105–1115.

Grube M, Cernava T, Soh J, Fuchs S, Aschenbrenner I, Lassek C, Wegner U, Becher D, Riedel K, Sensen CW, Berg G. Exploring functional contexts of symbiotic sustain within lichen-associated bacteria by comparative omics. *ISME J* 2015;**9**:412–424.

Herlemann DP, Lundin D, Labrenz M, Jürgens K, Zheng Z, Aspeborg H, Andersson AF. Metagenomic de novo assembly of an aquatic representative of the verrucomicrobial class Spartobacteria. *MBio* 2013;4:e00569–12.

Hodkinson BP, Gottel NR, Schadt CW, Lutzoni F. Photoautotrophic symbiont and geography are major factors affecting highly structured and diverse bacterial communities in the lichen microbiome. *Environ Microbiol* 2012;***14***:147–61.

Honegger (1998). Morphogenesis. p. 69,93. In: Nash TH (ed.), *Lichen Biology*, 2nd ed. Cambridge University Press, Cambridge, United Kingdom

Honegger R, Edwards D, Axe, L. The earliest records of internally stratified cyanobacterial and algal lichens from the Lower Devonian of the Welsh Borderland. *New Phytologist* 2013;**197**:264–275.

Huson DH, Mitra S, Weber N, Ruscheweyh H, Schuster SC. Integrative analysis of environmental sequences using MEGAN4. *Genome Res* 2011;**21**:1552–1560.

Janssen PH, Costa KC, Hedlund BP. 2011. Class III. Spartobacteria, p 834–841. In Krieg NR, Ludwig W, Whitman WB, Hedlund BP, Paster BJ,Staley JT, Ward N, Brown D, Oarte A (ed), Bergey's manual of systematic bacteriology, 2nd ed, vol 4. Springer Verlag, New York, NY.

Junttila S, Laiho A, Gyenesei A, Rudd S. Whole transcriptome characterization of the effects of dehydration and rehydration on *Cladonia rangiferina*, the grey reindeer lichen. *BMC Genomics* 2013;***14***:870.

Kant R, Van Passel MW, Palva A, Lucas S, Lapidus A, del Rio TG, Smidt H. Genome sequence of Chthoniobacter flavus Ellin428, an aerobic heterotrophic soil bacterium. *J Bacteriol* 2011;**193**:2902–2903.

Klappenbach JA, Dunbar JM, Schmidt TM. rRNA operon copy number reflects ecological strategies of bacteria. *Appl Environ Microbiol* 2000;**66**:1328–1333.

Klindworth A, Pruesse E, Schweer T, Peplies J, Quast C, Horn M, Glöckner FO. Evaluation of general 16S ribosomal RNA gene PCR primers for classical and next-generation sequencing-based diversity studies. *Nucleic Acids Res* 2013;**41**:1–11.

Kopylova E, Noé L, Touzet H. "SortMeRNA: Fast and accurate filtering of ribosomal RNAs in metatranscriptomic data". *Bioinformatics* 2012; doi: 10.1093/bioinformatics/bts611

Kosanić M., Ranković B. Lichen secondary metabolites as potential antibiotic agents. In: Ranković B. (ed.) Lichen secondary metabolites. Bioactive properties and pharmaceutical potential. Springer, Berlin. 2015;pp. 81–104.

Kukutla P, Steritz M, Xu J. Depletion of Ribosomal RNA for Mosquito Gut Metagenomic RNA-seq. *J. Vis. Exp*. 2013;**74**:e50093.

Lange OL, Green TA, Heber U. Hydration-dependent photosynthetic production of lichens: what do laboratory studies tell us about field performance? *J Exp Bot* 2001;***52***:2033–2042.

Lawrey JD, Diederich P. Lichenicolous Fungi : Interactions , Evolution , and Biodiversity. *The Bryologist* 2003;**106**:81–120.

Liba CM, Ferrara FIS, Manfio GP, Fantinatti-Garboggini F, Albuquerque RC, Pavan C, et al. Nitrogen-fixing chemo-organotrophic bacteria isolated from cyanobacteria-deprived lichens and their ability to solubilize phosphate and to release amino acids and phytohormones. *J Appl Microbiol* 2006;***101***:1076–1086.

Loy A, Maixner F, Wagner M, Horn M. probeBase - an online resource for rRNA-targeted oligonucleotide probes: new features 2007. *Nucleic Acids Res* 2007;**35**:D800–D804

Lundberg DS, Yourstone S, Mieczkowski P, Jones CD, Dangl JL. Practical innovations for high-throughput amplicon sequencing. *Nat Meth* 2013;**10**:999–1002.

Mavrodi DV, Peever TL, Mavrodi OV, Parejko JA, Raaijmakers JM, Lemanceau P, Mazurier S, Heide L, Blankenfeldt W, Weller DM, and Thomashow LS. Diversity and Evolution of the Phenazine Biosynthesis Pathway. *Appl Environ Microbiol* 2010;**76**:866–879.

Meyer F, Paarmann D, D'Souza M, Olson R, Glass EM, Kubal M et al. The metagenomics RAST server - a public resource for the automatic phylogenetic and functional analysis of metagenomes. *BMC Bioinformatics* 2008;**9**:386.

Nash, T.H. III. (2008) Introduction. p. 1–8. In: Nash TH (ed.), *Lichen Biology*, 2nd ed. Cambridge University Press, Cambridge, United Kingdom

Ondov BD, Bergman NH, and Phillippy AM. Interactive metagenomic visualization in a web browser. *BMC Bioinformatics* 2011;**12**:385.

Overbeek R, Begley T, Butler RM, Choudhuri JV, Chuang HY, Cohoon M, de Crécy-Lagard V, et al. The subsystems approach to genome annotation and its use in the project to annotate 1000 genomes. *Nucleic Acids Res* 2005;**33**:5691–702.

Pierson III LS, Pierson EA. Metabolism and function of phenazines in bacteria: impacts on the behavior of bacteria in the environment and biotechnological processes. *Appl Microbiol Biotechnol* 2010;**86**:1659–1670.

Pinto, AJ, Raskin L. PCR biases distort bacterial and archaeal community structure in pyrosequencing datasets. *PLoS ONE* 2012;**7**:e43093.

Pruesse E, Quast C, Knittel K, Fuchs BM, Ludwig WG, Peplies J, Glöckner FO. SILVA: a comprehensive online resource for quality checked and aligned ribosomal RNA sequence data compatible with ARB. *Nucl Acids Res* 2007;**35**: 7188–7196.

Quast C, Pruesse E, Yilmaz P, Gerken J, Schweer T, Yarza P, Peplies J, Glockner FO. The SILVA ribosomal RNA gene database project: improved data processing and web-based tools. *Nucleic Acids Res 2013;**41**:D590–D596*

Rajendhran J, Gunasekaran P. Microbial phylogeny and diversity: Small subunit ribosomal RNA sequence analysis and beyond. *Microbiol Res* 2011;**166**:99–110.

Remy W, Taylor TN, Hass H, Kerp H. Four hundred-million-year-old vesicular arbuscular mycorrhizae. *P Natl Acad Sci* 1994;***91***:11841–11843.

Rose F. Temperate forest management: its effect on bryophyte and lichen floras and habitats. In: Bates JW, Farmer AM, eds. *Bryophytes and Lichens in a Changing Environment.* Oxford, UK: Oxford University Press 1992; pp. 211–233.

Sangwan P, Chen X, Hugenholtz P, Janssen PH. *Chthoniobacter flavus* gen. nov., sp. nov., the first pure-culture representative of subdivision two, *Spartobacteria* classis nov., of the phylum *Verrucomicrobia*. *Appl Environ Microbiol* 2004;***70***:5875–5881.

Sangwan P, Kovac S, Davis KE, Sait M, Janssen PH. Detection and cultivation of soil Verrucomicrobia. *Appl Environ Microbiol* 2005;**71**:8402–8410.

Scheidegger C. Early development of transplanted isidioid soredia of *Lobaria pulmonaria* in an endangered population. *Lichenologist* 1995;**27**:361–374.

Schirrmeister BE, Dalquen DA, Anisimova M, Bagheri HC. Gene copy number variation and its significance in cyanobacterial phylogeny. *BMC Microbiology* 2012;***12***:177.

Schneider T, Schmid E, de Castro JV Jr, Cardinale M, Eberl L, Grube M, Berg G, Riedel K. Structure and function of the symbiosis partners of the lung lichen (*Lobaria pulmonaria* L. Hoffm.) analyzed by metaproteomics. *Proteomics* 2011;**11**:2752–2756.

Soto MJ, Sanjuán J, Olivares J. Rhizobia and plant-pathogenic bacteria: common infection weapons. *Microbiology* 2006;**152**:3167–3174.

Stach JEM, Bathe S, Clapp JP, Burns RG. PCR-SSCP comparison of 16S rDNA sequence diversity in soil DNA obtained using different isolation and purification methods. *FEMS Microbiol Ecol* 2001;**36**:139–151.

Stewart FJ, Ottesen EA, DeLong EF. Development and quantitative analyses of a universal rRNA-subtraction protocol for microbial metatranscriptomics. *The ISME J* 2010;***4***:896–907.

Susin MF, Baldini RL, Gueiros-Filho F, Gomes SL. GroES/GroEL and DnaK/DnaJ Have Distinct Roles in Stress Responses and during Cell Cycle Progression in Caulobacter crescentus. *J Bacteriol* 2006;**188**:8044–8053.

Wallner G, Amann R, Beisker W. Optimizing fluorescent in situ hybridization with rRNA-targeted oligonucleotide probes for flow cytometric identification of microorganisms. *Cytometry* 1993;**14**:136–143.

Waters VL. Conjugation between bacterial and mammalian cells. *Nature Genet* 2001;**29**:375–376.

Zwart G, Huismans R, van Agterveld MP, Van de Peer Y, De Rijk P, Eenhoorn H, Muyzer G, van Hannen EJ, Gons HJ, Laanbroek HJ. Divergent members of the bacterial division Verrucomicrobiales in a temperate freshwater lake. *FEMS Microbiol Ecol* 1998;**25**:159–169.

Figure legends

Figure 1: Taxonomical community composition for each omic-approach up to family level visualized in Krona-charts.

Figure 2: Relative sequence abundances of families within the highly abundant orders *Sphingobacteriales*, *Rhodospirillales*, *Sphingomonadales*, *Myxococcales* and *Chthoniobacterales* according to three omic approaches (16S rRNA amplicon-, metagenome and metatranscriptome analysis).

Figure 3: Scheme of the functional assignments of the metagenome and metatranscriptome based on SEED-classification. Functional categories of interest are visualized as pie charts representing the relative contributions of the five orders *Sphingobacteriales*, *Rhodospirillales*, *Sphingomonadales*, *Myxococcales* and *Chthoniobacterales* to each category. Functions associated with the primary metabolism and other categories are indicated in grey.

Figure 4: Confocal laser scanning microscopy images visualizing the colonization of *Spartobacteria* (A,B) and *Verrucomicrobia* (C) in general on the lichen thallus of *L. pulmonaria* stained by fluorescence *in situ* hybridization (FISH). Green: algae *Dictyochloropsis reticulata*; grey or blue/purple: lichenized fungus *L. pulmonaria*; yellow: *Spartobacteria*; red, other eubacteria. A, B**:** volume rendering of confocal stacks; C: three-dimensional model reconstruction visualized as isosurfaces and spheres. Arrows or circles indicate single colonies or areas with small clusters of *Spartobacteria* / *Verrucomicrobia* within the bacterial community.

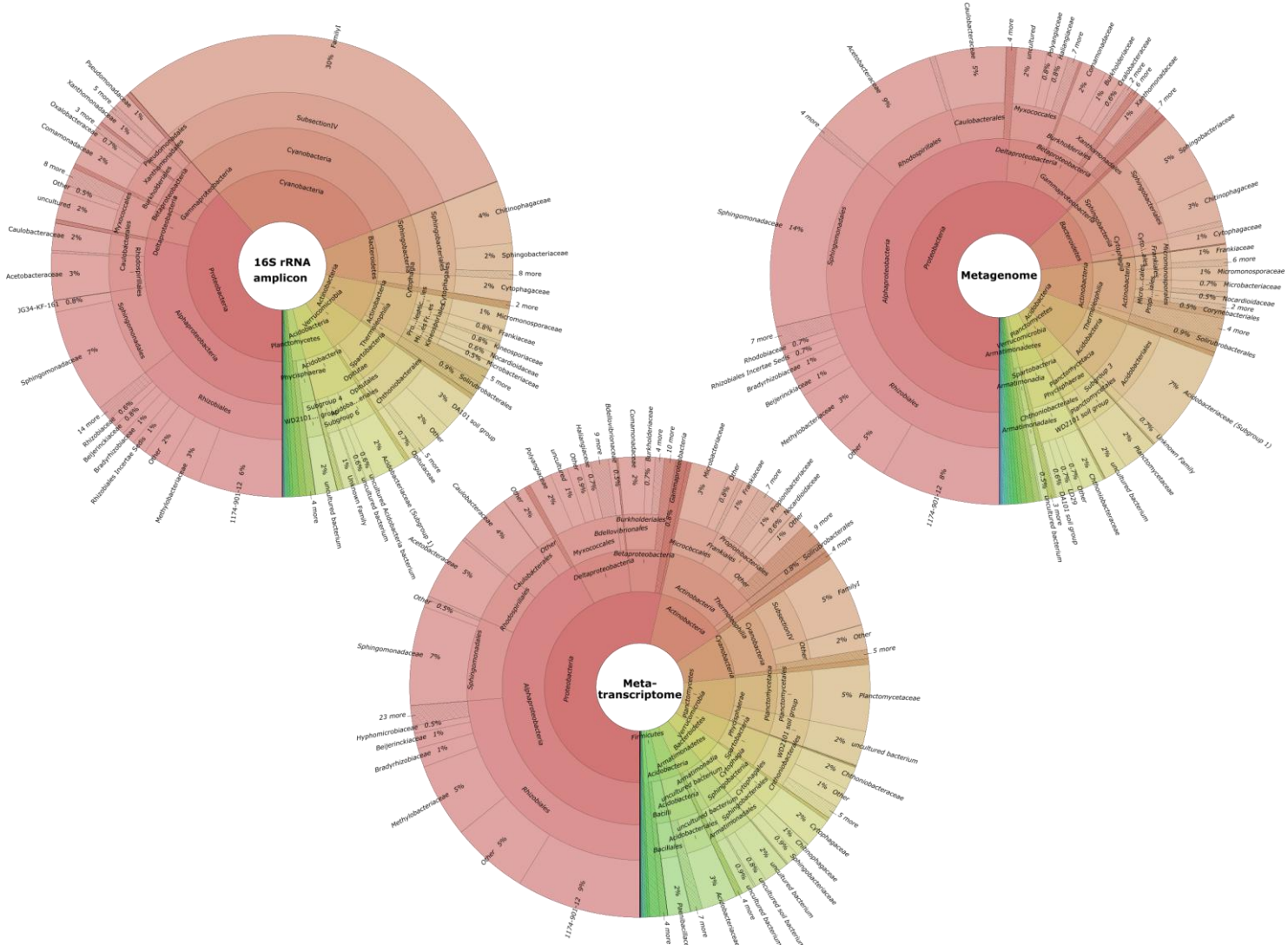

Figure 1

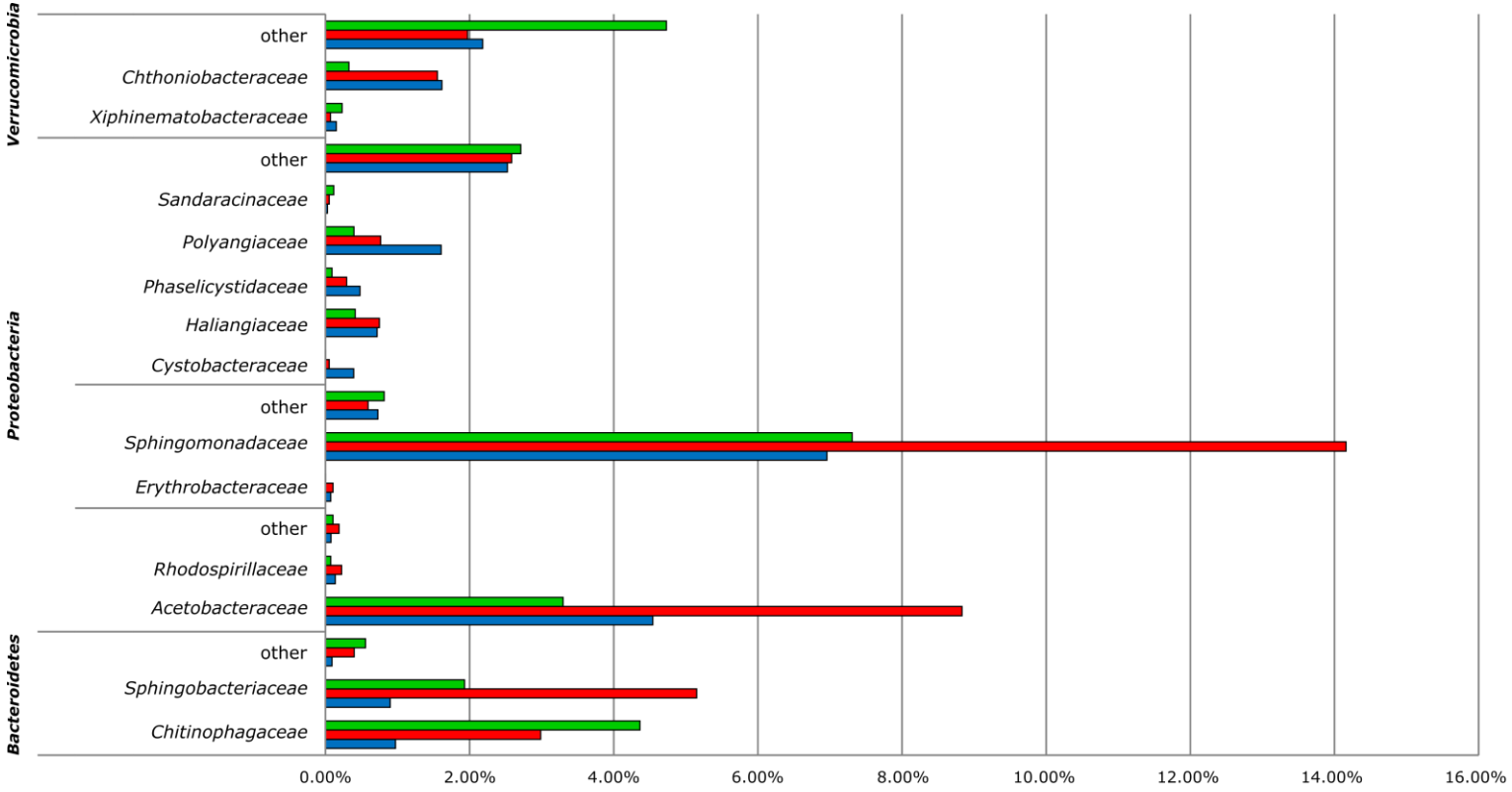

	Bacteroidetes			Proteobacteria												Verrucomicrobia		
	Sphingobacteriales			Rhodospirillales			Sphingomonadales			Myxococcales						Chthoniobacterales		
	Chitinophagaceae	Sphingobacteriaceae	other	Acetobacteraceae	Rhodospirillaceae	other	Erythrobacteraceae	Sphingomonadaceae	other	Cystobacteraceae	Haliangiaceae	Phaselicystidaceae	Polyangiaceae	Sandaracinaceae	other	Xiphinematobacteraceae	Chthoniobacteraceae	other
16S rRNA amplicon	4.36	1.93	0.56	3.30	0.08	0.11	0.00	7.31	0.82	0.00	0.41	0.09	0.40	0.12	2.71	0.23	0.33	4.73
meta-genome	2.99	5.15	0.40	8.83	0.23	0.19	0.10	14.16	0.59	0.05	0.75	0.30	0.77	0.05	2.58	0.07	1.55	1.97
meta-transcriptome	0.97	0.90	0.09	4.54	0.14	0.08	0.08	6.96	0.73	0.39	0.72	0.48	1.61	0.03	2.53	0.15	1.62	2.18

Figure 2

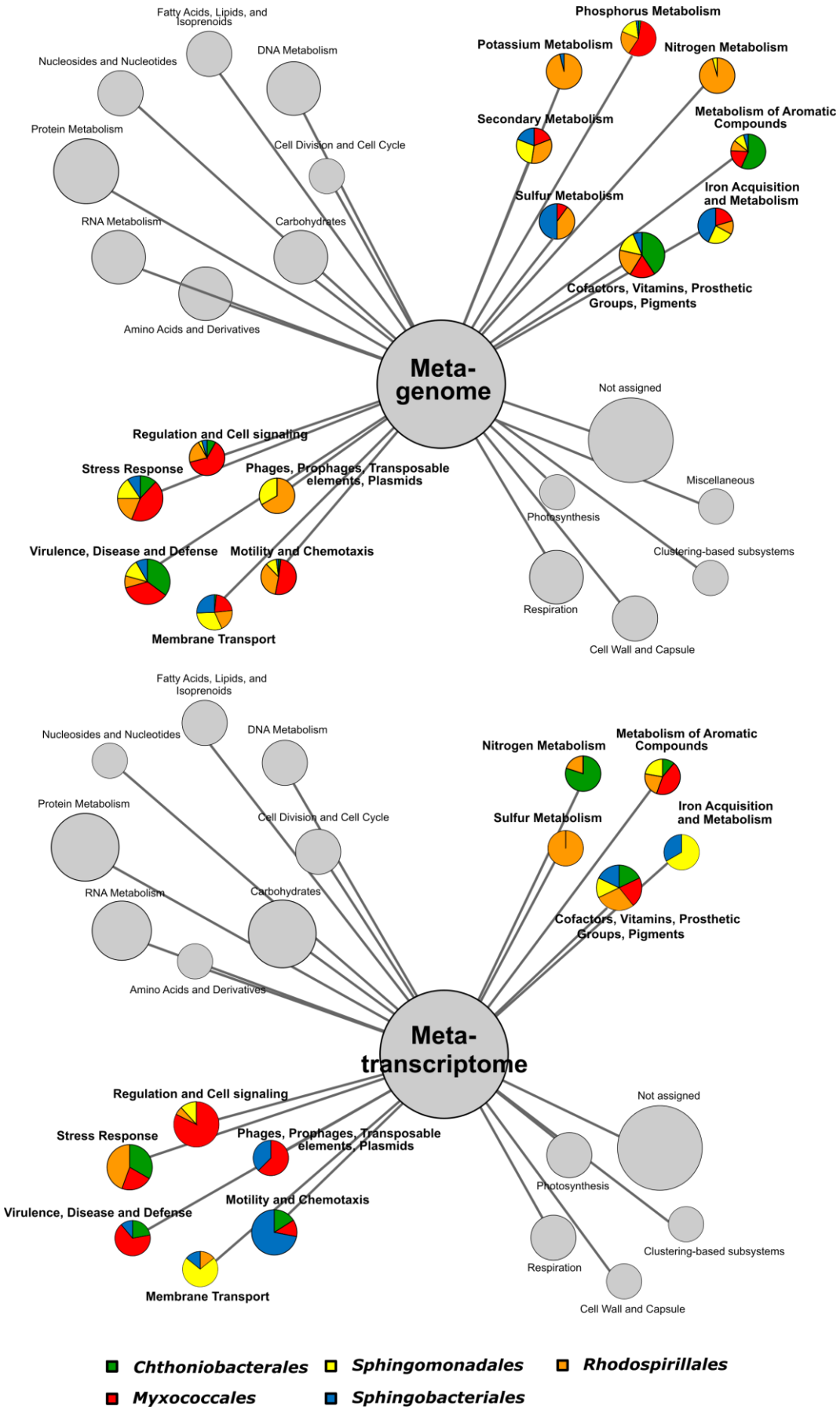
Meta-genome
Fatty Acids, Lipids, and Isoprenoids
DNA Metabolism
Nucleosides and Nucleotides
Protein Metabolism
Cell Division and Cell Cycle
RNA Metabolism
Carbohydrates
Amino Acids and Derivatives
Phosphorus Metabolism
Potassium Metabolism
Nitrogen Metabolism
Secondary Metabolism
Metabolism of Aromatic Compounds
Sulfur Metabolism
Iron Acquisition and Metabolism
Cofactors, Vitamins, Prosthetic Groups, Pigments
Regulation and Cell signaling
Stress Response
Phages, Prophages, Transposable elements, Plasmids
Virulence, Disease and Defense
Motility and Chemotaxis
Membrane Transport
Not assigned
Miscellaneous
Photosynthesis
Clustering-based subsystems
Respiration
Cell Wall and Capsule
Meta-transcriptome
Fatty Acids, Lipids, and Isoprenoids
DNA Metabolism
Nucleosides and Nucleotides
Protein Metabolism
Cell Division and Cell Cycle
RNA Metabolism
Carbohydrates
Amino Acids and Derivatives
Nitrogen Metabolism
Metabolism of Aromatic Compounds
Sulfur Metabolism
Iron Acquisition and Metabolism
Cofactors, Vitamins, Prosthetic Groups, Pigments
Regulation and Cell signaling
Stress Response
Phages, Prophages, Transposable elements, Plasmids
Virulence, Disease and Defense
Motility and Chemotaxis
Membrane Transport
Not assigned
Photosynthesis
Clustering-based subsystems
Respiration
Cell Wall and Capsule
Chthoniobacterales
Sphingomonadales
Rhodospirillales
Myxococcales
Sphingobacteriales

Figure 3

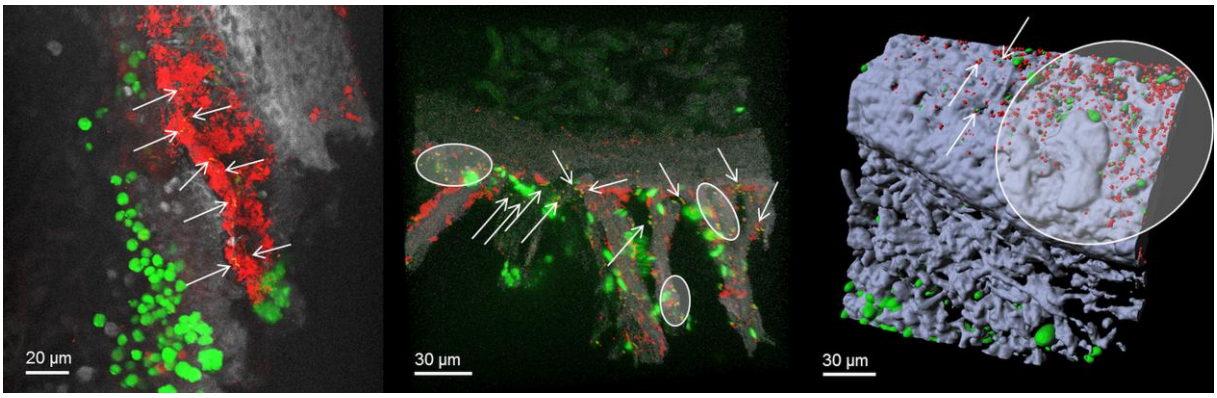

Figure 4

Manuscript II – Supplementary Data

Supplementary Tables

Table S 1: Primer sets for eukaryotic and prokaryotic rRNA gene fragment amplification. Bold: T7 promoter sequence; blue: enhancer sequence

Primer name	Sequence (5'-->3')
Eukaryotic SSU	
NS1	GTAGTCATATGCTTGTCTC
SR2_T7	GCCAGTGAATTG**TAATACGACTCACTATAGG**CGGCCATGCACCACC
SR8R	GAACCAGGACTTTTACCTT
NS8_T7	GCCAGTGAATTG**TAATACGACTCACTATAGG**TCCGCAGGTTCACCTACG
Eukaryotic LSU	
LR0R	ACCCGCTGAACTTAAGC
LR7_T7	GCCAGTGAATTG**TAATACGACTCACTATAGG**TACTACCACCAAGATCT
LR7R	GCAGATCTTGGTGGTAG
LR14_T7	GCCAGTGAATTG**TAATACGACTCACTATAGG**AGCCAAACTCCCCACCTG
Prokaryotic SSU	
803R_T7	GCCAGTGAATTG**TAATACGACTCACTATAGG**NCTACCTGGGTATCTAATCC
347F	GGAGGCAGCAGTRRGGAAT
1492R_T7	GCCAGTGAATTG**TAATACGACTCACTATAGG**GACGGCTACCTTGTTACGACTT
Prokaryotic LSU	
189F	GAASTGAAACATCTHAGTA
2490R_T7	GCCAGTGAATTG**TAATACGACTCACTATAGG**GCGACATCGAGGTGCCAAAC
1075F	GTTGGCTTRGARGCAGC
2241R_T7	GCCAGTGAATTG**TAATACGACTCACTATAGG**GACCGCCCCAGTHAAACT

Table S 2: Basic information about the three omic-approaches

meta-omic method	sequencing platform	# of sequences (post QC)	mean sequence length (post QC)	additional information
Genome	Illumina HiSeq 2000	67,731,962	143 ± 29 bp	Grube et al. (2015) MG-RAST ID: 4530091.3
Transcriptome total RNA	Illumina HiSeq 2500	3,932,528	105 ± 19 bp	
Transcriptome Depleted RNA	Illumina Hiseq 2500	23,118,362	113 ± 28 bp	
16S rDNA amplicons	Illumina MiSeq	415,693	290 ± 10 bp	Aschenbrenner et al. (2015)

ADDITIONAL PUBLICATION I

The ISME Journal (2015) **9**, 412–424

Exploring functional contexts of symbiotic sustain within lichen-associated bacteria by comparative omics

Martin Grube,[2*] Tomislav Cernava,[1*] Jung Soh,[3] Stephan Fuchs,[4] Ines Aline Aschenbrenner,[1,2] Christian Lassek,[4] Uwe Wegner,[4] Dörte Becher,[4] Katharina Riedel,[4] Christoph W. Sensen,[3] and Gabriele Berg[1]

[1]Institute of Environmental Biotechnology
Graz University of Technology, Austria

[2]Institute of Plant Sciences
University of Graz, Austria

[3]Department of Biochemistry & Molecular Biology
University of Calgary, Canada

[4]Institute of Microbiology
Ernst-Moritz-Arndt University of Greifswald, Germany

*These authors contributed equally to this work.

The ISME Journal (2015) 9, 412–424

www.nature.com/ismej

ORIGINAL ARTICLE

Exploring functional contexts of symbiotic sustain within lichen-associated bacteria by comparative omics

Martin Grube[1,5], Tomislav Cernava[2,5], Jung Soh[3,5], Stephan Fuchs[4], Ines Aschenbrenner[1,2], Christian Lassek[4], Uwe Wegner[4], Dörte Becher[4], Katharina Riedel[4], Christoph W Sensen[3] and Gabriele Berg[2]

[1]*Institute of Plant Sciences, Karl-Franzens-University, Graz, Austria;* [2]*Institute of Environmental Biotechnology, Graz University of Technology, Graz, Austria;* [3]*Department of Biochemistry & Molecular Biology, University of Calgary, Calgary, Alberta, Canada and* [4]*Institute of Microbiology, Ernst-Moritz-Arndt University of Greifswald, Greifswald, Germany*

Symbioses represent a frequent and successful lifestyle on earth and lichens are one of their classic examples. Recently, bacterial communities were identified as stable, specific and structurally integrated partners of the lichen symbiosis, but their role has remained largely elusive in comparison to the well-known functions of the fungal and algal partners. We have explored the metabolic potentials of the microbiome using the lung lichen *Lobaria pulmonaria* as the model. Metagenomic and proteomic data were comparatively assessed and visualized by Voronoi treemaps. The study was complemented with molecular, microscopic and physiological assays. We have found that more than 800 bacterial species have the ability to contribute multiple aspects to the symbiotic system, including essential functions such as (i) nutrient supply, especially nitrogen, phosphorous and sulfur, (ii) resistance against biotic stress factors (that is, pathogen defense), (iii) resistance against abiotic factors, (iv) support of photosynthesis by provision of vitamin B_{12}, (v) fungal and algal growth support by provision of hormones, (vi) detoxification of metabolites, and (vii) degradation of older parts of the lichen thallus. Our findings showed the potential of lichen-associated bacteria to interact with the fungal as well as algal partner to support health, growth and fitness of their hosts. We developed a model of the symbiosis depicting the functional multi-player network of the participants, and argue that the strategy of functional diversification in lichens supports the longevity and persistence of lichens under extreme and changing ecological conditions.

The ISME Journal (2015) **9,** 412–424; doi:10.1038/ismej.2014.138; published online 29 July 2014

Introduction

Symbiosis, one of the most common lifestyles on earth, is a long-term interaction, which acts as source of evolutionary innovation (Margulis and Fester, 1991; Martin and Schwab, 2013). The term symbiosis was introduced by Frank (1877) in a study of lichens, which are today considered a classic example for self-sustaining partnerships of species belonging to different kingdoms of life (Nash, 2008). Lichens represent one of most diversified and oldest symbiotic lifestyles of fungi, with more than 18 000 recognized fungal species and a typical stratified morphology that evolved at least 415 million years ago (Honegger *et al.*, 2013). The light-exposed lichen thalli are shaped by outer layers of fungal hyphae, which shelter internalized phototrophic partners. Lichen thalli develop only with proper combinations of fungal and algal species. Once the symbiotic phenotype is established, lichens may reach indeterminate ages and may even survive even the harshest conditions on earth (Øvstedal and Lewis-Smith, 2001). One reason for the ecological success of this fungal-algal partnership is the mutually enhanced ability to survive oxidative stress by suspended animation and rapid resumption of metabolism under permissive conditions (Kranner *et al.*, 2005). However, additional and hitherto unidentified forces might have helped lichens to adapt to nutrient-poor and hostile habitats with strong fluctuation of abiotic parameters.

Most biology textbooks characterize lichens as an association solely between a fungal (mycobiont) and

Correspondence: G Berg, Institute of Environmental Biotechnology, Graz University of Technology, Petersgasse 12, 8010 Graz, Austria.
E-mail: gabriele.berg@tugraz
[5]These authors contributed equally to this work.
Received 7 March 2014; revised 13 June 2014; accepted 17 June 2014; published online 29 July 2014

an algal (photobiont) partner. Our recent studies, however, revealed a high diversity of bacteria that are also associated with lichens. We have visualized biofilm-like communities, dominated by *Alphaproteobacteria* on the surfaces of thalli (Cardinale *et al.*, 2008, 2012a, b). Their structure suggests some degree of host specificity of the bacterial communities (Grube *et al.*, 2009; Hodkinson *et al.*, 2011; Bates *et al.*, 2011). The ubiquity and abundance of lichen-associated bacteria challenge the classic view of lichens as a two-tier partnership and support an extended concept that also includes the universally present bacterial communities. With this new perspective in mind, we have now explored the potential functions of the bacterial communities with the goal of understanding their symbiotic context in a more holistic way. Functional analysis of the culturable fraction of the lichen-associated bacteria suggested their involvement in several roles, including iron and phosphate mobilization, hormone production, nitrogen fixation as well as several lytic activities (Liba *et al.*, 2006; Grube *et al.*, 2009). The culturable fraction usually represents only a minor part of the total lichen-associated microbiome and therefore most likely does not cover the host-dependent majority of the bacterial species (Cardinale *et al.*, 2008). Recently developed omics approaches and subsequent bioinformatics tools are therefore required for a more comprehensive understanding of the role of the microbiome.

The objective of our study was therefore to investigate the function and metabolic potential of the bacterial lichen microbiome using a combined omics approach, together with a comprehensive spectrum of molecular, microscopic and physiological assays. The results were comparatively assessed and visualized using bioinformatics tools. For our study, we chose the lung lichen *Lobaria pulmonaria* (L.) Hoffm., a lichen which is considered to be endangered in many areas. *L. pulmonaria* serves as an indicator of primeval forest ecological continuity (Scheidegger and Werth, 2009). The mycobiont of *L. pulmonaria* engulfs a green-algal photobiont (*Dictyochloropsis reticulata*; found in 90% of the lichen surface) and a minor cyanobacterial partner, *Nostoc* sp. (Cornejo and Scheidegger, 2013). Schneider *et al.* (2011) provided an initial insight into the *L. pulmonaria* proteome and suggested *Lobaria* as an ideal model to study symbiotic processes. In our study, we extended this work and now provide results from the comparison of metagenomic and metaproteomic data.

Material and methods

Sampling strategy and preparation

L. pulmonaria was sampled from a rich population on maple tress (*Acer* spp.) in the Alps (Johnsbach, Austria; N 47°32′35″, E 14°37′38″) after visual inspection to avoid contamination by lichenicolous fungi and other organisms (Supplementary Figure S1). Using integrated sampling, a total amount of 176.3 g lichen was shock frozen with liquid nitrogen and immediately ground with mortar and pestle. The sample was homogenized in 360 ml 0.85% NaCl and filtered using a 63 μm mesh sieve; larger lichen parts were retained and colonizing bacteria were enriched in the filtrate. The filtrate was centrifuged at 8,000 r.p.m. at 4 °C for 20 min and the pellet was resuspended in 16×1.5 ml 0.85% NaCl aliquots. After a subsequent centrifugation step at 13 000 r.p.m. at 4 °C for 20 min, the supernatant was discarded and the pellets were used for DNA isolation (PowerSoil DNA Isolation Kit, MO BIO Laboratories Inc., Carlsbad, CA, USA). Following the DNA isolation, an aliquot containing 22 μg of metagenomic DNA was sent to GATC Biotech (Konstanz, Germany) for Illumina sequencing (HiSeq 2000 paired-end runs, Illumina Inc., San Diego, CA, USA).

Quality control and assembly of Illumina reads

Illumina HiSeq 2000 paired-end metagenomic DNA sequencing reads (GATC Biotech) were initially quality-checked using the FastQC program. The adapter sequence (5′-GATC GGAA GAGC ACAC GTCT GAAC TCCAG TCAC GTCC GCAC ATCT CGTAT-3′: identified as part of the Illumina TruSeq Indexed Adapter) was found in over 1% of the reads in set 1, and diminishing quality scores were observed towards the end of reads. Based on this observation, quality trimming and filtering was performed on each raw read set, using a custom-developed Perl script (written in-house by JS). The adapter sequences were removed and the sequence ends were trimmed, when the base quality score was smaller than 20. After the trimming step, reads were filtered out (i) if the length was shorter than 75 bp; (ii) or the read contained one or more ambiguous (N) bases; or (iii) the average quality score overall bases of the read was <25. After quality control, we did not observe overrepresented sequences, significant degradation of base qualities, or any other major quality issues. The sequence quality was confirmed again using the FastQC program. After quality control, some reads from set 1 did not have matching reads from set 2 due to read filtering, and vice versa. Therefore, to use paired-end information during assembly, only those reads that formed a matching pair were retained for further analysis.

Assembly of the reads into contiguous sequences (contigs) was performed using the Velvet *de novo* assembly software (Zerbino and Velvet, 2008; http://www.ebi.ac.uk/~zerbino/velvet/). Multiple trial assemblies with different *k*-mer lengths (57, 61, 65, 67, 69, 71 and 73) were performed and assembly statistics were compared with find the best *k*-mer length. All assemblies were conducted with an insert length of 350. The final *k*-mer length chosen was 71, which resulted in the maximum N50 value (2411 nts).

Taxonomic and functional analysis of assembled Illumina reads
The number of actual contigs used for this analysis was 368 424 (out of 503 528 overall contigs), based on the default Velvet minimum contig-length threshold of two times the *k*-mer length and the default coverage cutoff of half the median coverage. The Tera-BLASTN program (www.timelogic.com/documents/TeraBLAST_2009.pdf) was run on the 368 424 contigs, using TimeLogic (Active Motif, Carlsbad, CA, USA) DeCypher boards against the 'nt' database from NCBI (ftp://ftp.ncbi.nlm.nih.gov/blast/db). The blastn results were imported into MEGAN (Metagenome Analyzer, v4.70.4; Huson *et al.*, 2011) to produce several taxonomy profiles. For assembly-based functional analysis, we used a similar approach as above but using BLASTX (www.timelogic.com/documents/TeraBLAST_2009.pdf), which was run against the 'non-redundant protein sequence' database from NCBI (ftp://ftp.ncbi.nlm.nih.gov/blast/db). The blastx results were imported into MEGAN (v4.70.4) for functional analysis. Both SEED and KEGG functional analyses were conducted with MEGAN.

MG-RAST analysis of Illumina reads
Unprocessed Illumina HiSeq 2000 reads were uploaded on the MG-RAST v3 public server (Meyer *et al.*, 2008) to undergo paired-end reads joining and quality filtering (with default settings). 67 731 962 (88.8%) out of 76 310 051 sequences passed quality control; therein 60 015 088 (78,7%) sequences contained predicted proteins of either known or unknown function, while 1 788 100 (2.3%) sequences contained ribosomal RNA genes. SEED Subsystems Annotation was conducted with a maximum e-value cutoff of $1e^{-5}$ and a minimum 60% identity cutoff. Rarefaction analysis based on identified ribosomal RNA genes was done using best-hit classification and the Greengenes database (http://greengenes.lbl.gov) as the annotation source (with a minimum e-value cutoff of $1e^{-5}$; Supplementary Figure S2). The *Lobaria* metagenome was compared within a Principal Coordinates Analysis (annotation source: subsystems) with 20 publicly available datasets on MG-RAST. The functional abundance of eight particular habitats was compared using a minimum e-value cutoff of $1e^{-5}$. A table with all compared habitats together with their MG-RAST accession numbers is provided in the Supplementary Material (Supplementary Table S1). The metagenomic dataset is available under MG-RAST ID 4530091.3.

Quantitative real-time PCR
Quantification of *nifH* genes in the lichen DNA extract was conducted with primer pair *nifH*-F/*nifH*-R, as described by Hai *et al.* (2009). Standards containing the *nifH* fragments were prepared according to Bragina *et al.* (2013). Briefly, the gene fragments from *Erwinia carotovora* subsp. *atroseptica* SCRI1043 were cloned into the pGEM-T Easy Vector (Promega, Madison, WI, USA) and later re-amplified with vector-specific primers. Amplification-grade DNase I (Sigma-Aldrich, St Louis, MI, USA) treated total DNA extract was used to determine inhibitory effects of co-extracted substances. Based on this experiment, the total community DNA was diluted to 1:25 and target genes were amplified using KAPA SYBR FAST qPCR Kit (Kapa Biosystems, Woburn, MA, USA). Two independent runs, with three replicates for each sample, were performed on the Rotor Gene 6000 (Corbett Research, Mortlake, VIC, Australia), according to Bragina *et al.* (2013). The specificity of the amplicons was confirmed with both melting-curve analysis and gel electrophoresis of the qPCR products, respectively. Gene copy numbers for *nifH* were calculated per gram of lichen fresh weight.

Sample preparation for protein extraction
The collected thalli (Johnsbach, Austria; N 47°32′35″, E 14°37′38″) were cleaned with sterile tweezers from moss, bark and other visible contaminations. Samples from different thalli were pooled to a total amount of 2 g. Liquid nitrogen was added to the pooled thalli, which were subsequently ground to a fine powder using mortar and pestle. Proteins were extracted as described by Wang *et al.* (2006).

Gel electrophoresis with extracted proteins
One-dimensional SDS-polyacrylamide gel electrophoresis was performed as described earlier (Laemmli, 1970), and by loading 50 µg of extracted lichen protein mixture per lane. The sample was analyzed in three technical replicates (three lanes). Electrophoresis was carried out at 150 V and 250 mA for 45 min, afterwards proteins were fixed by shaking the gel in an aqueous solution containing 40% ethanol and 10% acetic acid for 30 min. Finally, proteins were stained with 25 ml of colloidal Coomassie Brilliant Blue G (Sigma-Aldrich, Steinheim, Germany), as described earlier (Neuhoff *et al.*, 1988). The gel was scanned on a standard light scanner (Microtek, Hsinchu, Taiwan) for documentation. Afterwards each of the three lanes was cut into 20 pieces, as shown in the Supplementary Material (Supplementary Figure S3).

In-gel digestion after SDS-polyacrylamide gel electrophoresis
Each of the 20 gel pieces from the three technical replicates was cut into small cubes (1 mm^3), which were destained by adding 700 µl of 30% acetonitrile containing 0.2 M NH_4HCO_3, and shaking for 15 min at 37 °C and 1500 r.p.m. This step was repeated

twice. After destaining, the pieces were dried in a vacuum concentrator (Eppendorf, Hamburg, Germany). In-gel digestion was performed with 50-μl-modified sequence-grade trypsin (Promega), with an enzyme concentration of $2\,\mu g\,ml^{-1}$ overnight at 37 °C. Subsequently, peptides were eluted by sonication for 15 min (Ultra sonic cleaner, VWR, Darmstadt, Germany). The eluted peptides were transferred into vials, dried in a vacuum concentrator (Eppendorf) again, and finally dissolved in 10 μl of ultrapure water.

Mass spectrometry analysis

Peptide mixtures resulting from in-gel tryptic cleavage were subjected to liquid chromatography-tandem mass spectroscopy measurements, using an EASYnLC 1000 (Thermo Scientific, Odense, Denmark), with self-packed columns (Luna 3 μ C18(2) 100 A, Phenomenex, Aschaffenburg, Germany) in a one-column setup online, coupled to an Orbitrap Elite mass spectrometer (Thermo Fisher, Bremen, Germany). Samples were loaded and desalted in 0.1% acetic acid, with a flow rate of $700\,nl\,min^{-1}$, followed by peptide separation achieved by a binary non-linear 170 min gradient from 5–50% acetonitrile in 0.1% acetic acid at a flow rate of $300\,nl\,min^{-1}$. Mass spectrometric measurement was performed in the Orbitrap Elite (Thermo Fisher Scientific) at a spray voltage of 2.4 kV applied to the emitter. After a survey scan in the Orbitrap ($R = 30\,000$) tandem mass spectroscopy data were recorded for the 20 most intensive precursor ions in the linear ion trap. Singly charged ions were not taken into account for tandem mass spectroscopy analysis. The lock mass option was enabled throughout all analyses.

Database construction for metaproteome analysis, database search and metaproteome data analysis

Due to the lack of translated metagenomic sequences of *L. pulmonaria,* a synthetic metagenomic-based database was created. This database contained all protein sequences available in the NCBI NR protein database (state of 13.09.26) which have been predicted to be present in the sample based on similarity searches of the metagenomic reads by BLAST (Altschul *et al.*, 1990). Because neither the fungal nor the algal symbiont genomes of *L. pulmonaria* have been sequenced yet, all available NCBI protein sequences from fungi and algae were added to the database, together with a set of typical contaminations (for example, porcine trypsin, human keratin). Entries with the same protein sequence, but different headers were combined into one entry by an in-house php script (written by SF). The final database contained 2 473 550 protein sequences, pointing to 2 581 850 GenBank identifiers (bacteria: 1 564 300; algae: 226 723; fungi: 513 152; archaea: 26 952; other unclassified: 250 723).

The raw files were converted to mgf-files by MSconvert (www.Proteowizard.org), and searched with the Mascot search engine (version 2.2.04, Matrix Science Inc., Boston, MA, USA) with the following parameters: parent mass tolerance 10 ppm, fragment mass tolerance 0.5 Da, maximum missed cleavages 2; charge state 1+; variable modifications and oxidation of methionine. The Mascot search was followed by an X-tandem analysis in Scaffold (version 4.0.7, Proteome Software Inc., Portland, OR, USA). This analysis was performed as a 'MudPit experiment' to merge the individual mascot result files into a single file. The results were filtered as follows: 99% peptide probability, 1 peptide, 99% protein probability. Only proteins detected in two out of three technical replicates were considered for further analyses.

For functional classification and taxonomical distribution the in-house developed metaproteome analyses pipeline 'Prophane 2.0' was used (http://www.prophane.de; Schneider *et al.*, 2011). Briefly, peptide to protein matches were clustered in groups by the Scaffold software. To standardize functional annotation all peptide to protein matches were functionally characterized based on TIGRFAMs (release 12; Haft *et al.*, 2013) using HMMER3 (e-value $\leqslant 1E-10$; Haft *et al.*, 2013; Eddy, 2011). Functional data were transferred to the protein group if the members share the same predicted function. If these proteins share multiple predicted functions the function with the lowest overall e-value were assigned to the respective protein group. Groups of proteins sharing no functional prediction were named heterogeneous on functional level.

Moreover, protein groups were taxonomically classified based on the annotation of the respective protein members. Protein quantification was based on normalized spectral abundance factor values (Zybailov *et al.*, 2006), however, only exclusive spectral counts were considered.

Voronoi treemaps

Voronoi treemaps were generated using Paver (Decodon, Greifswald, Germany, http://www.decodon.com/).

Fluorescence *In Situ* Hybridization and Confocal Laser Scanning Microscopy samples were collected from the same *Lobaria* population used for the metagenomics and metaproteomics analysis. Lichen thalli were fixed with 4% paraformaldehyde/phosphate-buffered saline (PBS) (v/v, 3:1) at 4 °C for at least 4 h, followed by three washing steps with ice-cold PBS. The samples were stored at −20 °C in ethanol absolute/PBS (v/v, 1:1). Before the hybridization step of the thallus, 30-μm thick cryosections were made. Fluorescence *In Situ* Hybridization was carried out in tubes, as outlined in Cardinale *et al.*,

(2008) and samples were analyzed using a Leica TCS SPE microscope (Leica Microsystems, Heidelberg, Germany), as well as image analysis and three-dimensional modeling, using the software Image Surfer (http://imagesurfer.cs.unc.edu/) and Imaris 7.0 (Bitplane, Zurich, Switzerland), respectively.

Isolation of lichen-associated bacteria
Lichen thalli of *L. pulmonaria* were sampled from three different locations in Austria (Tamischbachgraben, N 47°32′40″, E 14°37′35″, Johnsbach, N 47°32′35″, E 14°37′38″, and St. Oswald, N 46°44′50″, E 15°04′26″). After grinding lichen samples with mortar and pestle, a homogenate was prepared using sterile 0.85% NaCl in a 1:10 (w/v) ratio, together with a lab stomacher (BagMixer; Interscience, St Nom, France). Diluted fractions were plated on R2A agar (Carl Roth, Karlsruhe, Germany), R2A agar with 25 μg ml^{-1} cycloheximide, starch casein agar (Kuester and Williams, 1964) and ISP2 agar (Shirling and Gottlieb, 1966). Bacterial colonies were randomly picked within 5 days of incubation at room temperature.

Screening of isolates for in vitro antagonistic activity towards particular bacteria and fungi
Dual-culture experiments were carried out as confrontation assays, using different media and target organisms according to Berg *et al.* (2002) and Opelt *et al.* (2007). Lichen-associated isolates were spotted on solid media pre-inoculated with *E. coli* XL1 and *S. aureus* ATCC 25923 and assessed for inhibition zones after 4 days of incubation at 30 °C. Antagonistic activity against the fungus *Botrytis cinerea Pers.* (TU Graz culture collection, Graz, Austria) was tested by dual culture on Waksman agar, according to Berg *et al.* (2002) and assessed after 5–7 days of incubation at 20 °C. Cultures of the lichen-colonizing fungus *Rhinocladiella* sp. (TU Graz culture collection) were homogenized and resuspended in sterile 0.85% NaCl. Aliquots from one batch (50 μl) were used to inoculate each well of 24-well plates, containing solid potato dextrose agar (Carl Roth, Karlsruhe, Germany). Subsequently, 100-μl culture filtrate obtained from each lichen-associated isolate was added to particular wells. After 3 weeks of incubation, the wells were checked for growth reduction. All experiments were conducted with replicates and carried out twice.

Functional assays with Lobaria-associated bacteria
Altogether, 388 randomly selected bacterial cultures were subjected to functional assays based on different growth media. Protease, β-glucanase and chitinase activity were analyzed according to Berg *et al.* (2002), and phosphate solubilization of strains as described by Nautiyal (1999). *Chromobacterium violaceum* CV026 was used to detect C4–C6 AHL-mediated quorum sensing by visualizing purple pigmentation of the reporter strain (McClean *et al.*, 1997). *Pseudomonas putida* F117 pAS-C8 and *P. putida* F117 pAS-C12 (Steidle *et al.*, 2001) were used to detect C8 AHLs and C12 AHLs, respectively. Visualization of the green fluorescent protein-based AHL sensor was achieved through epifluorescence imaging, using an Universal Hood III (Bio-Rad, Hercules, CA, USA). All strains were incubated at 30 °C for 48 h.

Results

Taxonomic structure of the bacterial lichen microbiome
The analysis of 368 424 contigs revealed the taxonomic profile represented in Figure 1 that shows the overall composition of the metagenome and a more detailed structure of the dominant bacterial taxa within. Among the *Proteobacteria*, *Alphaproteobacteria* was the prominent taxon, with *Rhizobiales* and *Sphingomonadales* as the most frequently called orders. Within *Rhizobiales*, *Methylobacteriaceae* and *Bradyrhizobiaceae* are prominent, with *Rhizobiaceae*, *Beijerinckiaceae*, *Xanthobacteriaceae* and *Phylobacteriaceae* in minor quantities. Almost all of the *Sphingomonadales* belonged to the *Sphingomonadaceae*, and we estimate that a total of more than 800 bacterial species represent the diversity of the associated bacterial community, according to the rarefaction analysis (Supplementary Figure S2). Results derived from the present metaproteomic analysis presented an outmost similar community structure to the metagenome analysis. *Proteobacteria* were the predominant phylum and accounted for 361 distinct database hits, followed by *Cyanobacteria* with 47 hits and *Acidobacteria* with 28 hits. A complementary Fluorescence *In Situ* Hybridization visualization with *Alphaproteobacteria* and *Betaproteobacteria* specific probes, together with unspecific eubacteria probes illustrated and generally confirmed the taxonomic distribution observed by the metagenome analysis. *Alphaproteobacteria* were predominant and widespread on both, the upper and lower surface of the leaf-like lichen thallus, respectively, while *Betaproteobacteria* were less abundant and locally restricted (Figure 2a).

Metagenome and proteome of the bacterial lichen microbiome
Functional analyses of the lichen metagenome focused on bacterial contigs, as the sampling procedure was designed to enrich the bacterial metagenome, using both SEED and KEGG functional analyses. SEED functional analysis was used for finding a set with functions of interest (that is, carbohydrate, virulence, cofactors and so on), many of which are standard SEED functional terms. Out of the 368 424 contigs, 69 823 were assigned to a functional term and the breakdown of the assignments at the top level is shown as a bar graph

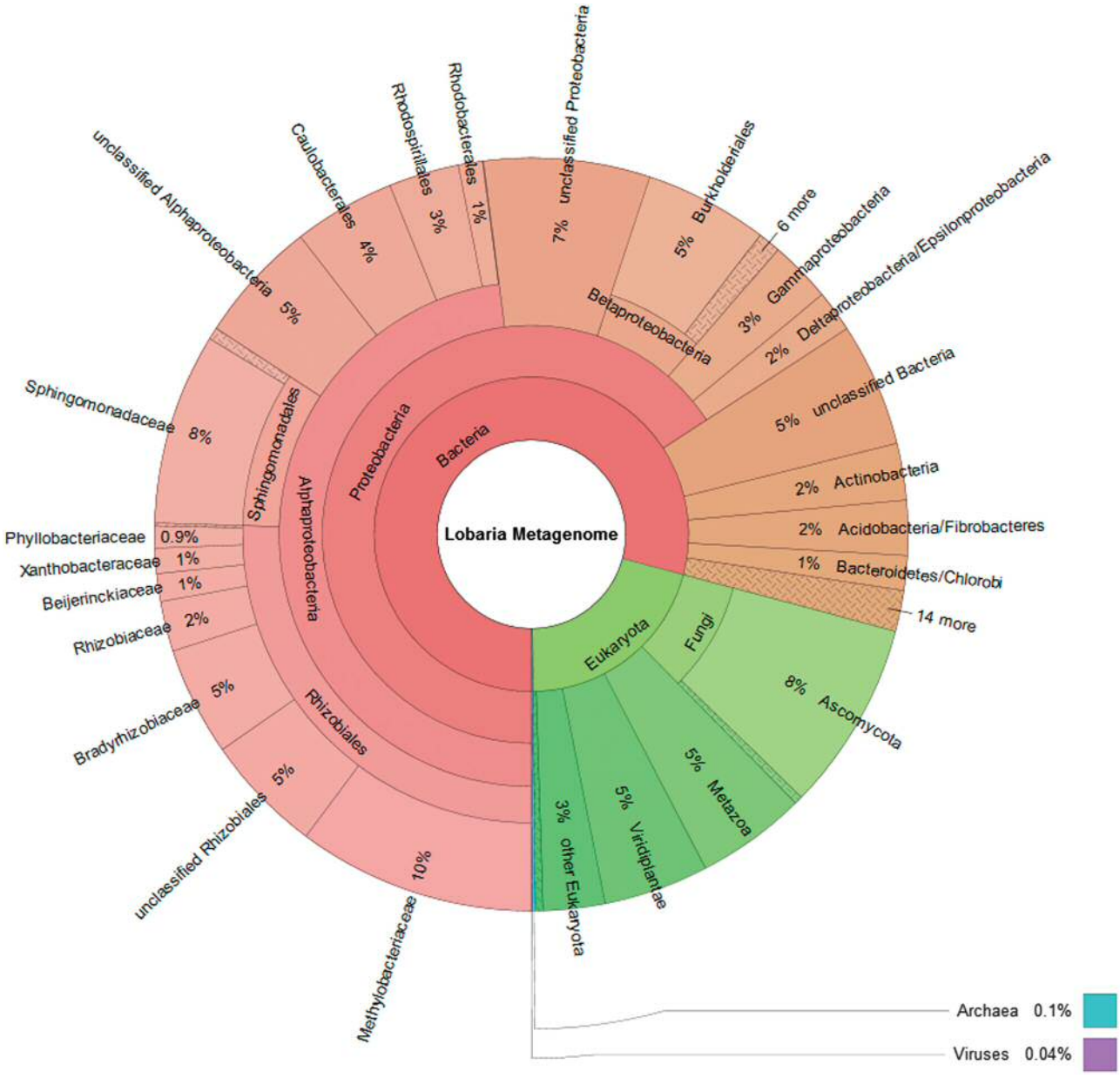

Figure 1 Taxonomic spectrum visualized with Krona (www.krona.sourceforge.net/) of contigs in the metagenome for all domains of life. Circles represent taxonomic classifications in ascending order up to the family level (outermost circle). Less-abundant taxa are listed outside the charts together with their relative abundance.

(Supplementary Figure S4). A significant number of contigs represented primary metabolic functions of bacteria (amino acids and derivatives: 6440; central carbohydrate metabolism: 2770; fatty acids, lipids and isoprenoids: 2721). Taxonomic separation of functional assignments revealed that up to 50% of different functional terms were covered by *Alphaproteobacteria*, while less-abundant bacteria account for the remaining contigs (Figure 3). Moreover MG-RAST visualization of functional abundance with SEED subsytems annotation showed presence of all level 4 functional terms. Out of the 368 424 contigs, 66 739 were assigned to KEGG pathways. Although the KEGG pathway assignment is primarily developed using mammalian genome information, it covers central capabilities of universal primary metabolism (carbohydrate metabolism: 12 823, energy metabolism: 7616, lipid metabolism: 5301, nucleotide metabolism: 5909, amino acid metabolism: 12 784, metabolism of other amino acids: 4068, glycan biosynthesis and metabolism: 2181 and genetic information processing: 12 258). Principal Coordinates Analysis carried out with MG-RAST revealed a unique functional distribution most similar to the one found on the plant phyllosphere (Figure 4; Supplementary Table S1).

Lichen samples used for metagenome analyses were investigated in parallel on metaproteomics

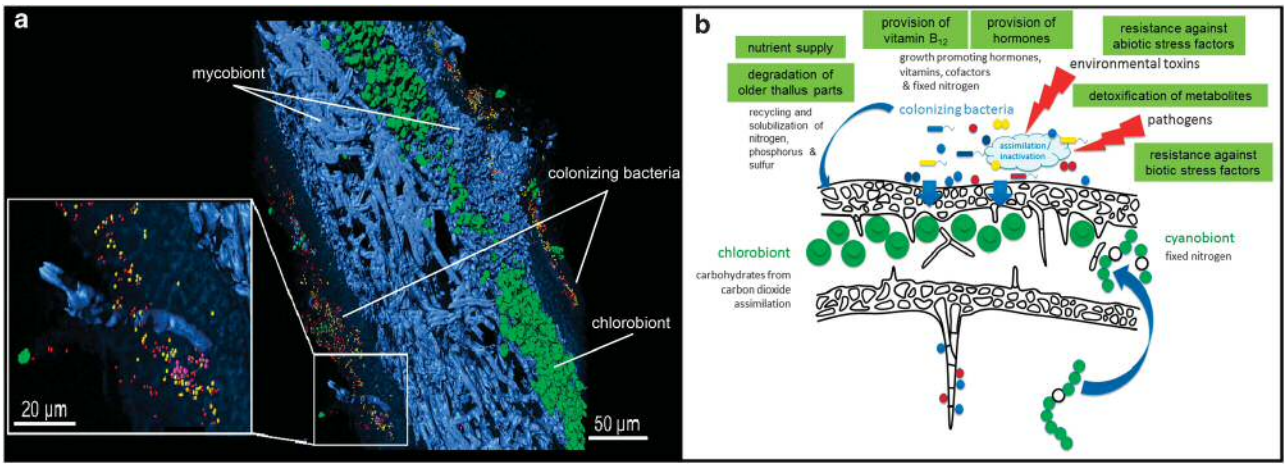

Figure 2 (**a**) Leaf-like thallus visualization of bacteria on a cross-section by 3D reconstruction of FISH image stacks. *Eubacteria* (red) and *Alphaproteobacteria* (yellow) were found widespread on both, the upper and the lower cortex, while *Betaproteobacteria* (pink) were less abundant and locally contained. Fungal hyphae (blue) and algae located under the upper cortex (green) were visualized without specific FISH probes, due to the naturally occurring fluorescence of the internal structures. (**b**) Model of the lichen symbiosis depicting the functional network of the participants. The model includes relevant functions of the colonizing bacteria, which are derived from metagenomic/metaproteomic analysis, as well as cultivation-dependent experiments.

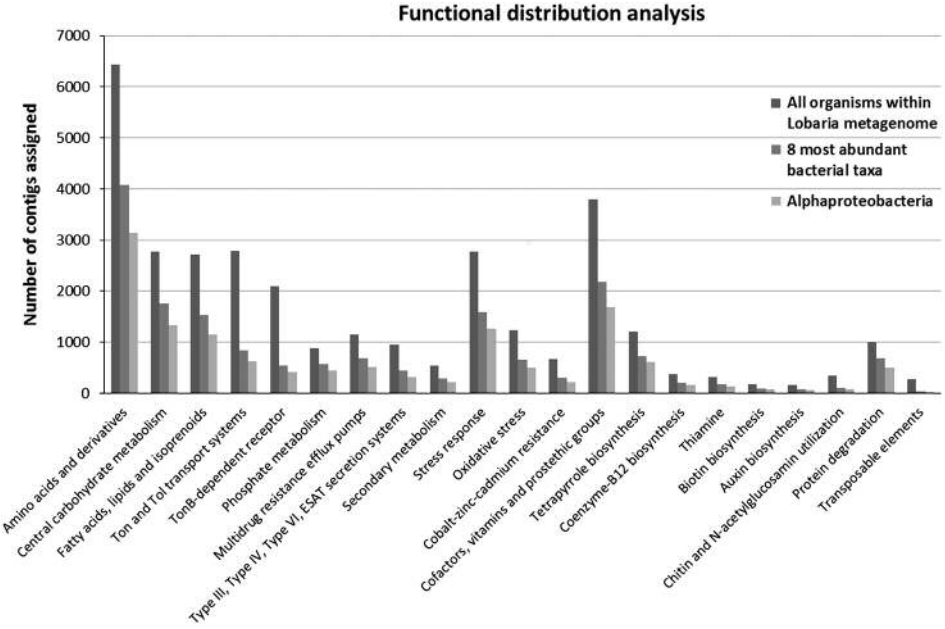

Figure 3 Distribution of particular functions prior and after exclusion of less-abundant taxa. The number of contigs assigned to all organisms within the sample (blue bars) is visualized in contrast to assigned contigs of the eight most-abundant taxa (*Alphaproteobacteria*, *Betaproteobacteria*, *Gammaproteobacteria*, *Deltaproteobacteria*, *Actinobacteria*, *Acidobacteria*, *Bacteroidetes* and *Firmicutes*; red bars) and *Alphaproteobacteria* (green bars). The full colour version of this figure is available at *ISME* Journal online.

level. For this a in-gel tryptic digestion followed by liquid chromatography-tandem mass spectrometry based metaproteomics approach was used as recently described (Schneider *et al.*, 2011) combined with a database containing all BLAST protein hits of the metagenomic reads (best hit per read). In total, our metaproteome analyses revealed 4405 different proteins, which were covered by at least one peptide-to-spectrum match (99% peptide probability, 99% protein probability) in at least two of three replicates. All proteins were divided into 3226 groups, based on shared peptide-to-spectrum matches by the Scaffold software (Koskinen *et al.*, 2011). Out of these, 2676 and 541 groups could be unambiguously assigned to a eukaryotic and eubacterial origin, respectively, employing the Prophane workflow (Schneider *et al.*, 2011). As our study aims for a better understanding of structure and functionality of the bacterial lichen microbiome, further functional analyses based on TIGRFAMs (e-value $\leqslant 1E-10$) focused exclusively on protein groups of bacterial origin. Functional

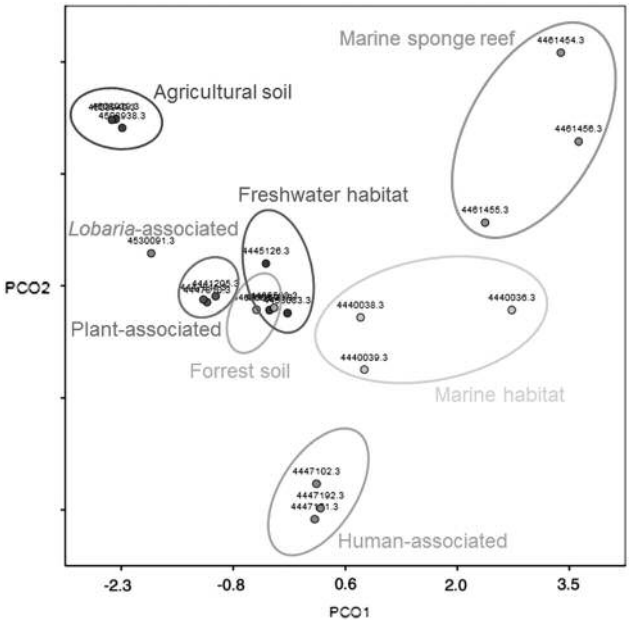

Figure 4 Principal Coordinates Analysis (PCoA) including 20 publicly available metagenomic datasets from MG-RAST and the *Lobaria* metagenome (red dot). All datasets were compared with subsytems and calculated using normalized values and the Bray-Curtis distance matrix. Single metagenomes from different biomes are labeled with their MG-RAST accession numbers and grouped in colored ellipses. The full colour version of this figure is available at *ISME* Journal online.

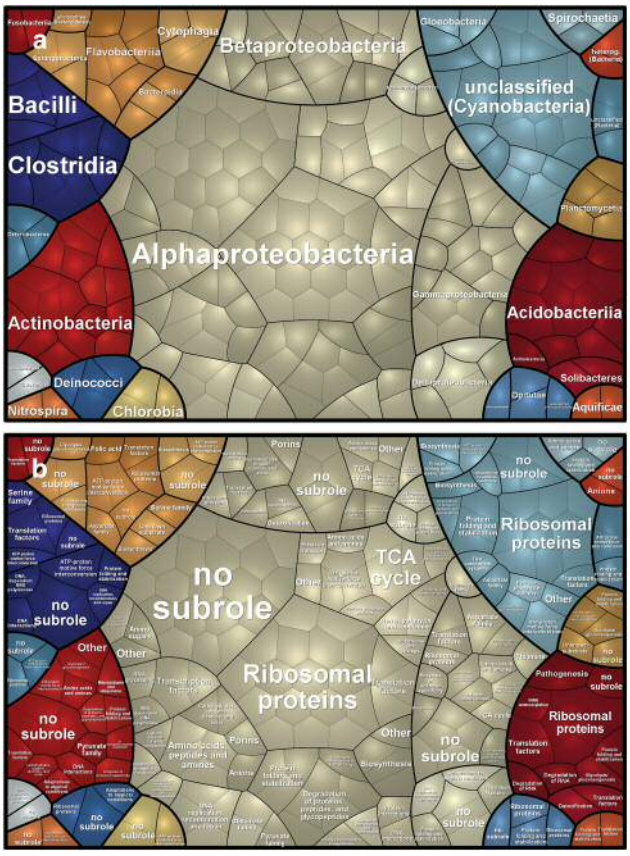

Figure 5 Voronoi Treemap visualization of the prokaryotic metaproteome on the taxonomic (**a**) and functional (**b**) level. The taxonomic and functional distributions were carried out by Prophane 2.0. Taxonomic groups are indicated by different colors (**a** and **b**) and the functional classes are separated by black lines (based on TIGRRoles). Each cell represents at least one protein (or protein group) assigned to the respective phylum.

data were only transferred to bacterial protein groups whose members share the same functional prediction (424 out of 541, see material and methods for details). To gain a view on the role of bacterial proteins, the data were visualized with Voronoi treemaps, which also show the participation of different eubacterial groups in functions (Figure 5). In addition, we integrated the metaproteomic data with metagenomic data using the Voronoi treemap (Figure 6). Generally, most of the functional classes predicted by the metagenome analysis are also represented by at least one protein. As expected, numerous proteins assigned to functions involved in protein synthesis, DNA replication, recombination and repair were found in the metaproteome. Moreover, a significant number of proteins involved in protein fate and central energy metabolism, for example, tricarbonic acid cycle, were recovered from the bacterial lichen microbiome.

Selected functions of the bacterial lichen microbiome

Nutrient supply. About 2793 contigs suggested the presence of Ton and Tol transport systems, some of which are also involved in iron uptake. The TonB-dependent receptor, a family of beta-barrel proteins from the outer membrane of Gram-negative bacteria and responsible for siderophore transport into the periplasm, was present in 2094 contigs. Metaproteome analysis indicated at least four different types of TonB-dependent receptors, which were derived from two different bacterial phyla (*Proteobacteria* and *Bacteroidetes*, respectively). Phosphate metabolism is represented in 885 contigs, as well as in two PFAM classifications within the metaproteome and also includes proteins involved in solubilization of phosphates. Corresponding to this finding, 19.6% of all bacterial isolates from *Lobaria* formed clearing zones on NBRIP agar and thus underscored the potential role of lichen-associated bacteria in the solubilization of phosphates. Moreover, we utilized a quantitative real-time PCR approach, based on total community DNA, to evaluate the bacterial potential for nitrogen fixation. Therewith $\log_{10}$ 5.0 ± 0.1 *nifH* copies were identified per gram of lichen fresh weight.

Resistance against biotic stress factors (pathogen defense). Virulence functions are common among the lichen-associated bacteria. About 1152 contigs were assigned to multidrug resistance efflux pumps, and multiple genes that code for resistance against antibiotics were also found (fluoroquinolone, vancomycin, methicillin, penicillin and cephalosporine) in addition to the 955 contigs that contribute

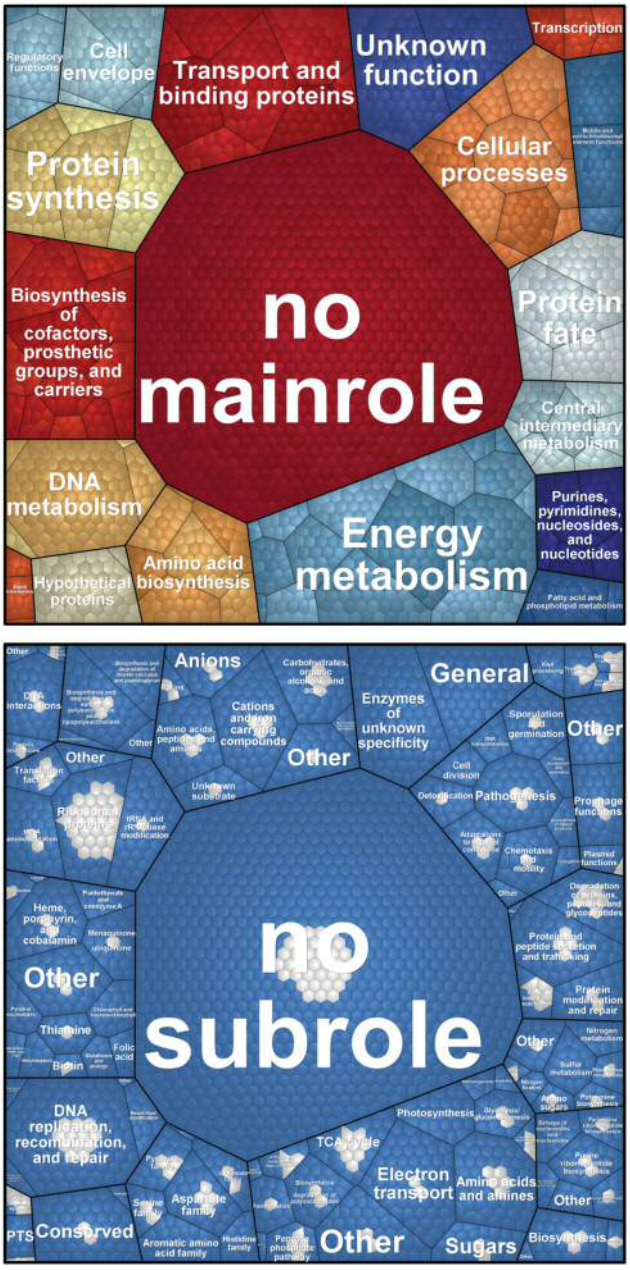

Figure 6 Functional recovery of the bacterial lichen microbiome metagenome on the metaproteomic level using Voronoi treemaps. The protein sequences were compared with metagenomic contigs by BLAST and then functionally characterized using HMMER3 and TIGRFAMs. Upper panel shows all functions covered by the metagenome (third level) and the respective subroles (second level) and main roles (first level). The mainrole labels are shown. On the lower panel, metaproteomic coverage is shown (blue cells: functions present only in the metagenome; grey cells: functions present in both metagenome and metaproteome).

to Type III, Type IV, Type VI and ESAT secretion systems. Type VI secretion systems were represented by three different variants in the metaproteome data, as well as one specific hit for an acriflavin-resistance protein. A moderate number of genes were also found which contribute to secondary metabolism, according to SEED analysis (548 contigs); some of the secondary metabolites are known as antibacterials or antifungals, but are represented by a fairly low number of contigs (phenazine biosynthesis protein PhzF: 26 contigs, clavulanic acid biosynthesis: 11 contigs). Furthermore, results from cultivation-dependent studies involving *Lobaria*-associated bacteria combined with taxonomic data from the present metagenomic approach suggest that around 7% of the taxa present have an antagonistic potential. The majority of these showed antagonism against fungi (data not shown).

Resistance against abiotic stress factors. Stress-related functions are distinct in the bacterial microbiome (2769 contigs; oxidative stress: 1238). About 891 contigs indicated genes conferring resistance to metals (copper, cobalt-zinc-cadmium, silver, mercury and arsenic). Interestingly, a similar proportion of oxidative-stress protectants to heavy metal efflux pumps was observed in the metaproteome (3 and 1, respectively). In addition, we looked for genes involved in dormancy and sporulation, as we expected this to be an important aspect of bacteria adapted to the poikilohydric life on lichens. However, only 13 contigs were related to this function.

Photosynthesis support by vitamin B_{12}. Numerous genes are involved in the metabolism of cofactors, vitamins and prostethic groups (3799 contigs), according to SEED functional analysis, and a relatively high number of 1203 contigs was annotated to tetrapyrrole biosynthesis. Among these, for example, 365 contigs coded for coenzyme-B_{12} biosynthesis, 312 contigs for thiamine and 174 contigs indicated biotin biosynthesis. In the KEGG analysis, 5479 contigs were linked with the metabolism of cofactors and vitamins. Metaproteome analysis resulted in 2 hits that support the presence of enzymes involved in cobalamin biosynthesis, while folic acid and thiamine biosynthesis were represented by 1 hit each, respectively.

Hormone production. For the potential production of hormones, we found that auxin biosynthesis was represented by 156 contigs.

Detoxification of metabolites. In the KEGG analysis, many of the contigs that indicate xenobiotics biodegradation and metabolism (5482 contigs) seem to also be involved in the degradation of phenolic compounds. The presence of enzymes involved in degradation of phenolic compounds was reinforced by three hits in the metaproteome data.

Lytic activities. Degradation of older thallus parts could provide nutrients for the young and growing thallus parts. Such function is enhanced by bacterial enzymes involved in specific degradation procedures. 341 contigs within the metagenome are connected to chitin and N-acetylglucosamine utilization. Additionally, 1000 contigs were found for

protein degradation of which 957 contigs were derived from bacteria. The cultivation-based functional screening underlines that *Lobaria*-associated bacteria are key-players in the recycling of old lichen parts: 33% of the isolates demonstrated protease activity, while 6.7 and 12.9% have shown chitinase and glucanase activity, respectively.

Other functions. In the KEGG analysis, the biosynthesis of polyketides and terpenoids was suggested in 2975 contigs, and the biosynthesis of other secondary metabolites is suggested by a further 2012 contigs. This set also includes known antibiotics such as betalain, penicillin, streptomycin, butirosin, neomycin and novobiocin, as well as phenylpropanoids, stilbenoids and alkaloids. A substantial number of contigs in the KEGG analysis was linked with pathways of environmental information processing (12 053 contigs), and of these, membrane transport forms a fraction of 7629 contigs. Some bacteria also undergo CO_2-fixation, of which about 757 bacterial contigs were assigned. Notably, polyol utilization is represented in 301 contigs (ribitol-, xylitol-, arabitol-, mannitol- and sorbitol-utilization).

Quorum sensing was rather poorly represented in our dataset with only 25 contigs. Metaproteome analysis supports the under-represented role of quorum sensing within the *Lobaria* microbiome, no relevant sequences were identified. It was therefore not surprising, that cultivation-dependent experiments involving lichen-associated bacteria revealed that $<1\%$ of tested isolates produced detectable N-acyl homoserine–lactone-derived quorum sensing molecules. In addition, phages, prophages and transposable elements were not particularly common among the lichen-associated microbiome (275 contigs).

Comparison with an algal partner. To confirm that the selected functions noted above are truly dominant in the lichen-associated bacteria, we have compared the SEED function analysis of the *Lobaria* metagenome with that of a transcriptome of *D. reticulata*, the green-algal photobiont of *L. pulmonaria*. The transcriptome data were obtained from the Joint Genome Institute repository (sequencing of three cultured partners of *L. pulmonaria*, http://genome.jgi.doe.gov/Lobpulcupartners/Lobpulcupartners.info.html). There are a total of 102 102 contigs in the assembly (about 27.71% of the 368 424 contigs of the lichen metagenome). The SEED analysis for the *D. reticulata* data was performed in exactly the same way as was done for the lichen metagenome. Supplementary Table S2 shows a comparison of the selected microbiome function assignments between these two datasets, whereas Supplementary Table S3 shows the same kind of comparison of top-level SEED functions. As Supplementary Table S2 clearly shows, for every selected function discussed until now, the lichen data has far more contigs assigned than the *D. reticulata* data has. Although a genomic/transcriptomic comparison with both fungal and algal partners is currently not feasible, some bacterial functions, which contribute greatly to the overall symbiosis, have been confirmed.

Discussion

The analysis of our data has revealed metabolic capacities and potential roles of the lichen-associated bacteria, especially in the areas of stability and survival of the overall symbiosis. Using our multiphasic approach, combining omics technologies and physiological assays, we found diverse and previously unknown potential functions of the microbiome, such as nutrient supply, resistance against biotic and abiotic stress, support for the photosynthesis and for the growth of the two eukaryotic partners, as well as detoxification and thallus degradation abilities. Supportive roles of associated microbiomes are well-known from humans, animals and plants (Berg, 2009; Bragina *et al.*, 2013; Cho and Blaser, 2012). With our present results, we have found new hints that a similar helper effect can be present in lichen symbioses. This supports our concept of lichens as complex microbial ecosystem (Grube *et al.*, 2009). Combining metagenomic analysis of a bacteria-enriched *Lobaria* sample with a metaproteomic approach provided an additional insight into the functional and structural diversity of bacterial inhabitants. The identified potential functions of the lichen microbiome suggest interactions with the algal as well as with the fungal partner. Metagenomic and proteomic experiments have provided evidence for the capability of production of vitamin B12 and other cofactors supporting the beneficial algae–bacteria interaction. Many algae are auxotroph for vitamin B12, which is often synthesized by prokaryotes in symbiotic interactions (Croft *et al.*, 2005). Other functions such as nutrient supply and resistance against biotic and abiotic stress factors indicate interactions with the fungal partner. Lichens are exposed to abiotic stress and a well-known target for parasitic fungi (Grube *et al.*, 2012). In addition, hormones such as auxin produced by bacteria can support the growth of algae as well as fungi (Gutjahr, 2014). Although results confirmed by both metagenomics and proteomics data corroborated functionalities, a more detailed view is often limited by the availability of annotated data and the lack of completely sequenced genomes, for comparison. Some differences between the two approaches might also be explained by variation of the actual metabolic activity of the involved microorganisms at the time of sample preparation. However, the present results agree with a previous metaproteomic approach of an independent sample of the same lichen, covering the entire lichen holobiome. Schneider *et al.* (2011)

showed that algal proteins are involved in energy production and a diverse set of functions of the fungal proteins relates to the role of the mycobiont in energy consumption and symbiotic control. Similar findings resulted from the analysis of the eukaryotic metatranscriptome in another lichen symbiosis (Juntilla and Rudd, 2012; Juntilla *et al.*, 2013). The present study extends the previous studies in resolution of bacterial functionality. Focusing on the bacterial fraction, the comparison of the new proteomic and metagenomic datasets revealed an overall similarity in the taxonomic representation of bacterial organisms. In both datasets, *Proteobacteria* are the most prominent phylum, with *Alphaproteobacteria* as the most prevalent class. In contrast, cyanobacterial proteins were much more abundant as expected from the contig counts; they might be more active than other phylogenetic groups. As potential carbon and nitrogen fixing organisms, they are known for a long time as substantial part of lichen symbioses (Honegger *et al.*, 2013).

Bacterial communities on long-living lichen thallus surface remain largely constant over seasons (Grube *et al.,* 2009), despite they are exposed to substantial periodicity of abiotic factors in the habitat. Our data show that bacteria living on the surfaces of lichens are well-adapted to abiotic stress, in particular osmotic and oxidative stress. These properties match with the general property of lichens to tolerate periodic drought in their natural habitats. The periodic desiccation and rehydration cycles lead to repeated oxidative bursts at the surfaces of the fungal textures. Release of free radicals under these circumstances has been demonstrated and was interpreted as pathogen defense mechanism of lichens (Minibayeva and Beckett, 2001; Beckett *et al.*, 2013). Thus, thallus-colonizing thalli bacteria without pronounced tolerance to oxidative stress and other selective conditions barely survive. By oxidative degradation of these non-adapted bacteria, a broad spectrum of additional nutrients is accessible. This source might be more important for oligotrophic lichens than for soil-provisioned plants (Paunfoo-Lonhienne *et al.*, 2010; White *et al.*, 2012). Consequently we hypothesize that periodic hydration acts as selective pressure for enrichment of specific and stress-tolerant bacterial communities, which can contribute to longevity and persistence of lichens under extreme and changing ecological conditions.

As we found little evidence of quorum sensing, we hypothesize that bacterial colonization of the thallus is mostly regulated by the fungal partner in the symbiotic community. It is well-established that the secondary metabolites of diverse lichen species have broad antibacterial properties (Boustie and Grube, 2005). The surprising abundance of bacteria on the surfaces and between crystals of secondary metabolites in lichens (for example, *Lecanora polytropa*; Grube *et al.*, 2009) can only be explained by differences in the susceptibility to antibiotic compounds, which may be considered another factor of bacterial selection in lichens. Because we found significant numbers of multidrug resistance efflux pumps, the phylogenetically old lichen symbiosis could represent a natural reservoir of bacterial resistance mechanisms. Moreover, some of the adapted bacteria are potentially involved in the degradation of fungal secondary metabolites, as indicated by contigs of genes whose products may process complex and cyclic carbohydrates. These genes might also be interesting for biotechnological approaches, aiming at the degradation of xenobiotics. The presence of genes for the metabolism of typical bacterial antibiotics in our dataset suggests potential competition among bacterial strains on the lichen surfaces or a defense against other strains entering the microbial surface community. The ecological significance of these functions is pending further experimentation.

The morphological design of lichen structures could have a profound effect on the organization of the symbiotic networking. Bacterial communities primarily colonize the (hydrophilic) lichen surfaces, yet this pattern is strikingly different from the internalized symbionts in lichens, such as the green algae (*D. reticulata* in *L. pulmonaria*), which primarily contribute to the provision of photosynthetically produced carbohydrates. The green-algal strain is massively enriched within the fungal structures, while cyanobacterial *Nostoc* strains are acquired from the surfaces of *L. pulmonaria* recurrently during the life-time of the thallus to form internal organs devoted to nitrogen fixation in lichens (Hyvärinen *et al.*, 2002, Cornejo and Scheidegger, 2013). Conversely, the external presence of other bacteria in the lichen symbiosis recalls the helper bacteria of mycorrhizal symbioses, which provide multiple functions to mutually support and stabilize the root symbioses, including exchange of carbohydrates and vitamin provision (Frey-Klett *et al.*, 2007; Deveau *et al.*, 2010). The long-living lichen thallus is formed by tightly packed fungal hyphae, which are conglutinated by their cell walls. Lichen-adapted bacteria benefit from the persistent cell walls for nutrition, and in return provide multiple helper functions for the longevity of lichen thalli (Figure 2b) to enhance fitness of the holobiome (symbiome). Although we have found a lot of supportive facts for this symbiosis model within our datasets, the evidence for fulfilled contribution of bacterial communities to the lichen symbiosis can only be found by additional experiments, for example, using isotope-labeled compounds and/or comparative physiological analysis between lichens with and without the bacterial microbiota. Both are currently difficult to establish due to slow metabolism and high diversity of bacteria. Despite these facts, we consider lichens as an interesting model for multi-biont symbioses, with different distributions of functions among

the symbionts. It appears that partners with narrowly specified functions, such as carbohydrate or nitrogen fixation, are preferentially internalized by fungal structures and massively enriched in the lichen thallus. Internalization of a partner may help to provide a more uniform and stable environment for these partners. This symbiotic design has evolved as a convergence in unrelated fungal lineages (Grube and Hawksworth, 2007; Honegger, 2012). It has been optimized not only for the association with carbon-providing algal photobionts (Kranner *et al.*, 2005), but also for the enrichment of bacterial supporters. Genome sequences of the eukaryotic partners, which are now becoming available (for example, Wang *et al.*, 2014), will further help to address the intricacies of one of the oldest known symbiosis and its interactions with their bacterial helpers.

Conflict of Interest

The authors declare no conflict of interest.

Acknowledgements

This work was supported by a joint grant of the Austrian and German Science Foundation (FWF, DFG) to GB, MG and KR (FWF-DACH Project I882).

References

Altschul SF, Gish W, Miller W, Myers EW, Lipman DJ. (1990). Basic local alignment search tool. *J Mol Biol* **215**: 403–410.

Bates ST, Cropsey GWG, Caporaso JG, Knight R, Fierer N. (2011). Bacterial communities associated with the lichen symbiosis. *Appl Environ Microbiol* **77**: 1309–1314.

Beckett RP, Zavarzina AG, Liers C. (2013). Oxidoreductases and cellulases in lichens: possible roles in lichen biology and soil organic matter turnover. *Fungal Biol* **117**: 431–438.

Berg G. (2009). Plant-microbe interactions promoting plant growth and health: perspectives for controlled use of microorganisms in agriculture. *Appl Microbiol Biotechnol* **84**: 11–18.

Berg G, Roskot N, Steidle A, Eberl L, Zock A, Smalla K. (2002). Plant-dependent genotypic and phenotypic diversity of antagonistic rhizobacteria isolated from different *Verticillium* host plants. *Appl Environ Microbiol* **68**: 3328–3338.

Boustie J, Grube M. (2005). Lichens—a promising source of bioactive secondary metabolites. *Plant Gen Res* **3**: 273–287.

Bragina A, Berg C, Müller H, Moser D, Berg G. (2013). Insights into functional bacterial diversity and its effects on Alpine bog ecosystem functioning. *Sci Rep* **3**: 1995.

Cardinale M, Müller H, Berg G, de Castro Jr JV, Grube M. (2008). *In situ* analysis of the bacteria community associated with the reindeer lichen Cladonia arbuscula reveals predominance of Alphaproteobacteria. *FEMS Microbiol Ecol* **66**: 63–71.

Cardinale M, Steinova J, Rabensteiner J, Berg G, Grube M. (2012a). Age, sun, and substrate: triggers of bacterial communities in lichens. *Environ Microbiol Rep* **4**: 23–28.

Cardinale M, Grube M, de Castro Jr JV, Müller H, Berg G. (2012b). Bacterial taxa associated with the lung lichen Lobaria pulmonaria are differentially shaped by geography and habitat. *FEMS Microb Lett* **329**: 111–115.

Cho I, Blaser MJ. (2012). The human microbiome: at the interface of health and disease. *Nat Rev Gen* **13**: 260–270.

Cornejo C, Scheidegger C. (2013). New morphological aspects of cephalodium formation in the lichen *Lobaria pulmonaria* (Lecanorales, Ascomycota). *Lichenologist* **45**: 77–87.

Croft MT, Lawrence AD, Raux-Deery E, Warren MJ, Smith AG. (2005). Algae acquire vitamin B12 through a symbiotic relationship with bacteria. *Nature* **438**: 90–93.

Deveau A, Brulé C, Palin B, Champmartin D, Rubini P, Garbaye J *et al.* (2010). Role of fungal trehalose and bacterial thiamine in the improved survival and growth of the ectomycorrhizal fungus Laccaria bicolor S238N and the helper bacterium Pseudomonas fluorescens BBc6R8. *Environ Microbiol Rep* **4**: 560–568.

Eddy SR. (2011). Accelerated profile HMM searches. *PLoS Comput Biol* **7**: e1002195.

Frank AB. (1877). Über die biologischen Verhältnisse des Thallus einiger Krustenflechten. *Beitr Biol Pflanzen* **2**: 123–200.

Frey-Klett P, Garbaye J, Tarkka M. (2007). The mycorrhiza helper bacteria revisited. *New Phytol* **176**: 22–36.

Grube M, Hawksworth DL. (2007). Trouble with lichen: the re-evaluation and re-interpretation of thallus form and fruit body types in the molecular era. *Mycol Res* **111**: 1–1132.

Grube M, Cardinale M, Vieira de Castro J, Müller H, Berg G. (2009). Species-specific structural and functional diversity of bacterial communities in lichen symbioses. *ISME J* **3**: 1105–1115.

Grube M, Köberl M, Lackner S, Berg C, Berg G. (2012). Host-parasite interaction and microbiome response: effects of fungal infections on the bacterial community of the Alpine lichen *Solorina crocea*. *FEMS Microbiol Ecol* **82**: 472–481.

Gutjahr C. (2014). Phytohormone signaling in arbuscular mycorhiza development. *Curr Opin Plant Biol* **21**: 26–34.

Hai B, Diallo NH, Sall S, Haesler F, Schauss K, Bonzi M *et al.* (2009). Quantification of key genes steering the microbial nitrogen cycle in the rhizosphere of sorghum cultivars in tropical agroecosystems. *Appl Environ Microbiol* **75**: 4993–5000.

Haft DH, Selengut JD, Richter RA, Harkins D, Basu MK, Beck E. (2013). TIGRFAMs and genome properties in 2013. *Nucleic Acids Res* **41**(Database issue): D387–D395.

Hodkinson BP, Gottel NR, Schadt CW, Lutzoni F. (2011). Photoautotrophic symbiont and geography are major factors affecting highly structured and diverse bacterial communities in the lichen microbiome. *Environ Microbiol* **14**: 147–161.

Honegger R. (2012). The symbiotic phenotype of lichen-forming Ascomycetes and their endo- and epibionts.

In: Hock B (ed.) *The Mycota IX*. Springer: Berlin, pp 287–339.

Honegger R, Edwards D, Axe L. (2013). The earliest records of internally stratified cyanobacterial and algal lichens from the Lower Devonian of the Welsh Borderland. *New Phytol* **197**: 264–275.

Huson DH, Mitra S, Weber N, Ruscheweyh H, Schuster SC. (2011). Integrative analysis of environmental sequences using MEGAN4. *Genome Res* **21**: 1552–1560.

Hyvärinen M, Härdling R, Tuomi J. (2002). Cyanobacterial lichen symbiosis: the fungal partner as an optimal harvester. *Oikos* **98**: 498–502.

Juntilla S, Rudd S. (2012). Characterization of a transcriptome from a non-model organism, *Cladonia rangiferina*, the grey reindeer lichen, using high-throughput next generation sequencing and EST sequence data. *BMC Genomics* **13**: 575.

Junttila S, Laiho A, Gyenesei A, Rudd S. (2013). Whole transcriptome characterization of the effects of dehydration and rehydration on *Cladonia rangiferina*, the grey reindeer lichen. *BMC Genomics* **14**: 870.

Kranner I, Cram WJ, Zorn M, Wornik S, Yoshimura I, Stabentheiner E, Pfeifhofer HW. (2005). Antioxidants and photoprotection in a lichen as compared with its isolated symbiotic partners. *PNAS* **102**: 3142–3146.

Koskinen VR, Emery PA, Creasy DM, Cottrell JS. (2011). Hierarchical clustering of shotgun proteomics data. *Mol Cell Proteomics* **10**: M110.003822.

Kuester E, Williams ST. (1964). Selection of media for isolation of *Streptomycetes*. *Nature* **202**: 928–929.

Laemmli UK. (1970). Cleavage of structural proteins during the assembly of the head of bacteriophage T4. *Nature* **227**: 680–685.

Liba CM, Ferrara FIS, Mangio GP, Fantinatti-Garboggini F, Albuquerque RC, Pavan C *et al.* (2006). Nitrogen-fixing chemo–organotrophic bacteria isolated from cyanobacteria-deprived lichens and their ability to solubilize phosphate and to release amino acids and phytohormones. *J Appl Microbiol* **101**: 1076–1086.

Margulis L, Fester R. (1991). *Symbiosis as a source of evolutionary innovation: speciation and morphogenesis*. MIT Press: Cambridge, pp 454.

Martin BD, Schwab E. (2013). Current usage of symbiosis and associated terminology. *Int J Biol* **5**: 32–45.

McClean KH, Winson MK, Fish L, Taylor A, Chhabra SR, Camara M *et al.* (1997). Quorum sensing and *Chromobacterium violaceum*: exploitation of violacein production and inhibition for the detection of N-acylhomoserine lactones. *Microbiology* **143**: 3703–3711.

Meyer F, Paarmann D, D'Souza M, Olson R, Glass EM, Kubal M *et al.* (2008). The metagenomics RAST server - a public resource for the automatic phylogenetic and functional analysis of metagenomes. *BMC Bioinformatics* **9**: 386.

Minibayeva F, Beckett RP. (2001). High rates of extracellular superoxide production in bryophytes and lichens, and an oxidative burst in response to rehydration following desiccation. *New Phytol* **152**: 333–343.

Mushegian AA, Peterson CN, Baker CCM, Pringle A. (2011). Bacterial diversity across individual lichens. *Appl Environ Microbiol* **77**: 4249–4252.

Nash III TH. (2008). *Lichen Biology*, 2nd edn. Cambridge University Press: Cambridge, UK.

Nautiyal CS. (1999). An efficient microbiological growth medium for screening phosphate solubilizing microorganisms. *FEMS Microbiol Lett* **170**: 265–270.

Neuhoff V, Arold N, Taube D, Ehrhardt W. (1988). Improved staining of proteins in polyacrylamide gels including isoelectric focusing gels with clear background at nanogram sensitivity using Coomassie Brilliant Blue G-250 and R-250. *Electrophoresis* **9**: 255–262.

Opelt K, Chobot V, Hadacek F, Schönmann S, Eberl L, Berg G. (2007). Investigations of the structure and function of bacterial communities associated with *Sphagnum* mosses. *Environ Microbiol* **9**: 2795–2809.

Øvstedal D, Lewis-Smith R. (2001). *Lichens of Antarctica and South Georgia, A guide to their identification and ecology*. Cambridge University Press: Cambridge, UK.

Paungfoo-Lonhienne C, Rentsch D, Robatzek S, Webb RI, Sagulenko E, Näsholm T *et al.* (2010). Turning the table: plants consume microbes as a source of nutrients. *PLoS One* **5**: e11915.

Scheidegger C, Werth S. (2009). Conservation strategies for lichens: insights from population biology. *Fungal Biol Rev* **23**: 55–66.

Schneider T, Schmid E, de Castro Jr JV, Cardinale M, Eberl L, Grube M *et al.* (2011). Structure and function of the symbiosis partners of the lung lichen (*Lobaria pulmonaria* L. Hoffm.) analyzed by metaproteomics. *Proteomics* **11**: 2752–2756.

Shirling EB, Gottlieb D. (1966). Methods for characterization of *Streptomyces* species. *Int J Syst Bacteriol* **16**: 313–340.

Steidle A, Sigl K, Schuhegger R, Ihring A, Schmid M, Gantner S *et al.* (2001). Visualization of N-acylhomoserine lactone-mediated cell-cell communication between bacteria colonizing the tomato rhizosphere. *Appl Environ Microbiol* **67**: 5761–5770.

Wang W, Vignani R, Scali M, Cresti M. (2006). A universal and rapid protocol for protein extraction from recalcitrant plant tissues for proteomic analysis. *Electrophoresis* **27**: 2782–2786.

Wang YY, Liu B, Zhang XY, Zhou QM, Zhang T, Li H *et al.* (2014). Genome characteristics reveal the impact of lichenization on lichen-forming fungus *Endocarpon pusillum* Hedwig (Verrucariales, Ascomycota). *BMC Genomics* **15**: 34.

White Jr JF, Crawford H, Torres MS, Mattera R, Irizarry I, Bergen M. (2012). A proposed mechanism for nitrogen acquisition by grass seedlings through oxidation of symbiotic bacteria. *Symbiosis* **57**: 161–171.

Zerbino DR, Velvet BE. (2008). Algorithms for *de novo* short read assembly using de Bruijn graphs. *Genome Res* **18**: 821–829.

Zybailov B, Mosley AL, Sardiu ME, Coleman MK, Florens L, Washburn MP. (2006). Statistical analysis of membrane proteome expression changes in *Saccharomyces cerevisiae*. *J Proteome Res* **5**: 2339–2347.

Supplementary Information accompanies this paper on The ISME Journal website (http://www.nature.com/ismej)

Additional Publication I – Supplementary Data

Supplementary Figures

Figure S1: *Lobaria pulmonaria* thalli before sampling. All lichen thalli were checked for infection with lichenicolous fungi and other contaminants.

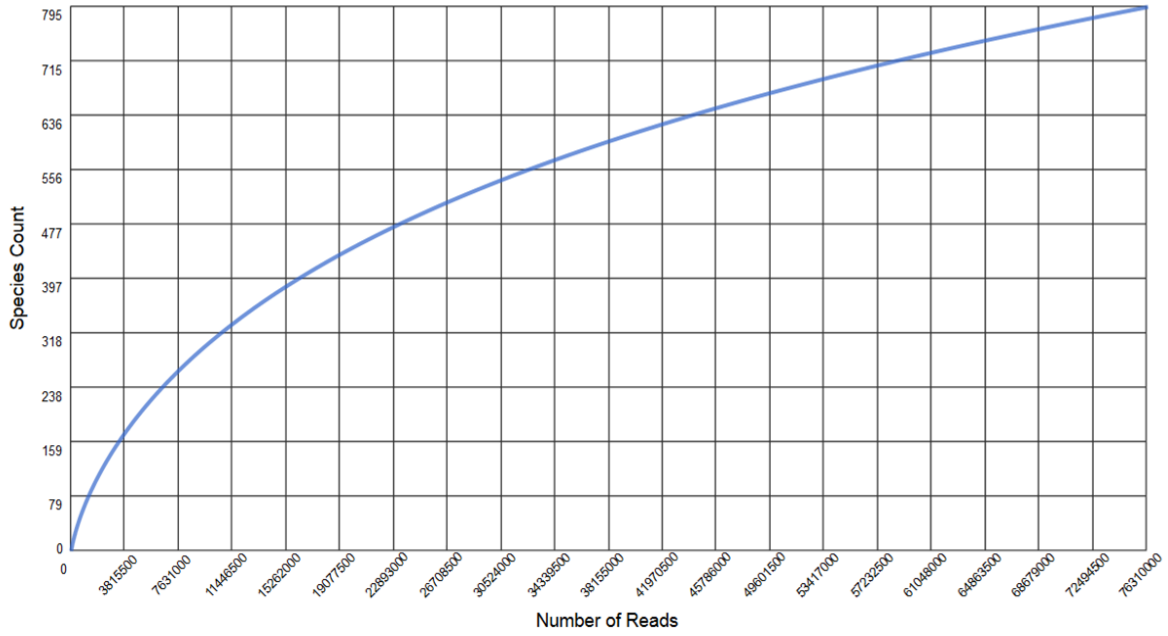

Figure S2: Rarefaction analysis indicating species richness that can be expected in the *Lobaria* metagenome. The data was compared to Greengenes using standard MG-RAST terms for RNA databases.

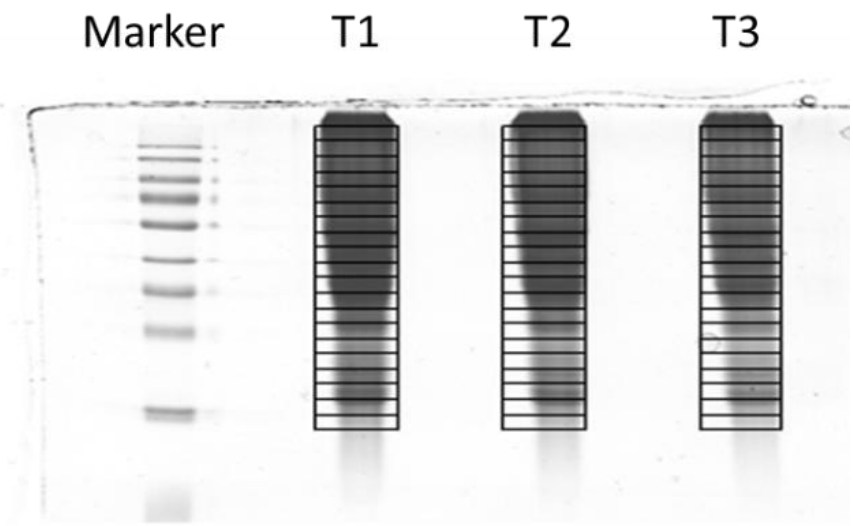

Figure S3: Colloidal Coomassie-stained 1D SDS-PAGE of three technical replicates T1 – T3 of proteins extracted from *L. pulmonaria*. The cutting of the lanes into 20 individual gel pieces is indicated by the lines.

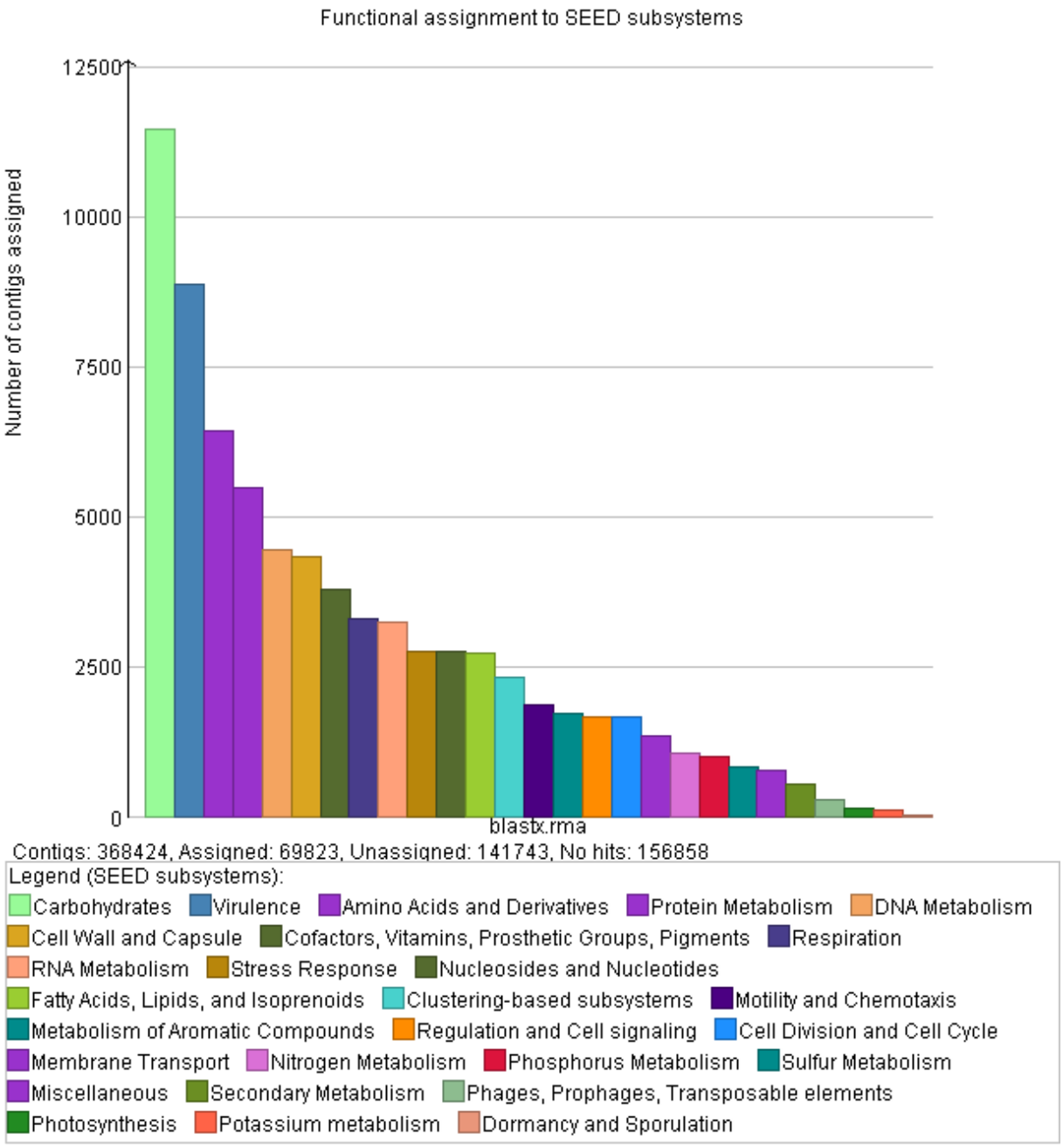

Figure S4. Functional assignments processed with MEGAN (v4.70.4) and SEED Subsystems analysis. SEED functions were arranged in a decreasing sequence based on the total contig count assigned to certain functions. The most prominent assignments are connected to functions involved in primary metabolism, but also to virulence-related genes, biosynthesis and transport of vitamins, cofactors, prosthetic groups and pigments as well as genes involved in stress response.

Supplementary Tables

Table S1. Brief sample description and corresponding MG-RAST metagenome IDs for all datasets used in the PCoA.

Metagenome ID	Habitat	Country or location	# of sequences	Alpha-diversity
4530091.3	*L. pulmonaria*	Austria	76,310,051	563.852
4447810.3	*A. thaliana* phyllosphere	Spain	1,098,311	470.804
4447811.3	Clover phyllosphere	Switzerland	1,028,814	421.794
4441205.3	Soybean phyllosphere	Switzerland	523,769	381.345
4453083.3	Freshwater	Australia	409,743	1030.286
4441590.3	Freshwater	Panama	296,355	785.38
4445126.3	Freshwater	Canada	256,849	585.456
4447101.3	Human oral cavity	Spain	295,072	299.147
4447102.3	Human oral cavity	Spain	244,881	217.806
4447192.3	Human oral cavity	Spain	204,218	217.793
4461456.3	*A. brasiliensis*	Brazil	64,933	440.293
4461455.3	*A. brasiliensis*	Brazil	167,475	521.743
4461454.3	*A. brasiliensis*	Brazil	85,431	489.784
4440036.3	Seawater	Kingman Atoll	94,915	432.738
4440038.3	Seawater	Christmas Atoll	283,390	250.197
4440039.3	Seawater	Palmyra Atoll	351,205	358.14
4508939.3	Agricultural soil	USA (IN)	16,923,988	641.538
4508938.3	Agricultural soil	USA (IN)	9,999,775	678.281
4508940.3	Agricultural soil	USA (IN)	17,442,824	621.506
4465558.3	Forrest soil	Spain	257,697	715.306
4465556.3	Forrest soil	Spain	412,302	621.136

Table S2. Comparison of the numbers of contigs assigned to selected functions of the lichen microbiome (described in the Results section), between *Lobaria pulmonaria* metagenome and *Dictyochloropsis reticulata* transcriptome (Transcriptome assembly downloaded from http://genome.jgi.doe.gov/Lobpulcupartners/Lobpulcupartners.info.html)

SEED function	***L. pulmonaria*** **contigs assigned (total=69,823)**		***D. reticulata*** **contigs assigned (total=28,072)**	
	Number	Percentage	Number	Percentage
Ton and Tol transport systems	2,793	4.00	8	0.03
TonB-dependent receptor	2,094	3.00	0	0.00
Phosphate metabolism	885	1.27	11	0.04
Multidrug resistance efflux pumps	1,152	1.65	1	0.00
Type III, Type IV, Type VI, ESAT secretion systems	955	1.37	0	0.00
Secondary Metabolism	548	0.78	53	0.19
Stress Response	2,769	3.97	155	0.55
Oxidative stress	1,238	1.77	63	0.22
Cofactors, Vitamins, Prosthetic Groups, Pigments	3,799	5.44	258	0.92
Tetrapyrroles	1,203	1.72	107	0.38
Coenzyme B12 biosynthesis	365	0.52	3	0.01
Thiamin biosynthesis	312	0.45	11	0.04
Biotin biosynthesis	174	0.25	5	0.02
Auxin biosynthesis	156	0.22	15	0.05
Chitin and N-acetylglucosamine utilization	341	0.49	5	0.02
Protein degradation	1,000	1.43	111	0.40

Table S3. Comparison of the numbers of contigs assigned to top-level SEED functions (as depicted in Fig. S4) between *Lobaria pulmonaria* metagenome and *Dictyochloropsis reticulata* transcriptome (Transcriptome assembly downloaded from http://genome.jgi.doe.gov/Lobpulcupartners/Lobpulcupartners.info.html)

Top-level SEED functions	***L. pulmonaria*** **contigs assigned (total=69,823)**		***D. reticulata*** **contigs assigned (total=28,072)**	
	Number	Percentage	Number	Percentage
Carbohydrates	11,462	16.42	329	1.17
Virulence	8,861	12.69	70	0.25
Amino Acids and Derivatives	6,440	9.22	264	0.94
Protein Metabolism	5,481	7.85	527	1.88
DNA Metabolism	4,446	6.37	68	0.24
Cell Wall and Capsule	4,325	6.19	44	0.16
Cofactors, Vitamins, Prosthetic Groups, Pigments	3,799	5.44	258	0.92
Respiration	3,299	4.72	70	0.25
RNA Metabolism	3,248	4.65	121	0.43
Stress Response	2,769	3.97	155	0.55
Nucleosides and Nucleotides	2,761	3.95	92	0.33
Fatty Acids, Lipids, and Isoprenoids	2,721	3.90	111	0.40
Clustering-based subsystems	2,328	3.33	112	0.40
Motility and Chemotaxis	1,880	2.69	15	0.05
Metabolism of Aromatic Compounds	1,734	2.48	48	0.17
Regulation and Cell signaling	1,673	2.40	21	0.07
Cell Division and Cell Cycle	1,669	2.39	36	0.13
Membrane Transport	1,361	1.95	27	0.10
Nitrogen Metabolism	1,060	1.52	30	0.11
Phosphorus Metabolism	1,011	1.45	11	0.04
Sulfur Metabolism	836	1.20	17	0.06
Miscellaneous	767	1.10	23	0.08
Secondary Metabolism	548	0.78	53	0.19
Phages, Prophages, Transposable elements	275	0.39	7	0.02
Photosynthesis	139	0.20	27	0.10
Potassium metabolism	103	0.15	5	0.02
Dormancy and Sporulation	13	0.02	1	0.00

ADDITIONAL PUBLICATION II

Frontiers in Microbiology (2015) **6**:620

Analyzing the antagonistic potential of the lichen microbiome against pathogens by bridging metagenomic with culture studies

Tomislav Cernava,[1] Henry Müller,[1] Ines Aline Aschenbrenner,[1,2] Martin Grube,[2] and Gabriele Berg[1]

[1]Institute of Environmental Biotechnology
Graz University of Technology, Austria

[2]Institute of Plant Sciences
University of Graz, Austria

frontiers in Microbiology

ORIGINAL RESEARCH
published: 22 June 2015
doi: 10.3389/fmicb.2015.00620

Analyzing the antagonistic potential of the lichen microbiome against pathogens by bridging metagenomic with culture studies

*Tomislav Cernava[1], Henry Müller[1], Ines A. Aschenbrenner[1,2], Martin Grube[2] and Gabriele Berg[1]**

[1] *Institute of Environmental Biotechnology, Graz University of Technology, Graz, Austria,* [2] *Institute of Plant Sciences, University of Graz, Graz, Austria*

OPEN ACCESS

Edited by:
Jesús Mercado-Blanco, Consejo Superior de Investigaciones Científicas, Spain

Reviewed by:
Yusuke Saijo, Max Planck Institute for Plant Breeding Research, Germany
Diogo Neves Proença, University of Aveiro and CEMUC – University of Coimbra, Portugal

***Correspondence:**
Gabriele Berg, Institute of Environmental Biotechnology, Graz University of Technology, Petersgasse 12, 8010 Graz, Austria
gabriele.berg@tugraz.at

Specialty section:
This article was submitted to Plant-Microbe Interaction, a section of the journal Frontiers in Microbiology

Received: *03 April 2015*
Accepted: *08 June 2015*
Published: *22 June 2015*

Citation:
Cernava T, Müller H, Aschenbrenner IA, Grube M and Berg G (2015) Analyzing the antagonistic potential of the lichen microbiome against pathogens by bridging metagenomic with culture studies. Front. Microbiol. 6:620. doi: 10.3389/fmicb.2015.00620

Naturally occurring antagonists toward pathogens play an important role to avoid pathogen outbreaks in ecosystems, and they can be applied as biocontrol agents for crops. Lichens present long-living symbiotic systems continuously exposed to pathogens. To analyze the antagonistic potential in lichens, we studied the bacterial community active against model bacteria and fungi by an integrative approach combining isolate screening, omics techniques, and high resolution mass spectrometry. The highly diverse microbiome of the lung lichen [*Lobaria pulmonaria* (L.) Hoffm.] included an abundant antagonistic community dominated by *Stenotrophomonas, Pseudomonas,* and *Burkholderia.* While antagonists represent 24.5% of the isolates, they were identified with only 7% in the metagenome; which means that they were overrepresented in the culturable fraction. Isolates of the dominant antagonistic genus *Stenotrophomonas* produced spermidine as main bioactive component. Moreover, spermidine-related genes, especially for the transport, were identified in the metagenome. The majority of hits identified belonged to *Alphaproteobacteria*, while *Stenotrophomonas*-specific spermidine synthases were not present in the dataset. Evidence for plant growth promoting effects was found for lichen-associated strains of *Stenotrophomonas.* Linking of metagenomic and culture data was possible but showed partly contradictory results, which required a comparative assessment. However, we have shown that lichens are important reservoirs for antagonistic bacteria, which open broad possibilities for biotechnological applications.

Keywords: lichen, antagonistic bacteria, plant growth promotion, *Stenotrophomonas,* spermidine

Introduction

Plant pathogens and the diseases they cause are major threats to humanity. Each year we globally lose over one third of the total harvest to bacterial and fungal pathogens. The past two decades have seen an increasing number of virulent infectious diseases in plants (Fisher et al., 2012), and human activity is intensifying pathogen dispersal as well as reducing diversity in agricultural systems (Schmid et al., 2011). However, microbial diversity is a key factor in avoiding pathogen outbreaks (Mendes et al., 2012; van Elsas et al., 2012). Therefore, biocontrol of plant pathogens is

a promising solution to control plant pathogens (Berendsen et al., 2012; Berg et al., 2013; Berg, 2015) because it was also shown that it enhances general microbial diversity (Erlacher et al., 2015a). Naturally occurring antagonists toward plant pathogens play an important role for biocontrol approaches. In natural ecosystems, which often contain a high proportion of antagonistic microorganisms, such antagonists potentially function in stabilizing the community, but might also protect the community against pathogen outbreaks (Opelt et al., 2007; Zachow et al., 2008; Grube et al., 2015). However, the ecology of naturally occurring antagonistic microorganisms is only partly understood and not yet exploited.

Lichens, which are classic examples of self-sustained symbioses, are interesting models for antagonism studies because within these mini-ecosystems the cooperation between microbial partners facilitates stability and longevity under extreme ecological conditions although they are often attacked by allochthonous bacteria and fungi (Lawrey and Diederich, 2003; Bates et al., 2011; Mushegian et al., 2011). While the lichen-specific structure is provided by fungal symbionts, which also is the naming component of the symbiosis, green algae, and/or cyanobacteria are incorporated into specific layers or compartments and contribute with photosynthetically fixed carbohydrates to the symbiosis (Nash, 2008). Lichen-associated bacteria were only recently shown to be highly diverse and omics approaches have indicated that they are functional contributors to robustness of the lichen holobiome (Grube et al., 2009, 2015). The intricate association of members of different organismal kingdoms in well-delimited and long-living symbiotic structures – as symbiotic hotspots of terrestrial life – highlights lichens as a veritable treasure chest for interorganismal communication, regulation, and bioactivity in general (Boustie and Grube, 2005; Boustie et al., 2011). Conditioned by the slow growth of many lichens and difficulties in culturing the symbionts, biotechnological exploitation of lichens was lagging behind other natural resources. With the advent of modern technologies, however, the secondary metabolism and antagonistic potentials in lichens receive new impulses, and this will particularly apply to culturable bacterial partners. Although, lichens are equipped with various secondary compounds with antagonistic effects (Oksanen, 2006; Lawrey, 2009; Boustie et al., 2011), we hypothesize that only a diverse protective microbiome can efficiently maintain stability over longer periods to prevent pathogen attacks.

The objective of this study was to analyze the antagonistic potential of the lichen microbiome against model pathogens by a novel approach bridging metagenomic with culture techniques. Model pathogens associated with human, lichen and plant diseases were accessed to screen for a broad spectrum of antagonistic activity. Furthermore, we utilized the lung lichen *Lobaria pulmonaria* (L.) Hoffm., which is one of the fastest growing leaf-like lichens (MacDonald and Coxson, 2013) and used as indicator species of undisturbed forests and air pollution (Rose, 1976; Scheidegger, 1995). We also characterized the most active as well as the most abundant lichen-associated antagonists *Stenotrophomonas,* which were already identified as versatile antagonists from plant origin (Ryan et al., 2009; Alavi et al., 2014; Berg and Martinez, 2015). Beneficial *Stenotrophomonas* strains produced osmoprotectans and spermidine in response to eukaryotic hosts (Alavi et al., 2013). In our study we applied multidisciplinary techniques to link metagenomic data with those obtained from bacterial cultures. Moreover, we could show that lichens are important reservoirs for antagonistic bacteria, which can also be used for biological control approaches to protect plants against biotic and abiotic stress.

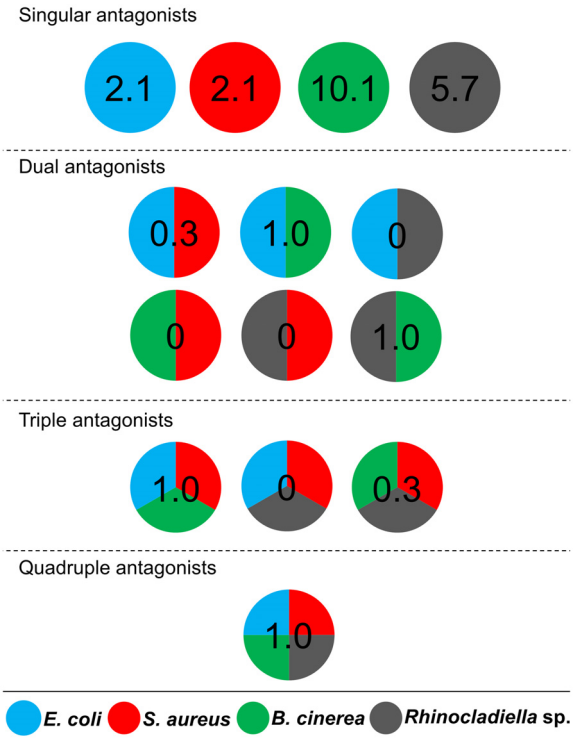

FIGURE 1 | Distribution of antagonistic bacteria isolated from multiple *Lobaria pulmonaria* thalli. Dual-culture experiments with 388 bacterial cultures were used to identify antagonists against four different model pathogens. *Escherichia coli* and *Staphylococcus aureus* were used as models for human pathogens, *Botrytis cinerea* and *Rhinocladoniella* sp. were used as models for plant and lichen pathogens, respectively. Results are presented in a schematic illustration of antagonists, targeting a specific pathogen (indicated by relative numbers and different colors, respectively). Divided circles indicate particular combinations of pathogens, which were inhibited by an assigned percentage of *Lobaria*-associated isolates. Singular antagonists: *Lobaria*-associated isolates that inhibited only one model pathogen; Dual antagonists: isolates that inhibited two distinct model pathogens; Triple antagonists: isolates that inhibited three distinct model pathogens; Quadruple antagonists: isolates that inhibited four distinct model pathogens.

Materials and Methods

Sampling Strategy and Isolation of Lichen-Associated Bacteria

Lichen thalli of *L. pulmonaria* were sampled from three different locations in Austria (Tamischbachgraben, N47°32′40″, E14°37′35″, Johnsbach, N47°38′07″, E14°44′45″, and St. Oswald

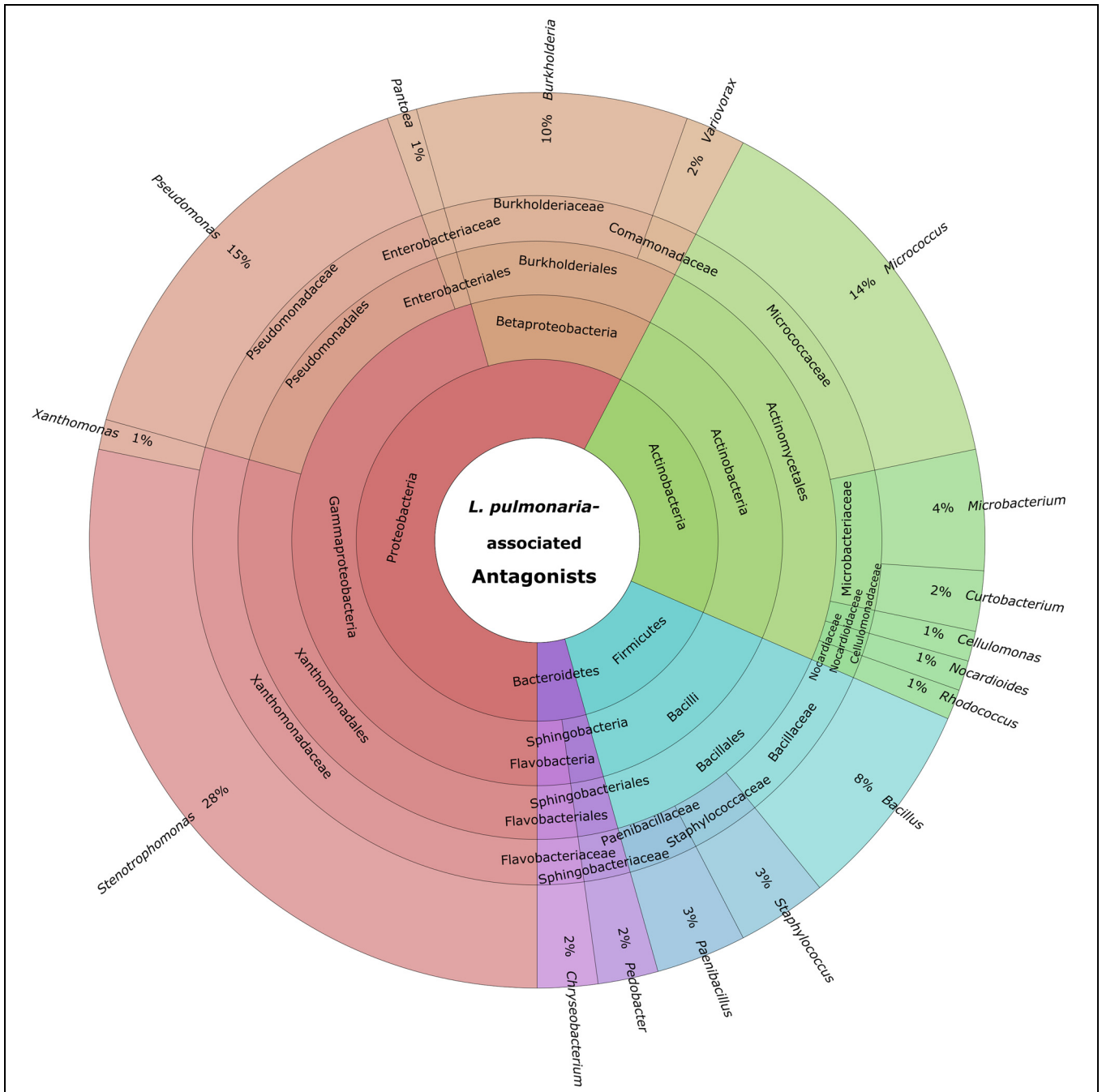

FIGURE 2 | Summary of identified antagonistic bacteria in a multi-level chart (http://sourceforge.net/p/krona). The displayed taxa were shown to inhibit growth of one or more of the utilized model pathogens: *B. cinerea*, *E. coli*, *S. aureus,* and *Rhinocladionella* sp. The inner circles represent higher taxonomic ranks, while more detailed taxonomic ranks (up to genus level) are presented in the outer circles.

ob Eibiswald, N46°44′ 50″, E15° 04′ 26″) after visual inspection to avoid contamination by lichenicolous fungi and other organisms. Five separate lichen thalli were sampled from each sampling site. The samples were stored on dry ice and were, shortly after, ground with mortar and pestle. A homogenate was prepared using sterile 0.85% NaCl in a 1:10 (w/v) ratio, together with a lab stomacher (BagMixer; Interscience, St Nom, France). Diluted fractions were plated on R2A agar (Carl Roth, Karlsruhe, Germany), R2A agar with 25 μg ml^{-1} cycloheximide, starch casein agar (SCA; Küster and Williams, 1964) and ISP2 agar (Shirling and Gottlieb, 1966). Bacterial colonies were randomly picked within 5 days of incubation at room temperature (RT) and a total of 388 isolates was obtained. The isolates were stored in glycerol stocks at −70°C prior to cultivation-based experiments.

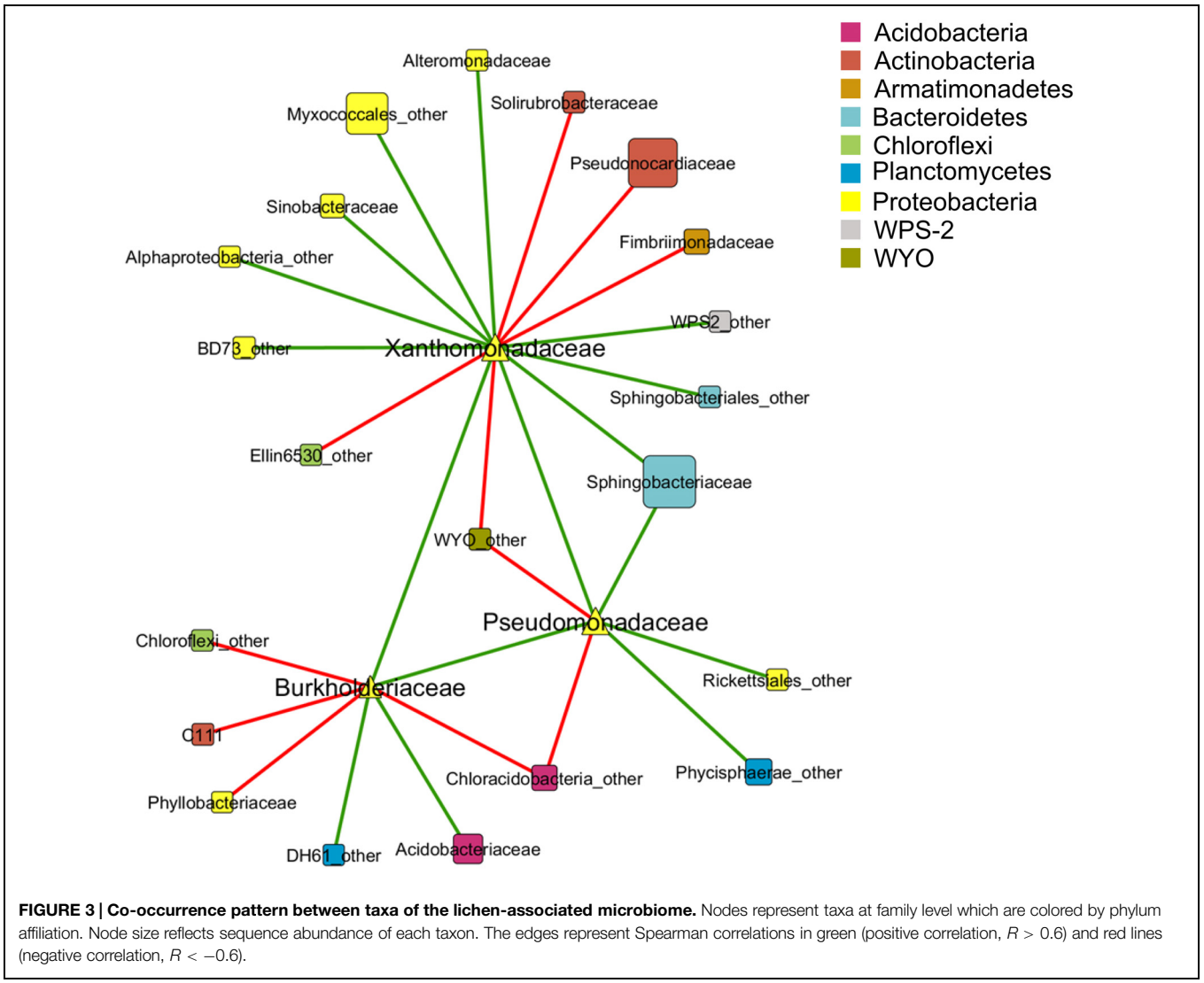

FIGURE 3 | Co-occurrence pattern between taxa of the lichen-associated microbiome. Nodes represent taxa at family level which are colored by phylum affiliation. Node size reflects sequence abundance of each taxon. The edges represent Spearman correlations in green (positive correlation, $R > 0.6$) and red lines (negative correlation, $R < -0.6$).

Screening of Isolates for *In Vitro* Antagonistic Activity Toward Particular Bacteria and Fungi

Dual-culture experiments were carried out as confrontation assays, using different media and target organisms according to Berg et al. (2002) and Opelt et al. (2007). Lichen-associated isolates were spotted on solid media pre-inoculated with *Escherichia coli* XL1 and *Staphylococcus aureus* ATCC 25923 and assessed for inhibition zones after 4 days of incubation at 30°C. Antagonistic activity against the fungus *Botrytis cinerea* Pers. (in-house culture collection) was tested by dual culture on Waksman agar (WA), according to Berg et al. (2002) and assessed after 5–7 days incubation at 20°C. Cultures of the lichen-pathogenic fungus *Rhinocladiella* sp. (culture collection of Lucia Muggia; Institute of Plant Sciences, University of Graz) were homogenized and re-suspended in sterile 0.85% NaCl. In the following step, 50 μL aliquots from one batch were used to inoculate each well of 24-well plates which contained solid potato dextrose agar (PDA; Carl Roth, Karlsruhe, Germany). Subsequently, 100 μL culture filtrate obtained from each lichen-associated isolate was added to particular wells. After 3 weeks of incubation, the wells were checked for growth reduction. All experiments were conducted with three independent replicates.

Amplicon Library Preparation and Co-Occurrence Analysis

Amplicon libraries obtained by Aschenbrenner et al. (2014) were used to extract distinct taxa for additional studies. The utilized 454-pyrosequencing data was obtained from lichen samples from the same sampling sites that were used for isolation of lichen-associated bacterial cultures. Out of the 454-amplicon dataset 15 thallus samples (five for each sampling site) were used for a co-occurrence analysis. Therefore OTUs (Operational Taxonomic Units) were clustered with UCLUST (Edgar, 2010) at 95% similarity (correlates with the taxonomic genus level). Mitochondrial, chloroplast, and *Nostoc* sequences were excluded as well as all OTUs with less than three sequences. Co-occurrence patterns were created with calculated Spearman correlations

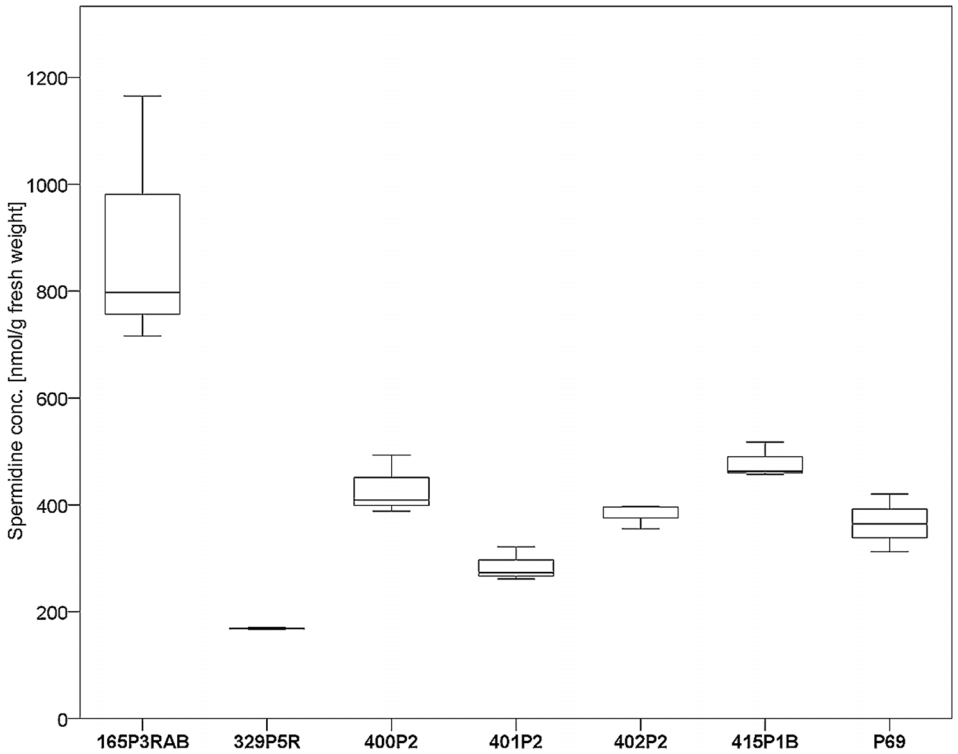

FIGURE 4 | Analysis of internal spermidine concentrations and lichen-associated *Stenotrophomonas* sp. isolates. The isolates were cultivated on solid cultivation media followed by cell disruption and quantification of internal spermidine levels ($n = 21$). A total of six *Lobaria*-associated isolates were utilized together with one plant-associated isolate (P69) in a comparative approach. *Stenotrophomonas* sp. 165P3RAB was shown to contain the highest internal spermidine concentration ($p < 0.1$) compared to all other isolates, while isolate 329P5R had the lowest concentration ($p < 0.01$).

between taxa at family level (>0.6 and <−0.6; R environment version 3.1.2[1]). Only families, which showed a correlation to *Pseudomonadaceae, Xanthomonadaceae,* and *Burkholderiaceae* were considered for further analysis and visualized as network with Cytoscape (organic layout; version 3.2.1; Saito et al., 2012). Node size within the network reflects the sequence abundance of each taxon and nodes were colored according to phylum affiliation.

16S rRNA-Based Identification of Antagonistic Bacteria and Phylogenetic Analysis

Primer pair 27F/1492r was used to amplify specific 16S rRNA gene fragments from antagonistic bacterial cultures. Subsequent sequencing and BLASTn searches within the 16S ribosomal RNA sequence database (NCBI) were conducted for identification of antagonists. These sequences were later trimmed to the hypervariable V4 region to allow alignments with 454-pyrosequencing data of the same rRNA region. QIIME 1.6.0 (Quantitative Insights Into Microbial Ecology, Caporaso et al., 2010) and the implemented Greengenes database (DeSantis et al., 2006) was used to search for bacterial OTUs in the corresponding amplicon dataset (Aschenbrenner et al., 2014) that were assigned to the three most dominant proteobacterial genera within prior identified antagonists. OTUs which could not be assigned to any particular phylum or to species level within *Proteobacteria* were additionally analyzed with Seqmatch (RDP database) for taxonomic assignment. The representative sequences of these additionally identified OTUs were used for further phylogenetic analyses. The phylogenetic tree was constructed with V4-trimmed 16S rRNA sequences from antagonistic bacteria cultures and an amplicon subset. Sequences were aligned with MEGA6 (Tamura et al., 2013) and processed for bootstrapped neighbor-joining with PHYLIP work package v.3.695[2]. Confidence levels for the internal branches were assessed by bootstrap analysis with 100 re-samplings. FigTree v.1.4.0[3] was used for annotation and final graphic visualization of the phylogenetic tree. All utilized 16S rRNA gene fragment sequences from isolate and amplicon sequencing were deposited at GenBank[4] (accession numbers: KP739786–KP739797 and KR611621–KR611709).

Metagenomic Mining for Specific Genes of Interest

All metagenome-based analyzes were carried out on the assembled dataset described in a previous study by Grube

[1]http://www.r-project.org

[2]http://evolution.genetics.washington.edu/phylip

[3]http://tree.bio.ed.ac.uk/software/figtree

[4]http://www.ncbi.nlm.nih.gov/genbank

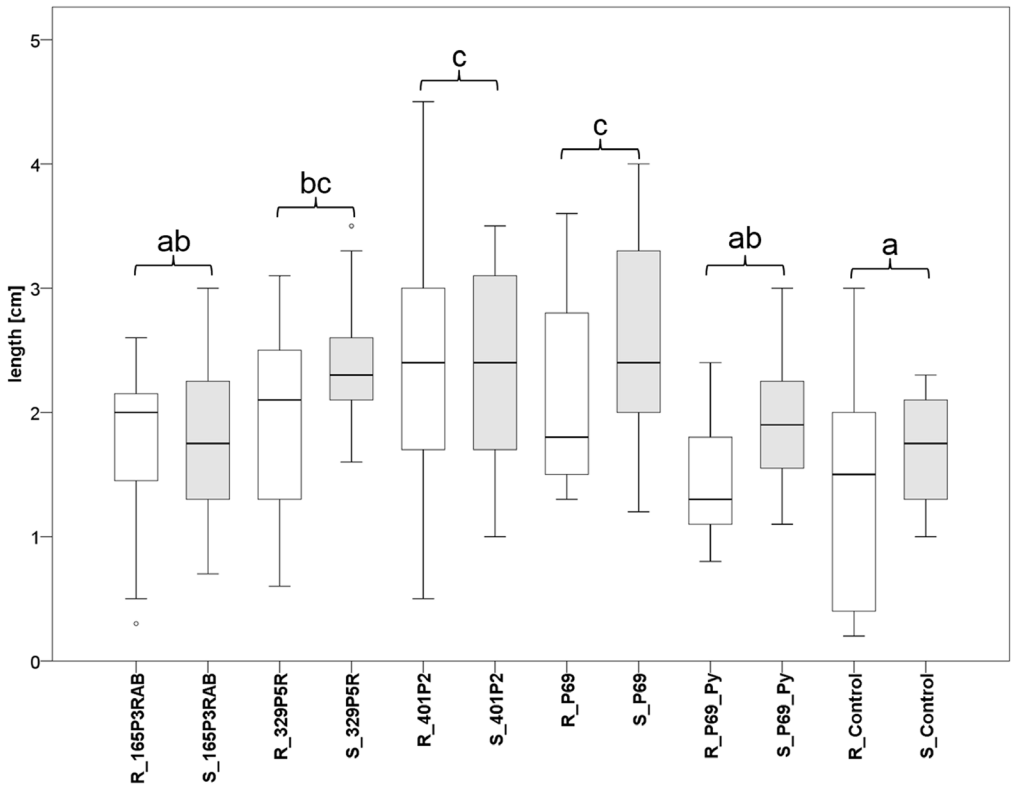

FIGURE 5 | Greenhouse experiment with *Stenotrophomonas*-primed tomato seeds and two distinctive controls (P69_Py and Control). Three *Lobaria*-associated isolates (165P3RAB, 329P5R, and 401P2) were utilized together with a plant-associated isolate (P69). Root (R; $n = 64$) and stem (S; $n = 66$) lengths were measured after 2 weeks plant growth under limited water supply. White (root lengths) and gray (stem lengths) plot pairs represent the treatments with specific isolates and complementary controls. Statistical analysis was employed to identify significant ($p < 0.05$) differences in combined root and stem lengths. Different letters were used to differentiate between statistically discriminative groups.

et al. (2015). CLUSTER CONTROL (Stocker et al., 2004) was used to search with the blastn algorithm for specific spermidine synthase matches (NCBI accession numbers: NC_010943.1, NC_011071.1, NC_015947.1, and NC_017671.1) within the dataset (368,424 contigs). MEGAN (v4.70.4) was used to retrieve taxonomic classification and relevant SEED functions.

Metabolite Extraction from Bacterial Cultures Grown on Solid Medium

Bacterial cultures were washed from several densely colonized Nutrient Agar (NA; Sifin, Berlin, Germany) plates after 48 h incubation at 30°C and homogenized in 9 mL 0.85% NaCl solution. The homogenate was centrifuged for 20 min, 2,000 *g* at 4°C. This step was repeated two times to remove residual media from bacterial cells. The pellet was re-suspended in 2 mL ddH_2O followed by centrifugation for 15 min, 18,000 *g* at 4°C. Precooled 90% methanol at −70°C was used for reproducible extraction and to avoid further degradation of metabolites. Subsequently, 1 mL was added to each pellet and the bacterial cells were mechanically disrupted with glass beads for 2 × 45 s at 6 m/s. Followed by a final centrifugation step for 15 min, 18,000 *g* at 4°C, 100 µl of each supernatant was collected and immediately placed in a deep freezer at −70°C until further analysis. Three independent biological replicates were prepared for each isolate.

Preparation of Culture Supernatants for Spermidine Quantification

Bacterial cultures were used to prepare overnight cultures (ONC) in fluid Nutrient Broth II (NBII; Sifin, Berlin, Germany) medium. These ONCs were used to inoculate 50 mL NBII flasks, which were then incubated at 30°C, 120 rpm for 48 h. In the following step, 2 mL aliquots were taken from the cultures and centrifuged for 20 min, 18,000 *g* at 4°C. The supernatants were filtered with 0.25 µm filters and immediately placed in a deep freezer at −70°C until further analysis. Three independent biological replicates were prepared for each isolate.

Quantification of Specific Bacterial Metabolites with High Resolution Mass Spectrometry

Samples were analyzed in nine biological/technical replicates with a combined HPLC-hybrid quadrupole-orbitrap mass spectrometer (Q Exactive; Thermo Scientific, Bremen, Germany). A Luna 5u NH2 100A 250 × 4.6 column (Phenomenex,

Aschaffenburg, Germany) was used to separate different metabolites from the cell extracts. Formic acid (0.1%, v/v) in acetonitrile was used as solvent A and aqueous formic acid (0.1%, v/v) as solvent B. Starting conditions for the gradient elution were 10% A and 90% B. The conditions were gradually changed to 80% A and 20% B within 15 min. This step was followed by 5 min at 10% A and 90% B for readjustment to initial conditions. The eluent flow was maintained at 0.8 mL/min together with a column temperature of 25°C. Sample analysis was carried out with negative ion ESI detection. ESI conditions were set to 3.2 kV spray voltage and 350°C capillary temperature. Scans were recorded in the range 100.0–300.0 m/z with the AGC target set to 500,000 and maximal accumulation time of 200 ms. The resolution was adjusted to 200,000. Altering full MS-SIM and targeted MS^2 cycles were employed and a specific inclusion mass of 146.16517 amu was selected. Standard calibration was obtained with 0, 0.02, 0.03, 0.04, 0.05, 0.1, and 0.2 μM spermidine standard (Duchefa Biochemie, Haarlem, The Netherlands) diluted in 0.2 mM HCL.

Plant Growth Experiments with *Stenotrophomonas*-Primed Seeds

Overnight cultures with selected *Stenotrophomonas* isolates were used to inoculate main cultures in fluid NBII. In addition to the lichen-associated isolates, a plant-associated isolate *Stenotrophomonas rhizophila* P69 (Minkwitz and Berg, 2001; Wolf et al., 2002) was also utilized for comparisons. After 2 h of growth at 30°C and 120 rpm the fluid cultures were diluted to 5×10^6–1×10^7 cells per mL in sterile 0.85% NaCl solution. Tomato (*Solanum lycopersicum* L. cv. Kremser Perle; Austrosaat, Graz, Austria) seeds were surface sterilized with 4% NaHClO for 10 min followed by drying at RT. The sterilized seeds were put into the respective bacterial suspensions and incubated for 4 h at 120 rpm and RT. The control samples were put in 0.85% NaCl solution without bacteria. Ground and homogenized seeds from each inoculum were plated on NA to test priming efficiency after the incubation time. The remaining seeds were planted in sterile soil (150 g/tray) with vermiculite (1:3 ratio) and watered with 30 mL sterile H_2O. Beside the control with non-primed seeds an additional control with P69-primed seeds was added. Therefore, 60 μL 5-sec-butyl-2,3-dimethylpyrazine (Sigma–Aldrich, Steinheim, Germany) was supplemented into 30 mL sterile H_2O used for irrigation after planting. The closed trays were placed without further irrigation for 2 weeks into a greenhouse with 12 h day/night cycles and a constant temperature of 24°C. Root ($n = 64$) and stem ($n = 66$) lengths of the plantlets were assessed separately for all samples.

Statistical Analysis

Statistical analyses were performed with SPSS v.20.0.0 (SPSS Inc, Chicago, IL, USA). Data were tested for normal distribution with the Kolmogorov–Smirnov test. Sets with normally distributed data were analyzed with univariate ANOVA and Duncan tests at $p < 0.05$. The *t*-test was employed for statistical analysis of data that was not normally distributed ($p < 0.05$ and $p < 0.1$).

Results

Antagonistic Bacteria within the *Lobaria* Microbiome

Cultivable bacteria, which have been isolated from 15 *L. pulmonaria* samples, were tested in dual-culture assays against the bacterial model pathogens *E. coli*, *S. aureus*, the plant pathogen *B. cinerea* and the lichenicolous fungus *Rhinocladoniella* sp. to determine the general antagonistic potential. In these experiments, lichen-associated antagonists were shown to primarily target lichen and plant pathogenic fungi (20.1% of all isolates) while a lower proportion was directed against bacterial model pathogens (7.7% of all isolates). A total of 95 isolates (24.5%) showed inhibition of growth of at least one of the model pathogens (**Figure 1**). Singular antagonists (active against only one target microorganism) were dominated by *Stenotrophomonas* spp. (31% of singular antagonists) followed by *Pseudomonas* spp. (19%) and *Burkholderia* spp. (12%; Supplementary Figure S1). Dual antagonists (active against two microorganisms) comprised nine isolates. *Stenotrophomonas* and *Micrococcus* were represented by three isolates and *Chryseobacterium*, *Microbacterium,* and *Paenibacillus* by only one isolate, respectively. Nine bacterial strains inhibited the growth of either three or four model pathogens simultaneously. These cultures were identified at genus level as *Bacillus* (five isolates), *Micrococcus* (one isolate), and *Paenibacillus* (three isolates). A complete taxonomic breakdown for all identified antagonists was visualized in **Figure 2**.

Comparison of the hypervariable V4 rRNA region from the most abundant proteobacterial antagonistic isolates: *Stenotrophomonas* spp., *Pseudomonas* spp., and *Burkholderia* spp. with filtered OTUs from an amplicon library constructed with *Lobaria* samples from the same sampling sites, revealed high homology of sequences within the same genus (Supplementary Figure S2). Specific branches (bootstrap values > 70%) were detected for amplicon- and isolate-based sequences. OTUs that were assigned to *Stenotrophomonas* sp., *Pseudomonas* sp., and *Burkholderia* sp. comprised, respectively, 0.06, 0.56, and 0.09% of all analyzed OTUs in the amplicon library. Interestingly three of the highly active antagonistic genera (*Bacillus*, *Micrococcus,* and *Paenibacillus*) were not substantially represented in the amplicon library.

A co-occurrence pattern between different taxa at family level was created with the calculated Spearman correlations based on 15 lichen thallus samples. In total, 24 correlations between the families *Pseudomonadaceae*, *Burkholderiaceae,* and *Xanthomonadaceae* to other taxa within the microbiome could be detected and were visualized as a co-occurrence network (**Figure 3**). Most correlations (10 out of 24) were found within the phylum *Proteobacteria* followed by *Actinobacteria* (3). The strongest positive correlations (Spearman correlation > ±0.7) showed *Xanthomonadaceae* with *Pseudomonadaceae* and *Alteromonadaceae*, all assigned to *Gammaproteobacteria*, whereas the strongest negative correlations were found between *Burkholderiaceae* (*Betaproteobacteria*) and *Phyllobacteriaceae* (*Alphaproteobacteria*) and a family within the class

Chloracidobacteria (*Acidobacteria*) which was not further classified in the utilized database.

In addition, the abundance of antagonistic taxa was extracted from the *Lobaria* metagenome. The proportion of retrievable antagonistic genera was determined for *Stenotrophomonas* (0.22% of all bacteria within the metagenome), *Pseudomonas* (1.14%), *Burkholderia* (2.81%), *Xanthomonas* (0.43%), *Nocardiodes* (0.10%), *Rhodococcus* (0.18%), *Bacillus* (0.08%), and *Staphylococcus* (0.02%). The remaining antagonistic taxa could not be retrieved at genus level. However, they comprised at family level together 2.14% of all bacteria. Altogether, antagonistic taxa comprised 7.12% of the total bacterial community. Neither the genus *Cellulomonas* nor the family *Cellulomonadaceae* was present in the assembled metagenomic dataset.

Spermidine Production *In Vitro* and Spermidine-Related Genes within the *Lobaria*-Associated Metagenome

Genes coding for spermidine synthases were analyzed from the *Lobaria* metagenome and taxonomically assigned. In addition, spermidine production and secretion was analyzed *in vitro*.

Seven antagonistic *Stenotrophomonas* sp. isolates were cultivated on solid agar plates and in liquid media prior to the extraction of spermidine. The detection limit for spermidine on the utilized instruments was determined to be <30 nM. Externalized spermidine levels detected in liquid cultivation media were in the range between 8.2 and 10.5 μmol/g fresh weight. Extracellular spermidine concentration differences between utilized *Stenotrophomonas* isolates were not statistically significant (Supplementary Figure S3). Conversely, the same isolates were shown to contain different internal spermidine concentrations after cultivation on solid media (**Figure 4**). The lowest internal spermidine concentration was found to be 168 nmol/g fresh weight, which was around fourfold lower than the highest observed concentration. Isolate 165P3RAB was found to contain significantly higher spermidine concentrations than all other isolates. In contrast, *Stenotrophomonas* isolate 329P5R contained the lowest spermidine concentrations.

For BLASTn searches, reference sequences for spermidine synthases from four different *Stenotrophomonas* strains were utilized. Additionally, SEED assignments were searched for related functions. *Stenotrophomonas*-specific contigs that contain known spermidine synthases were not found in the utilized metagenome, while three other bacteria-derived contigs were present. Two spermidine synthase contigs that were retrieved with SEED-based analysis were assigned to *Proteobacteria*. One contig was assigned to *Burkholderiaceae* and the other contig to *Acetobacteraceae*. A third contig could not be assigned to any taxon. Conversely, spermidine putrescine transporter permeases were more abundant in the metagenome. A total of 50 contigs were assigned to this specific transporter protein (Supplementary Figure S4). More than a half of these contigs were assigned to bacteria (58%), while 42% remained unassigned to a specific kingdom. The hits were predominantly associated with *Proteobacteria* (52%) and more specifically to *Rhizobiales* (28%).

Stenotrophomonas Treatments Increased Plant Growth of Tomato Under Greenhouse Conditions

Tomato (*Solanum lycopersicum* L.) seeds were inoculated with three lichen-associated and one plant-associated *Stenotrophomonas* isolate and stress protecting agent as reference (Alavi et al., 2013) to analyze the effect of bacterial inoculants on plants. The primed seeds were grown with limited irrigation for 2 weeks in sterile soil. Two control types were implemented to evaluate growth promotion effects by the inoculants. One control (P69_Py) was supplemented with 60 μL 5-sec-butyl-2,3-dimethylpyrazine per tray during the initial irrigation of *Stenotrophomonas* P69-primed seeds. This heterocyclic compound was found to limit the growth of *Stenotrophomonas* isolates in previous experiments. Correspondingly, the growth of P69-primed samples that were treated with 5-sec-butyl-2,3-dimethylpyrazine (R_P69_Py and S_P69_Py), was similar to non-primed control samples (**Figure 5**). Also, the plant growth was not enhanced by isolate 165P3RAB, which was shown to contain the highest internal spermidine concentrations when compared to both implemented controls. *Stenotrophomonas* isolates 329P5R, 401P2, and P69 enhanced the plant growth significantly when compared to both controls. These isolates were shown to produce low internal spermidine concentrations in previous experiments. Treatments with the lichen-associated isolate 401P2 and the plant-associated isolate P69 resulted in similar plant growth.

Discussion

The lichen symbiosis was discovered as reservoir for antagonistic bacteria. Interestingly, it was possible to transfer selected isolates from lichens to cultivated plants while maintaining beneficial effects. In addition, we have shown the usability as well as limits of various applied techniques to efficiently screen for specific characteristics and how to reasonably couple classic microbiology with high-end techniques in a comprehensive approach. Starting from a culture collection and dual-culture experiments to screen for active antagonists, the approach was expanded with detailed specification of continuously filtered isolates.

The microbiome involved in the lichen symbiosis is highly diverse (Aschenbrenner et al., 2014) and was identified as bioresource for antagonistic bacteria. *L. pulmonaria* is predominately colonized by *Alphaproteobacteria* (Grube et al., 2015), in particular by various members of *Rhizobiales* (Erlacher et al., 2015b), which harbor many bacterial genera known for a beneficial host-microbe interaction especially with plants. Interestingly, all antagonistic genera identified for lichens – *Stenotrophomonas, Pseudomonas, Burkholderia, Micrococcus, Chryseobacterium*, *Microbacterium,* and *Paenibacillus* – are well-known from plant studies (Haas and Défago, 2005; Ryan et al., 2009; Rybakova et al., submitted). This is an interesting finding because it shows that these bacteria have the same redundant function independent of the habitat. This observation is underlined by the greenhouse experiments, which have shown

that lichen-associated antagonists are active on plants. This also supports the hypothesis that natural ecosystems are interesting reservoirs for biotechnologically relevant bacteria. The present study depicts that cultivable bacterial taxa with lower occurrence on lichens are mainly responsible for the protection against biotic disturbance. A highly diversified bacterial microbiome enhances the available functional repertoire, which might play a crucial role for the stability and longevity of the lichen symbiosis. Comparison of isolate-derived 16S rRNA gene fragments and amplicon-based sequences of abundant antagonists has indicated that a high proportion of *Burkholderia* spp., *Pseudomonas* spp., and *Stenotrophomonas* spp. can be retrieved from lichen symbioses by cultivation experiments on conventional growth media. It was also demonstrated that several isolated antagonists, such as *Bacillus, Paenibacillus*, and *Micrococcus*, were not detectable in the amplicon library but partially in the metagenomic dataset. The most reasonable explanation is that these antagonistic species occur with low abundance within this lichen microbiome and therefore these species might be below the detection limit of the utilized 454 pyrosequencing approach. Other methods with higher coverage might be more suitable to uncover all present bacterial colonizers. Further studies that address this question should preferably subject less multiplexed samples to high-throughput sequencing platforms to obtain a higher read number per sample. This would allow more accurate characterizations of the rare microbial population.

The majority of the antagonistic isolates was assigned to the genus *Stenotrophomonas*. These bacteria have been reported to protect plants against unaffordable conditions like drought and elevated salinity by exudation of protective compounds like spermidine and different osmolytes (Berg et al., 2010; Alavi et al., 2013). Corresponding to this, polyamines which also include spermidine were shown to be involved in plant response to abiotic stress in prior studies (Alcazar et al., 2006; Liu et al., 2007). Environmental strains of *S. maltophilia* and *S. rhizophila* were reported to exert a certain degree of tolerance toward salinity of up to 9% (w/v) NaCl which was correlated with the ability to produce the osmolytes trehalose and glucosylglycerol (Ribbeck-Busch et al., 2005). Even though *Stenotrophomonas*-specific spermidine synthases were not present in the analyzed metagenome, it was evident that utilization of spermidine is widely distributed among various detected organisms. Since lichens presents a habitat that is frequently subjected to drought, the association with bacteria having protective properties appears favorable. However, lichens themselves have mechanisms to account for desiccation, which also includes osmolytes (Green et al., 2011). Moreover, protection mechanisms against oxidative stress-related damage act in a mutual manner among the eukaryotic partners (Kranner et al., 2005). Therefore, we consider stress-protective functions of lichen-associated bacteria to act as an enhancer, which might react more flexibly to local fluctuations of the conditions than their hosts.

Although synthesized and excreted in different amounts, for all selected *Stenotrophomonas* isolates, *in vitro* spermidine production was detected. According to the result, we assume that the function of lichen-associated bacteria includes assistance in the protection against pathogens as well as against damage caused by desiccation. *Stenotrophomonas* is a well-known antagonist of plant-associated origin (Ryan et al., 2009) and connected with a beneficial effect on plant hosts (Berg et al., 1996; Egamberdieva et al., 2011; Alavi et al., 2013). *Stenotrophomonas* strains might also have the same function independent of the habitat. However, in the last two decades, they have received additional attention for opportunistic infections in humans (Berg and Martinez, 2015). It is difficult to identify specific factors of pathogenicity of the virulent isolates but the ability of persistence, resistance and survival – also essential to colonize lichens – allowed a colonization of immunocompromised patients with predisposition. Similar to the plant rhizosphere (Berg et al., 2005), lichens may act as a reservoir for facultative human pathogenic bacteria, or close relatives thereof.

The host-microbiome balance as well as indigenous diversity is essential for functional stability in ecosystems. This balance also depends on the mutual effects among bacteria within the microbiome. In our co-occurrence analyses we found indications for positive and negative correlations among bacterial groups on samples of the same host lichen symbiosis in the same habitat, which is a strong indication of antagonistic and synergistic effect in the lichen habitat. Further analyses are required for clarifying the mechanisms responsible for these effects, as these might involve direct interactions or diffusible metabolites in the system or both. The present results have already shown that lichen symbioses are valuable bioresources to discover bacteria with antagonistic potential and we suggest that a systematic screening of a broader range of lichens may be useful for finding biocontrol solutions that are specifically tailored for ecologically different plant habitats.

Acknowledgments

We appreciate the help of Armin Erlacher (Graz) with statistical analyses and his generous contributions to the study. Christoph W. Sensen (Graz) and Jung Soh (Calgary) provided valuable support with metagenomics analyses. We also want to thank Angelika Schäfer (Graz) and Kenneth B. Jensen (Graz) for their support during preparation and realization of LC/MS experiments. We are grateful to Lucia Muggia (Graz) for providing the culture of *Rhinocladiella* sp. We also would like to thank Rocel A. Ortega (Graz) for proof-reading the manuscript and her helpful remarks. This work was supported by a grant of the Austrian Science Fund (FWF) to GB and MG (FWF Project I882). Parts of the study were conducted in the Central Lab 'Environmental, Plant and Microbial Metabolomics' funded by NAWI Graz.

Supplementary Material

The Supplementary Material for this article can be found online at: http://journal.frontiersin.org/article/10.3389/fmicb.2015.00620

References

Alavi, P., Starcher, M. R., Thallinger, G. G., Zachow, C., Müller, H., and Berg, G. (2014). *Stenotrophomonas* comparative genomics reveals genes and functions that differentiate beneficial and pathogenic bacteria. *BMC Genomics* 15:482. doi: 10.1186/1471-2164-15-482

Alavi, P., Starcher, M. R., Zachow, C., Müller, H., and Berg, G. (2013). Root-microbe systems: the effect and mode of interaction of stress protecting agent (SPA) *Stenotrophomonas rhizophila* DSM14405T. *Front. Plant Sci.* 4:141. doi: 10.3389/fpls.2013.00141

Alcazar, R., Marco, F., Cuevas, J. C., Patron, M., Ferrando, A., Carrasco, P., et al. (2006). Involvement of polyamines in plant response to abiotic stress. *Biotechnol. Lett.* 28, 1867–1876. doi: 10.1007/s10529-006-9179-3

Aschenbrenner, I. A., Cardinale, M., Berg, G., and Grube, M. (2014). Microbial cargo: do bacteria on symbiotic propagules reinforce the microbiome of lichens?. *Environ. Microbiol.* 16, 3743–3752. doi: 10.1111/1462-2920.12658

Bates, S. T., Cropsey, G. W., Caporaso, J. G., Knight, R., and Fierer, N. (2011). Bacterial communities associated with the lichen symbiosis. *Appl. Environ. Microbiol.* 77, 1309–1314. doi: 10.1128/AEM.02257-10

Berendsen, R. L., Pieterse, C. M., and Bakker, P. A. (2012). The rhizosphere microbiome and plant health. *Trends Plant Sci.* 17, 478–486. doi: 10.1016/j.tplants.2012.04.001

Berg, G. (2015). Beyond borders: investigating microbiome interactivity and diversity for advanced biocontrol technologies. *Microb. Biotechnol.* 8, 5–7. doi: 10.1111/1751-7915.12235

Berg, G., Eberl, L., and Hartmann, A. (2005). The rhizosphere as a reservoir for opportunistic human pathogenic bacteria. *Environ. Microbiol.* 7, 1673–1685. doi: 10.1111/j.1462-2920.2005.00891.x

Berg, G., Egamberdieva, D., Lugtenberg, B., and Hagemann, M. (2010). "Symbiotic plant–microbe interactions: stress protection, plant growth promotion, and biocontrol by *Stenotrophomonas*," in *Symbioses and Stress*, eds J. M. G. Seckbach and M. Grube (Netherlands: Springer), 445–460. doi: 10.1007/978-90-481-9449-0_22

Berg, G., Marten, P., and Ballin, G. (1996). *Stenotrophomonas maltophilia* in the rhizosphere of oilseed rape - occurrence, characterization and interaction with phytopathogenic fungi. *Microbiol. Res.* 151, 19–27. doi: 10.1016/S0944-5013(96)80051-6

Berg, G., and Martinez, J. L. (2015). Friends or foes: can we make a distinction between beneficial and harmful strains of the *Stenotrophomonas maltophilia* complex? *Front. Microbiol.* 6:241. doi: 10.3389/fmicb.2015.00241

Berg, G., Roskot, N., Steidle, A., Eberl, L., Zock, A., and Smalla, K. (2002). Plant-dependent genotypic and phenotypic diversity of antagonistic rhizobacteria isolated from different *Verticillium* host plants. *Appl. Environ. Microbiol.* 68, 3328–3338. doi: 10.1128/AEM.68.7.3328-3338.2002

Berg, G., Zachow, C., Müller, H., Phillips, J., and Tilcher, R. (2013). Next-generation bio-products sowing the seeds of success for sustainable agriculture. *Agronomy* 3, 648–656. doi: 10.3390/agronomy3040648

Boustie, J., and Grube, M. (2005). Lichens—a promising source of bioactive secondary metabolites. *Plant Genet. Resour.* 3, 273–287. doi: 10.1079/PGR200572

Boustie, J., Tomasi, S., and Grube, M. (2011). Bioactive lichen metabolites: alpine habitats as an untapped source. *Phytochem. Rev.* 10, 287–307. doi: 10.1007/s11101-010-9201-1

Caporaso, J. G., Kuczynski, J., Stombaugh, J., Bittinger, K., Bushman, F. D., Costello, E. K., et al. (2010). QIIME allows analysis of high-throughput community sequencing data. *Nat. Methods* 7, 335–336. doi: 10.1038/nmeth.f.303

DeSantis, T. Z., Hugenholtz, P., Larsen, N., Rojas, M., Brodie, E. L., Keller, K., et al. (2006). Greengenes, a chimera-checked 16S rRNA gene database and workbench compatible with ARB. *Appl. Environ. Microbiol.* 72, 5069–5072. doi: 10.1128/AEM.03006-05

Edgar, R. C. (2010). Search and clustering orders of magnitude faster than BLAST. *Bioinformatics* 26, 2460–2461. doi: 10.1093/bioinformatics/btq461

Egamberdieva, D., Kucharova, Z., Davranov, K., Berg, G., Makarova, N., Azarova, T., et al. (2011). Bacteria able to control foot and root rot and to promote growth of cucumber in salinated soils. *Biol. Fertil. Soils.* 47, 197–205. doi: 10.1007/s00374-010-0523-3

Erlacher, A., Cardinale, M., Grube, M., and Berg, G. (2015a). Biotic stress shifted structure and abundance of enterobacteriaceae in the lettuce microbiome. *PLoS ONE* 10:e0118068. doi: 10.1371/journal.pone.0118068

Erlacher, A., Cernava, T., Cardinale, M., Soh, J., Sensen, C. W., Grube, M., et al. (2015b). Rhizobiales as functional and endosymbiontic members in the lichen symbiosis of *Lobaria pulmonaria L. Front. Microbiol.* 6:53. doi: 10.3389/fmicb.2015.00053

Fisher, M. C., Henk, D. A., Briggs, C. J., Brownstein, J. S., Madoff, L. C., McCraw, S. L., et al. (2012). Emerging fungal threats to animal, plant and ecosystem health. *Nature* 484, 186–194. doi: 10.1038/nature10947

Green, T. G. A., Sancho, L. G., and Pintado, A. (2011). "Ecophysiology of desiccation/rehydration cycles in mosses and lichens," in *Plant Desiccation Tolerance*, eds U. Lüttge, E. Beck, and D. Bartels (Berlin: Springer), 89–120. doi: 10.1007/978-3-642-19106-0_6

Grube, M., Cardinale, M., de Castro, J. V., Müller, H., and Berg, G. (2009). Species-specific structural and functional diversity of bacterial communities in lichen symbioses. *ISME J.* 3, 1105–1115. doi: 10.1038/ismej.2009.63

Grube, M., Cernava, T., Soh, J., Fuchs, S., Aschenbrenner, I., Lassek, C., et al. (2015). Exploring functional contexts of symbiotic sustain within lichen-associated bacteria by comparative omics. *ISME J.* 9, 412–424. doi: 10.1038/ismej.2014.138

Haas, D., and Défago, G. (2005). Biological control of soil-borne pathogens by fluorescent pseudomonads. *Nat. Rev. Microbiol.* 3, 307–319. doi: 10.1038/nrmicro1129

Kranner, I., Cram, W. J., Zorn, M., Wornik, S., Yoshimura, I., Stabentheiner, E., et al. (2005). Antioxidants and photoprotection in a lichen as compared with its isolated symbiotic partners. *Proc. Natl. Acad. Sci. U.S.A.* 102, 3141–3146. doi: 10.1073/pnas.0407716102

Küster, E., and Williams, S. T. (1964). Selection of media for isolation of *Streptomycetes*. *Nature* 202, 928–929. doi: 10.1038/202928a0

Lawrey, J. D. (2009). "Chemical defense in lichen symbioses," in *Defensive Mutualism in Microbial Symbiosis*, eds J. F. Jr. White and M. S. Torres (Boca Raton, FL: CRC Press), 167–176. doi: 10.1201/9781420069327.pt3

Lawrey, J. D., and Diederich, P. (2003). Lichenicolous fungi: interactions, evolution, and biodiversity. *Bryologist* 106, 81–120. doi: 10.1639/0007-2745(2003)106[0080:LFIEAB]2.0.CO;2

Liu, J. H., Kitashiba, H., Wang, J., Ban, Y., and Moriguchi, T. (2007). Polyamines and their ability to provide environmental stress tolerance to plants. *Plant Biotechnol.* 24, 117–126. doi: 10.5511/plantbiotechnology.24.117

MacDonald, A., and Coxson, D. (2013). A comparison of *Lobaria pulmonaria* population structure between subalpine fir (*Abies lasiocarpa*) and mountain alder (*Alnus incana*) host-tree species in British Columbia's inland temperate rainforest. *Botany* 91, 535–544. doi: 10.1139/cjb-2013-0025

Mendes, R., Kruijt, M., de Bruijn, I., Dekkers, E., van der Voort, M., Schneider, J. H., et al. (2012). Deciphering the rhizosphere microbiome for disease-suppressive bacteria. *Science* 332, 1097–1100. doi: 10.1126/science.1203980

Minkwitz, A., and Berg, G. (2001). Comparison of antifungal activities and 16S ribosomal DNA sequences of clinical and environmental isolates of *Stenotrophomonas maltophilia*. *J. Clin. Microbiol.* 39, 139–145. doi: 10.1128/JCM.39.1.139-145.2001

Mushegian, A. A., Peterson, C. N., Baker, C. C. M., and Pringle, A. (2011). Bacterial diversity across individual lichens. *Appl. Environ. Microbiol.* 77, 4249–4252. doi: 10.1128/AEM.02850-10

Nash, T. H. III. (2008). "Introduction," in *Lichen Biology*, ed. T. H. Nash (Cambridge: Cambridge University Press), 1–3. doi: 10.1017/cbo9780511790478.002

Oksanen, I. (2006). Ecological and biotechnological aspects of lichens. *Appl. Microbiol. Biotechnol.* 73, 723–734. doi: 10.1007/s00253-006-0611-3

Opelt, K., Berg, C., and Berg, G. (2007). The bryophyte genus *Sphagnum* is a reservoir for powerful and extraordinary antagonists and potentially facultative human pathogens. *FEMS Microbiol. Ecol.* 61, 38–53. doi: 10.1111/j.1574-6941.2007.00323.x

Ribbeck-Busch, K., Roder, A., Hasse, D., De Boer, W., Martínez, J. L., Hagemann, M., et al. (2005). A molecular biological protocol to distinguish potentially human pathogenic *Stenotrophomonas maltophilia* from plant-associated *Stenotrophomonas rhizophila*. *Environ. Microbiol.* 7, 1853–1858. doi: 10.1111/j.1462-2920.2005.00928.x

Rose, F. (1976). "Lichenological indicators of age and environmental continuity in woodlands," in *Lichenology: Progress and Problems*, eds D. H. Brown, D. L. Hawksworth, and R. H. Bailey (London: Academic Press), 279–307.

Ryan, R. P., Monchy, S., Cardinale, M., Taghavi, S., Crossman, L., Avison, M. B., et al. (2009). The versatility and adaptation of bacteria from the genus *Stenotrophomonas*. *Nat. Rev. Microbiol.* 7, 514–525. doi: 10.1038/nrmicro2163

Saito, R., Smoot, M. E., Ono, K., Ruscheinski, J., Wang, P. L., Lotia, S., et al. (2012). A travel guide to *Cytoscape plugins*. *Nat. Methods* 9, 1069–1076. doi: 10.1038/nmeth.2212

Scheidegger, C. (1995). Early development of transplanted isidioid soredia of *Lobaria pulmonaria* in an endangered population. *Lichenologist* 27, 361–374. doi: 10.1017/s0024282995000478

Schmid, F., Moser, G., Müller, H., and Berg, G. (2011). Functional and structural microbial diversity in organic and conventional viticulture: organic farming benefits natural biocontrol agents. *Appl. Environ. Microbiol.* 77, 2188–2191. doi: 10.1128/AEM.02187-10

Shirling, E. T., and Gottlieb, D. (1966). Method for characterization of *Streptomyces* species. *Int. J. Syst. Bacteriol.* 16, 313–340. doi: 10.1099/00207713-16-3-313

Stocker, G., Rieder, D., and Trajanoski, Z. (2004). Cluster Control: a web interface for distributing and monitoring bioinformatics applications on a Linux cluster. *Bioinformatics* 20, 805–807. doi: 10.1093/bioinformatics/bth014

Tamura, K., Stecher, G., Peterson, D., Filipski, A., and Kumar, S. (2013). MEGA6: molecular evolutionary genetics analysis version 6.0. *Mol. Biol. Evol.* 30, 2725–2729. doi: 10.1093/molbev/mst197

van Elsas, J. D., Chiurazzi, M., Mallon, C. A., Elhottovā, D., Krištůfek, V., and Salles, J. F. (2012). Microbial diversity determines the invasion of soil by a bacterial pathogen. *Proc. Natl. Acad. Sci. U.S.A.* 109, 1159–1164. doi: 10.1073/pnas.11093 26109

Wolf, A., Fritze, A., Hagemann, M., and Berg, G. (2002). *Stenotrophomonas rhizophila* sp. nov., a novel plant-associated bacterium with antifungal properties. *Int. J. Sys. Evol. Microbiol.* 52, 1937–1944. doi: 10.1099/ijs.0. 02135-0

Zachow, C., Tilcher, R., and Berg, G. (2008). Sugar beet-associated bacterial and fungal communities show a high indigenous antagonistic potential against plant pathogens. *Microb. Ecol.* 55, 119–129. doi: 10.1007/s00248-007-9257-7

Conflict of Interest Statement: The authors declare that the research was conducted in the absence of any commercial or financial relationships that could be construed as a potential conflict of interest.

Additional Publication II – Supplementary Data

Supplementary Figures

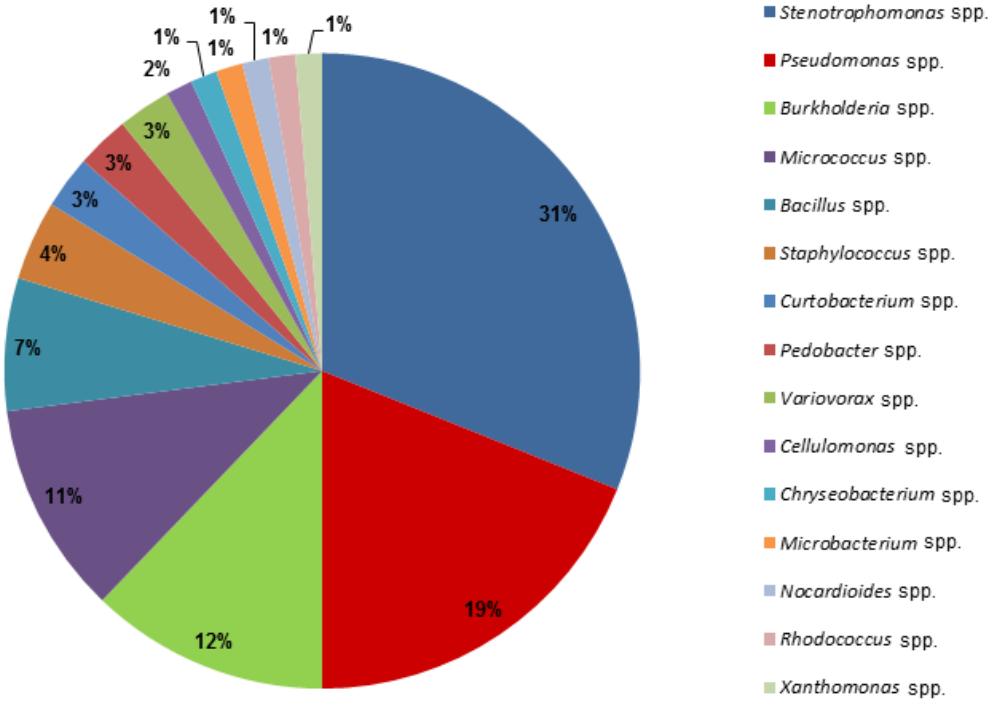

Figure S1: Visualization of lichen-associated antagonistic bacteria which targeted only one utilized model pathogen. The depicted taxa inhibited growth of either *B. cinerea*, *E. coli*, *S. aureus* or *Rhinocladionella* sp.

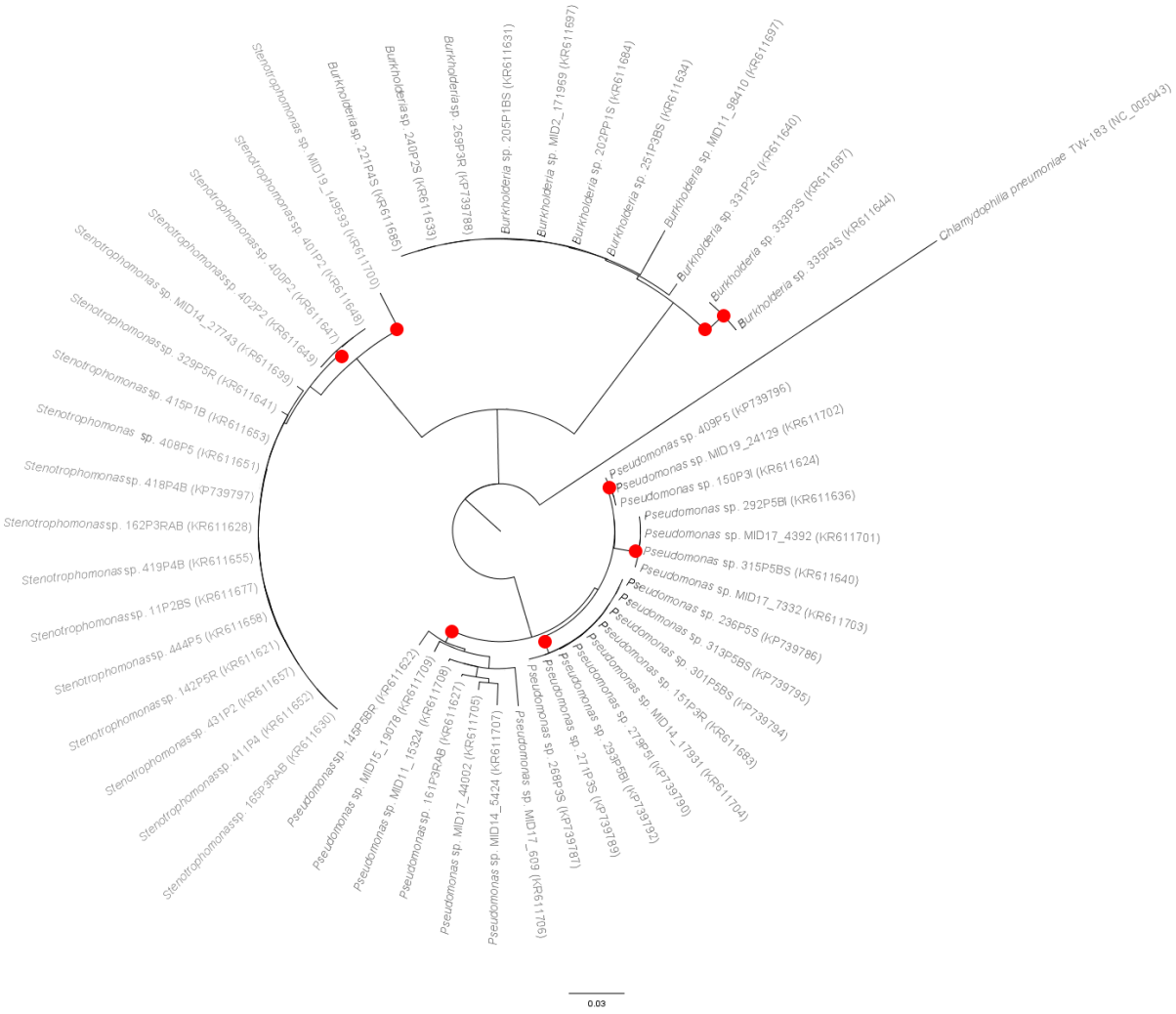

Figure S2: Neighbor-joining tree based on isolated-derived 16S rRNA gene fragments and specific amplicon sequences from the V4 region. Amplicon-based sequences are labelled with 'MID' in the respective sequence names. *Chlamydophila pneumoniae* TW-183 (NC_005043.1) was used as an out-group. Red dots mark nodes with bootstrap values > 70%. Distance bar: 0.03 substitutions per site.

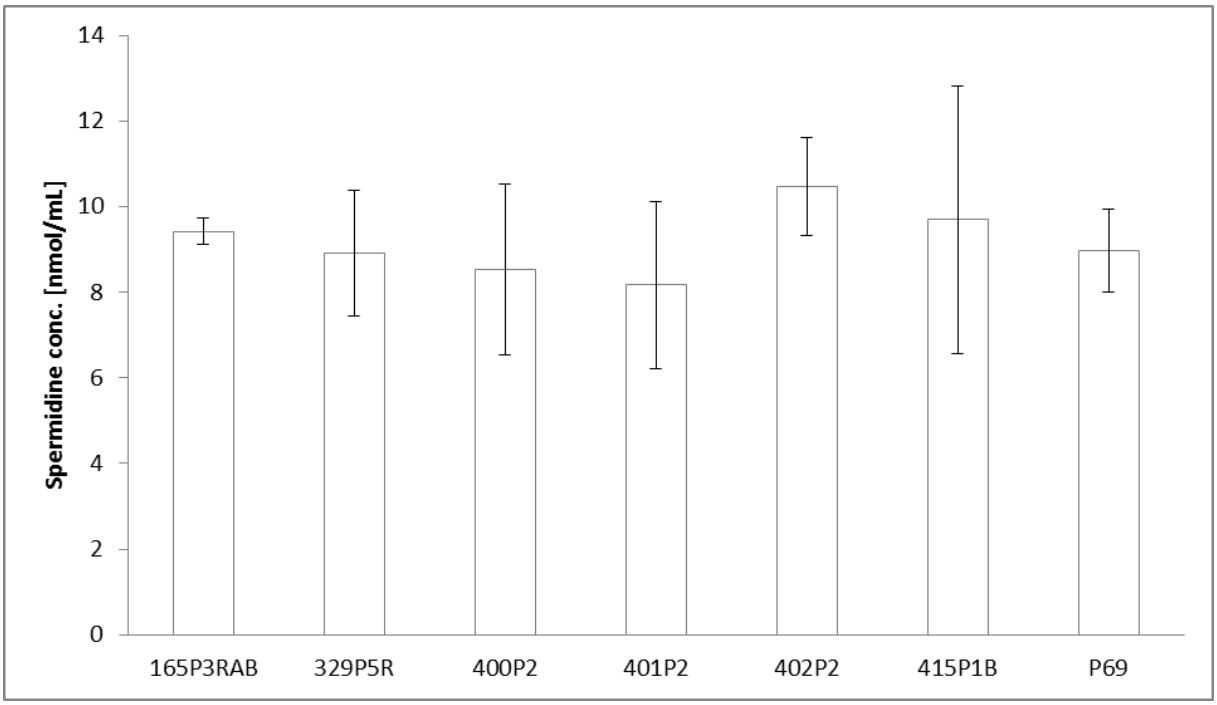

Figure S3 Analysis of extracellular spermidine concentrations and lichen-associated *Stenotrophomonas* spp. isolates. The isolates were cultivated in fluid cultivation media followed by cell removal and quantification of extracellular spermidine levels. HPLC-MS analysis was utilized to quantify spermidine concentrations. A total of six *Lobaria*-associated isolates was utilized together with one plant-associated isolate (P69) in a comparative approach. ANOVA and Tukey's HSD post hoc tests did not show significant differences between the samples.

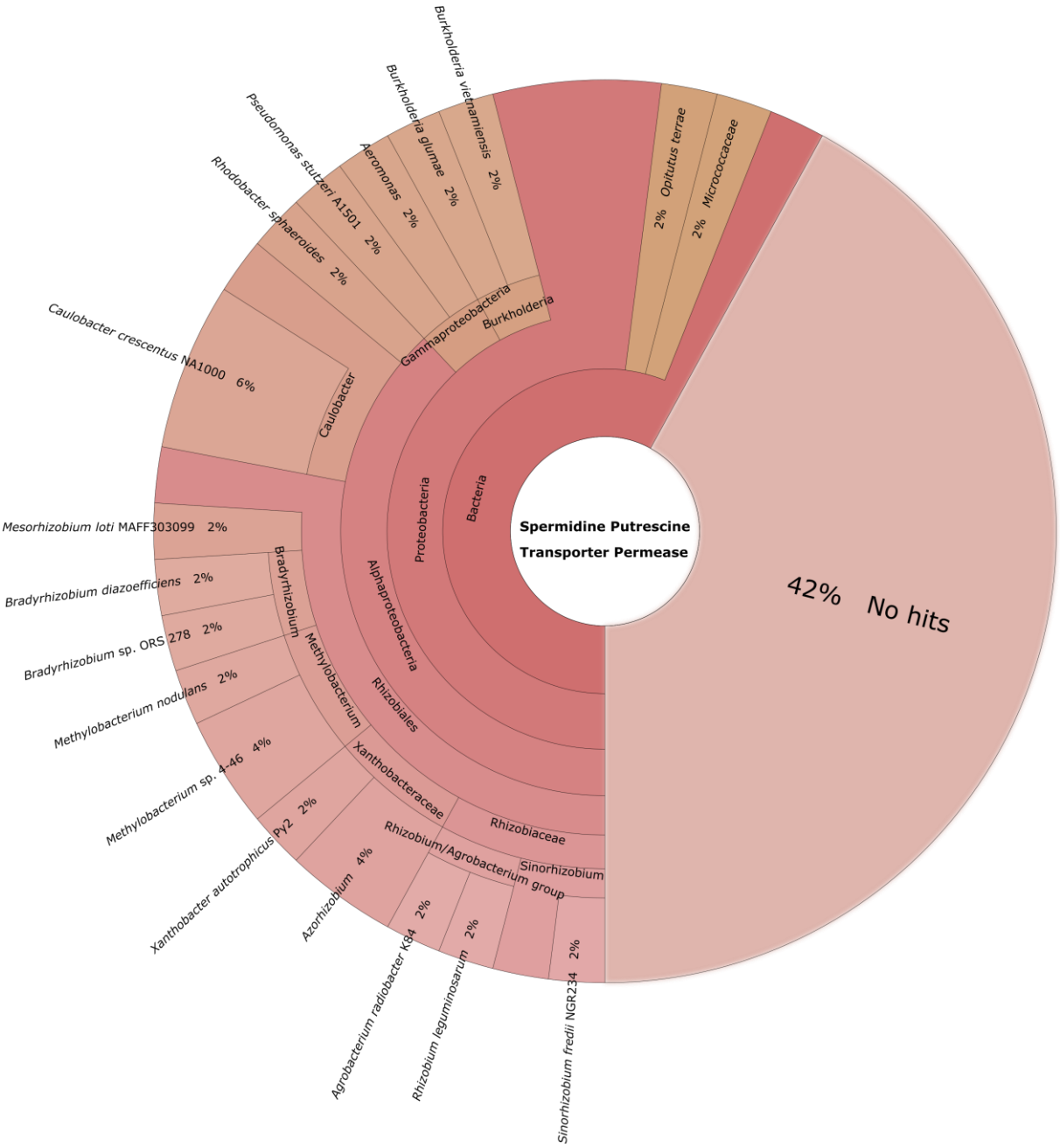

Figure S4: Visualization of taxonomic assignments of spermidine putrescine transporter permease hits within a *L. pulmonaria* metagenome. The data is visualized in a multi-level chart (http://sourceforge.net/p/krona) with different taxonomic resolutions.

ADDITIONAL PUBLICATION III

Frontiers in Microbiology (2015) **6**:398

A novel assay for the detection of bioactive volatiles evaluated by screening of lichen-associated bacteria

Tomislav Cernava,[1] Ines Aline Aschenbrenner,[1,2] Martin Grube,[2] Stefan Liebminger,[1] and Gabriele Berg[1]

[1]Institute of Environmental Biotechnology
Graz University of Technology, Austria

[2]Institute of Plant Sciences
University of Graz, Austria

frontiers in Microbiology

METHODS
published: 01 May 2015
doi: 10.3389/fmicb.2015.00398

A novel assay for the detection of bioactive volatiles evaluated by screening of lichen-associated bacteria

Tomislav Cernava[1], *Ines A. Aschenbrenner*[1,2], *Martin Grube*[2], *Stefan Liebminger*[3] and *Gabriele Berg*[1]*

[1] Institute of Environmental Biotechnology, Graz University of Technology, Graz, Austria, [2] Institute of Plant Sciences, University of Graz, Graz, Austria, [3] Roombiotics GmbH, Graz, Austria

Volatile organic compounds (VOCs) produced by microorganisms are known both for their effect on pathogens and their role as mediators in various interactions and communications. Previous studies have demonstrated the importance of VOCs for ecosystem functioning as well as their biotechnological potential, but screening for bioactive volatiles remained difficult. We have developed an efficient testing assay that is based on two multi-well plates, separated by a sealing silicone membrane, two tightening clamps, and variable growth media, or indicators. The experiment design as presented here is a novel and robust technique to identify positive as well as negative VOC effects on the growth of a target organism and to test for specific substances e.g., hydrogen cyanide which can be detected with a suitable indicator. While the first pre-screening assay is primarily based on indicator color change and visible growth diameter reduction, we also introduce an advanced and quantitatively precise experiment design. This adaptation involves qPCR-based quantification of viable target cells after concluding the treatment with VOCs. Therefore, we chose preselected active isolates and compared the partial 16S rRNA gene copy number of headspace-exposed *E. coli* with non-treated controls. Separately obtained headspace SPME and GC/MS-based profiles of selected bacterial isolates revealed the presence of specific and unique signatures which suggests divergent modes of action. The assay was evaluated by screening 100 isolates of lung lichen-associated bacteria. Approximately one quarter of the isolates showed VOC-based antibacterial and/or antifungal activity; mainly *Pseudomonas* and *Stenotrophomonas* species were identified as producers of bioactive volatiles.

Keywords: volatiles, VOCs, antifungal, antibacterial, lichen symbiosis

OPEN ACCESS

Edited by:
Paolina Garbeva, Netherlands Institute of Ecology (NIOO-KNAW), Netherlands

Reviewed by:
Laure Weisskopf, Agroscope, Switzerland
Marco Kai, University of Rostock, Germany

***Correspondence:**
Gabriele Berg, Institute of Environmental Biotechnology, Graz University of Technology, Petersgasse 12, 8010 Graz, Austria
gabriele.berg@tugraz.at

Specialty section:
This article was submitted to Plant-Microbe Interaction, a section of the journal Frontiers in Microbiology

Received: *05 January 2015*
Accepted: *17 April 2015*
Published: *01 May 2015*

Citation:
Cernava T, Aschenbrenner IA, Grube M, Liebminger S and Berg G (2015) A novel assay for the detection of bioactive volatiles evaluated by screening of lichen-associated bacteria. Front. Microbiol. 6:398. doi: 10.3389/fmicb.2015.00398

Introduction

Volatile organic compounds (VOCs) are organic compounds that have a high vapor pressure at ordinary room temperature. VOCs are produced by the majority of organisms and they often function as communication molecules (Effmert et al., 2012). The most notable characteristic of all VOCs is the extent of their range of influence as compared to non-volatile substances. While other secreted metabolites rely on close contact between interacting organisms or diffusion through

separating matter, VOCs can overcome much greater distances. Bacterial as well as fungal strains produce a broad spectrum of bioactive VOCs with multi-functional effects, which are not restricted to the same species. Their action across organismal kingdoms was shown by Ryu et al. (2003) who demonstrated that bacterial volatiles promoted growth in *Arabidopsis thaliana*. In contrast, some bacterial isolates were also shown to reduce the growth of *A. thaliana* through emission of bioactive volatiles (Vespermann et al., 2007; Blom et al., 2011; Weise et al., 2013). Moreover, bacterial VOCs were shown to be able to suppress the growth of soil-borne pathogenic fungi, e.g., *Rhizoctonia solani* (Kai et al., 2007). Bacteria are able to communicate over long distances within the root system, both among bacteria and with plant hosts, where they elicit induced systemic resistance (ISR) and growth promotion (Farag et al., 2013). VOCs emitted by different soil bacteria can affect the growth, antibiotic production, and gene expression of soil bacteria (Garbeva et al., 2014). Owing to these multi-functional roles of VOCs, they have an enormous potential for biotechnological applications (Strobel, 2006; Schalchli et al., 2014). Currently, there is no efficient testing assay that allows for rapid screening of bioactive volatile metabolites in interrelation between two different microorganisms within the same headspace.

Host-associated microbiomes are important reservoirs for VOC-producing organisms because communication and pathogen defense are essential functions of the microbiome, and recently shown to be integral for healthy plant and human life (Blaser et al., 2013; Philippot et al., 2013). For the rhizosphere microbiome located on/in plant roots, the proportion of VOC producers is often high because in plants the root-associated microbiome acts as a primary protection shield against soil-borne pathogens (Cook, 1990; Weller et al., 2002). A similar role was also attributed to bacteria in the self-sustaining lichen symbiosis (Grube et al., 2015). In each microbiome a certain proportion of microorganisms with antagonistic activity against pathogens is involved in this function. Using a combination of metagenomic, -proteomic, and cultivation approaches, a proportion of 7% antagonists was identified for the lung lichen (Grube et al., 2015). Identification of antagonistic microorganisms is still a challenge (Berg et al., 2013), but nevertheless important for a more profound understanding of ecosystem functioning and also a necessary tool for bioprospecting in biotechnology (Strobel, 2006). The discovery of novel bioactive compounds facilitates improvement in disinfection strategies and drug discovery, both of which are in high demand due to the increasing rates of resistance to antibiotics (Woolhouse and Farrar, 2014). Antagonistic microorganisms harbor a vast potential to produce active biomolecules for direct activity against pathogens but also for mediators in various interactions, e.g., pathogen defense, quorum sensing, microorganism-host-interaction. Some of these biomolecules are highly active modifications of known antimicrobial substances and are therefore less susceptible to existing resistance mechanisms. In the past, most efforts focused on antibiotics for which high-throughput screening strategies were already developed (Conery et al., 2014; Seyedsayamdost, 2014). Although previous studies have demonstrated promising effects of bacterial and fungal volatile compounds, they are difficult to detect as well as to identify. Due to their inspiring odors, lichen extracts are used as raw materials in perfumery (Joulain and Tabacchi, 2009). As the specificity of bacterial communities in this phylogenetically old symbiosis was only recently detected (Grube et al., 2009), nothing is yet known about VOCs produced by the abundant lichen-associated bacteria.

The objective of our study was to develop a well plate-based and cost-effective testing assay for the emission of bioactive VOCs. We chose lichen-associated bacteria for evaluation purposes. One hundred lichen-associated bacterial isolates were tested for volatile antagonistic activity in order to evaluate our assay. A noteworthy screening assay for biological hydrogen production developed by Schrader et al. (2008) was used as the basis for developing our testing system. The assay is based on two micro-well plates, separated by a sealing silicone membrane, two tightening clamps, and variable growth media or indicators. The suggested experiment design can be used to differentiate between target organism inhibition or growth promotion by a pure substance and also for the same effects caused by volatile mixtures emitted by living microorganisms. This, as well as an increased throughput compared to classic single plate-tests illustrates the novelty of the presented assay in comparison to already described experiment setups. In addition, it can be employed to test for specific substances which can be detected with a suitable indicator (**Figure 1**). Using this design we identified 30 out of 100 lichen-associated bacterial isolates, which produced bioactive volatiles and induced growth inhibition in two distinct target organisms. Since many lichenicolous organisms are characterized by slow growth rates and difficult or impossible to grow on media, two classic model targets were employed for evaluation purposes. *E. coli* was used in this experimental approach as a model for a typical human pathogen and *B. cinerea* as a model for a plant pathogen. Additional GC/MS-based headspace analysis with different lichen-associated isolates was applied to demonstrate the occurrence of isolate-specific VOC profiles.

Material and Methods

Isolation of Lichen-Associated Bacteria

Lobaria pulmonaria lichen thalli were sampled from three different locations in Austria (Tamischbachgraben, N 47°32′40″, E 14°37′35″, Johnsbach, N 47°38′07″, E 14°44′45″, and St. Oswald ob Eibiswald, N 46°44′50″, E 15°04′26″). The lichen samples were ground with mortar and pestle, and subsequently combined with a ratio of 1:10 0.85% sterile NaCl in a lab stomacher to form a homogenate (BagMixer; Interscience, St Nom, France). The diluted fractions were then plated onto agars R2A (Carl Roth, Karlsruhe, Germany), R2A with 25 μg ml^{-1} cycloheximide, starch casein agar (SCA; Küster and Williams, 1964), and ISP2 (Shirling and Gottlieb, 1966). Distinctive bacterial colonies were transferred onto R2A plates for sub-cultivation within 5 days of incubation at room temperature. After subsequent testing for antagonism against different pathogens among other physiological tests, 100 lichen-associated bacterial isolates were selected out of 388 available isolates from the in-house culture collection. All of these isolates met at least one of the following criteria: (i) antagonistic activity against *E. coli* K12, (ii) antagonistic

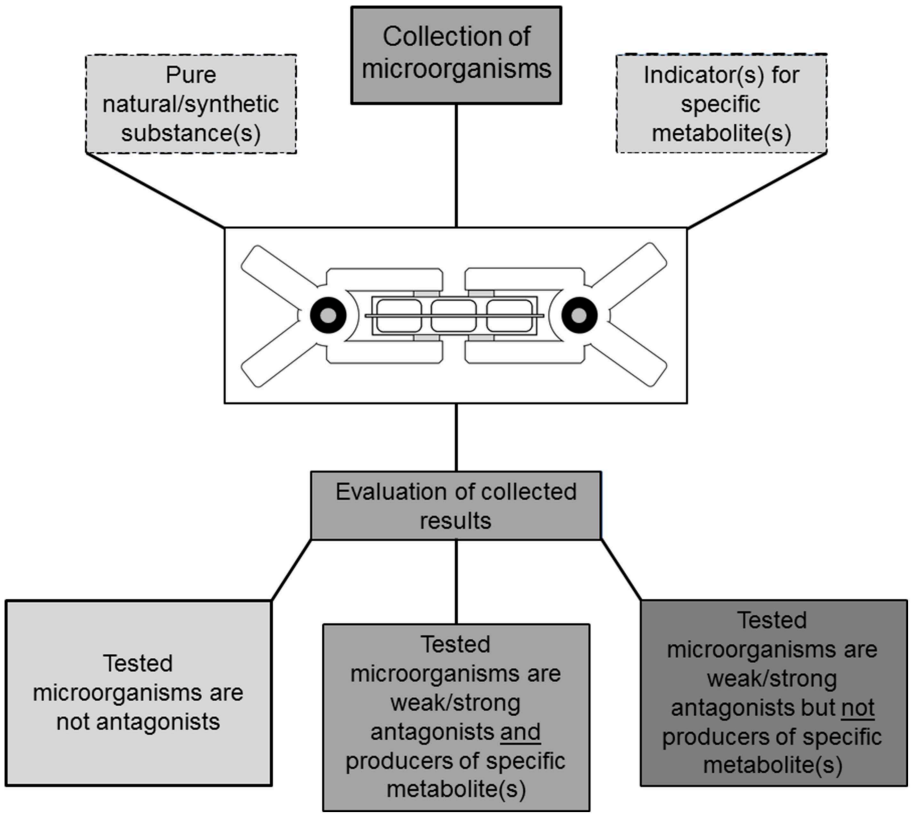

FIGURE 1 | Illustration of a TCVA-based screening approach for bioactive volatile compounds. The experiments are based on microorganism cultures suitable for cultivation in well-plates. Parallel setup of different experiments facilitates selectivity and can be used to eliminate producers of predefined compounds e.g., HCN if indicator substances are available. Utilization of additional reference substances enables gradual evaluation of visually inspected experiments.

activity against *Staphylococcus aureus* ATCC 25923, (iii) antagonistic activity against *Botrytis cinerea* (SCAM, culture collection of the institute of Environmental Biotechnology, Austria), (iv) antagonistic activity against *Rhinocladiella* sp. (culture collection of the Institute of Plant Sciences, University of Graz) in dual-culture experiments, (v) chitinase activity on chitin agar and in chitin-RBV assay, (vi) β-glucanase activity with chromogenic AZCL-Barley β-glucan.

Two Clamp VOCs Assays (TCVAs)

Depending on the experiment type, 6-, 12-, and 24-well plates (Greiner Bio-One, Frickenhausen, Germany) were used together with a perforated (0.5 cm ø) 1 mm silicone foil (detailed specifications are presented in Table S1) for tightening connected wells and usual clamps for fixation. Sterile plates were acquired and the silicone foils used were washed and autoclaved at 121°C (holding time of 20 min). 6-, 12-, and 24-well plates were filled with respectively 5, 3.5, and 1.5 mL sterile media per well. The preparation steps and the final setup are pictured sequentially in Figure S1.

TCVA with *B. cinerea* and Lichen-Associated Bacteria

The bacterial isolates were streaked onto Nutrient Agar (NA; Sifin, Berlin, Germany) in 6-well plates and pre-incubated for 24 h at 30°C. Next, 5 mm diameter plugs were cut from a donor plate evenly covered with *B. cinerea*. These plugs were placed in the center of each well in the 6-well plates containing Synthetic Nutrient-Poor Agar (SNA). After the inoculated plates were checked for sufficient growth, silicone foils were placed between plate pairs containing lichen isolates and *B. cinerea,* respectively. The plates were then clamped together; the lichen-associated bacteria plate was placed upside-down over the *B. cinerea* plates on the bottom. The plates were incubated in the dark at 21°C for 4 days and subsequently visually inspected for mycelium growth and compared to untreated controls (**Figure 2A**). Two types of controls were implemented; one containing NA wells without any bacteria and one inoculated with *E. coli* K12 instead of lichen-associated isolates.

TCVA with *E. coli* and Lichen-Associated Bacteria

The bacterial isolates were streaked onto NA in 12-well plates and pre-incubated for 24 h at 30°C. Following the incubation time, a fluid Nutrient Broth (NB; Sifin, Berlin, Germany) culture of *E. coli* K12 was grown to an OD_{600} = 0.4–0.6. 6 mL aliquots were then sequentially transferred to 200 mL NA (20%) supplemented with 0.2 mg/mL 2–(4–iodophenyl)–3–(4–nitrophenyl)–5–phenyltetrazolium chloride (INT; Sigma-Aldrich, St. Louis, MO, USA) and immediately pipetted into sterile 12-well plates.

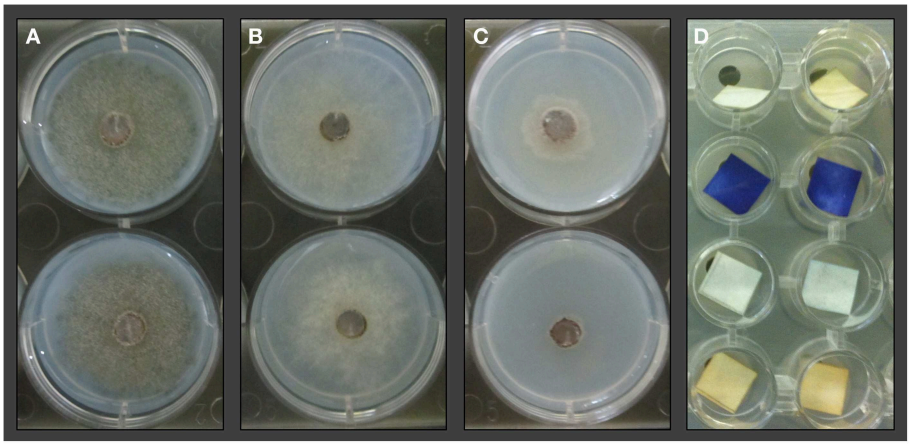

FIGURE 2 | TCVA with lichen-associated bacterial isolates and *Botrytis cinerea*. Mycelium growth and sporulation was compared to untreated controls **(A)** after 4 days of co-incubation. Inhibition of sporulation was recorded for wells where discoloring of the mycelium was not observable **(B)**. Inhibition of mycelial growth was recorded for wells with 50% or less mycelium proliferation **(C)** compared to negative controls. TCVA with HCN indicator **(D)** based on copper(II) ethyloacetoacetate and 4,4'-methylenebis(N,N-dimethylaniline). The second row shows positive reactions where bacterial isolates from counterpart wells secreted HCN into the headspace which led to the color change of indicator strips.

INT can be utilized to detect dehydrogenase activity due to visible color changes. Hence, approximate differences in bacterial abundance can be correlated to the grade of visible discoloring of INT-supplemented growth medium. After solidification of the *E. coli* K12 containing plates, silicone foils were placed between plate pairs containing lichen isolates and *E. coli* K12, respectively. The plates were then clamped together; the lichen-associated bacteria plate was placed upside-down over the *E. coli* K12 plates on the bottom. After 24 h incubation at 21°C, the plates were checked for differences in indicator color change and compared to positive and negative controls. Positive controls were obtained using different commercial disinfectants to determine sufficient OD_{600} values (0.4–0.6) for *E. coli* K12 and an adequate concentration of INT (Figure S2). Two types of negative controls were implemented: one containing NA wells without any bacteria, and one inoculated with *E. coli* K12 instead of lichen-associated isolates.

qPCR Validation of TCVA Results

This experiment is an adaption of the aforementioned TCVA with *E. coli* K12, the only modification being that semi-solid 0.3% NA was used instead of solid 1.5% NA in the initial steps of the experiment. After the incubation time, 500 µL of the semi-solid medium with *E. coli* K12 and INT was transferred into 2 mL reaction tubes with 1 mL 0.85% NaCl and subsequently dissolved via vortex. Each tube was supplemented with 10 µL (1:100 solution) propidium monoazide (PMA; GenIUL, Barcelona, Spain) and incubated on ice in the dark while shaking at 100 rpm for 50 min. The tube lids were then opened after incubation and placed under a LED light source for activation of PMA with an emission maximum of 520 nm for 10 min. PMA forms covalent bonds with available DNA but cannot pass through undisrupted cell membranes. This step was performed to exclusively detect gene fragments from living *E. coli* K12 in the qPCR-based quantification. The suspension was then transferred to glass bead containing tubes and mechanically disrupted for 2 × 45 s at 6 m/s with a FastPrep®-24 Instrument (MP Biomedicals Europe, Illkirch, France) and centrifuged at 3000 × g for 2 min to sediment beads and residual Agar. DNA was subsequently extracted from 500 µL of supernatant using the GeneJET Genomic DNA Purification Kit (Thermo Scientific, Waltham, MA, USA). Quantification of 16S rDNA fragments from the DNA extract was conducted with primer pair Unibac-II-515f/Unibac-II-927r as described by Lieber et al. (2003), and standards containing the Unibac-II fragments were prepared according to Köberl et al. (2011). For standard preparation, the gene fragments from *Bacillus subtilis* subsp. *subtilis* Sd3-12 were cloned into the pGEM®-T Easy Vector (Promega, Madison, WI, USA) and later re-amplified with vector specific primers. Total DNA extract treated with amplification-grade DNase I (Sigma-Aldrich, St. Louis, MO, USA) was used to determine the inhibitory effects of co-extracted substances. Based on these results, the extracted DNA was then diluted 1:10 and the target regions were amplified using KAPA SYBR FAST qPCR Kit (Kapa Biosystems, Woburn, MA, USA). Two independent runs with three replicates for each sample were performed on the Rotor Gene 6000 (Corbett Research, Mortlake, Australia) according to Bragina et al. (2013). The specificity of the amplicons and qPCR products was confirmed using melting-curve analysis and gel-electrophoresis, respectively.

TCVA with a Hydrogen Cyanide (HCN) Indicator and Lichen-Associated Bacteria

The bacterial isolates were streaked onto NA in 24-well plates and pre-incubated for 24 h at 30°C. Indicator strips were prepared using blotting paper submerged in 10 mL chloroform (Carl Roth, Karlsruhe, Germany) solution with 50 mg copper(II) ethylacetoacetate (Sigma-Aldrich, St. Louis, MO, USA) and 50 mg 4,4-methylenebis(N,N-dimethylaniline) (Sigma-Aldrich, St. Louis, MO, USA) and left to air dry. After the pre-incubation time,

1 × 1 cm HCN indicator strips were placed in each well of a 24-well plate. Silicone foils were placed between the upside-down lichen-associated bacteria plates and those containing the HCN indicators. The plate pairs were then clamped together and incubated for 48 h at 30°C. Lastly, the indicator plates were checked for an intense blue color change in the corresponding upper wells. Negative controls were conducted with non-inoculated NA wells.

Identification of Active Isolates by 16S rDNA Sequencing

Isolated DNA from pure cultures was amplified with primer pair 27F/1492r according to Lane (1991). The PCR product was purified with Wizard® SV Gel and PCR Clean-Up System (Promega, Madison; WI, USA) followed by Sanger sequencing (LGC Genomics, Berlin, Germany). The sequences were aligned with BLASTn (http://blast.ncbi.nlm.nih.gov/Blast.cgi) and 16S ribosomal RNA sequences database. Identification of the closest match was applied for the retrieved results.

Headspace SPME and GC/MS Analysis of Bacterial VOCs

The utilized GC/MS SPME headspace method was adapted with minor changes from Verginer et al. (2010). For sample preparation from bacterial isolates, single colonies were transferred with an inoculating loop on 10 mL NA slope agar (1.5%) in 20 mL headspace vials (75.5 × 22.5 mm; Chromtech, Idstein, Germany). The isolates were streaked out in 3 parallel lanes to ensure similar bacterial lawn density after incubation. Following 48 h of incubation at 30°C the vials were sealed with adequate crimp seals and incubated for additional 2 h. Solid phase micro extraction (SPME) was performed with an automated sampler and 50/30 μm Divinylbenzen/CarboxenTM/ Polydimethylsiloxane (PDMS) 2 cm Stableflex/SS fiber (Supelco, Bellefonte, PA, USA). Volatile compounds were enriched for 30 min at 30°C. Compound separation and detection was performed on a system combining a GC 7890A with a quadrupol MS 5975C (Agilent Technologies, Waldbronn, Germany). Samples were run through a (5%-phenyl)methylpolysiloxane column, 60 m × 0.25 mm i.d., 0.25 μm film thickness (DB-5MS; Agilent Technologies, Waldbronn, Germany), followed by electron ionization (EI; 70 eV) and detection (mass range 25–350). The inlet temperature was adjusted to 270°C. For the temperature gradient the GC column was kept at 40°C for 2 min, raised to 110°C at a rate of 5°C/min, then to 280°C at 10°C/min and finally maintained at 280°C for 3 min. The helium flow rate was set to 1.2 mL/min. Serial analysis was done with up to 12 samples per run. Obtained spectra were compared with NIST Mass Spectral Database 08 entries. Specific compounds were identified based on their retention indices and comparison to reference substances (Sigma-Aldrich, St. Louis, MO, USA). Origin 8.5 (OriginLab, Northampton, MA, USA) was applied for visualization of total ion chromatograms (TICs). Background-subtracted mass spectra were used for the depiction of unidentified substances.

Statistical Analysis

The statistical analysis was conducted with ANOVA within RStudio (version 0.97.551) and one-sided *t*-test ($P < 0.001$). Gene copy numbers of the UniBac-II fragment from TCVA-exposed samples ($n = 36$) were compared to untreated controls ($n = 12$). The gene copy numbers were obtained from two biological samples and three qPCR repeats respectively.

Results

Testing Volatile Activity Against *E. coli* and Botrytis Cinerea

The here presented Two Clamp VOCs Assay (TCVA) made it possible to detect bioactive VOC producers within 100 lichen-associated bacterial isolates. Sporulation reduction (**Figure 2B**) was demonstrated for five isolates; four isolates reduced sporulation of *B. cinerea* in three out of four replicate experiments, while one isolate reduced sporulation in all four trials. *B. cinerea* growth was repeatedly reduced after exposure to 21 different lichen-associated bacterial isolates in the TCVA, and mycelium proliferation was visibly affected (**Figure 2C**) for these isolates when compared to negative controls. Moreover, 16 isolates reduced proliferation in three out of four replicate experiments, while five isolates reduced proliferation in all four trials. Only one of the identified growth-reducing isolates was later shown to release HCN into the headspace. TCVAs with *E. coli* allowed identification of 10 lichen-associated isolates that are associated with the exertion of antagonistic activity through headspace. Low INT-based growth media discoloring indicating a reduced number of metabolically active bacteria was observed in all three replicate experiments. Comparison to the corresponding HCN TCVAs showed that two of the growth-reducing isolates did not release HCN into headspace. Only one isolate inhibited the growth of both target organisms and was later identified as *Pseudomonas umsongensis* 313P5BS. From all identified antagonists we have selected the 15 most active isolates against one or both target organisms and one non-inhibiting isolate for Sanger sequencing (**Table 1**).

Screening for HCN Producers

All lichen isolates were tested for HCN production in a modified TCVA by imposing indicator strips to the headspace. Nine bacterial isolates induced dark blue discoloring of the indicator strips in all three replicate experiments. Eight of the identified HCN-producing isolates also reduced growth of *E. coli* in previous experiments. These isolates were later assigned to *Pseudomonas* spp., while the non-antagonistic HCN producer had the highest sequence similarity to a *Bacillus pumilus* isolate.

Validation of TCVA Results by Quantitative PCR

DNA extracts from wells containing *E. coli* that had shown low discoloring of INT after exposition to lichen-associated bacteria were used to determine the gene copy number of the Unibac-II fragment. DNA from dead or disrupted cells was blocked by PMA which enabled a correlation between gene copy number and living cells. A significantly lower gene copy number compared to controls was shown for all samples exposed to the headspace of highly active antagonists that were pre-screened based on INT discoloring. An approximately 4-fold decrease of the gene copy

TABLE 1 | Overview of identified isolates including corresponding activity in TCVAs.

Strain ID	Closest BLASTn match	GenBank accession #	Inhibition of *E. coli*	Inhibition of *B. cinerea*	HCN producer
43P2BR	*Bacillus pumilus*	KP739785		✓	
236P5S	*Pseudomonas umsongensis*	KP739786	✓		✓
268P3S	*Pseudomonas umsongensis*	KP739787	✓		✓
269P3R	*Burkholderia sordidicola*	KP739788	✓		
271P3S	*Pseudomonas umsongensis*	KP739789	✓		✓
279P5I	*Pseudomonas umsongensis*	KP739790	✓		✓
288P4R	*Burkholderia sordidicola*	KP739791	✓		
293P5BI	*Pseudomonas umsongensis*	KP739792	✓		✓
300P5BR	*Chryseobacterium piscium*	KP739793		✓	
301P5BS	*Pseudomonas umsongensis*	KP739794	✓		✓
313P5BS	*Pseudomonas umsongensis*	KP739795	✓	✓	✓
409P5	*Pseudomonas lini*	KP739796	✓		✓
418P4B	*Stenotrophomonas rhizophila*	KP739797		✓	
439P1B	*Stenotrophomonas rhizophila*	KP739798		✓	
460P5B	*Stenotrophomonas rhizophila*	KP739799		✓	
471P3B	*Bacillus pumilus*	KP739800			✓

Listed species represent the closest match of BLASTn searches within the 16S ribosomal RNA sequences database (NCBI). The 16S gene fragment sequences were deposited at GenBank (http://www.ncbi.nlm.nih.gov/genbank).

number was observed with the least inhibiting antagonist *Pseudomonas* sp. 279P5I, while the most effective antagonist *Pseudomonas* sp. 236P5S decreased the gene copy number of *E. coli* approx. 15-fold (**Figure 3**).

Taxonomic Assignment of Active Lichen-Associated Isolates

Sanger sequencing revealed multiple occurrence of some dominant genera. Furthermore, sequencing of 16S rRNA gene fragments from the 15 most active isolates and a non-antagonistic HCN producer revealed the majority belonging to the genus *Pseudomonas* (8 isolates), followed by *Stenotrophomonas* (3 isolates) and three other genera with lower occurrence: *Bacillus*, *Burkholderia,* and *Chryseobacterium.* Utilization of the TCVA demonstrated that *E. coli* inhibition was mostly observed after exposure to the headspace of *Pseudomonas* sp., while *B. cinerea* growth reduction was mostly observed after exposition to the headspace of *Stenotrophomonas rhizophilia*. Moreover the sequencing approach revealed that different *Pseudomonas* sp. inhibited *E. coli* growth accompanied by HCN release into headspace. Identified isolates are presented together with corresponding TCVA results in **Table 1**.

GC/MS-Based Headspace Analysis with Selected Isolates

Three representative isolates which were shown to inhibit growth of headspace-exposed target microorganisms and which were taxonomically assigned to reoccurring genera were used for subsequent GC/MS headspace SPME profiling. Isolate-specific VOCs were identified by overlays of total ion chromatograms (TIC; **Figure 4**). A total of 21 compounds (Table S2) were found to be unique and only present in TICs of a specific isolate. *Bacillus pumilus* 43P2BR emitted nine distinctive volatile compounds (compound IDs: 2, 5, 8, 10, 13, 14, 15, 18, and 21), followed by *Pseudomonas umsogensis* 313P5BS with eight distinctive compounds (compound IDs: 1, 6, 7, 9, 16, 17, 19, and 20). *S. rhizophila* 418P4B was shown to emit only four distinctive compounds (compound IDs: 3, 4, 11, and 12). Compound identification indicated that *B. pumilus* 43P2BR emitted 1-butanol, 3-methyl-2-pentanone and seven unidentified substances (Figures S3-18). 2-butanol, 2-methyl-1-propanol and two unidentified substances were found within spectra of *S. rhizophila* 418P4B. Conversely, *P. umsogensis* 313P5BS emitted methyl thiocyanate as well as seven unidentified substances.

Discussion

The results of the screening for bacteria-derived bioactive VOCs demonstrated the applicability of a novel testing system, which is not restricted to bacteria associated with lichens, but can be widely applied with microorganisms sampled in other habitats. With the presented setup several 100 isolates can be tested simultaneously for VOCs-driven effects on target microorganisms and occurrence of specific metabolites. This facilitates screening programs for strain-specific biological effects. Thus, the method is also not limited to observations of growth inhibition such as demonstrated in the present study, but could also be used to identify growth promoting effects. The method, however, reveals the effect of the total "volatilome" of a bacterial strain and does not dissect the effect of individual substances. The composition of the mixture of volatile substances must still be assessed by chemical analysis, after which individual compounds might be tested separately.

We have selected 100 isolates for evaluation purposes that met predefined criteria such as antagonism in classic dual-culture experiments. Thus, we expected to identify a sufficient number of isolates which emit bioactive VOCs to validate the experimental design and the presented workflow. Utilization of different TCVA variations allowed the identification of 30 growth inhibiting bacterial isolates with a novel and reliable technique. Subsequent analysis of the headspace from taxonomically dissimilar bacterial isolates by employing headspace SPME GC/MS demonstrated the presence of isolate-specific TIC profiles and unique compounds in each sample. We have identified five out of 21 unique compounds, emitted by three distinct bacterial strains, to exemplify the presented workflow. While some compounds most likely originate from bacterial degradation of growth media

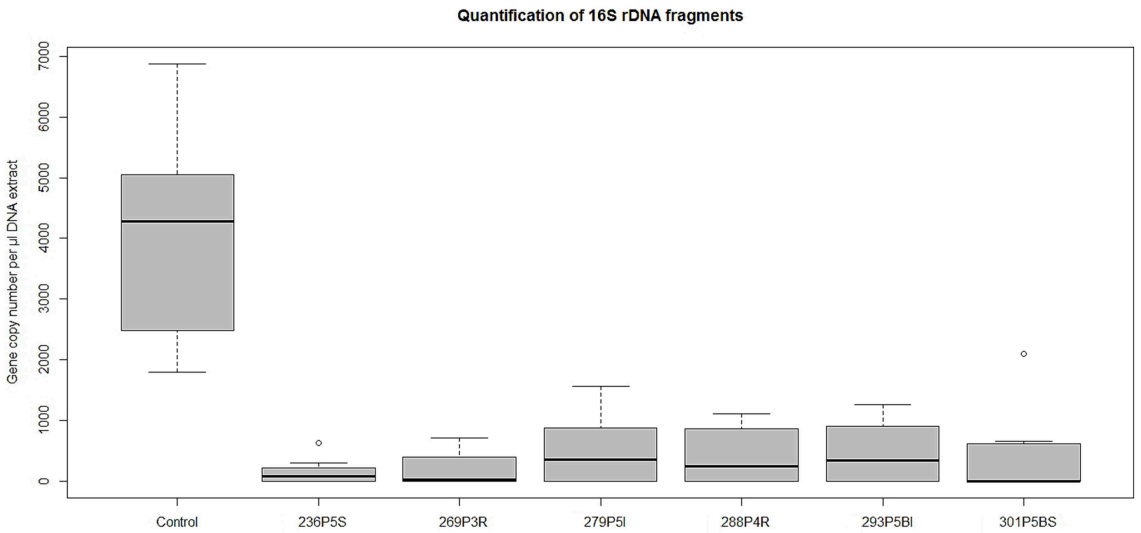

FIGURE 3 | A qPCR approach was used to determine gene copy numbers of *E. coli* K12 after exposition to strong VOCs antagonists. TCVA-exposed samples were treated with PMA and gene copy numbers of viable cells were quantified with Unibac-II primers. Values for the treated samples were obtained from respectively six qPCR runs and additional 12 qPCR runs for untreated controls. Statistical analysis with ANOVA and one-sided *t*-test confirmed a highly significant decrease of gene copy numbers of the treated samples compared to the control group ($P < 0.001$).

(waste products of bacterial metabolism) and therefore do not target pathogens specifically, other compounds might either be involved in molecular signaling or inhibition of competing organisms. These differences and their significance in natural systems merit further exploration. It might be hypothesized that bacterial bioconversion of the natural substrate may result in volatile compounds with signaling effect. Specifically, the odor of lichens, which may attract reindeer or is part of perfumes, could be influenced not only by the genuine compounds produced by the fungal or algal symbiont, but possibly also by VOCs produced by the bacteria themselves or by compounds released from the fungal matrix due to the metabolic activity of associated bacteria.

The presented workflow includes a pre-incubation of the tested isolates to minimize their inhibition by volatiles emitted by the target organisms. Due to intended growth advantage of the tested organisms, emitted volatiles from the target organisms might not play an important role during the co-incubation. Still, such effects cannot be completely avoided with the presented setup. An inverted approach where the "target" is pre-incubated and subsequently tested against the respective isolate collection could be implemented to obtain a more holistic view on occurring interactions.

Interestingly, *P. umsongensis,* a bacterial species isolated from soil as well as from fungal hyphae and described as "fungiphilic" (Warmink et al., 2009), was the only representative of *Pseudomonas* isolates that consistently inhibited *B. cinerea* growth. This may have resulted from better and faster growth on solid medium compared to the other utilized strains and therefore a higher accumulation of cyanide in the headspace. Various *Pseudomonas* species are known to be cyanogenic bacteria and therefore enhanced toxicity toward various prokaryotes and eukaryotes can be expected even if they are not in close contact. While the employed headspace SPME GC/MS method was not suitable for detection of hydrogen cyanide, we were able to detect methyl thiocyanate above cultures of *P. umsongensis* 313P5BS. Conversion of cyanide to thiocyanate is accomplished by bacterial rhodanese and these co-occurring molecules can be extracted simultaneously from headspace above living cultures (Broderick et al., 2008). Weise et al. (2013) have highlighted the importance of bacterial ammonia production and demonstrated accompanied growth inhibition of *Arabidopsis thaliana*. Specific indicator stripes in the TCVA would allow to test for ammonia in the headspace, which would also imply an unspecific inhibition of target organisms.

Some bacteria are well known for pronounced antifungal effects against phytopathogenic fungi. This effect is typical for several strains belonging to *Stenotrophomonas* (Wolf et al., 2002), which was also observed with headspace experiments (Ryan et al., 2009). *Bacillus* species were shown in prior studies not only to produce antifungal VOCs (Fiddaman and Rossall, 1993), but also volatiles that promoted growth in *A. thaliana* (Ryu et al., 2003). Our study demonstrates such antagonistic effects with a robust well plate-based approach and provides various options for modifications to study further effects e.g., growth promotion of bacteria on plants in an adaptable testing system. Moreover, this approach could also be applied to study the prevalence of similar bioactive effects across entire bacterial genera and to correlate volatile effects with the occurrence of strains in particular ecological niches.

As we are convinced that bacterial volatiles might play an important role to modify the composition of host-associated communities, future research needs to focus on the, possibly context-dependent, effects of such small molecules. We anticipate

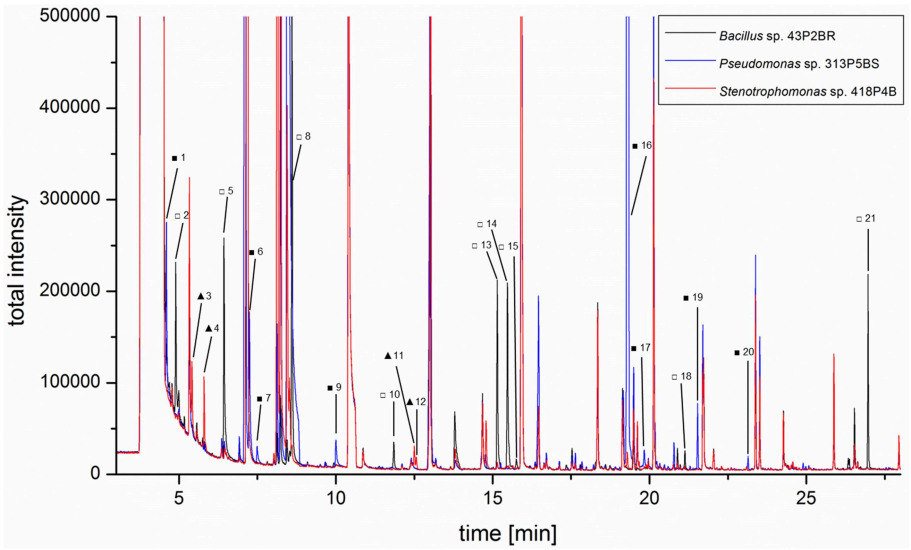

FIGURE 4 | Three lichen-associated bacterial isolates were subjected to headspace SPME GC/MS analysis to identify isolate-specific VOC profiles. An overlay of the respective TIC chromatograms illustrates the presence of specific metabolites in the headspace of *Bacillus pumilus*43P2BR (empty squares), *Pseudomonas umsongensis* 313P5BS (filled squares), and *Stenotrophomonas rhizophila* 418P4B (filled triangles). Identified *Bacillus*-specific compounds were: 1-butanol (5□) and 3-methyl-2-pentanone (8□). Methyl thiocyanate (7■) was identified as *Pseudomonas*-specific compound. *Stenotrophomonas*-specific compounds were: 2-butanol (3▲) and 2-methyl-1-propanol (4▲). More details in Table S2.

that this newly developed testing approach will be a major step forward to facilitate such studies.

Acknowledgments

This work was supported by a grant of the Austrian Science Fund (FWF) to GB and MG (FWF Project I882). We want to thank Angelika Schäfer (Graz), Nicole Pabi (Graz), and Georg Raber (Graz) for their generous support and the provision of required instruments for headspace analytics. We are grateful to Lucia Muggia (Graz) for providing the culture of *Rhinocladiella* sp. We appreciate the provision of pictures used in **Figure 2** by Rocel Amor Ortega (Graz) and the valuable support of Alexander Mahnert (Graz) with RStudio. We also want to thank Timothy Mark (Graz) for proof-reading the manuscript and informative discussions.

Supplementary Material

The Supplementary Material for this article can be found online at: http://journal.frontiersin.org/article/10.3389/fmicb.2015.00398/abstract

References

Berg, G., Zachow, C., Müller, H., Philipps, J., and Tilcher, R. (2013). Next-generation bio-products sowing the seeds of success for sustainable agriculture. *Agronomy* 3, 648–656. doi: 10.3390/agronomy3040648

Blaser, M., Bork, P., Fraser, C., Knight, R., and Wang, J. (2013). The microbiome explored: recent insights and future challenges. *Nat. Rev. Microbiol.* 11, 213–217. doi: 10.1038/nrmicro2973

Blom, D., Fabbri, C., Connor, E. C., Schiestl, F. P., Klauser, D. R., Boller, T., et al. (2011). Production of plant growth modulating volatiles is widespread among rhizosphere bacteria and strongly depends on culture conditions. *Environ. Microbiol.* 13, 3047–3058. doi: 10.1111/j.1462-2920.2011.02582.x

Bragina, A., Berg, C., Müller, H., Moser, D., and Berg, G. (2013). Insights into functional bacterial diversity and its effects on Alpine bog ecosystem functioning. *Sci. Rep.* 3:1955. doi: 10.1038/srep01955

Broderick, K. E., Chan, A., Balasubramanian, M., Feala, J., Reed, S. L., Panda, M., et al. (2008). Cyanide produced by human isolates of Pseudomonas aeruginosa contributes to lethality in *Drosophila melanogaster*. *J. Infect. Dis.* 197, 457–464. doi: 10.1086/525282

Conery, A. L., Larkins-Ford, J., Ausubel, F. M., and Kirienko, N. V. (2014). High-throughput screening for novel anti-infectives using a *C. elegans* pathogenesis model. *Curr. Protoc. Chem. Biol.* 6, 25–37. doi: 10.1002/9780470559277.ch130160

Cook, R. J. (1990). "Towards biological control with introduced antagonists," in *Biological Control of Soil-Borne Plant Pathogens*, ed D. Hornby (Wallingford: CAB International), 6–10.

Effmert, U., Kalderás, J., Warnke, R., and Piechulla, B. (2012). Volatile mediated interactions between bacteria and fungi in the soil. *J. Chem. Ecol.* 38, 665–703. doi: 10.1007/s10886-012-0135-5

Farag, M. A., Zhang, H., and Ryu, C. M. (2013). Dynamic chemical communication between plants and bacteria through airborne signals: induced resistance by bacterial volatiles. *J. Chem. Ecol.* 39, 1007–1018. doi: 10.1007/s10886-013-0317-9

Fiddaman, P. J., and Rossall, S. (1993). The production of antifungal volatiles by *Bacillus subtilis*. *J. Appl. Bacteriol.* 74, 119–126. doi: 10.1111/j.1365-2672.1993.tb03004.x

Garbeva, P., Hordijk, C., Gerards, S., and de Boer, W. (2014). Volatile-mediated interactions between phylogenetically different soil bacteria. *Front. Microbiol.* 5:289. doi: 10.3389/fmicb.2014.00289

Grube, M., Cardinale, M., de Castro, J. V. Jr., Müller, H., and Berg, G. (2009). Species-specific structural and functional diversity of bacterial communities in lichen symbioses. *ISME J.* 3, 1105–1115. doi: 10.1038/ismej.2009.63

Grube, M., Cernava, T., Soh, J., Fuchs, S., Aschenbrenner, I., Lassek, C., et al. (2015). Exploring functional contexts of symbiotic sustain within lichen-associated bacteria by comparative omics. *ISME J.* 9, 412–424. doi: 10.1038/ismej.2014.138

Joulain, D., and Tabacchi, R. (2009). Lichen extracts as raw materials in perfumery. *Flavour Frag. J.* 24, 105–116.

Kai, M., Effmert, U., Berg, G. and Piechulla, B. (2007). Volatiles of bacterial antagonists inhibit mycelial growth of the plant pathogen *Rhizoctonia solani*. *Arch. Microbiol.* 187, 351–60. doi: 10.1002/ffj.1923

Köberl, M., Müller, H., Ramadan, E. M., and Berg, G. (2011). Desert farming benefits from microbial potential in arid soils and promotes diversity and plant health. *PLoS ONE* 6:e24452. doi: 10.1371/journal.pone.0024452

Küster, E., and Williams, S. T. (1964). Selection of media for isolation of Streptomycetes. *Nature* 202, 928–929.

Lane, D. J. (1991). "16S/23S rRNA sequencing," in *Nucleic Acid Techniques in Bacterial Systematics*, eds E. Stackebrandt and M. Goodfellow(Chichester: John Wiley and Sons), 115–147.

Lieber, A., Kiesel, B., and Babel, W. (2003). "Microbial diversity of soil by SSCP fingerprinting technique using TGGE Maxi System," in *Ökophysiologie des Wurzelraumes*, eds W. Merbach, B. W. Hütschand and J. Augustin (Stuttgart: Teubner Verlag), 61–65.

Philippot, L., Raaijmakers, J. M., Lemanceau, P., and van der Putten, W. H. (2013). Going back to the roots: the microbial ecology of the rhizosphere. *Nat. Rev. Microbiol.* 11, 789–799. doi: 10.1038/nrmicro3109

Ryan, R. P., Monchy, S., Cardinale, M., Taghavi, S., Crossman, L., Avison, M. B., et al. (2009). The versatility and adaptation of bacteria from the genus *Stenotrophomonas*. *Nat. Rev. Microbiol.* 7, 514–525. doi: 10.1038/nrmicro2163

Ryu, C. M., Farag, M. A., Hu, C. H., Reddy, M. S., Wei, H. X., Paré, P. W., et al. (2003). Bacterial volatiles promote growth in *Arabidopsis*. *Proc. Natl. Acad. Sci. U.S.A.* 100, 4927–4932. doi: 10.1073/pnas.0730845100

Schalchli, H., Tortella, G. R., Rubilar, O., Parra, L., Hormazabal, E., and Quiroz, A. (2014). Fungal volatiles: an environmentally friendly tool to control pathogenic microorganisms in plants. *Crit. Rev. Biotechnol.* 8, 1–9. doi: 10.3109/07388551.2014.946466

Schrader, P. S., Burrows, E. H., and Ely, R. L. (2008). High-throughput screening assay for biological hydrogen production. *Anal. Chem.* 80, 4014–4019. doi: 10.1021/ac702633q

Seyedsayamdost, M. R. (2014). High-throughput platform for the discovery of elicitors of silent bacterial gene clusters. *Proc. Natl. Acad. Sci. U.S.A.* 111, 7266–7271. doi: 10.1073/pnas.1400019111

Shirling, E. T., and Gottlieb, D. (1966). Method for characterization of Streptomyces species. *Int. J. Syst. Bacteriol.* 16, 313–340.

Strobel, G. (2006). Harnessing endophytes for industrial microbiology. *Curr. Opin. Microbiol.* 9, 240–244. doi: 10.1016/j.mib.2006.04.001

Verginer, M., Leitner, E., and Berg, G. (2010). Production of volatile metabolites by grape-associated microorganisms. *J. Agric Food Chem.* 58, 8344–8350. doi: 10.1021/jf100393w

Vespermann, A., Kai, M., and Piechulla, B. (2007). Rhizobacterial volatiles affect the growth of fungi and Arabidopsis thaliana. *Appl. Environ. Microbiol.* 73, 5639–5641. doi: 10.1128/AEM.01078-07

Warmink, J. A., Nazir, R., and van Elsas, J. D. (2009). Universal and species-specific bacterial 'fungiphiles' in the mycospheres of different basidiomycetous fungi. *Environ. Microbiol.* 11, 300–312. doi: 10.1111/j.1462-2920.2008.01767.x

Weise, T., Kai, M., and Piechulla, B. (2013). Bacterial ammonia causes significant plant growth inhibition. *PLoS ONE* 8:e63538. doi: 10.1371/journal.pone.0063538

Weller, D. M., Raaijmakers, J. M., Gardener, B. B. M., and Thomashow, L. S. (2002). Microbial populations responsible for specific soil suppressiveness to plant pathogens. *Annu. Rev. Phytopathol.* 40, 309–348.

Wolf, A., Fritze, A., Hagemann, M., and Berg, G. (2002). Stenotrophomonas rhizophila sp. nov., a novel plant-associated bacterium with antifungal properties. *Int. J. Syst. Evol. Microbiol.* 52, 1937–1944. doi: 10.1099/ijs.0.02135-0

Woolhouse, M., and Farrar, J. (2014). Policy: an intergovernmental panel on antimicrobial resistance. *Nature* 509, 555–557. doi: 10.1038/509555a

Conflict of Interest Statement: The authors declare that the research was conducted in the absence of any commercial or financial relationships that could be construed as a potential conflict of interest.

Additional Publication III – Supplementary Data

Supplementary Figures

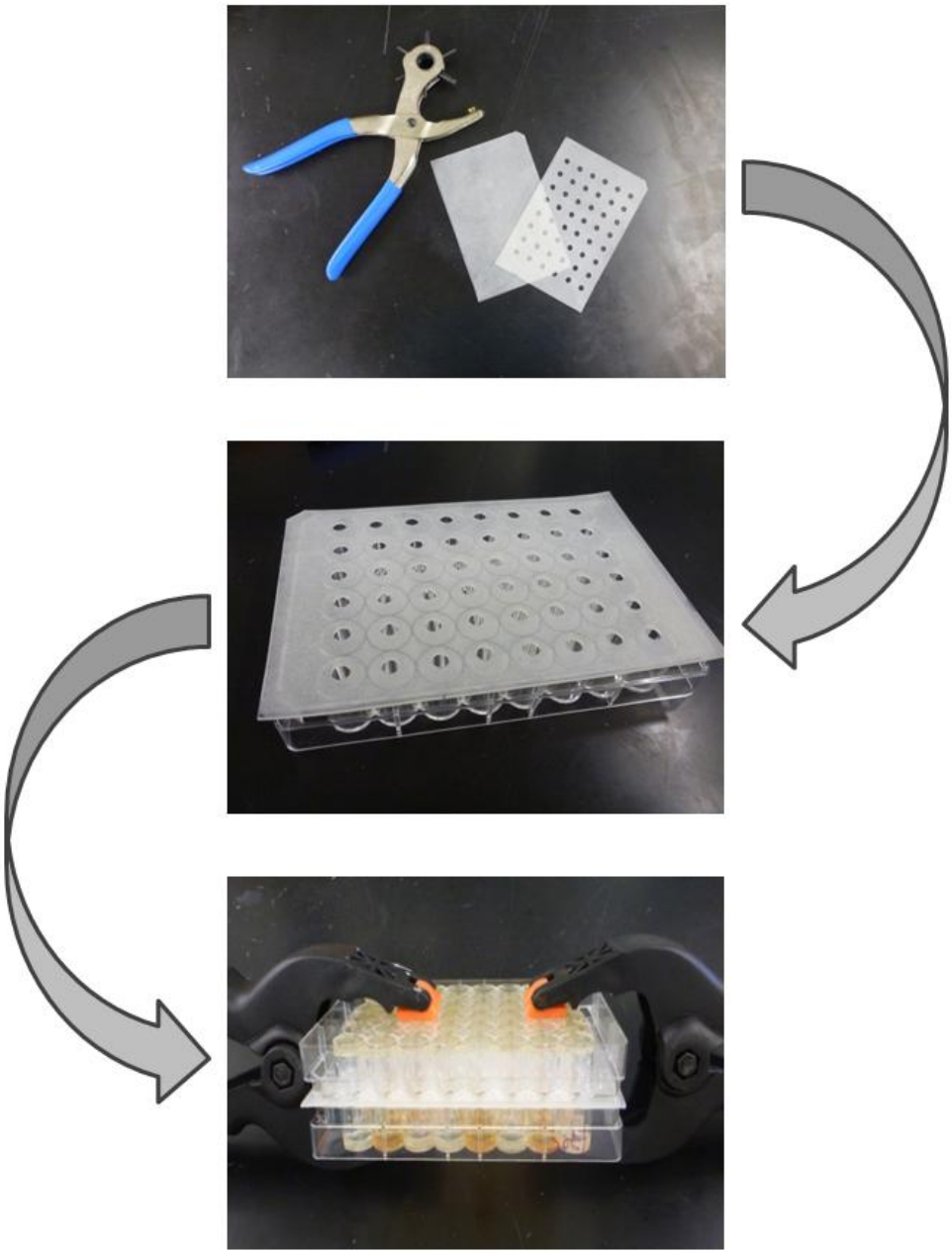

Figure S1: Step by step illustration of a TCVA with two microorganism-containing well-plates. Perforated silicone foil together with two clamps per plate was used to seal adjacent wells and join them into separate chambers. After a microorganism-specific incubation time, the plates were separated again and visually inspected for growth reduction within wells of the target plate.

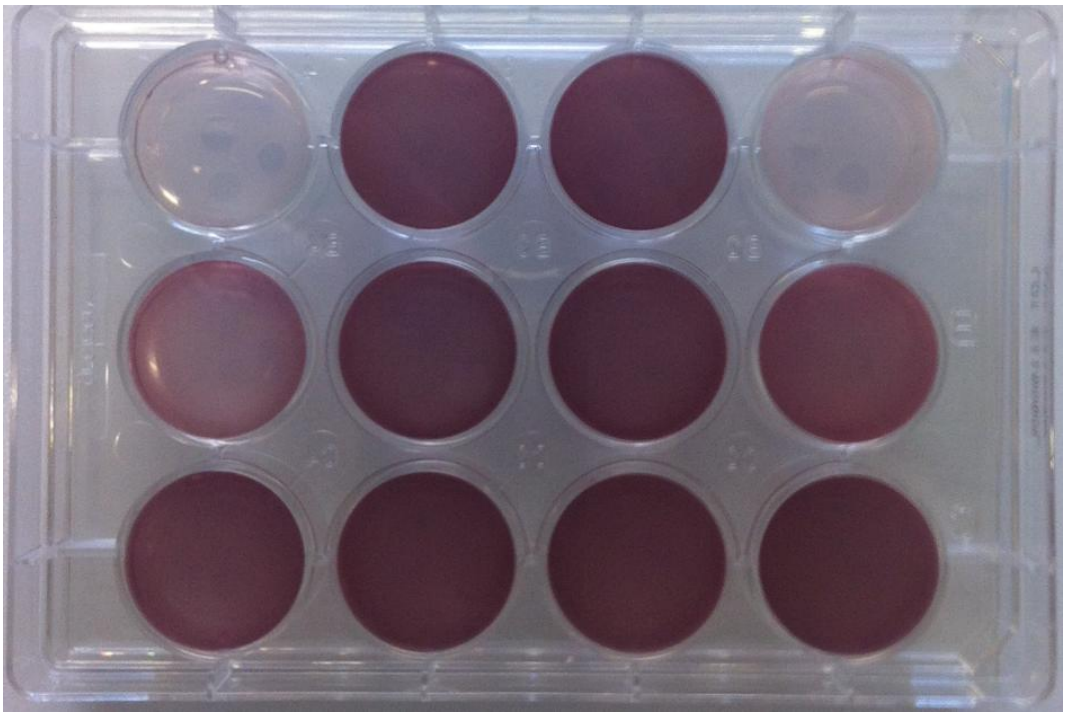

Figure S2: Pretest with *E. coli* K12 and 2–(4–iodophenyl)–3–(4–nitrophenyl)–5–phenyltetrazolium chloride (INT; 0.2 mg/mL) supplemented nutrient agar (NA) 12-well plates. The left plate compartment (A1-A6) was exposed to different Sterilium™ concentrations, while the right plate compartment (B1-B6) was exposed to different Bacilol™ concentrations. High inhibition of *E. coli* was observed with 100 µL Sterilium™ and Bacilol™, respectively (A1 and B1). Lower inhibition was observed with decreasing Sterilium™ and Bacilol™ concentrations (A2-A5 and B2-B5). Two negative controls without any disinfectant were additionally conducted (A6 and B6).

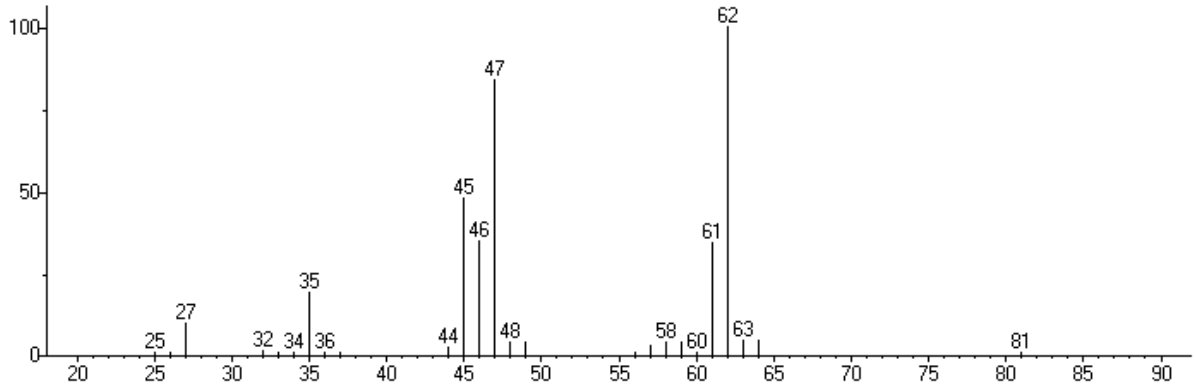

Figure S3: Mass spectrum of unidentified substance (compound ID: 1).

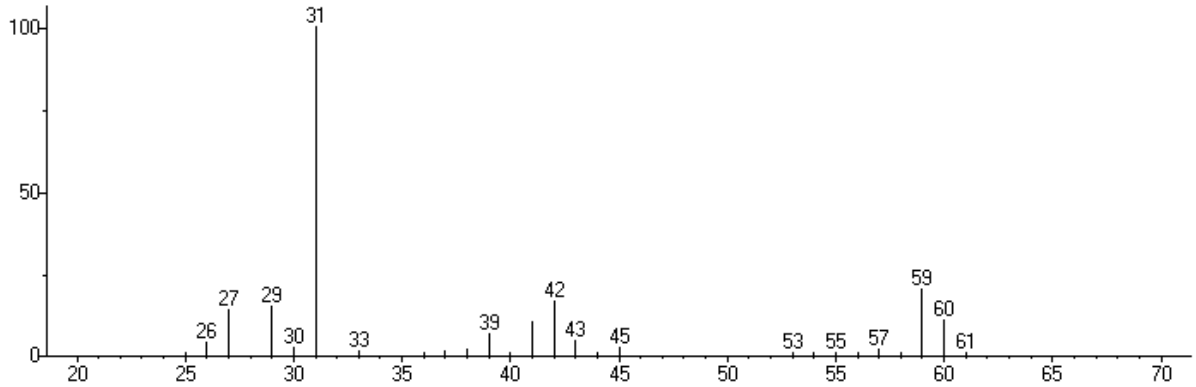

Figure S4: Mass spectrum of unidentified substance (compound ID: 2).

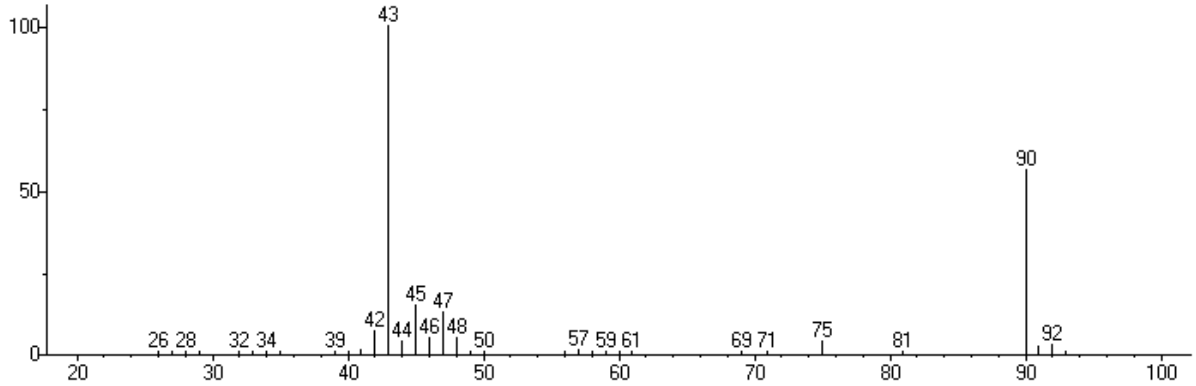

Figure S5: Mass spectrum of unidentified substance (compound ID: 6).

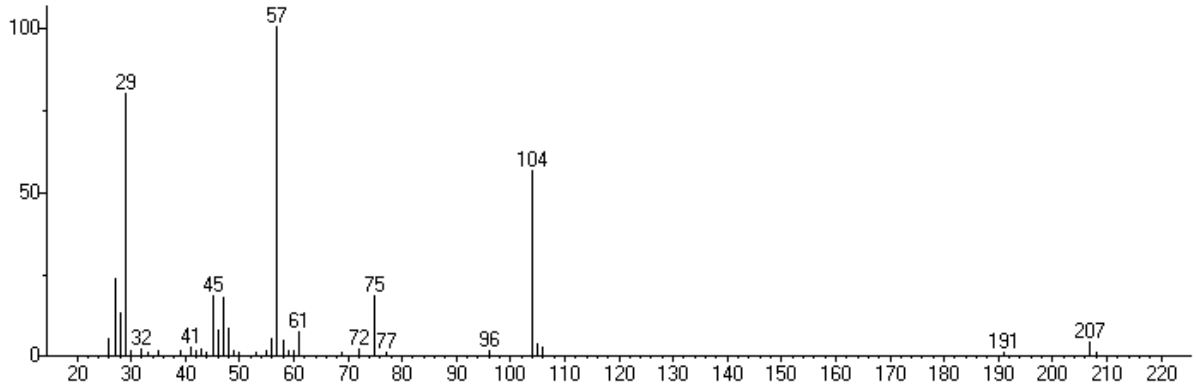

Figure S6: Mass spectrum of unidentified substance (compound ID: 9).

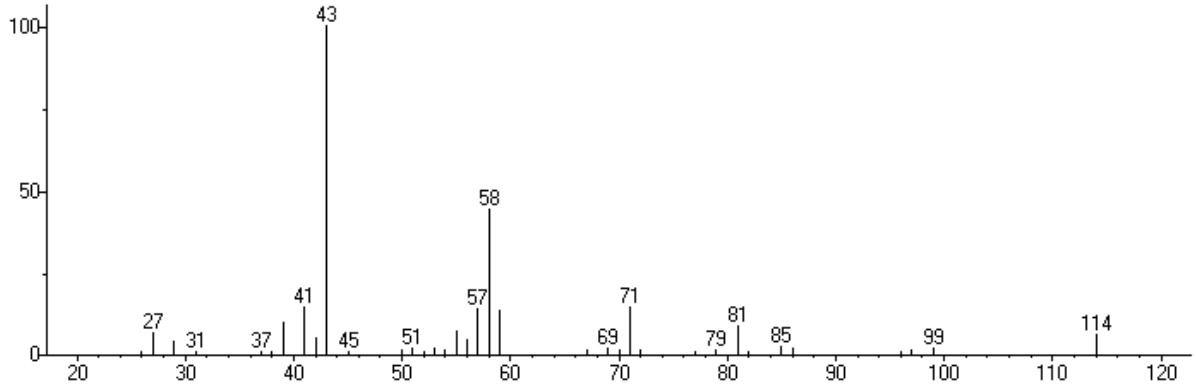

Figure S7: Mass spectrum of unidentified substance (compound ID: 10).

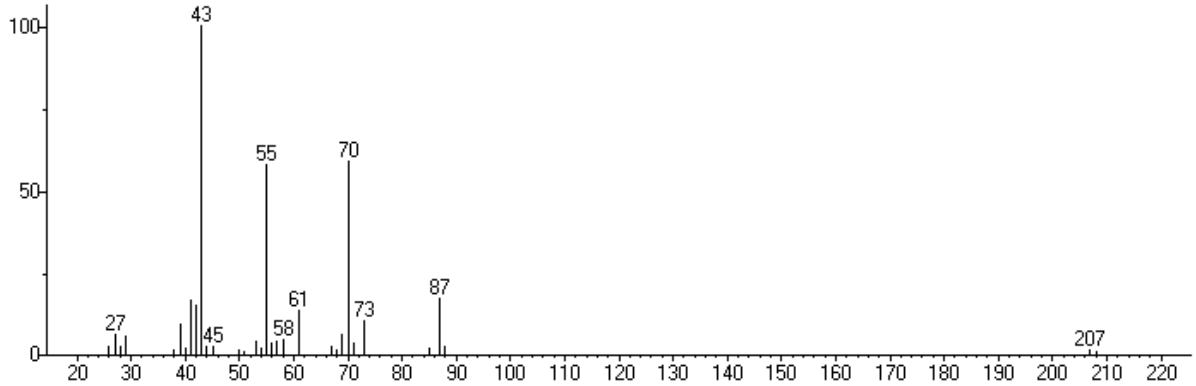

Figure S8: Mass spectrum of unidentified substance (compound ID: 11).

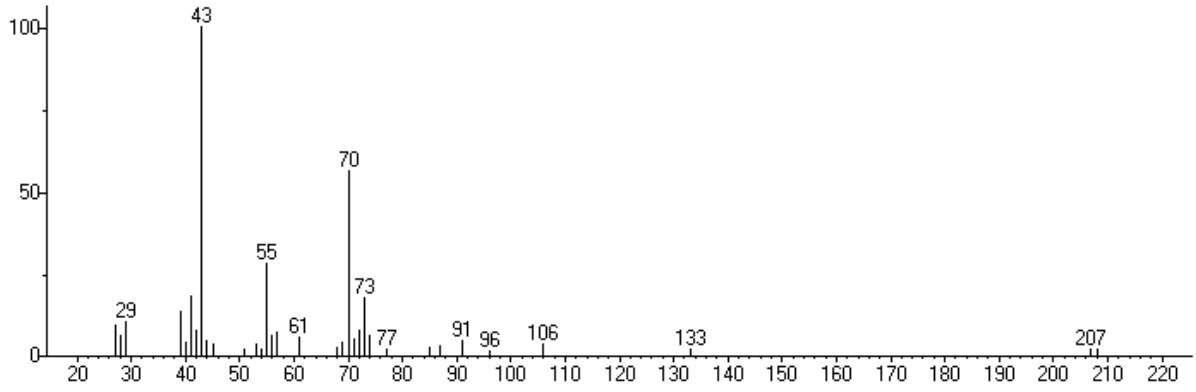

Figure S9: Mass spectrum of unidentified substance (compound ID: 12).

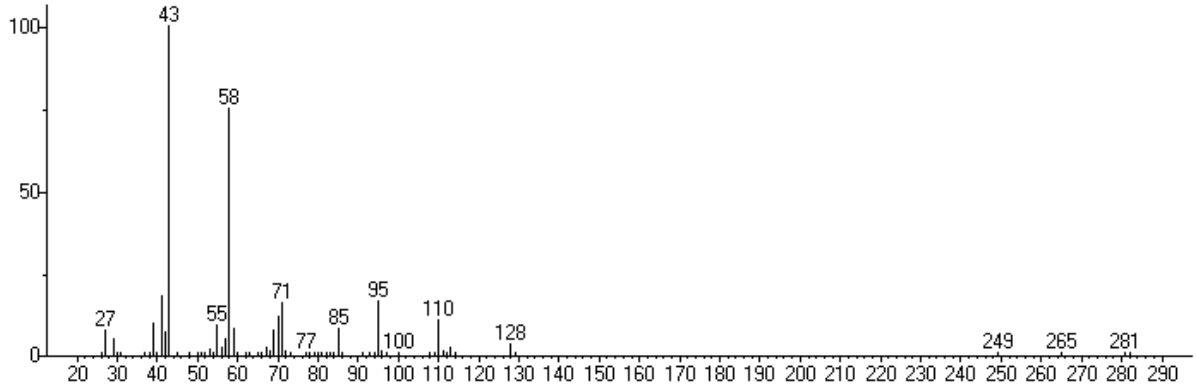

Figure S10: Mass spectrum of unidentified substance (compound ID: 13).

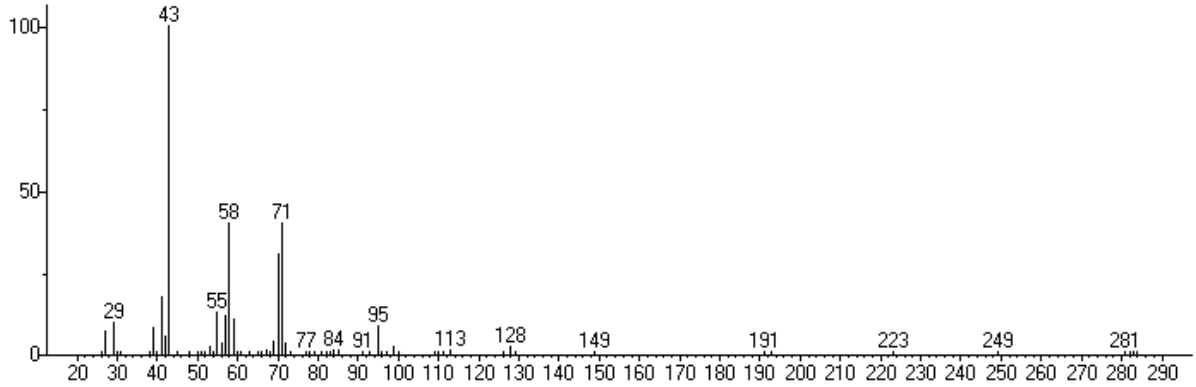

Figure S11: Mass spectrum of unidentified substance (compound ID: 14).

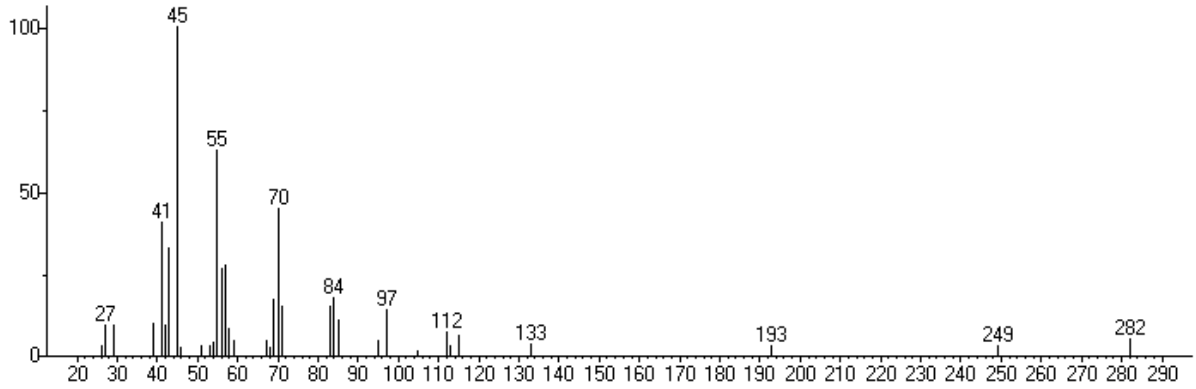

Figure S12: Mass spectrum of unidentified substance (compound ID: 15).

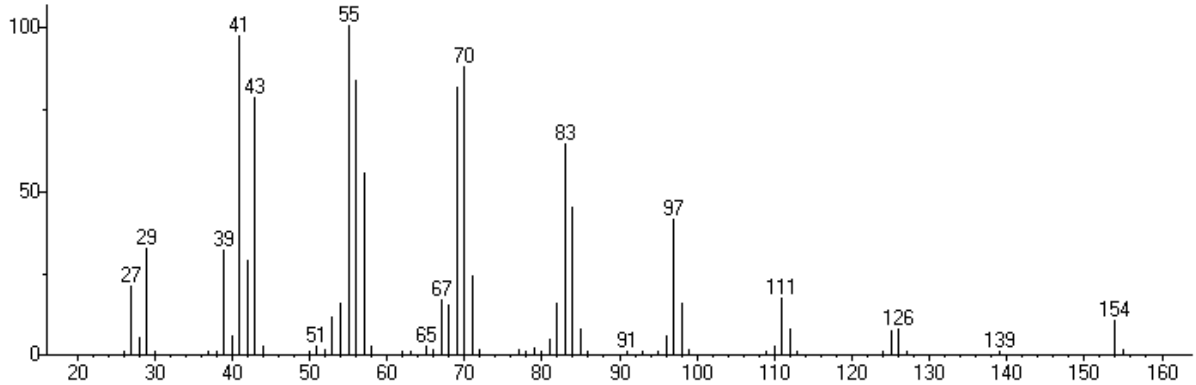

Figure S13: Mass spectrum of unidentified substance (compound ID: 16).

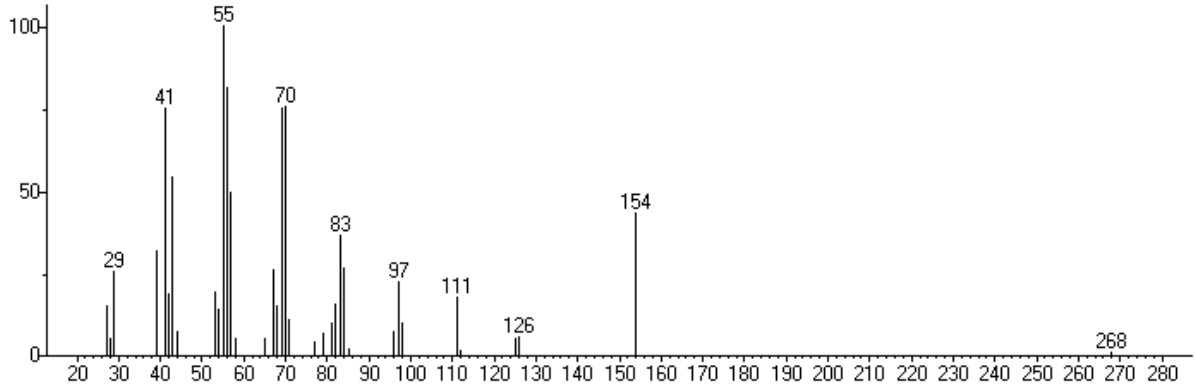

Figure S14: Mass spectrum of unidentified substance (compound ID: 17).

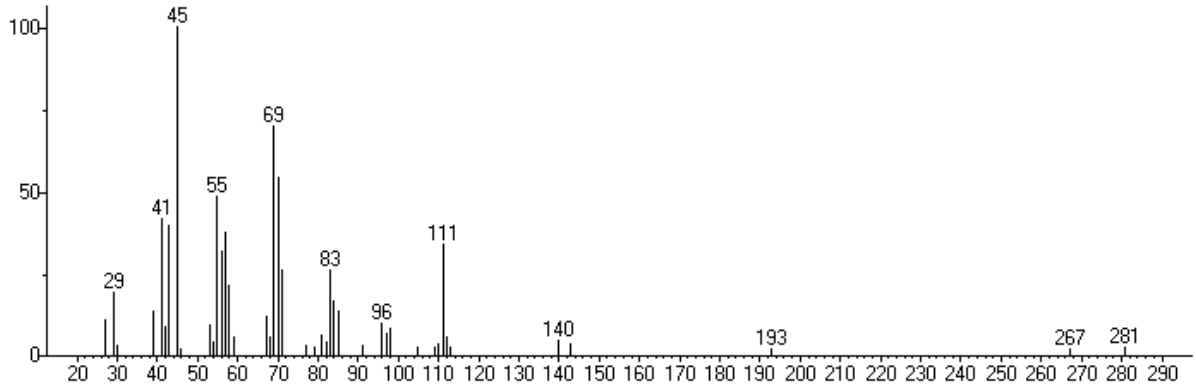

Figure S15: Mass spectrum of unidentified substance (compound ID: 18).

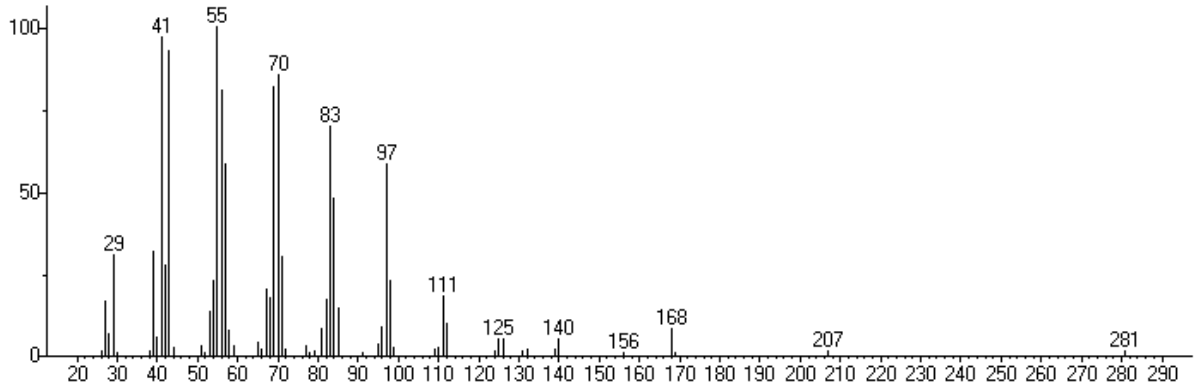

Figure S16: Mass spectrum of unidentified substance (compound ID: 19).

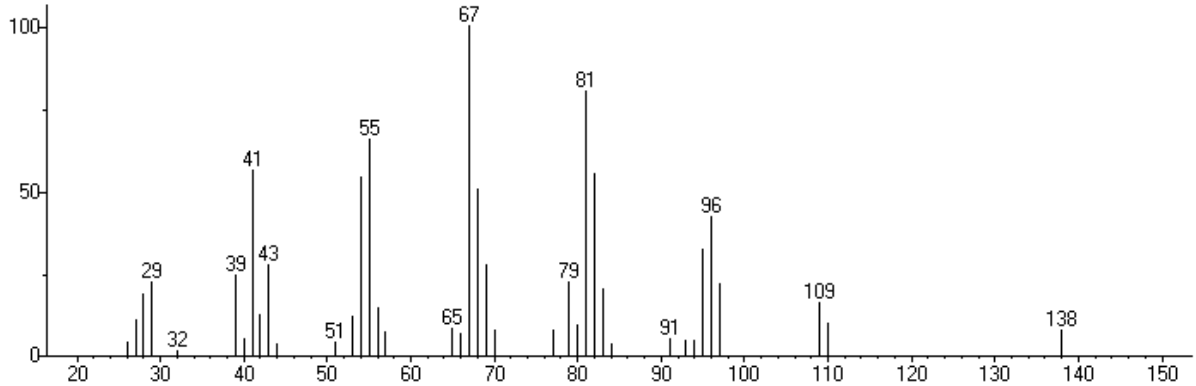

Figure S17: Mass spectrum of unidentified substance (compound ID: 20).

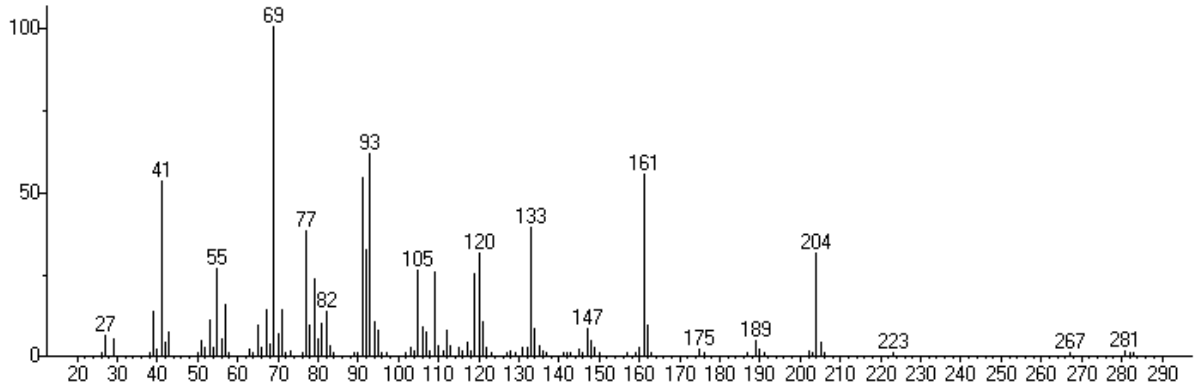

Figure S18: Mass spectrum of unidentified substance (compound ID: 21).

Supplementary Tables

Table S1: The utilized silicone foils were obtained from a local reseller (Hostra GmbH, Graz, Austria). To allow reproducibility of our experiments we have summarized the most important properties.

Detailed properties of the utilized tightening foil	
Material	silicone
Thickness	1 mm
Density	1.14 g/cm^3
Hardness Shore A DIN 53505	55–65 SHA
Temperature Range	-60 – +230 °C
Elongation at Brake DIN 53504	250%
Compression Set ISO 815	24 h, 150 °C = 30%
Color	transparent

Table S2: Unique volatile metabolites in the headspace of three bacterial isolates. VOCs from *Bacillus* sp. 43P2BR, *Pseudomonas* sp. 313P5BS and *Stenotrophomonas* sp. 418P4B were detected and specific peaks for each isolate were extracted from chromatogram overlays. Compounds were identified by comparison with reference substance mass spectra and their respective retention indices.

Strain ID	RI[a]	Substance	Substance ID
43P2BR	n.a.[b]	unidentified substance	2
	645	1-butanol	5
	738	3-methyl-2-pentanone	8
	855	unidentified substance	10
	954	unidentified substance	13
	963	unidentified substance	14
	972	unidentified substance	15
	1175	unidentified substance	18
	1540	unidentified substance	21
313P5BS	n.a.[b]	unidentified substance	1
	680	unidentified substance	6
	691	methyl thiocyanate	7
	798	unidentified substance	9
	1094	unidentified substance	16
	1106	unidentified substance	17
	1193	unidentified substance	19
	1279	unidentified substance	20
418P4B	617	2-butanol	3
	632	2-methyl-1-propanol	4
	875	unidentified substance	11
	876	unidentified substance	12

[a]Calculated Kovats retention indices

[b]The substance was not retained within in the utilized n-alkane series

ACKNOWLEDGEMENTS

Foremost, I would like to express my sincere gratitude to my supervisors Univ.-Prof. Dr. Gabriele Berg and Ao. Univ.-Prof. Dr. Martin Grube for giving me this great opportunity to work in this interdisciplinary scientific field of symbiotic organisms and modern technologies. I would like to thank Gabriele for her scientific guidance and support in each of the last three years and Martin for his unconventional mindset and contagious enthusiasm, which often brought forward new and interesting ideas.

Besides my advisors, I would like to thank our cooperation partners Univ.-Prof. Dr. Kathrin Riedel and her team in Greifswald as well as Univ.-Prof. Dr. Christoph W. Sensen and Dr. Jung Soh for their important contributions in Proteome studies and bioinformatic analyses.

Furthermore, I want to thank Tomislav Cernava, MSc and Dr. Christian Westendorf for their encouragement and constructive comments, Melanie Marek and Tobija Glawogger for their help in processing our lichen specimens in the laboratory, Herbert Koller for technical support and to Dr. Armin Erlacher, Dr. Henry Müller, Dr. Fernando Fernandez Mendoza and Dr. Massimiliano Cardinale for their valuable contributions and helpful advices. Special thanks to all my colleagues and friends from the Institute of Environmental Biotechnology and the Institute of Plant Sciences for a supportive and productive working environment. In particular, I would like to thank Mag. Barbara Klug, Stefanie Maier, MSc, Mag. Theodora Kopun, Dr. Lucia Muggia and Antonia Fleischhacker, MSc for inspiring conversations during the coffee breaks in the botanical gardens and Mag. Philipp Resl to accompany our breaks with provocative music. It was a great time and a lot of fun being part of these friendly and ambitious working groups.

Finally, I want to thank my dear family: my parents, my brother and sister, and my boyfriend Manuel for their continuous support, motivation and patience over so many years and for always believing in me.

CURRICULUM VITAE

Personal Data

Name	**Ines Aline Aschenbrenner, BSc MSc**
Address	Plüddemanngasse 75 / 9 8010 Graz Austria
Telephone	+43 664 1397972
E-mail	ines.aschenbrenner@tugraz.at
Date of Birth	November 7th 1986
Place of Birth	Berlin, Germany
Citizenship	Austrian

Education

2012-2015	PhD studies in *Biotechnology* at Graz University of Technology and University of Graz.
2009-2011	Master studies in *Molecular Microbiology* at University of Graz and Graz University of Technology within the NAWI Graz project.
2005-2009	Bachelor studies in *Molecular Biology* at University of Graz and Graz University of Technology within the NAWI Graz project.
1999-2005	High school (Realgymnasium) in Leibnitz, Styria at BG/BRG Leibnitz.
1997-1999	Grammar school (AHS) in Leibnitz, Styria at BG/BRG Leibnitz.

Work experience

05/2012-10/2015	Doctoral Thesis: "*Stability and change in the lichen microbiome*" in *Biotechnology* at the Institute of Environmental Biotechnology, Graz University of Technology. Supervisor: Univ.-Prof. Dr.rer.nat. Gabriele Berg. Methods: next generation sequencing techniques and data analyses, fluorescence in situ hybridization and confocal laser scanning microscopy, metagenomics and metatranscriptomics analyses.
05/2010-11/2011	Master Thesis: "*Interaction-analyses between the transcription activator protein TraJ and the bacterial RNA polymerase*" in *Molecular Microbiology* at the Institute of Molecular Biosciences, University of Graz.

Supervisor: Ao.Univ.-Prof.Dr.phil. Günther Koraimann.

Methods: standard microbiological and molecular biological techniques, bacterial two-hybrid system assay for protein-protein interaction analyses, model organism: *Escherichia coli.*

Teaching experience

10/2014-01/2015	Co-Supervisor, at Institute of Environmental Biotechnology, Graz University of Technology, course: "*Microbiology Laboratory Course*".
10/2011-01/2012	Student Assistant, at Institute of Molecular Biosciences, University of Graz, course: "*Bacteriology and bacterial genetics*".
03/2011-06/2011	Student Assistant, at Institute of Molecular Biosciences, University of Graz, course: "*Molecular Biology Laboratory Course II*".
10/2010-01/2011	Student Assistant, at Institute of Molecular Biosciences, University of Graz, courses: "*Molecular Biology Laboratory Course I*" and "Bacteriology and bacterial genetics".

Additional training

04/2014	*Introduction to statistical data analysis with R* at the Institute of Plant Sciences, University of Graz.
06/2010	*Communicational training* at Center for social competence, University of Graz.
03/2010	*Leading working groups* at Center for social competence, University of Graz.
06/2004	*First Certificate in English (ESOL Examination),* University of Cambridge.
07/2003	*European computer driving license* core certificate, Austrian Computer Society.

PUBLICATION LIST

Peer-reviewed Publications

Aschenbrenner, I. A., Cardinale, M., Berg, G., & Grube, M. (2014). Microbial cargo: do bacteria on symbiotic propagules reinforce the microbiome of lichens? *Environmental microbiology*, *16*, 3743–3752.

Cernava, T., Aschenbrenner, I. A., Grube, M., Liebminger, S., and Berg, G. (2015). A novel assay for the detection of bioactive volatiles evaluated by screening of lichen associated bacteria. *Frontiers in microbiology*, *6*, 398.

Cernava, T., Müller, H., Aschenbrenner, I. A., Grube, M., and Berg, G. (2015). Analyzing the antagonistic potential of the lichen microbiome against pathogens by bridging metagenomic with culture studies. *Frontiers in microbiology*, *6*, 620.

Grube, M., Cernava, T., Soh, J., Fuchs, S., Aschenbrenner, I., Lassek, C., Wegner, U., Becher, D., Riedel, K., Sensen, C. W., and Berg, G. (2015). Exploring functional contexts of symbiotic sustain within lichen-associated bacteria by comparative omics. *The ISME journal*, *9*, 412–424.

Oral Presentation

Aschenbrenner, I., Cardinale, M., Berg, G., and Grube, M. Microbial cargo: bacteria on symbiotic propagules of lichens. 16th Conference of Austrian botanists. Graz, Austria 26.09.2014.

Poster Presentations

Aschenbrenner, I., Cernava, T., Maier, S., Cardinale, M., Berg, G., and Grube, M. Bacterial cargo on symbiotic propagules of the lung lichen *Lobaria pulmonaria*. FEMS 2013 - 5th Congress of European Microbiologists. Leipzig, Germany 22.07.2013.

Cernava, T., Aschenbrenner, I., Riedel, K., Soh, J., Sensen, C. W., Grube, M., and Berg, G. Deciphering a functional network of symbiotic sustain with the microbiome of lichens by comparative omics. NAWI Graz Fest 2014. Graz, Austria 10.07.2014.

Aschenbrenner, I., Cernava, T., Cardinale, M., Berg, G., and Grube, M. Microbial Cargo: Do bacteria on symbiotic propagules reinforce the lichen microbiome. IMC10 2014 - 10th Mycological Congress. Bangkok, Thailand 14.08.2014.

Grube, M., Cernava, T., Soh, J., Fuchs, S., Aschenbrenner, I., Riedel, K., Sensen, C. W., and Berg, G. Functional roles of bacteria in lichen-associated bacteria studied by comparative omics. BAGECO 13. 13th Symposium on Bacterial Genetics and Ecology. Milano, Italy 15.06.2015.

Aschenbrenner, I., Cernava, T., Berg, G., and Grube, M. Bacterial cargo on symbiotic propagules of the lung lichen *Lobaria pulmonaria*. BAGECO 13. 13th Symposium on Bacterial Genetics and Ecology. Milano, Italy 15.06.2015.